ICLIAD 67 (2), 165-321, 2026

p-ISSN 0535-5133
e-ISSN 2477-9393

Volumen 67
No. 2
Junio
2026

Investigación Clínica

Universidad del Zulia
Facultad de Medicina
Instituto de Investigaciones Clínicas
"Dr. Américo Negrette"
Maracaibo, Venezuela

Investigación Clínica

https://sites.google.com/site/revistainvestigacionesclinicas

Revista arbitrada dedicada a estudios humanos, animales y de laboratorio relacionados con la investigación clínica y asuntos conexos.

La Revista es de Acceso Abierto, publicada trimestralmente por el Instituto de Investigaciones Clínicas "Dr. Américo Negrette", de la Facultad de Medicina, de la Universidad del Zulia, Maracaibo, Venezuela.

Investigación Clínica está indizada en Science Citation Index Expanded (USA), Excerpta Medica/EMBASE y Scopus (Holanda), Tropical Diseases Bulletin y Global Health (UK), Biblioteca Regional de Medicina/BIREME (Brasil), Ulrich's Periodicals, Journal Citation Reports (USA), Index Copernicus (Polonia), SIIEC Data Bases, Sección Iberoamérica (Argentina) e Infobase Index (India), Redalyc y las bases de datos: SciELO (www.Scielo.org.ve), Revencyt, LILACS, LIVECS, PERIODICA y web de LUZ: http://www.produccioncientificaluz.org/revistas

Para cualquier otra información dirigir su correspondencia a:

Dra. Elena Ryder, Editora
Instituto de Investigaciones Clínicas "Dr. Américo Negrette"
Facultad de Medicina, Universidad del Zulia
Maracaibo, Venezuela.

Teléfono:
+58-0414-6305451

Correos electrónicos:
elenaryder@gmail.com
riclinicas@gmail.com

Páginas web:
https://sites.google.com/site/revistainvestigacionesclinicas

http://www.produccioncientificaluz.org/revistas

For any information please address correspondence to:

Dr. Elena Ryder, Editor
Instituto de Investigaciones Clínicas "Dr. Américo Negrette"
Facultad de Medicina, Universidad del Zulia
Maracaibo, Venezuela.

Phone:
+58-0414-6305451

E-mails:
elenaryder@gmail.com
riclinicas@gmail.com

Web pages:
https://sites.google.com/site/revistainvestigacionesclinicas

http://www.produccioncientificaluz.org/revistas

Universidad del Zulia
Publicación auspiciada por el
Vicerrectorado Académico
Serbiluz-CONDES

CODEN: ICLIAD
Versión impresa ISSN: 0535-5133
Depósito legal pp 196002ZU37
Versión electrónica ISSN: 2477-9393
Depósito legal ppi 201502ZU4667

Artes finales:
Lisbeny Valencia
lisbenyvalencia@gmail.com

ASESORES CIENTÍFICOS (2025-2027)

Invest Clin 67(2): 165 - 167, 2026 https://doi.org/10.54817/IC.v67n2a00

EDITORIAL
La reemergencia de la fiebre amarilla en Venezuela.

La fiebre amarilla es una enfermedad viral aguda, clasificada como una patología icterohemorrágica. Es una zoonosis que también afecta a primates de diferentes especies, los cuales son el reservorio principal de la infección, y se transmite al humano por diversos géneros de mosquitos (*Haemagogus, Sabethes* o *Aedes*), con ciclos urbanos y selváticos en las regiones endémicas[1]. Esta arbovirosis, causada por un flavivirus, se transmite de forma accidental al humano cuando este invade áreas de riesgo sin la debida protección, denominándose fiebre amarilla selvática.

Venezuela forma parte de las zonas tropicales en América del Sur, junto a Brasil, Colombia, Bolivia, Perú, Ecuador, Guyana, Argentina y Paraguay, con circulación emergente y remergente de esta arbovirosis. El virus fue aislado por primera vez en 1927 y fue una evidencia certera en el país desde 1961, cuando se realizó el primer aislamiento venezolano del virus de la fiebre amarilla a partir de un mono y de un caso humano fallecido en el estado Táchira [1-3].

En Venezuela, la fiebre amarilla se ha presentado en tres focos enzoóticos: San Camilo, en los estados Apure y Táchira; Sur del Lago de Maracaibo, en el estado Zulia; y Guayana, en el estado Bolívar, con extensiones hacia Amazonas. La existencia de estos focos y la casi inexistencia del control de vectores, junto al deterioro sanitario en el país, y al intercambio fronterizo y migratorio, han hecho que reaparezcan enfermedades que ya estaban controladas, con un impacto severo en la salud pública local, especialmente las prevenibles por vacunación como la fiebre amarilla [3-5].

La situación de la fiebre amarilla en Venezuela ha escalado recientemente a un estado de alerta sanitaria tras confirmarse un brote que abarca varias regiones del país. Hasta mayo de 2026, los reportes de organismos oficiales de salud pública indican que se han registrado al menos 40 casos en humanos: 32 en 2025 y 8 en 2026, con 21 fallecimientos confirmados, lo que representa una tasa de letalidad superior al 50%, que históricamente ha caracterizado a esta infección [6,7].

El virus ha circulado recientemente en 14 estados del país, con mayor incidencia en Barinas, Monagas, Amazonas y Bolívar. También se ha detectado propagación hacia zonas previamente consideradas de bajo riesgo, lo que representa una propagación geográfica mayor que la de brotes anteriores, involucrando los focos enzoóticos existentes con mayor actividad en San Camilo. Hasta el momento, la transmisión se mantiene en el ciclo selvático, sin evidencia de circulación urbana. Estas infecciones se han caracterizado por un 57,5% de los casos concentrados en la población de sexo masculino, mayor incidencia en el grupo etario de 20 a 29 años (22,5%) y el riesgo ocupacional con alta vulnerabilidad en los agricultores, con historial de falta de vacunación, muy por debajo del 95% establecido como margen para prevenir epidemias [8].

Este brote forma parte de un resurgimiento regional no solo en Venezuela, sino también en América Latina desde finales de 2024, que afecta a países como Colombia, Brasil, Perú, Bolivia, Ecuador y Guyana. En este contexto, Venezuela ocupa el cuarto lugar en incidencia de casos reportados [7].

Por tal motivo, instituciones nacionales de salud e internacionales, como la Organización Panamericana de la Salud (OPS), mantienen una vigilancia estrecha debido a la detección de virus en primates (epizootias) en 88 localidades de ocho estados, lo que indica una circulación viral activa en zonas boscosas y un riesgo inminente de desbordamiento hacia áreas periurbanas [6,8].

El resurgimiento de la fiebre amarilla en Venezuela, representa una grave amenaza para la seguridad sanitaria regional [5]. Análisis previos subrayan que la precariedad de los sistemas de vigilancia y las demoras diagnósticas, propician el reconocimiento clínico tardío de esta arbovirosis, agravando sus desenlaces [3,7]. Ante el incremento de casos, es imperativo establecer protocolos estrictos de movilidad en las zonas afectadas y ampliar la cobertura vacunal conforme a estándares internacionales, garantizando una vigilancia diferenciada en grupos vulnerables, como gestantes y adultos mayores.

Es fundamental destacar que la fiebre amarilla es una enfermedad prevenible mediante vacunación. De hecho, su inmunización es considerada uno de los logros más exitosos en la historia de la inmunología: una sola dosis de la cepa 17D (desarrollada en la década de 1930) basta para conferir protección de por vida a la mayoría de las personas. No obstante, investigaciones recientes sugieren que esta inmunidad difiere de la inducida por las cepas de tipo salvaje; el alcance de tales diferencias y sus mecanismos subyacentes aún no se han esclarecido por completo [9]. En consecuencia, es necesario profundizar en el estudio de la respuesta inmunitaria frente a este virus, especialmente en contextos enzoóticos.

Asimismo, cabe subrayar que, a pesar de la eficacia de la dosis única, la falta de inversión en vacunas y las deficiencias logísticas para asegurar la cadena de frío y mantener su viabilidad, en especial en zonas rurales remotas, persisten como las principales barreras para el control de la enfermedad [9].

La reemergencia de la fiebre amarilla como desafío de salud pública se debe a una compleja red de factores ecológicos, logísticos y sociales. Entre ellos destacan la dinámica poblacional de vectores y reservorios, el aumento de la movilidad humana y las brechas en la cobertura vacunal. Además, las dificultades críticas en la producción y distribución de vacunas reflejan, en gran medida, el impacto de las prioridades y políticas gubernamentales en la gestión sanitaria [6].

Como la mayoría de las arbovirosis emergentes y reemergentes, la fiebre amarilla comparte determinantes que favorecen la permanencia y circulación de estos virus, como son el cambio climático, el uso de la tierra y la alteración de los ecosistemas (especialmente la incursión humana desmedida en ecosistemas vírgenes, impulsada por la minería ilegal y la deforestación), factores que obligan a los vectores selváticos y a los reservorios a desplazarse hacia asentamientos humanos, aumentando el riesgo de salida hacia el ciclo urbano. También contribuyen la urbanización no planificada, las fallas en la vigilancia epizoótica y el limitado trabajo conjunto entre los organismos pertinentes [4].

En definitiva, esta reemergencia no es un evento fortuito, sino el resultado de la convergencia de fallas en la vigilancia virológica, entomológica e inmunológica, de cambios ambientales drásticos y de un silencio epidemiológico prolongado. Como una solución se ha planteado que la adopción del enfoque “Una Salud” (One Health) reduciría el riesgo de incidencia y brotes de fiebre amarilla en el futuro [10]; sin embargo, a pesar de que puede ser factible y previsible el éxito de este modelo, se debe tomar como base imprescindible, la colaboración y comunicación entre las diversas partes interesadas, así como la publicación inmediata y regular de boletines epidemiológicos que alerten proactivamente y permitan la toma de acciones oportunamente.

Nereida Valero-Cedeño
ORCID 0000-0003-3496-8848

The reemergence of yellow fever in Venezuela

The reemergence of yellow fever in Venezuela poses a critical threat to the region's health security. After years of control, the persistent crisis has shifted surveillance from proactive to reactive. As of May 2026, official public health agencies report at least 40 human cases and 21 confirmed deaths, corresponding to a case fatality rate exceeding 50%. In addition to the inherent predisposing factors of arboviruses, increasing human mobility without adequate protection in jungle areas and the accumulation of susceptible, unvaccinated individuals are identified as key determinants. The epidemiological impact shows a notable demographic bias, predominantly affecting young men of working age (57.5% of cases), which exacerbates the socioeconomic consequences of this outbreak. Furthermore, ongoing enzootic and epizootic circulation of the virus, both in known hotspots and in border areas and regions previously considered low-risk, indicates a high potential for expansion. Under the One Health approach, given active viral circulation, it is imperative to reinstate vaccination protocols to close susceptibility gaps in rural and peri-urban regions that have not yet achieved the recommended immunization coverage, thereby completely blocking transmission and preventing the urban cycle. Similarly, it is necessary to optimize diagnostic turnaround times, strengthen entomological and ecological surveillance, bolster international cooperation to reduce the risk of spread to neighboring countries, provide timely alerts about epizootics, and issue travel protection recommendations.

REFERENCIAS

1. **Valero N**. A propósito de la fiebre amarilla en Venezuela. Invest Clin. 2003; 44(4): 269-271. Disponible en: http://ve.scielo.org/scielo.php?script=sci_arttext&pid=S0535-51332003000400001&lng=es.
2. **Finol E, Berrueta E, Levy A, Añez F, Espina LM, Maldonado M, et al.** Evaluación retrospectiva de fiebre amarilla selvática en Venezuela, período 2003 - 2005. Kasmera. 2008;36(1):67-78. Disponible en: http://ve.scielo.org/scielo.php?script=sci_arttext&pid=S0075-52222008000100008&lng=es.
3. **Espinosa L, Mirinaviciute G.** Health crisis in Venezuela: Status of communicable diseases and implications for the European Union and European Economic Area, May 2019. Euro Surveill. 2019;24(22):1900308. *https://doi.org/10.2807/1560-7917.ES.2019.24.22.1900308.*
4. **Chavero M, Guevara O, Figuera L, Viera M, Sandoval-De Mora M, Carrión-Nessi FS, et al.** Reemergence of yellow fever in Venezuela: Report of the first case after 14 years. Travel Med Infect Dis. 2021; 41:102025. *https://doi.org/10.1016/j.tmaid.2021.102025.*
5. **Rodríguez-Morales AJ, Bonilla-Aldana DK, Suárez JA, Franco-Paredes C, Forero-Peña DA, Mattar S, et al.** Yellow fever reemergence in Venezuela - Implications for international travelers and Latin American countries during the COVID-19 pandemic. Travel Med Infect Dis. 2021; 44:102192. *https://doi.org/10.1016/j.tmaid.2021.102192.*
6. **Pan American Health Organization**. Current Yellow fever situation in the Americas: call for strengthened surveillance and vaccination efforts in enzootic and newly affected areas. Rev Panam Salud Publica. 2026;50: e51. *https://doi.org/10.26633/ RPSP.2026.51.*
7. **Rodriguez-Morales AJ, Navarro JC, Forero-Peña DA, Romero-Alvarez D.** Reemergence of yellow fever in Venezuela, 2025/2026. New Microbes New Infect. 2026; 70:101737. *https://doi.org/10.1016/j.nmni.2026.101737.*
8. **Ministerio del Poder Popular para la Salud**. Venezuela. Boletin Epidemiológico. Semana Epidemiológica 14 del 5-11 de abril de 2026. Disponible en: https://mpps.gob.ve/wp-content/uploads/2026/04/SE14-BOLETIN-EPIDEMIOLOGICO-SEMANA-14-2026-DEF-1.pdf
9. **Gonçalves AP, Almeida LT, Rezende IMd, Fradico JRB, Pereira LS, Ramalho DB, et al.** Evaluation of humoral immune response after yellow fever infection: an observational study on patients from the 2017-2018 sylvatic outbreak in Brazil. Microbiol Spectr. 2024;12(5): e0370323. *https://doi.org/10.1128/spectrum.03703-23.*
10. **Mensah EA, Gyasi SO, Nsubuga F, Alali WQ.** A proposed One Health approach to control yellow fever outbreaks in Uganda. One Health Outlook. 2024;6(1):9. *https://doi.org/10.1186/s42522-024-00103-x.*

Invest Clin 67(2): 168 - 177, 2026 https://doi.org/10.54817/IC.v67n2a01

Expressions of Lipocalin-2 in nasal tissues and secretions of patients with chronic rhinosinusitis with nasal polyps and correlations with inflammatory factors.

Yang Li, Youxiong Yang, Jun Xu and Yun Zhu

Department of Otorhinolaryngology Head and Neck Surgery, Ningbo Hospital of Integrated Traditional Chinese and Western Medicine, Ningbo, Zhejiang Province, China.

Keywords: Inflammation Mediators; Lipocalin-2; Nasal polyps; Rhinosinusitis.

Abstract. Chronic rhinosinusitis with nasal polyps (CRSwNP) is a common inflammatory disease of the upper airway. Lipocalin-2, an inflammation-related glycoprotein involved in innate immune regulation, has been linked to several chronic inflammatory disorders, but its role in CRSwNP remains unclear. This study aimed to examine the expression of Lipocalin-2 in nasal tissues and secretions of CRSwNP patients and its relationship with inflammatory factors. Seventy patients diagnosed with CRSwNP between January 2023 and January 2025 were enrolled in the case group, while 60 patients with simple nasal septal deviation served as controls. NP tissues and nasal secretions were collected from CRSwNP patients, whereas inferior turbinate mucosal tissues and nasal secretions were obtained from controls. Levels of Lipocalin-2, interleukin-5 (IL-5), IL-6, and tumor necrosis factor-alpha (TNF-α) were measured and analyzed. Compared with controls, CRSwNP patients showed significantly higher levels of Lipocalin-2 and inflammatory cytokines in nasal secretions ($p<0.05$). Stratification based on Visual Analog Scale (VAS) scores and computed tomography Lund-Mackay (CT L-M) scores indicated that these markers were notably higher in the moderate-to-severe group than in the mild disease group ($p< 0.05$). Lipocalin-2 was positively correlated with IL-5, IL-6, TNF-α, as well as VAS, Lund-Kennedy endoscopy, and CT L-M scores (all $p<0.05$). In summary, Lipocalin-2 is highly expressed in nasal polyp tissues and secretions of CRSwNP patients and closely associated with inflammatory cytokine levels and clinical severity, implying its potential as a biomarker for disease activity in CRSwNP.

Corresponding author: Yang Li. Department of Otorhinolaryngology Head and Neck Surgery, Ningbo Hospital of Integrated Traditional Chinese and Western Medicine, Ningbo 315100, Zhejiang Province, China. Email: liyangny2h@hosp-edu.cn

Expresión de Lipocalina-2 en los tejidos nasales y secreciones de pacientes con rinosinusitis crónica con pólipos nasales y su correlación con factores inflamatorios.

Invest Clin 2026; 67 (2): 168 – 177

Palabras clave: Mediadores de Inflamación; Lipocalina 2; Pólipos Nasales**;** Rinosinusitis.

Resumen. La rinosinusitis crónica con pólipos nasales (CRSwNP) es una enfermedad inflamatoria frecuente de las vías respiratorias superiores. La lipocalina-2, una glicoproteína asociada a la inflamación e implicada en la regulación de la inmunidad innata, se ha relacionado con diversas enfermedades inflamatorias crónicas; sin embargo, su papel en la CRSwNP aún no ha sido completamente aclarado. El objetivo de este estudio fue investigar la expresión de la lipocalina-2 en los tejidos y en las secreciones nasales de pacientes con CRSwNP, así como su asociación con factores inflamatorios. Setenta pacientes diagnosticados con CRSwNP entre enero de 2023 y enero de 2025 fueron incluidos en el grupo de casos, mientras que 60 pacientes con desviación simple del tabique nasal sirvieron como grupo control. Se recogieron tejidos de pólipos nasales y secreciones nasales de los pacientes con CRSwNP, mientras que en los controles se obtuvieron tejidos de la mucosa del cornete inferior y secreciones nasales. Se midieron y analizaron los niveles de lipocalina-2, interleucina-5 (IL-5), interleucina-6 (IL-6) y del factor de necrosis tumoral alfa (TNF-α). En comparación con los controles, los pacientes con CRSwNP presentaron niveles significativamente elevados de lipocalina-2 y citocinas inflamatorias en las secreciones nasales ($p<0,05$). La estratificación basada en la escala visual analógica (VAS) y en las puntuaciones de la tomografía computarizada Lund-Mackay (CT L-M) mostró que estos marcadores eran notablemente más altos en el grupo con enfermedad moderada a grave que en el grupo con enfermedad leve ($p<0,05$). La lipocalina-2 se correlacionó positivamente con IL-5, IL-6 y TNF-α, así como con las puntuaciones de VAS, Lund-Kennedy endoscópica y CT L-M (todas con $p<0,05$). En conclusión, la lipocalina-2 se expresa de forma elevada en los tejidos de los pólipos nasales y en las secreciones nasales de pacientes con CRSwNP, y se asocia estrechamente con los niveles de citocinas inflamatorias y la gravedad clínica, lo que sugiere su posible utilidad como biomarcador de la actividad de la enfermedad en la CRSwNP.

Received: 30-07-2025 Accepted: 20-02-2026

INTRODUCTION

Chronic rhinosinusitis with nasal polyps (CRSwNP) is a common nasal disease characterized by ongoing inflammation and polypoid hyperplasia in the nasal cavity or sinus mucosa, often accompanied by bone damage and mucus retention [1]. The incidence of CRS in China is approximately 8%, with CRSwNP patients making up about one-third of the total cases [2]. CRSwNP has a complex cause involving infection, environmental factors, allergies, and several other elements, with clinical signs like purulent nasal dis-

charge, nasal blockage, and reduced sense of smell, which seriously impact patients' quality of life [3]. In clinical treatment, managing CRSwNP mainly involves medication and surgery, but the disease is often persistent and prone to recurrence due to factors such as low immunity, recurrent infections, and the limited precision of current therapies [4]. The rate of recurrence after surgical removal can be as high as 40-60% [5]. Therefore, it is particularly important to explore new diagnostic and therapeutic targets for CRSwNP to improve patient outcomes.

As a secretory glycoprotein isolated from neutrophils in the early stage, Lipocalin-2 has the typical β-barrel structure of the lipocalin family and participates in many physiological processes, including iron metabolism, cytokine secretion, and extracellular trap regulation through binding to various ligands and receptors. It is also clear that Lipocalin-2 plays a crucial role in tumor cell proliferation and apoptosis, as well as in chronic inflammatory responses [6]. In inflammatory diseases such as asthma and atopic dermatitis, the widespread expression of Lipocalin-2 is positively associated with eosinophil counts and inflammatory factor levels, indicating its strong potential as a target for disease risk [7]. However, systematic clinical studies on the expression pattern of Lipocalin-2 in CRSwNP nasal tissues and secretions, and the mechanisms through which it correlates with inflammatory factors, including interleukin-5 (IL-5) and IL-6, have not yet been conducted.

Given this, an in-depth analysis was conducted on the relationship between Lipocalin-2 expression levels and the characteristics of nasal tissues and secretions from CRSwNP patients, and its correlations with inflammatory factors were explored in the present study.

PATIENTS AND METHODS

Subjects

Seventy patients diagnosed with CRSwNP and visiting our hospital from January 2023 to January 2025 were included in the case group. Additionally, a control group (n=60) consisting of patients with simple nasal septal deviation was established. Demographic and clinical characteristics, such as sex, age, body mass index, and comorbid allergic rhinitis, are summarized in Table 1. There were no statistically significant differences in baseline characteristics between the two groups ($p>0.05$).

Inclusion criteria were as follows: (1) patients in the case group diagnosed with CRSwNP through examinations showing clinical signs, rhinoscopy, and computed tomography (CT), and treated with functional endoscopic sinus surgery; (2) individuals in the control group meeting the diagnostic criteria for nasal septum deviation as specified in the Volume of Otolaryngology Head and Neck Surgery Clinical Practice Guidelines[8], without NP or sinusitis based on clinical examinations; and (3) patients aged 18-65 years. The following exclusion criteria were

Table 1. General data of patients.

Group	n	Gender (male/female)	Age (year)	Body mass index (kg/m^2)	Comorbid allergic rhinitis (n)
Case	70	40/30	42.39±10.24	22.97±2.01	28 (40.00%)
Control	60	36/24	41.92±10.46	22.67±1.97	40 (66.67%)
χ^2/t		0.109	0.258	0.856	0.617
p		0.742	0.797	0.394	0.432

Data are presented as mean ± standard deviation (SD) or number (percentage). Comparisons between groups were performed using the independent-samples t-test for continuous variables and the chi-square (χ^2) test for categorical variables. A p value < 0.05 was considered statistically significant.

applied: (1) patients who had been treated with a large amount of antibiotics, immunosuppressants, or antihistamines in the past month; (2) those with severe cardiac or pulmonary diseases or coagulation disorders; (3) individuals with strict surgical contraindications; (4) those complicated by fungal sinusitis, asthma, or nasal cavity neoplasm; and (5) individuals with serious psychiatric or psychological disorders or who cannot communicate normally. This study was reviewed and approved by the ethics committee of Ningbo Yinzhou No. 2 Hospital, and all patients in both groups signed the informed consent form.

Sample collection and treatment

During surgery, nasal polyps (NP) tissues and nasal secretions were collected from the case group, while inferior turbinate mucosal tissues and nasal secretions were obtained from the control group. NP tissues: The harvested samples were immediately rinsed with 4°C normal saline to remove blood clots and surface impurities. Then, the samples were cut into two tissue blocks of similar size and volume using a sterile scalpel. One tissue block was immersed in 10% (v/v) formalin solution for 12-24 hours for fixation, then embedded in wax. The other was placed in a sterile cryotube for 1-3 hours and then frozen in liquid nitrogen for later use. Nasal secretions: An aseptic cotton swab or cotton pad was gently rotated deep into the nasal cavity and NP for 15 minutes to obtain at least 2 mL of secretions. These were processed in an H1850 centrifuge (Hunan Xiangyi Laboratory Instrument Development Co., Ltd.) at 3,000 rpm for 10 minutes. The supernatant was aspirated and stored in a -80°C freezer.

Detection of Lipocalin-2 and inflammatory factors

Lipocalin-2 expression in tissues: The sections, dipped and embedded in wax, were sequentially hydrated in ethanol and xylene of varying concentrations. Following deparaffinization, a high-temperature, high-pressure retrieval method was used to expose cell and tissue antigens, and a hydrogen peroxide blocking solution was added in drops to inhibit peroxidase activity. Next, goat serum was added dropwise, followed by a 10-minute incubation at room temperature; the supernatant was discarded, and a Lipocalin-2-specific primary antibody was added for overnight incubation at 4°C. The next day, streptavidin-biotin-peroxidase complex solution was added dropwise and incubated for 15 minutes at room temperature, followed by color development with DAB solution, observation under an optical microscope (400×), rinsing, and counterstaining with hematoxylin. Afterward, the sections were placed in an alkaline solution until they turned blue, dehydrated in a graded alcohol series, cleared in xylene, and mounted with neutral resin added dropwise.

The expression levels of Lipocalin-2 in nasal tissues, as well as Lipocalin-2 and inflammatory factors [interleukin-5 (IL-5), IL-6, and tumor necrosis factor-α (TNF-α)] in nasal secretions, were quantified using an ELISA kit (Shanghai Fengshou Biotechnology Co., Ltd.) strictly following the manufacturer's instructions. Specifically, nasal tissue samples were homogenized and processed for ELISA-based measurement of Lipocalin-2, while nasal secretion samples were centrifuged at 300× g at 4°C for 10 minutes; the supernatant was then collected and stored at -80°C in aliquots for testing. Before testing, the kit was brought to room temperature for 30 minutes, and the washing solution (diluted using distilled water at 1:20) and sample diluent [phosphate-buffered saline with Tween-20 (PBST) containing 1% bovine serum albumin (BSA)] were prepared. Next, the standard substance was serially diluted (e.g., Lipocalin-2 standard range: 156-10,000 pg/mL). Then, 100 μL of each sample and standard (nasal secretion supernatants pre-diluted with sample diluent at 1:2-1:10 as needed) were added to a microtiter plate pre-coated with specific an-

tibodies (polyclonal antibody for Lipocalin-2 measurement), followed by incubation at 37°C for 90 minutes and 3 washes with PBST after discarding the liquid (allowing the plate to stand for 30 seconds after each filling, then pat dry). Subsequently, each well was blocked with 200 μL of blocking solution (5% skim milk or 1% BSA/PBS) at 37°C for 2 hours and washed 3 times. Afterward, 100 μL of biotin-labeled detecting antibodies (diluted as specified in the instructions) were added, incubated at 37°C for 60 minutes, and washed 5 times (samples with high background could be washed up to 7 times). Then, 50 μL of TMB chromogenic substrate (A/B solution, 50 μL each) was added for room temperature development, protected from light, for 15 minutes or until positive wells turned light blue. Next, 50 μL of 2 M H_2SO_4 stop buffer was added to each well, and the absorbance (optical density, OD) was immediately measured at 450 nm, with a reference wavelength of 630 nm, using a microplate reader. Finally, target factor concentrations were calculated using the standard curve (four-parameter logistic regression fitting, $R^2 > 0.99$), with a CV value of less than 15% among replicate wells.

Assessment of disease severity

A visual analog scale (VAS) was used for the quantitative evaluation of four clinical symptoms in patients, namely nasal obstruction [9], runny nose, hyposmia, and dizziness and headache. Each item was scored on a 0-2 scale, with a total of 10 points; higher scores indicated more severe symptoms. Additionally, the Lund-Kennedy nasal endoscopy (L-K) score was used to quantify dimensions such as NP area [10], secretions, mucosal edema, and scars, with each item scored 0-2 points and a total score of 0-12 points. The higher the scores, the greater the NP load and the higher the disease activity. Furthermore, the Lund-MacKay sinus computed tomography (L-M) score was applied for standardized scoring based on patients' computed tomography (CT) imaging results [11], where the inflammation in the maxillary sinus, ethmoidal sinus, frontal sinus, and sphenoidal sinus on both sides and the degree of ostiomeatal complex obstruction in patients were mainly observed. Each item was scored 0-2 points, and the total score was 0-24 points, with higher scores representing a wider range of inflammation and a higher degree of the disease.

Statistical analysis

SPSS 24.0 software was adopted for statistical analysis. Measurement data in line with normal distribution were expressed by ($\bar{x} \pm s$) and compared between groups *via* the independent-samples *t*-test. Count data were represented as [n (%)] and subjected to the χ^2 test for intergroup comparison. The correlations of the expression levels of Lipocalin-2, IL-5, IL-6, and TNF-α with the VAS, L-K, and CT L-M scores were identified through Pearson's correlation analysis. $p<0.05$ denoted a statistically significant difference.

RESULTS

Lipocalin-2 expression levels in nasal tissues

The expression level of Lipocalin-2 in nasal tissues was significantly higher in the case group than in the control group ($p<0.05$) (Table 2).

Table 2. Lipocalin-2 expression levels in nasal tissues.

Group	n	Lipocalin-2 (ng/mL)
Case	70	50.36±16.24
Control	60	26.19±9.21
t		10.204
p		<0.001

Data are presented as mean ± standard deviation (SD). Comparisons between groups were performed using the independent-samples t-test.

Levels of Lipocalin-2 and inflammatory factors in nasal secretions from the two groups

The case group showed higher levels of Lipocalin-2, IL-5, IL-6, and TNF-α in nasal

secretions compared to the control group, and these differences were statistically significant ($p<0.05$) (Table 3).

Correlation between Lipocalin-2 and inflammatory factors in nasal secretions obtained from the case group

Pearson's correlation analysis revealed that Lipocalin-2 had positive correlations with IL-5, IL-6, and TNF-α in nasal secretions from the case group ($p<0.05$) (Table 4).

Levels of Lipocalin-2 and inflammatory factors in the case group with different disease severities

Based on the stratification using the VAS score (≤5 points for mild and >5 points for moderate-to-severe) and CT L-M score (≤12 points for mild-to-moderate and >12 points for severe), all indicators were significantly higher in the moderate-to-severe group compared to the mild group ($p< 0.05$) (Table 5).

Correlations of Lipocalin-2 and inflammatory factors with disease severity in the case group

In the case group, the VAS, L-K, and CT L-M scores were positively correlated with the expression levels of Lipocalin-2 and inflammatory factors in patients ($p<0.05$) (Table 6).

DISCUSSION

Classified as an inflammatory disease of the upper respiratory tract secondary to CRS subtypes, CRSwNP is partially caused by abnormal anatomy, genetics, allergic edema, and other factors, with characteristic changes such as inflammatory cell infiltration, stromal edema, and NP growth. Clinically, it manifests as recurrent dizziness and headache, sinus ostium blockage, purulent nasal discharge, and anosmia [12,13]. Although immune responses dominated by T helper type 2 (Th2) inflammation are considered the main drivers of pathological imbalance in CRSwNP, the biological targets that regulate inflammatory factor expression levels remain undefined [14]. Lipocalin-2 is a pro-inflammatory, iron-shuttle molecule associated with neutrophil gelatinase. It participates in biological processes including cell differentiation, apoptosis, defense against bacterial infections, and fatty acid transportation. It also plays a crucial role in iron metabolism, oxidative stress, and inflammation regulation in the human body [15]. A recent study found that Lipocalin-2 can predict and reflect the degree of renal function im-

Table 4. Correlation between Lipocalin-2 and inflammatory factors in nasal secretions from the case group.

Inflammatory factor	Lipocalin-2	
	r	p
IL-5	0.827	<0.001
IL-6	0.465	<0.001
TNF-α	0.597	<0.001

Interleukin-5 (IL-5), interleukin-6 (IL-6), tumor necrosis factor-alpha (TNF-α). *r* indicates Pearson's correlation coefficient.

Table 3. Levels of Lipocalin-2 and inflammatory factors in nasal secretions.

Group	n	Lipocalin-2 (ng/mL)	IL-5 (pg/mL)	IL-6 (pg/mL)	TNF-α (pg/mL)
Case	70	62.15±14.26	46.92±4.52	58.36±14.21	113.68±9.14
Control	60	24.69±8.19	25.64±3.24	43.69±10.24	95.49±8.36
t		17.961	30.380	6.651	11.764
p		<0.001	<0.001	<0.001	<0.001

Data are presented as mean ± standard deviation (SD). Comparisons between groups were performed using the independent-samples t-test. Interleukin-5 (IL-5), interleukin-6 (IL-6), tumor necrosis factor-alpha (TNF-α).

Table 5. Levels of Lipocalin-2 and inflammatory factors in the case group with different disease severities.

Stratification indicator	n	Lipocalin-2 (ng/mL)	IL-5 (pg/mL)	IL-6 (pg/mL)	TNF-α (pg/mL)
VAS score					
≤5 points (mild)	25	48.21±12.35	40.23±3.89	52.14±11.56	105.32±8.23
>5 points (moderate-to-severe)	45	66.89±15.42	51.26±4.71	62.89±13.24	118.97±9.56
t		5.196	9.964	3.401	6.005
p		<0.001	<0.001	0.001	<0.001
CT L-M score					
≤12 points (mild-to-moderate)	32	52.36±13.18	43.56±4.12	55.21±12.34	108.65±8.78
>12 points (severe)	38	68.92±14.89	50.12±4.98	61.54±11.87	119.23±9.01
t		4.639	5.602	2.108	4.750
p		<0.001	<0.001	0.039	<0.001

Data are presented as mean ± standard deviation (SD). Comparisons between subgroups were performed using the independent-samples t-test. Interleukin-5 (IL-5), interleukin-6 (IL-6), tumor necrosis factor-alpha (TNF-α). Visual analog scale (VAS), Lund-MacKay sinus computed tomography (CT L-M).

Table 6. Correlations of Lipocalin-2 and inflammatory factors with disease severity in the case group.

Group	Lipocalin-2		IL-5		IL-6		TNF-α	
	r	*p*	*r*	*p*	*r*	*p*	*r*	*p*
VAS score	0.756	<0.001	0.613	<0.001	0.619	<0.001	0.078	<0.001
L-K score	0.647	<0.001	0.519	0.003	0.492	<0.001	0.069	0.004
CT L-M score	0.597	0.002	0.616	<0.001	0.473	<0.001	0.064	<0.001

r indicates Pearson's correlation coefficient. Correlation analyses were performed using Pearson correlation analysis. Interleukin-5 (IL-5), interleukin-6 (IL-6), tumor necrosis factor-alpha (TNF-α). Visual analog scale (VAS), Lund-Kennedy nasal endoscopy (L-K), Lund-MacKay sinus computed tomography (CT L-M).

pairment, offering clinical advantages like early monitoring, easy assessment, and high specificity [16]. As previously researched, Lipocalin-2 is a key player in the pathology of diseases such as alcoholic fatty liver and malignant tumors. It promotes disease progression by regulating inflammatory expression, mediating iron homeostasis, and participating in signaling pathways, making it a potential target for diagnosis and prevention [17]. However, studies on Lipocalin-2 and inflammatory factors in CRSwNP are still limited.

In this study, the case group exhibited significant increases in the expression level of Lipocalin-2 in nasal tissues as well as the levels of Lipocalin-2, IL-5, IL-6, and TNF-α in nasal secretions, in contrast to the control group, suggesting that Lipocalin-2 and inflammatory factors are highly expressed in the pathogenesis of CRSwNP, exerting a synergistic effect on NP formation. As a multifunctional pro-inflammatory protein, Lipocalin-2 induces the expression of chemokines, including CXCL8 and CCL2, and recruits neutrophils and eosinophils to NP tissues in combination with Th2 inflammatory factors such as IL-5, thereby exacerbating inflammatory infiltration. Moreover, TNF-α, IL-6, and other inflammatory factors can activate T lymphocytes to mediate neutrophil secretion of Lipocalin-2, form a synergistic cycle of inflammatory factors

and Lipocalin-2, and enhance the release of inflammatory signals [18]. The iron-chelating function of Lipocalin-2 can activate the ferroptosis pathway, disrupt the metabolic stability of the nasal mucosa, and elevate intracellular ferrous ion concentration. Besides, inflammatory factors released under oxidative stress activate the NF-κB signaling pathway, which up-regulates the expression of inflammatory factors and Lipocalin-2 again [19]. In addition, owing to its specific structure, Lipocalin-2 is capable of binding to and transporting various lipophilic small molecules including iron and fatty acids, affecting the metabolism of immune cells and polarization of macrophages. Finally, it collaborates with Th2 inflammatory factors to induce epithelial-mesenchymal transition, promote excessive deposition of the fibrous extracellular matrix, and facilitate hyperplasia and invasion of NP tissues. As indicated in the literature, in the diseased skin tissues of patients with psoriasis, keratinocytes exhibit high Lipocalin-2 expression within an activated inflammatory microenvironment, and Lipocalin-2 has synergistic effects with the pro-inflammatory factors TNF-α and IL-8. Once again, it demonstrates the regulatory roles of Lipocalin-2 and inflammatory factors in the disease validation cascade [20]. Through deep investigation, it was uncovered that Lipocalin-2 had positive relations to IL-5, IL-6, and TNF-α, together with significantly positive correlations with the VAS, L-K, and CT L-M scores in CRSwNP patients, suggesting that Lipocalin-2 forms a pathogenic network with inflammatory factors to jointly participate in and reflect the progression of CRSwNP. Combined with correlation analysis results, as a crucial cytokine regulating eosinophil maturation, activation, and tissue migration, IL-5 can work with Lipocalin-2 to recruit eosinophils, transfer them to NP tissues, and release toxic proteins to aggregate local mucosal edema and inflammation, resulting in increased NP size and thickened sinus mucosa, and triggering symptoms such as nasal obstruction and headache. TNF-α and IL-6 form a two-way feedback loop with Lipocalin-2 that continuously activates inflammation-related signaling pathways and accelerates the release of inflammatory mediators such as reactive oxygen species and proteases, thereby up-regulating ICAM-1 and other adhesion molecules, increasing vascular permeability of the nasal mucosa, and amplifying inflammatory responses. Meanwhile, Lipocalin-2 may exacerbate pain sensitization by activating trigeminal nerve endings in the nasal mucosa and promoting the release of neuroinflammatory substances, which directly affect the severity of the patient's subjective symptoms as measured by the VAS score. Existing studies have corroborated a positive correlation between Lipocalin-2 expression levels and the severity of ankylosing spondylitis [21]. In a study of hemorrhagic fever with renal syndrome, Lipocalin-2 is highly expressed in the serum of patients [22]. As demonstrated by the above literature and the present study, Lipocalin-2 is likely a broad-spectrum regulator of chronic inflammatory diseases, and its synergistic effects with inflammatory factors may serve as a potential indicator of clinical phenotypes and disease severity.

In conclusion, Lipocalin-2 exhibits high expression in NP tissues and secretions from CRSwNP patients, and it is not only significantly correlated with levels of inflammatory factors IL-5, IL-6, and TNF-α, but also positively associated with disease severity. This suggests that Lipocalin-2 could become a novel therapeutic target for monitoring disease progression, exploring the pathogenesis, and developing new treatments for CRSwNP. However, this study only identified a correlation between Lipocalin-2 and inflammatory factors, and there is a lack of scientific evidence regarding its regulatory mechanisms and signaling pathways, which can be examined in future research using cell models or animal studies.

Acknowledgements

None.

Funding

None.

ORCID ID of the authors

- Yang Li (YL): 0009-0000-9633-8038
- Youxiong Yang (YY): 0009-0007-3967-2559
- Jun Xu (JX): 0009-0003-8658-8537
- Yun Zhu (YZ): 0009-0008-7955-5530

Author's contributions

YL designed this study and significantly revised the paper; YY, JX, and YZ performed this study, analyzed the data, and drafted the paper. All authors have approved the submission and publication of this paper.

Conflict of interest

The authors declare no conflict of interest.

REFERENCES

1. **Chan Y, Thamboo AV, Han JK, Desrosiers M.** Remission: does it already exist in chronic rhinosinusitis with nasal polyposis? J Otolaryngol Head Neck Surg. 2023; 52(1): 50. *https://doi.org/10.1186/s40463-023-00657-2*
2. **Julka BS, Patil SB, Chandrakiran C.** Incidence and Prevalence of Fungal Sinusitis in Cases of Chronic Rhinosinusitis. Indian J Otolaryngol Head Neck Surg. 2023; 75(Suppl 1): 1041-1046. *https://doi.org/10.1007/s12070-023-03572-0*
3. **Viksne RJ, Sumeraga G, Pilmane M.** Antimicrobial and Defense Proteins in Chronic Rhinosinusitis with Nasal Polyps. Medicina. 2023; 59(7): 1259. *https://doi.org/10.3390/medicina59071259*
4. **Liu X, Charn TC, Wang DY.** Mepolizumab in chronic rhinosinusitis with nasal polyposis. Immunotherapy. 2023; 15(14): 1105-1116. *https://doi.org/10.2217/imt-2023-0026*
5. **Norwood TG, Grayson JW, Woodworth BA.** Advances in Sinus Surgery for Nasal Polyps. Am J Rhinol Allergy. 2023; 37(2): 162-167. *https://doi.org/10.1177/19458924221147783*
6. **Schröder SK, Gasterich N, Weiskirchen S, Weiskirchen R.** Lipocalin 2 receptors: facts, fictions, and myths. Front Immunol. 2023; 14: 1229885. *https://doi.org/10.3389/fimmu.2023.1229885*
7. **Pelaia G, Aiello V, Tinello C, Chiarella E, Piazzetta GL, Lobello N, et al.** Eosinophil-targeted treatment strategies for long-term outcomes in severe eosinophilic asthma. Expert Rev Respir Med. 2025; 19(8):827-842. *https://doi.org/10.1080/17476348.2025.2506551*
8. **Tysome JR.** Clinical Otolaryngology: Changing of the guard. Clin Otolaryngol. 2020; 45(1): 1. *https://doi.org/10.1111/coa.13482*
9. **Johnson EW.** Visual analog scale (VAS). Am J Phys Med Rehabil. 2001; 80(10): 717. *https://doi.org/10.1097/00002060-200110000-00001*
10. **Zhang Y, Jiang H, Long Y, Li J.** The Evaluation Value of the Modified Lund-Kennedy Nasal Endoscopy Score on the Efficacy of Sublingual Immunotherapy for Allergic Rhinitis. Am J Rhinol Allergy. 2024; 38(6): 366-372. *https://doi.org/10.1177/19458924241269786*
11. **Do BA, Lands LC, Mascarella MA, Fanous A, Saint-Martin C, Manoukian JJ, et al.** Lund-Mackay and modified Lund-Mackay score for sinus surgery in children with cystic fibrosis. Int J Pediatr Otorhinolaryngol. 2015; 79(8): 1341-1345. *https://doi.org/10.1016/j.ijporl.2015.06.007*
12. **Bandi S, Stephen E, Bansal K, Mahdavinia M.** Understanding the CRSwNP Patient as Whole. Am J Rhinol Aller-

gy. 2023; 37(2): 140-146. *https://doi.org/10.1177/19458924231152671*

13. **Gong MJ, Wang YS, Lou M, Ma RP, Hu ZZ, Zheng GX, et al.** A new marker for predicting postoperative recurrence of CRSwNP. Acta Otolaryngol. 2023; 143(2): 170-175. *https://doi.org/10.1080/00016489.2023.2168054*
14. **Shah SA, Kobayashi M.** Pathogenesis of chronic rhinosinusitis with nasal polyp and a prominent T2 endotype. Heliyon. 2023; 9(9): e19249. *https://doi.org/10.1016/j.heliyon.2023.e19249*
15. **Galaris A, Fanidis D, Tsitoura E, Kanellopoulou P, Barbayianni I, Ntatsoulis K, et al.** Increased lipocalin-2 expression in pulmonary inflammation and fibrosis. Front Med. 2023; 10: 1195501. *https://doi.org/10.3389/fmed.2023.1195501*
16. **Marques E, Alves Teixeira M, Nguyen C, Terzi F, Gallazzini M.** Lipocalin-2 induces mitochondrial dysfunction in renal tubular cells via mTOR pathway activation. Cell Rep. 2023; 42(9): 113032. *https://doi.org/10.1016/j.celrep.2023.113032*
17. **Živalj M, Van Ginderachter JA, Stijlemans B.** Lipocalin-2: A Nurturer of Tumor Progression and a Novel Candidate for Targeted Cancer Therapy. Cancers. 2023; 15(21): 5159. *https://doi.org/10.3390/cancers15215159*
18. **Sonmez Kaplan S, Sazak Ovecoglu H, Genc D, Akkoc T.** TNF-α, IL-1B and IL-6 affect the differentiation ability of dental pulp stem cells. BMC Oral Health. 2023; 23(1): 555. *https://doi.org/10.1186/s12903-023-03288-1*
19. **Simpson CA, Santoro AM, Carpenter TO, Deng Y, Parziale S, Insogna KL.** Circulating Levels of Leptin and Lipocalin-2 in Patients With X-Linked Hypophosphatemia. J Endocr Soc. 2023; 7(11): bvad116. *https://doi.org/10.1210/jendso/bvad116*
20. **Stisen ZR, Nielsen SM, Ditlev SB, Skougaard M, Egeberg A, Mogensen M, et al.** Treatment-related changes in serum neutrophil gelatinase-associated lipocalin (NGAL) in psoriatic arthritis: results from the PIPA cohort study. Scand J Rheumatol. 2024; 53(1): 21-28. *https://doi.org/10.1080/03009742.2023.2216046*
21. **Vogan K.** Immunotherapy for ankylosing spondylitis. Nat Genet. 2023; 55(12): 2020. *https://doi.org/10.1038/s41588-023-01612-7*
22. **Cvetko Krajinović L, Bodulić K, Laškaj R, Žibrat B, Svoboda Karić P, Kurolt IC, et al.** Hemorrhagic Fever with Renal Syndrome Patients Exhibit Increased Levels of Lipocalin-2, Endothelin-1 and NT-proBNP. Life. 2023; 13(11): 2189. *https://doi.org/10.3390/life13112189*.

Invest Clin 67(2): 178 - 188, 2026 https://doi.org/10.54817/IC.v67n2a02

The effect of vitamin D_3 combined with traction on the treatment of lumbar disc herniation.

Yina Yin and Jiaojiao Huang

Department of Rehabilitation, Xinhua Hospital Affiliated to Shanghai Jiaotong University School of Medicine, Changxing Branch, Shanghai, China.

Keywords: Cholecalciferol; Intervertebral Disc Herniation; Traction; Inflammation; Pain; Rehabilitation.

Abstract. This study examined the clinical effectiveness of vitamin D_3 combined with traction therapy in patients with lumbar disc herniation. It included 112 patients who received conservative rehabilitation at our hospital from January 2021 to December 2023. Participants were randomly assigned to two groups: one received supine mechanical traction, and the other received the same traction plus oral vitamin D_3 for 4 weeks. The study compared clinical outcomes and quality of life between the groups. Results showed that both groups experienced improvements in pain and lumbar spine function. However, the combined treatment group showed significantly better outcomes than the traction-only group. Inflammation and pain markers decreased significantly, and 25(OH)D_3 levels increased notably in both groups, with greater improvements in the combined treatment group. Additionally, negative mood and quality of life improved more in the combined group. There was no significant difference in the measured indicators between the one-month follow-up and the one-month treatment. In conclusion, vitamin D_3 combined with traction therapy can effectively enhance short-term clinical outcomes and quality of life for patients with lumbar disc herniation.

Corresponding author: Jiaojiao Huang, Department of Rehabilitation, Xinhua Hospital Affiliated to Shanghai Jiaotong University School of Medicine, Changxing Branch, No. 1008, Fengfu Road, Changxing Town, Chongming District, Shanghai 202150, China. Email: huangjiaojiao22@163.com

Evaluación de la eficacia clínica de la vitamina D_3 combinada con la tracción en pacientes con hernia de disco lumbar.

Invest Clin 2026; 67 (2): 178 – 188

Palabras clave: Vitamina D_3; Hernia de disco intervertebral; Tracción; Inflamación; Dolor; Rehabilitación.

Resumen. Este estudio se centró en evaluar la eficacia clínica de la terapia combinada con vitamina D_3 y tracción en pacientes con hernia de disco lumbar. Se incluyeron 112 pacientes que recibieron tratamiento de rehabilitación conservador en nuestro hospital entre enero de 2021 y diciembre de 2023. Los pacientes fueron asignados aleatoriamente a dos grupos: uno recibió únicamente tratamiento de tracción y el otro, tracción más tratamiento oral con vitamina D_3 durante 4 semanas. Se compararon la eficacia clínica y la calidad de vida entre ambos grupos. Los resultados mostraron que ambos tratamientos mejoraron el nivel de dolor y la función lumbar, aunque la combinación de vitamina D_3 con tracción produjo una mejora significativamente mayor. Los marcadores de inflamación y dolor disminuyeron notablemente, y los niveles de $25(OH)D_3$ aumentaron en ambos grupos, con una mejoría mayor en el grupo combinado. Además, el estado de ánimo y la calidad de vida mejoraron de forma más significativa en el grupo de tratamiento combinado. No se observaron diferencias estadísticamente significativas entre los indicadores de prueba al mes de seguimiento y al de tratamiento. En conclusión, la combinación de vitamina D_3 y terapia de tracción puede mejorar eficazmente los resultados clínicos a corto plazo y la calidad de vida de los pacientes con hernia discal lumbar.

Received: 27-08-2025 Accepted: 22-11-2025

INTRODUCTION

Lumbar degenerative disc disease (LDDD) is a leading cause of musculoskeletal disorders, with lumbar disc herniation (LDH) being its primary manifestation [1]. LDH occurs when disc material (nucleus pulposus or annulus fibrosus) displaces beyond the intervertebral disc space, causing symptoms such as nerve root pain, numbness, decreased sensation, and weakness [2,3]. In severe cases, it can result in paralysis or cardiovascular issues. It is more common in individuals aged 30 to 50, with men being twice as likely as women [4]. Over 50% of people with lumbar disc disease report lower back pain, which significantly impairs quality of life [5]. Conservative treatment remains the first choice for most LDH patients [6]. Pain relief is mainly achieved through medication, physiotherapy, exercise, traction, epidural steroid injections, and acupuncture [7]. Surgery is typically reserved for severe LDH cases that do not respond to conservative approaches. While minimally invasive procedures like microdiscectomy offer good long-term results for select patients, traditional open surgery carries risks such as recurrent herniation and post-operative complications [8].

Traction therapy is a conservative treatment commonly used in clinical practice that can increase the intervertebral space and reduce intervertebral pressure through physical pulling, thereby improving lum-

bar disc-related symptoms such as acidity, numbness, swelling, and pain [9]. However, traction therapy slightly raises the risk of lumbar spine injury [10]. Previous meta-analyses, including Tadano et al. [11], confirm that mechanical traction in the supine position offers short-term pain relief in radiculopathy, although long-term effectiveness varies and depends on the patient.

Vitamin D is a widely used neurosteroid hormone with multiple skeletal and non-skeletal functions. Vitamin D receptors have been identified in bone marrow, and several reports have demonstrated a regulatory role for vitamin D in bone metabolism and osteoporosis [12,13]. Research on the relationship between vitamin D receptors and lumbar disc degeneration and herniation has become a hot topic [14-16]. Mechanistic studies have found that vitamin D has a protective effect against neurotoxicity and can reduce pain by modulating neurons [17], in addition to reducing inflammation and pain in patients by down-regulating the release of pain-producing inflammatory factors from glial cells[18,19]. However, there is less information about the clinical application of vitamin D in LDH.

This study focuses on the short-term clinical effects of supine mechanical traction therapy and oral vitamin D_3 supplementation in patients with LDH.

MATERIALS AND METHODS

Study subjects

One hundred and twelve outpatients with LDH receiving conservative treatment at the Rehabilitation Department of Xinhua Hospital, affiliated with the Shanghai Jiaotong University School of Medicine (Changxing Branch, Shanghai, China), between January 2021 and December 2023, were enrolled. Inclusion criteria: (1) LDH confirmed by magnetic resonance imaging (MRI); (2) radicular pain (VAS ≥4); (3) no treatment in the previous six months. Exclusion criteria: (1) severe spinal pathology; (2) cardiac or hepatic dysfunction; (3) malignancy or autoimmune disease; (4) recent vitamin D use; (5) inability to comply. The study was approved by the Ethics Committee of Xinhua Hospital (Approval No. 2021-001).

Treatment protocol

The control group (CG) received supine mechanical traction using a Lumbar Traction Device (Model: TR-200, China). Pelvis and thorax were fixed, and intermittent traction was applied at 50–80% of body weight (adjusted for tolerance). Sessions lasted 20 minutes per day, 5 days a week, for 4 weeks. Patients rested in a supine position for 30 minutes after traction. The observation group (OG) received the same traction protocol plus oral vitamin D_3 (800 IU/day; Cholecalciferol, 1000 IU capsules, Shanghai Pharma) for 4 weeks.

Observation indicators

1. **Lumbar function/pain:** JOA [20], ODI [20], VAS [20].
2. **Efficacy:** Classified as significant (JOA↑>75%, VAS↓>75%), effective (JOA↑35–75%, VAS↓25–75%), ineffective (JOA↑<35%, VAS↓<25%) [21].
3. **Inflammation/pain:** Serum IL-1β, TNF-α, IL-6, IL-8, 25(OH)D_3, SP, 5-HT, PGE_2 (ELISA kits, R&D Systems).
4. **Complications:** Assessed via clinical evaluation and MRI at follow-up.
5. **Negative emotions:** SAS [21], SDS [21].
6. **Quality of life:** LHFQ [22].

Abbreviations: LDH – Lumbar Disc Herniation, VAS – Visual Analogue Scale, JOA – Japanese Orthopaedic Association Score, ODI – Oswestry Disability Index, IL-1β – Interleukin-1 Beta, TNF-α – Tumor Necrosis Factor-Alpha, IL-6 – Interleukin-6, IL-8 – Interleukin-8, 25(OH)D_3 – 25-Hydroxyvitamin D_3, SP – Substance P, 5-HT – 5-Hydroxytryptamine (Serotonin), PGE_2 – Prostaglandin E_2, SAS – Self-Rating Anxiety Scale, DS – Self-Rating Depression Scale, LHFQ – Lumbar Health Functional Questionnaire.

Statistical analysis

Data were analyzed with IBM SPSS Statistics for Windows, Version 25.0 (IBM Corp., Armonk, NY, USA). Continuous variables were reported as mean ± standard deviation (SD). The paired sample t-test was used for within-group (pre- and post-treatment) comparisons, while the independent sample t-test was employed for between-group comparisons. Categorical data were compared using the Chi-square (χ^2) test or Fisher's exact test when appropriate. Statistical significance was defined as $p<0.05$.

RESULTS

Improvement in lumbar spine function and pain level after treatment

As shown in Fig. 1, the JOA scores for both groups increased, while the ODI and VAS scores decreased after treatment, and the OG scores were significantly better than those of CG ($p<0.05$). The one-month follow-up results after treatment showed no statistically significant differences in lumbar spine function and pain levels compared to the post-treatment period ($p>0.05$).

Combination therapy improves clinical outcomes

As shown in Table 1, OG's treatment efficiency was significantly higher than CG's ($p<0.05$).

Combination therapy improves inflammatory factors and vitamin D levels

As shown in Fig. 2, the levels of IL-1β, TNF-α, IL-6, and IL-8 were lower in both groups after treatment, with a greater decrease in OG than in CG ($p<0.05$). The levels of $25(OH)D_3$ in the patients increased following vitamin D_3 supplementation.

As shown in Fig. 3, SP, 5-HT, and PGE_2 decreased in both groups, and OG decreased more than CG ($p<0.05$).

Assessment of the incidence of complications in both groups

As shown in Table 2, the complication rate of OG had a decreasing trend compared with that of CG, but there was no statistically significant difference between the two ($p>0.05$).

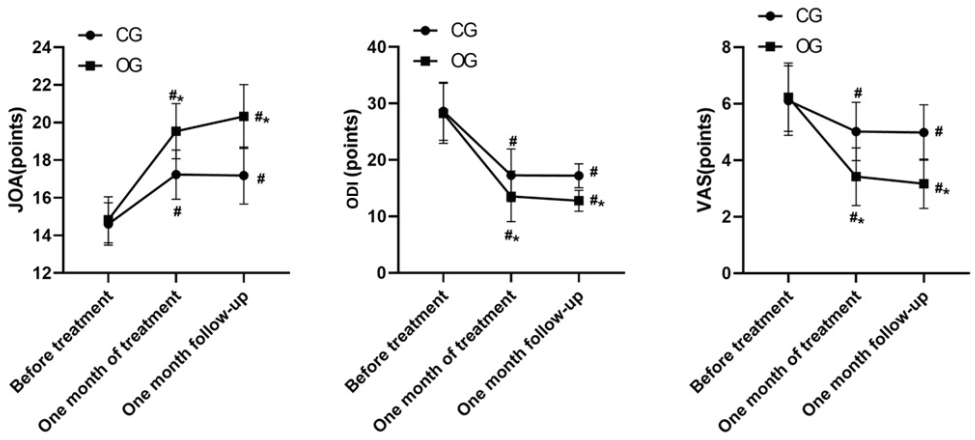

Fig. 1. Comparison of lumbar spine function and pain level. *$p<0.05$ compared with CG, #$p<0.05$ compared with before treatment. JOA: Japanese Orthopaedic Association Score; ODI: Oswestry Disability Index; VAS: Visual Analogue Scale; CG: Control Group; OG: Observational Group. Data are presented as mean ± SD. Independent sample t-test and paired sample t-test were used for between- and within-group comparisons, respectively.

Table 1. Comparison of treatment efficacy (%).

Groups	Obviously effective	Effective	Ineffective	Effective rate
CG (n =56)	30(53.57)	12(21.43)	14(25.00)	75.00
OG (n =56)	35(62.50)	15(26.79)	6(10.71)	89.29
$\chi 2$				3.896
p				0.048

CG: Control Group; OG: Observational Group. Data, expressed as n (%), were compared using the Chi-square (χ^2) test, $p<0.05$ indicates statistical significance.

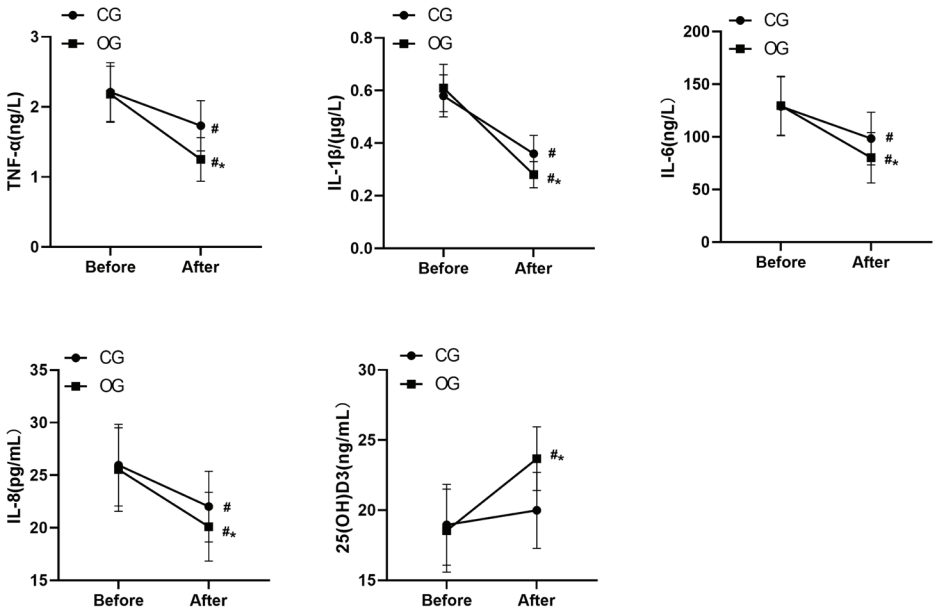

Fig. 2. Comparison of inflammatory factors and vitamin D levels. *$p<0.05$ compared with CG, #$p<0.05$ compared with before treatment. IL-1β: Interleukin-1 Beta; TNF-α: Tumor Necrosis Factor-Alpha; IL-6: Interleukin-6; IL-8: Interleukin-8; $25(OH)D_3$ – 25-Hydroxyvitamin D_3; CG: Control Group; OG: Observational Group. Data are presented as mean ± SD. Independent and paired sample t-tests were used.

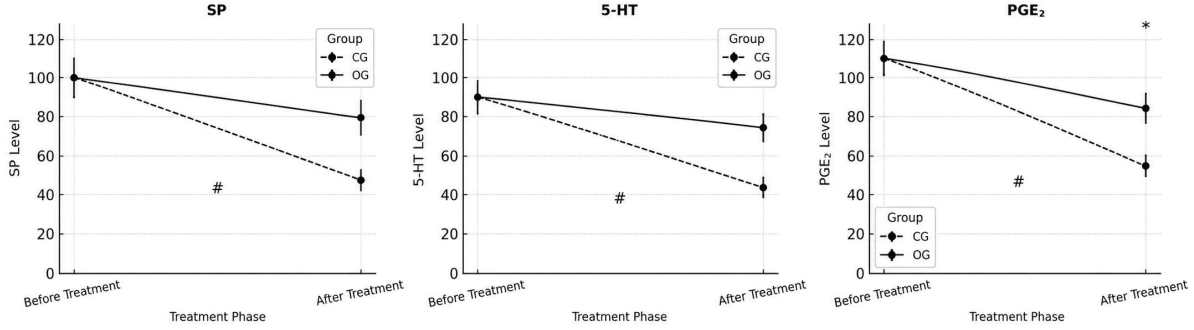

Fig. 3. Comparison of pain-related indicators. *$p<0.05$ compared with CG, #$p<0.05$ compared with before treatment. SP: Substance P; 5-HT: 5-Hydroxytryptamine; PGE_2: Prostaglandin E_2; CG: Control Group; OG: Observational Group. Data expressed as mean ± SD. Statistical comparisons were performed using independent sample t-tests and paired sample t-tests.

Table 2. Comparison of complications.

Groups	Nerve root compression	Intervertebral disc degeneration	Narrowing of the spinal canal	Total incidence rate
CG (n =56)	3 (5.36)	3(5.36)	2(3.57)	8(14.29)
OG (n =56)	1(1.79)	1(1.79)	0(0.00)	2(3.57)
$\chi 2$				-
p				0.094

CG: Control Group; OG: Observational Group. Data are expressed as n (%), compared using the Chi-square (χ^2) test, $p<0.05$ is considered statistically significant.

Combination therapy reduces negative emotions

As displayed in Fig. 4, SDS and SAS scores decreased in both groups after treatment, with OG scores being lower than CG ($p<0.05$). The follow-up results after one month showed no significant difference compared to those immediately after treatment ($p>0.05$).

Combination therapy improves Quality of Life (QOL)

As shown in Fig. 5, LHFQ scores improved after treatment in both groups, with OG scores lower than those in the CG ($p<0.05$).

DISCUSSION

This study assessed the short-term effectiveness of combining oral vitamin D_3 with supine mechanical traction for LDH. The primary finding was that combination therapy significantly enhanced pain relief, functional ability, inflammation reduction, and quality of life compared to traction alone. Specifically, this integrated approach led to a notable decrease in nerve root pain and better functional outcomes versus traditional conservative treatments. Nerve root pain is a common persistent issue that hampers daily activities for people with LDH. Local inflammatory responses are caused by malfunctioning muscles and soft tissues, which lead to herniation that compresses the nerve root. Disc inflammation contributes to disc degeneration or herniation through ongoing inflammation and production of inflammatory factors. Additionally, the nucleus pulposus releases inflammatory agents by activating the autoimmune system, worsening pain.

Traction therapy reduces soreness and pain by increasing the patient's lumbar intervertebral space and relieving the pressure caused by herniated nucleus pulposus. However, its effectiveness on lumbar intervertebral discs when used alone is limited, and prolonged traction can lead to drawbacks like instability of lumbar spinal muscles and ligaments. Vitamin D is a neurosteroid hormone that modulates the immune system, protects the central nervous system, and helps resist cell damage. Studies have shown a link between vitamin D and lumbar disc herniation. Yang et al. [23] found that levels of vitamin D receptor gene expression could serve as a marker for lumbar disc degeneration. Sedighi et al. [24] discovered that subcutaneous vitamin D_3 injections can decrease neural tension and improve sensory deficits related to lumbar discs. This study investigated the combined effects of traction therapy and vitamin D_3; unlike previous research, the vitamin therapy was administered orally, which is a new approach. Feedback on treatment effectiveness was assessed by observing changes in pain mediators and inflammatory factors.

Our results demonstrate that lumbar spine function and overall pain levels improved in both groups, with relief from com-

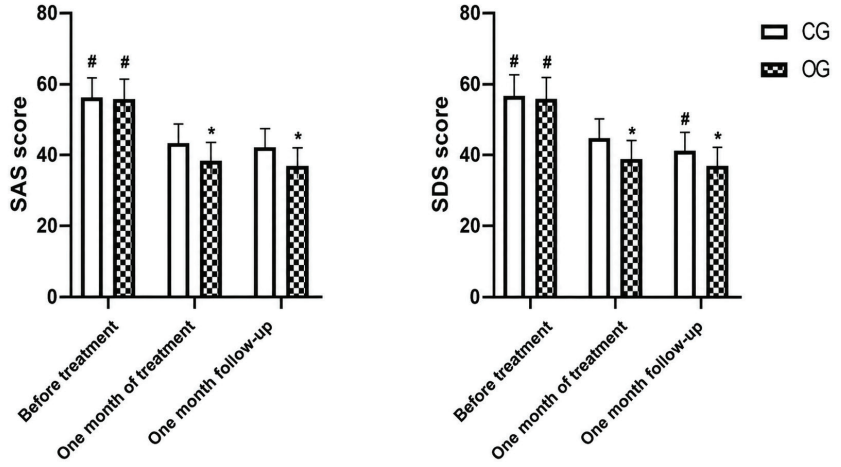

Fig. 4. Comparison of negative emotions. *p<0.05 compared with CG, #p<0.05 compared with one month of treatment. CG: Control Group; OG: Observational Group; SAS: Self-Rating Anxiety Scale; SDS: Self-Rating Depression Scale. Data are presented as mean ± SD. Statistical analysis performed using independent and paired sample t-tests.

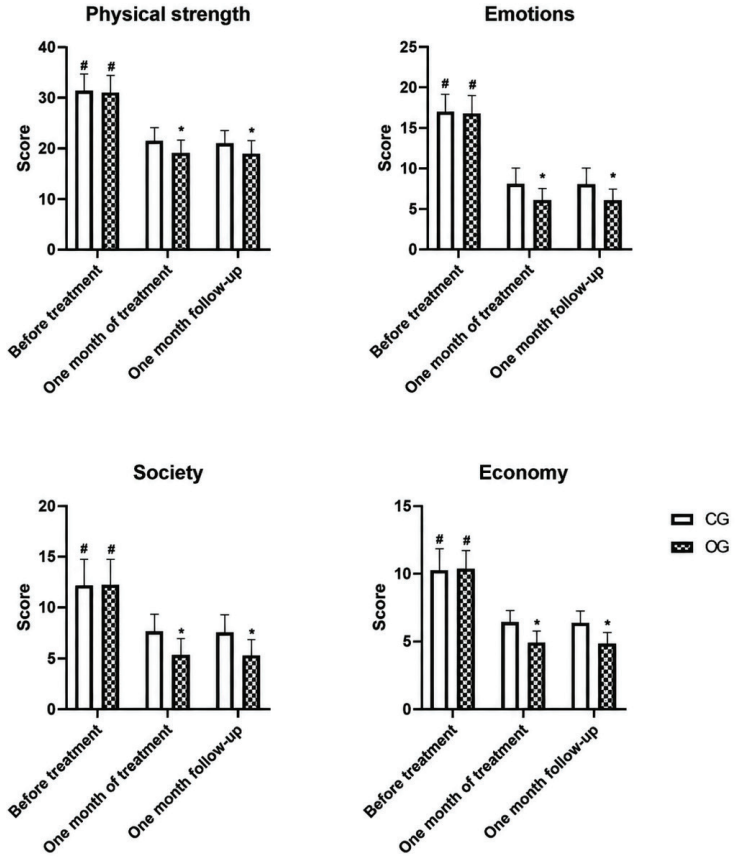

Fig. 5. Comparison of QOL. *p<0.05 compared with CG, #p<0.05 compared with one month of treatment. LHFQ: Lumbar Health Functional Questionnaire; CG: Control Group; OG: Observational Group. Data are presented as mean ± SD. Independent sample t-tests and paired sample t-tests were used for between- and within-group comparisons, respectively.

bination therapy exceeding that of monotherapy. The effectiveness of the treatments was assessed using the JOA and VAS scores, which showed superior results in the combined treatment group. To better understand the role of improved effectiveness, we tested patients for inflammatory and pain-related factors. Evidence suggests that vitamin D receptors, cytokines, apoptotic factors, and pain mediators contribute to the development of intervertebral disc herniation [25-27]. IL and TNF are the primary inflammatory mediators involved in lumbar disc disease. IL-1β is primarily secreted by mononuclear macrophages within the intervertebral disc, and elevated levels promote disc degeneration and pain. In one study, IL-1β was injected into the intervertebral space of a rat model, which caused inflammation and disc damage [28]. IL-8 and IL-6 can stimulate the release of inflammatory mediators, promote the recruitment of inflammatory cells, and accelerate the progression of intervertebral disc disease [29,30]. TNF-α is a potent inflammatory mediator that increases the release of other pro-inflammatory substances, induces apoptosis of chondrocytes, and affects osteoblast growth—key factors in lumbar disc pathology [31].

Furthermore, because pain mediators are key contributors to patient pain, we chose representative mediators—SP, 5-HT, and PGE_2—as our study subjects. Serum levels of SP, 5-HT, and PGE_2 were higher in patients with lumbar disc herniation than in healthy controls. SP is an injurious stimulatory neuropeptide found in nerve fibers with pain signaling capacity and has been linked to lumbar disc herniation pain [32]. 5-HT is a common pain mediator that transmits and modulates pain signals [33]. PGE_2 can activate sensory nerve receptors by lowering the pain threshold and increasing pain perception [34]. Our study showed that levels of inflammatory factors and pain mediators improved after treatment in both groups, with the combined treatment group experiencing greater relief.

Evidence suggests that vitamin D deficiency is prevalent among patients with lumbar degenerative spine conditions. Our findings showed that $25(OH)D_3$ levels in patients were at deficient levels prior to treatment, and after four weeks of vitamin supplementation, there was a significant increase, approaching the normal range. Mechanistic studies have found that vitamin D interacts with vitamin D receptors in the paravertebral muscles, supporting injury recovery. In addition, vitamin D can inhibit neurotoxic factors through immunomodulation and modulate inflammatory cell populations, thereby contributing to inflammation and pain relief. IL-6, TNF-α, and prostaglandins released by glial cells are downregulated by vitamin D [35-37]. Therefore, we hypothesize that the improved efficacy of combination therapy is due to vitamin D's ability to inhibit the expression of inflammatory and pain mediators.

Statistics on patients' mood and quality of life, as measured by questionnaires, revealed that combination therapy provided significantly greater benefits than monotherapy. One-month follow-up results suggested that the efficacy of combination therapy was maintained beyond one month.

However, there are still some limitations to this study. Firstly, the sample size was small, which may introduce bias into the findings. Secondly, the vitamin D_3 supplementation dose was not graded, and the optimal oral dose was not identified. These shortcomings represent directions for future research.

The present study demonstrates that combining vitamin D_3 supplementation with mechanical traction yields superior clinical benefits compared with traction alone in patients with lumbar disc herniation (LDH). Beyond alleviating pain and improving lumbar function, the combined regimen effectively modulates inflammatory and neurochemical pathways, reflected by reductions in IL-1β, TNF-α, IL-6, IL-8, SP, 5-HT, and PGE_2 levels. These biochemical improvements parallel

the enhancement in patients' quality of life and emotional well-being. The elevation of serum 25(OH)D_3 following therapy underscores the systemic contribution of vitamin D_3 to neuromuscular recovery and anti-inflammatory balance.

At a broader level, these findings substantiate the biopsychosocial impact of adjunctive vitamin D_3 therapy in musculoskeletal rehabilitation. By addressing both the physiological and psychological dimensions of LDH, vitamin D_3 with traction represents a biologically integrative and patient-centric approach that may redefine conservative management strategies. Future multicentric studies with larger cohorts and graded-dosing protocols are warranted to establish long-term efficacy, optimal dosing, and mechanistic insights into this synergistic interaction.

Funding

None.

ORCID ID of the authors

- Yina Yin (YY): 0009-0007-1907-5773
- Jiaojiao Huang (JH): 0009-0004-5828-156X

Author's contributions

Both authors contributed to the development and writing of the paper.

Conflict of interest

The authors state that there are no conflicts of interest to disclose.

Assurance of the originality of data

The author(s) assure the readers and the publishers that all the data presented here is original.

REFERENCES

1. **An HS, Thonar EJ, Masuda K**. Biological repair of intervertebral disc. Spine (Phila Pa 1976). 2003;28(15 Suppl):S86–92. *https://doi.org/10.1097/01.BRS.0000076904.99434.40.*
2. **Chen Z, Cao P, Zhou Z, Yuan Y, Jiao Y, Zheng Y.** Overview: the role of Propionibacterium acnes in nonpyogenic intervertebral discs. Int Orthop. 2016;40(6):1291–1298. *https://doi.org/10.1007/s00264-016-3115-5.*
3. **Urquhart DM, Zheng Y, Cheng AC, Rosenfeld JV, Chan P, Liew S, et al.** Could low grade bacterial infection contribute to low back pain? A systematic review. BMC Med. 2015;13:13. *https://doi.org/10.1186/s12916-015-0267-x.*
4. **Fjeld OR, Grøvle L, Helgeland J, Småstuen MC, Solberg TK, Zwart JA, et al.** Complications, reoperations, readmissions, and length of hospital stay in 34639 surgical cases of lumbar disc herniation. Bone Joint J. 2019;101-B(4):470-477. *https://doi.org/10.1302/0301-620X.101B4.BJJ-2018-1184.R1.*
5. **Cimmino MA, Ferrone C, Cutolo M.** Epidemiology of chronic musculoskeletal pain. Best Pract Res Clin Rheumatol. 2011;25(2):173–183. *https://doi.org/10.1016/j.berh.2010.01.012.*
6. **Amin RM, Andrade NS, Neuman BJ.** Lumbar Disc Herniation. Curr Rev Musculoskelet Med. 2017;10(4):507–516. *https://doi.org/10.1007/s12178-017-9441-4.*
7. **Kreiner DS, Hwang SW, Easa JE, Resnick DK, Baisden JL, Bess S, et al.** An evidence-based clinical guideline for the diagnosis and treatment of lumbar disc herniation with radiculopathy. Spine J. 2014;14(1):180–191. *https://doi.org/10.1016/j.spinee.2013.08.003.*
8. **Chou R, Loeser JD, Owens DK, Rosenquist RW, Atlas SJ, Baisden J, et al.** Interventional therapies, surgery, and interdisciplinary rehabilitation for low back pain: an evidence-based clinical practice guideline from the American Pain Society. Spine (Phila Pa 1976). 2009;34(10):1066–

1077. *https://doi.org/10.1097/BRS.0b013e3181a1390d.*

9. **Vanti C, Turone L, Panizzolo A, Guccione AA, Bertozzi L, Pillastrini P.** Vertical traction for lumbar radiculopathy: a systematic review. Arch Physiother. 2021;11(1):7. *https://doi.org/10.1186/s40945-021-00102-5.*
10. **Kumari A, Quddus N, Meena PR, Alghadir AH, Khan M.** Effects of One-Fifth, One-Third, and One-Half of the Bodyweight Lumbar Traction on the Straight Leg Raise Test and Pain in Prolapsed Intervertebral Disc Patients: A Randomized Controlled Trial. Biomed Res Int. 2021;2021:2561502. *https://doi.org/10.1155/2021/2561502.*
11. **Tadano M, Tanabe H, Arai S, Fujino K, Doi T, Akai M**. Lumbar mechanical traction: a biomechanical assessment of change at the lumbar spine. BMC Musculoskelet Disord. 2019;20(1): 155. *https://doi.org/10.1186/s12891-019-2545-9.*
12. **Cheng YH, Hsu CY, Lin YN.** The effect of mechanical traction on low back pain in patients with herniated intervertebral disks: a systematic review and meta-analysis. Clin Rehabil. 2020;34(1):13-22. *https://doi.org/10.1177/0269215519872528.*
13. **Gaydarski L, Sirakov I, Uzunov K, Chervenkov M, Ivanova T, Gergova R, et al.** A Case-Control Study of the FokI Polymorphism of the Vitamin D Receptor Gene in Bulgarians with Lumbar Disc Herniation. Cureus. 2023;15(9):e45628. *https://doi.org/10.7759/cureus.45628.*
14. **Kawaguchi Y, Kanamori M, Ishihara H, Ohmori K, Matsui H, Kimura T.** The association of lumbar disc disease with vitamin-D receptor gene polymorphism. J Bone Joint Surg Am. 2002;84(11):2022-2028. *https://doi.org/10.2106/00004623-200211000-00018.*
15. **Withanage ND, Perera S, Peiris H, Athiththan LV.** Serum 25-hydroxyvitamin D, serum calcium and vitamin D receptor (VDR) polymorphisms in a selected population with lumbar disc herniation – A case control study. PLoS One. 2018;13(10):e0205841. *https://doi.org/10.1371/journal.pone.0205841.*
16. **Garcion E, Wion-Barbot N, Montero-Menei CN, Berger F, Wion D.** New clues about vitamin D functions in the nervous system. Trends Endocrinol Metab. 2002;13(3):100-105. *https://doi.org/10.1016/s1043-2760(01)00547-1.*
17. **Myers RR, Campana WM, Shubayev VI.** The role of neuroinflammation in neuropathic pain: mechanisms and therapeutic targets. Drug Discov Today. 2006;11(1–2):8–20. *https://doi.org/10.1016/S1359-6446(05)03637-8.*
18. **Xu J, Hu Y.** Clinical Features and Efficacy Analysis of Redundant Nerve Roots. Front Surg. 2021;8:628928. *https://doi.org/10.3389/fsurg.2021.628928.*
19. **Lu Z, Ding A, Yu Q, Wang H, Ma L.** Effect of the preoperative assessment of the anteroposterior diameters of the spinal canal and dural area on the efficacy of oblique lumbar interbody fusion in patients with lumbar spinal stenosis. J Orthop Surg Res. 2023;18(1):440. *https://doi.org/10.1186/s13018-023-03913-3.*
20. **Eijsvogels TMH, Maessen MFH, Bakker EA, Meindersma EP, van Gorp N, Pijnenburg N, et al.** Association of Cardiac Rehabilitation with All-Cause Mortality Among Patients with Cardiovascular Disease in the Netherlands. JAMA Netw Open. 2020;3(7):e2011686. *https://doi.org/10.1001/jamanetworkopen.2020.11686.*
21. **Cosamalón-Gan I, Cosamalón-Gan T, Mattos-Piaggio G, Villar-Suárez V, García-Cosamalón J, Vega-Álvarez JA.** Inflammation in the intervertebral disc herniation. Neurocirugia (Engl Ed). 2021; 32(1):21-35. *https://doi.org/10.1016/j.neucir.2020.01.001.*
22. **Ozturk B, Gunduz OH, Ozoran K, Bostanoglu S.** Effect of continuous lumbar traction on the size of herniated disc material in lumbar disc herniation. Rheumatol Int. 2006;26(7):622-626. *https://doi.org/10.1007/s00296-005-0035-x.*
23. **Yang Q, Liu Y, Guan Y, Zhan X, Xiao Z, Jiang H, et al.** Vitamin D Receptor gene polymorphisms and plasma levels are associated with lumbar disc degeneration.

Sci Rep. 2019;9(1):7829. *https://doi.org/10.1038/s41598-019-44373-2.*

24. **Sedighi M, Haghnegahdar A.** Role of vitamin D_3 in treatment of lumbar disc herniation—pain and sensory aspects: study protocol for a randomized controlled trial. Trials. 2014;15:373. *https://doi.org/10.1186/1745-6215-15-373.*
25. **Martirosyan NL, Patel AA, Carotenuto A, Kalani MY, Belykh E, Walker CT, et al.** Genetic Alterations in Intervertebral Disc Disease. Front Surg. 2016;3:59. *https://doi.org/10.3389/fsurg.2016.00059.*
26. **Kim H, Hong JY, Lee J, Jeon WJ, Ha IH.** IL-1β promotes disc degeneration and inflammation through direct injection of intervertebral disc in a rat lumbar disc herniation model. Spine J. 2021;21(6):1031-1041. *https://doi.org/10.1016/j.spinee.2021.01.014.*
27. **Andrade P, Hoogland G, Garcia MA, Steinbusch HW, Daemen MA, Visser-Vandewalle V.** Elevated IL-1β and IL-6 levels in lumbar herniated discs in patients with sciatic pain. Eur Spine J. 2013;22(4):714-720. *https://doi.org/10.1007/s00586-012-2502-x.*
28. **Huang K, Hsu Y, Chen W, Tsai H, Yan J, Wang J, et al.** The roles of IL-19 and IL-20 in the inflammation of degenerative lumbar spondylolisthesis. J Inflamm (Lond). 2018;15:19. *https://doi.org/10.1186/s12950-018-0195-6*
29. **Zhang X, Wang X, Gao L, Yang B, Wang Y, Niu K, et al.** TNF-α induces methylglyoxal accumulation in lumbar herniated disc of patients with radicular pain. Front Behav Neurosci. 2021; 15:760547. *https://doi.org/10.3389/fnbeh.2021.760547.*
30. **Sella EJ.** Noncompressive spinal radiculitis. Orthop Rev. 1992;21(7):827-832. PMID: 1501920.
31. **Liu J, Ye YJ, Liu SM, Liu S.** [Analysis of the effect of midazolam on pain in a rat model of lumbar disc herniation based on the p38 MAPK signaling pathway]. Zhongguo Gu Shang. 2023;36(1):55-60. Chinese. *https://doi.org/10.12200/j.issn.1003-0034.2023.01.010.*
32. **Kawakami M, Matsumoto T, Kuribayashi K, Tamaki T.** mRNA expression of interleukins, phospholipase A_2, and nitric oxide synthase in the nerve root and dorsal root ganglion induced by autologous nucleus pulposus in the rat. J Orthop Res. 1999;17(6):941-946. *https://doi.org/10.1002/jor.1100170620.*
33. **Moalem G, Tracey DJ.** Immune and inflammatory mechanisms in neuropathic pain. Brain Res Rev. 2006;51(2):240-264. *https://doi.org/10.1016/j.brainresrev.2005.11.004.*
34. **Du P, Zhang Q, Zhang Y.** The role of IL-6, IL-10, and PGE_2 in the treatment of intervertebral disc herniation by dual-channel endoscopic lumbar discectomy. Cell Mol Biol (Noisy-le-grand). 2022;67(5):188-195. *https://doi.org/10.14715/cmb/2021.67.5.26.*
35. **Cheda A, Nowosielska EM, Gebicki J, Marcinek A, Chlopicki S, Janiak MK.** A derivative of vitamin B3 applied several days after exposure reduces lethality of severely irradiated mice. Sci Rep. 2021;11(1):7922. *https://doi.org/10.1038/s41598-021-86870-3.*
36. **Zung WW**. A self-rating depression scale. Arch Gen Psychiatry. 1965;12(1):63-70. *https://doi.org/10.1001/archpsyc.1965.01720310065008.*
37. **Patrick DL, Deyo RA, Atlas SJ, Singer DE, Chapin A, Keller RB.** Assessing health-related quality of life in patients with sciatica. Spine. 1995;20(17):1899-1908. *https://doi.org/10.1097/00007632-199509000-00011.*

Invest Clin 67(2): 189 - 204, 2026 https://doi.org/10.54817/IC.v67n2a03

Comparative efficacy of octreotide and somatostatin in acute pancreatitis: a controlled trial of inflammatory markers and hospital length of stay.

Qunchao Zhu[1], Tian Jiang[2], Yan Li[3], Sicong Jiang[1], Aifang Li[4] and Chendong Ma[1]

[1]Department of Emergency Medicine, The First People's Hospital of Jiashan, Jiashan Hospital Affiliated of Jiaxing University, Jiashan, Zhejiang Province, China.
[2]Department of Thoracic Oncology, Jiangxi Cancer Hospital, Nanchang, Jiangxi Province, China.
[3]Department of Endocrinology, Jiujiang Hukou County People's Hospital, Hukou, Jiangxi Province, China.
[4]Department of Hematology, Jiamusi University Affiliated First Hospital, Jiamusi, Heilongjiang Province, China.

Keywords: Acute Pancreatitis; Octreotide; Somatostatin; Inflammation; Hospitalization.

Abstract. Acute pancreatitis is an acute pancreatic injury with multiple etiologies. Octreotide and somatostatin are commonly used treatments, but their clinical efficacy remains controversial. This study compares their effects on inflammatory markers and hospital length of stay. One hundred and twenty patients with acute pancreatitis admitted to The First People's Hospital of Jiashan between January 2022 and December 2024 were retrospectively included and divided into two groups based on treatment modality, namely the control group (somatostatin treatment) and the experimental group (octreotide treatment), with 60 cases in each group. Serum amylase (AMY), serum lipase (LPS), C-reactive protein (CRP), interleukin-6 (IL-6), tumor necrosis factor-α (TNF-α), white blood cell count (WBC), serum albumin (ALB) content, procalcitonin (PCT), hospital stay duration, and the incidence of adverse reactions were assessed in both groups. Baseline data for the two groups were comparable, with no statistically significant differences ($p>0.05$). After seven days of medication, compared with the control group, patients in the experimental group had lower AMY, LPS, CRP, IL-6, TNF-α, WBC, and PCT ($p<0.05$), a shorter hospital stay ($p=0.011$), and a lower incidence of adverse reactions ($p=0.007$). ALB levels in the experimental group were significantly higher than those in the control group ($p=0.039$). Compared with somatostatin, octreotide shows superior therapeutic effects in acute pancreatitis, alleviating inflammation more effectively, promoting recovery, improving clinical outcomes, and shortening hospital stay. These findings provide a scientific basis for optimizing clinical medication.

Corresponding author: Chendong Ma, No. 1218, Tiyu South Road, Luoxing Street, Jiashan County, Jiaxing 314100, Zhejiang, China. Email: med9376@hotmail.com

Eficacia comparada de octreótido y somatostatina en pancreatitis aguda: ensayo controlado sobre marcadores inflamatorios y duración de la estancia hospitalaria.

Invest Clin 2026; 67 (2): 189 – 204

Palabras clave: Pancreatitis Aguda; Octreótido; Somatostatina; Inflamación; Hospitalización.

Resumen. La pancreatitis aguda es una lesión pancreática de etiología múltiple. El octreótido y la somatostatina son tratamientos habituales para esta condición, aunque su eficacia clínica sigue siendo controvertida. Este estudio compara sus efectos sobre los índices inflamatorios y el tiempo de hospitalización. Se incluyeron retrospectivamente 120 pacientes con pancreatitis aguda ingresados en el First People's Hospital of Jiashan entre enero de 2022 y diciembre de 2024, distribuidos en dos grupos según el tratamiento recibido: grupo control (tratamiento con somatostatina) y grupo experimental (tratamiento con octreótido), con 60 casos en cada grupo. Se evaluaron en ambos grupos la amilasa sérica (AMY), lipasa sérica (LPS), proteína C reactiva (PCR), interleucina-6 (IL-6), factor de necrosis tumoral α (TNF-α), recuento de leucocitos (WBC), albúmina sérica (ALB), procalcitonina (PCT), duración de la estancia hospitalaria e incidencia de reacciones adversas. Los datos basales de ambos grupos no mostraron diferencias estadísticamente significativas, lo que confirma su comparabilidad ($p>0,05$). Después de 7 días de medicación, en comparación con el grupo control, los pacientes del grupo experimental presentaron niveles más bajos de AMY, LPS, PCR, IL-6, TNF-α, WBC y PCT ($p<0,05$); la duración de la estancia hospitalaria fue menor ($p=0,011$); y la incidencia de reacciones adversas fue inferior ($p=0,007$). Los niveles de ALB en el grupo experimental fueron significativamente más altos que en el grupo control ($p=0,039$). En comparación con la somatostatina, el octreótido muestra una eficacia terapéutica superior en la pancreatitis aguda, aliviando la inflamación de forma más marcada, favoreciendo la recuperación, mejorando la eficacia clínica y acortando la hospitalización. Estos resultados aportan una base científica para optimizar el tratamiento farmacológico clínico.

Received: 27-01-2026 Accepted: 02-03-2026

INTRODUCTION

Acute pancreatitis arises from various etiological factors, leading to acute injury of pancreatic tissues, edema, hemorrhage, and necrosis, to name just a few [1]. It is an autodigestive disease of pancreatic tissue caused by the abnormal activation of pancreatic enzymes and may lead to dysfunction of other organs [2].

Acute pancreatitis usually occurs in adults, with an incidence of 5/100,000 to 30/100,000 per year. The incidence appears to be rising each year. In China, the leading cause of acute pancreatitis is cholelithiasis, with hypertriglyceridemia and excessive alcohol consumption as the next most common causes [3]. Early control of the underlying cause can help alleviate the condition, improve prognosis, and prevent recurrence

of acute pancreatitis [4]. Based on severity, acute pancreatitis is classified into three types: mild, moderately severe, and severe. According to pathology, it can be categorized as interstitial edema type and necrosis type [5]. Acute pancreatitis may lead to functional impairment of one or more organs, with respiratory and renal impairment being the most common [6]. In patients with acute pancreatitis, elevated serum amylase (AMY) and lipase (LPS) levels are commonly observed on laboratory testing [6].Originally isolated from hypothalamic extracts of pigs and sheep, somatostatin has a short biological half-life of approximately 3 minutes, which limits its duration of action in clinical therapy [7]. Common somatostatin analogs include somatostatin tetradecapeptide and octapeptide. Like somatostatin, somatostatin analogs effectively inhibit pancreatic enzyme secretion. However, unlike somatostatin, somatostatin analogs have a longer half-life, and their effects last for a relatively long time [8]. The specific mechanism of action is that, after medication use, somatostatin and its analogs, as the active ingredients, bind to somatostatin receptors on the patient's pancreatic cell surface [9], which weakens the pancreas's exocrine function, interferes with the release of acetylcholine, and downregulates adenosine release and the activity level of adenylyl cyclase. These effects can help reduce pancreatic duct pressure, inhibit the infiltration of pancreatic fluid into pancreatic tissues, and thereby reduce pancreatic auto-digestive function. In the early stages of the condition, patients' platelet levels are abnormally low, but platelet activity is markedly elevated. Treatment with somatostatin or somatostatin analogs can effectively reduce the patient's platelet activity level and block the abnormal release of platelet-activating factors [10]. Abnormal release of platelet-activating factors thus exacerbates the systemic inflammatory response in patients and blocks their disease progression[10].Octreotide is a widely used somatostatin analog that can significantly reduce the release of growth hormone and pancreatic enzymes, fully relax Oddi's sphincter of the biliary tract, reduce pancreatic duct pressure, prevent pancreatic juice reflux, control pancreatic self-digestion, reduce the secretion of pro-inflammatory factors, and thus alleviate the body's inflammatory response [11]. Octreotide is a cyclic octapeptide with greater physiological activity. It can inhibit the abnormal release of growth hormone and thyrotropin and reduce the release of gastric acid, glucagon, insulin, and pancreatic enzymes, thereby controlling gastrointestinal and pancreatic endocrine hormone pathology and ultimately inhibiting abnormal secretion in the intestinal tract.

In this study, the therapeutic efficacy of octreotide and somatostatin was compared in patients with acute pancreatitis, primarily using inflammatory markers such as AMY, LPS, C-reactive protein (CRP), interleukin-6 (IL-6), tumor necrosis factor-α (TNF-α), white blood cell count (WBC), and serum albumin (ALB), along with procalcitonin (PCT) and hospital stay duration for a comprehensive efficacy analysis. The aim was to compare the effects of octreotide and somatostatin in treating acute pancreatitis, to develop a more effective and personalized treatment plan for patients with acute pancreatitis, and to advance the discipline and contribute to the dual value of theory and practice.

PATIENTS AND METHODS

General information

This study retrospectively selected patients with acute pancreatitis admitted to The First People's Hospital of Jiashan from January 2022 to December 2024 as the research subjects, aiming to compare the efficacy of octreotide and somatostatin in treating acute pancreatitis. As shown in the experimental design flowchart in Fig. 1, a total of 132 cases were collected. After exclusions, 126 cases were included. Of these, two were lost, and four withdrew for personal reasons, leaving 120 cases for analysis.

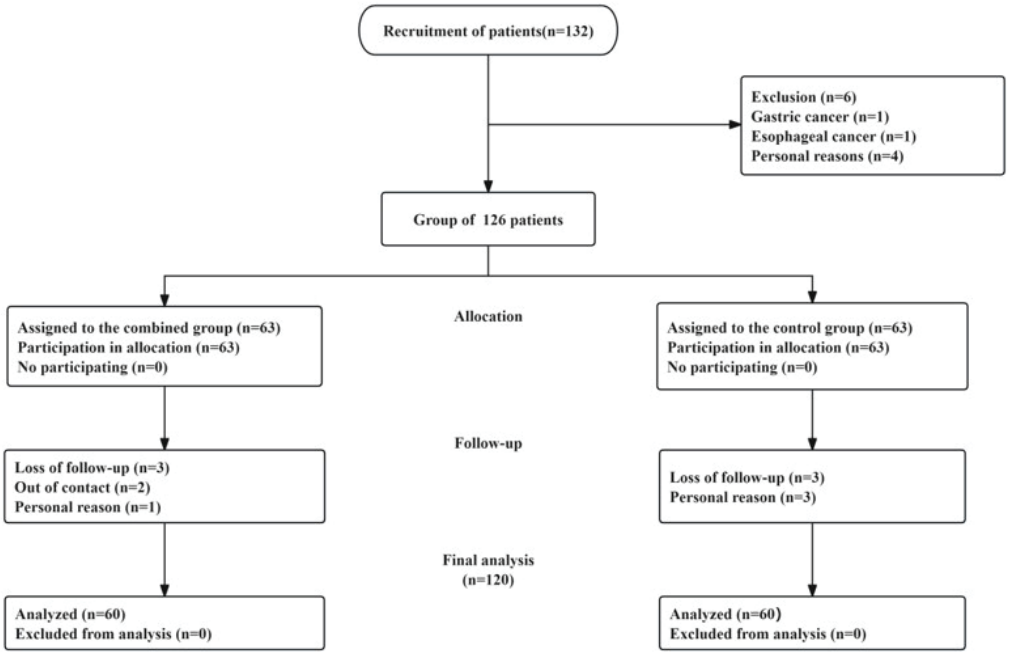

Fig. 1. Flowchart of experimental design.

These were divided into control and experimental groups based on treatment modality, with 60 cases in each group. Inclusion criteria: (1) patients with acute pancreatitis were diagnosed according to the Chinese Guide to Diagnosis and Treatment of Acute Pancreatitis in China (2021 Edition) [12], published by the Chinese Journal of Practical Surgery and written by the Pancreatic Surgery Group of the Surgical Branch of the Chinese Medical Association; (2) no other gastrointestinal or oncological diseases; (3) no history of allergy to the study drugs; (4) age 35-65 years; (5) complete clinical data and relevant examinations. Exclusion criteria [13]: (1) those with speech, mental, or psychological disorders that affect the smooth conduct of the study; (2) those with other digestive system malignant tumors; (3) patients with serious heart, liver, kidney, and lung problems; (4) female patients during pregnancy or breastfeeding; (5) a history of relevant drug treatment in the last four weeks; (6) those with serious infectious diseases.

Ethics statement

The clinical study followed the Declaration of Helsinki and other relevant ethical regulations, was reviewed and approved by the Hospital Ethics Committee, and the purpose, process, and potential risks of the study were explained in detail to the subjects or their proxies, with written informed consent obtained.

Mode of intervention

Both groups of patients received conventional treatment for acute pancreatitis. In practice, patients first underwent gastrointestinal decompression and fasting. Most patients had pain and required analgesic intervention as needed. Patients' basic vital signs were monitored to ensure that their water and electrolyte balance was maintained, and acid suppression and anti-infection treatment were provided. Meanwhile, patients received nutritional support based on their physical signs to support recovery, reduce symptoms, and prevent complications.

Patients in the control group received somatostatin as part of conventional treatment to inhibit pancreatic fluid secretion, administered by injection (trade name Sitanin, Laboratoires Serono S.A., H20090930, lyophilized powder, 250 μg). 250 μg of somatostatin was added to 500 mL of physiological saline, and the solution was infused intravenously. For patient [14,] the infusion was delivered at 250 μg per hour, twice daily for 7 consecutive days.

Patients in the experimental group received octreotide, in addition to conventional treatment, to inhibit pancreatic fluid secretion. Octreotide acetate (trade name Zenith, Novartis AG, Switzerland, H20090948), a colorless, clear liquid (1 mL: 0.1 mg), was used. It was diluted with 250 mL of saline injection and administered via intravenous drip at 0.3 mg every 12 hours. The patients were medicated for 7 consecutive days [15].

At the same time as administering drug treatment to patients, it was necessary to pay rigorous attention to the patient's respiratory status and blood pressure fluctuations, to observe whether there were any adverse reactions to the medication, and to actively prevent them, to avoid patients from experiencing shock and other adverse reactions, and to ensure the patient's life safety.

Observation indicators

AMY, serum LPS, CRP, and ALB

Procoagulant tubes were used to collect 5 mL of venous blood from patients on an empty stomach as test samples. After centrifugation for 10 min at 3000 r/min using a Beckman Microfuge® 20R centrifuge, the serum was separated and measured using a Beckman Counter DXC800 automatic blood biochemistry analyzer.

IL-6, TNF-α, and PCT

The serum was collected as described above, and the enzyme-linked immunosorbent assay (ELISA) was used to detect IL-6, TNF-α, and PCT [16] in the serum using the ELISA kits Beyotime PI330/PT518/PP790 from Shanghai Beyotime Biotechnology Co.

WBC count

A routine blood tube was used to collect 5 mL of fasting venous blood from the patients as a test sample, and a Beckman Vi-CELL BLU fully automated cell counter was used to perform the WBC count.

Hospital stay duration

Hospital stay duration is the total length of time a patient is hospitalized and an important indicator of the patient's condition and treatment effect [17].

Determine the admission time: the time when the patient completes admission procedures and officially becomes an inpatient.

Determine the discharge time: the point in time when the patient completes treatment and the nurse carries out the discharge instructions. The patient is considered to have completed treatment when the patient's condition is stable, with no obvious worsening symptoms, and vital signs are normal.

Calculate the total number of days: Subtract the discharge date from the admission date. The resulting number of days will be the total number of days in the hospital.

Attention to special circumstances: if there were cases such as a leave of absence or a temporary transfer, the calculation of hospitalization time should be adjusted accordingly.

Incidence rate of adverse reactions during treatment

The incidence rate of adverse drug reactions is the most important indicator for assessing drug safety and is used to measure the occurrence of adverse reactions during drug use. Calculating the incidence of adverse drug reactions can help doctors and patients better understand drug safety and make rational treatment decisions based on the risk of such reactions. In this study,

adverse conditions during the treatment of acute pancreatitis with somatostatin and octreotide mainly included abdominal pain, rash, nausea and vomiting, and dizziness and headache [18].

The formula for calculating the incidence of adverse drug reactions is shown below:

Incidence of adverse reactions = (number of people with adverse reactions/total number of patients using the drug) * 100%

Sample size calculation methods

Sample sizes were determined using G*Power 3.1.9.7 to estimate the number needed to detect statistically significant differences. The calculation was based on the primary outcome, the Inflammation Indicator. According to previous studies [14], IL-6 levels in patients with acute pancreatitis treated with somatostatin for 7 days were lower than in the healthy control group (p=0.025), with an effect size of 0.49. With a type I error rate (α) of 0.05 and 80% power, 53 patients were estimated to be needed in each group. To account for potential uncertainties, a total of 60 patients in the control group (n=60) and 60 in the experimental group (n=60) were ultimately selected for analysis in this study, and this sample size was considered sufficient to draw reliable conclusions.

Statistical Methods

SPSS version 28.0 was used to analyze the data. The data in this study were tested for normality. Baseline characteristics were described as counts and means (± SD). AMY, LPS, CRP, IL-6, TNF-α, WBC, ALB, PCT, and hospital stay duration were expressed as means ± SD. An independent-samples test was used to compare two groups. The incidence of adverse events was expressed as [n (%)], and comparisons between the two groups were analyzed using the χ^2 test. All statistical tests were two-sided, and $p<0.05$ was considered statistically significant.

RESULTS

Comparison of baseline data between the two groups

Comparing the baseline data of the patients in the control and experimental groups, Table 1 provided evidence that no significant differences were observed between the two groups in age, BMI, gender, classification of acute pancreatitis, APACHE II scores, disease duration, and etiology of the disease [16, 19] (p=0.816, 0.662, 0.36, 0.714, 0.896, 0.504, 0.559, 0.609, 0.793, 0.697), indicating that the groups were comparable before drug treatment.

Comparison of serum amylase and serum lipase between the two groups

As shown in Table 2, no significant difference was observed between the control and experimental groups in serum AMY and LPS levels on the day prior to dosing (AMY: 95% CI: -2.57-10.23, p=0.239; LPS: 95% CI: -2.78-12.17, p=0.216). After seven days of drug administration, these indices were significantly reduced in both groups (both $p<0.05$). In addition, compared with the control group (AMY: 44.85±8.17 U/L; LPS: 42.48±6.99 U/L), the experimental group (AMY: 42.15±5.87 U/L; LPS: 39.80±5.10 U/L) showed significantly lower levels (AMY: 95% CI: 0.13-5.28, p=0.04; LPS: 95% CI: 0.47-4.90, p=0.018), suggesting that, compared with somatostatin, octreotide can restore pancreatic function to normal more quickly in patients with acute pancreatitis.

Comparison of CRP between the two groups

As shown in Table 3, no significant difference in serum CRP levels was observed between the two groups on the first day of drug administration (95% CI: -3.50 to 5.01, p=0.726). After seven days of administration, CRP decreased in both the control and experimental groups (167.25±11.62 mg/L vs.

Table 1. Baseline information of patients.

Indicator	Control group (n=60)	Experimental group (n=60)	95% CI		*p*	Effect size
			Lower	Upper		
Age	50.58±9.03	50.2±8.96	-2.87	3.64	0.816	0.02
BMI(kg/m²)	22.62±1.7	22.76±1.80	-0.77	0.49	0.662	-0.04
Gender						
Male	35	30	0.681	2.878	0.36	0.084
Female	25	30				
Classification of Acute Pancreatitis						
Mild	33	31	0.558	2.344	0.714	0.033
Severe	27	29				
APACHE II scores	19.47±2.33	19.52±1.8	-0.80	0.70	0.896	-0.01
Disease duration (hours)	6.37±0.31	6.33±0.34	-0.08	0.16	0.504	0.06
Etiology						
Biliary	42	39	0.584	2.702	0.559	0.053
Alcoholic	8	10	0.281	2.107	0.609	-0.047
Hyperlipidemia	9	8	0.41	3.206	0.793	0.024
Other	3	4	0.158	3.443	0.697	-0.036

BMI: body mass index; APACHE II scores: acute physical and chronic health scores. Independent Samples t-test was used for continuous variables, and Chi-square Test was used for categorical variables.

Table 2. Comparison of serum amylase and serum lipase between the two groups.

Indicator	n	Time	Mean±SD		95% CI		*p*	Effect size
			Control group	Experimental group	Lower	Upper		
AMY (U/L)	60	1 day prior to dosing	261.53±17.59	257.70±17.83	-2.57	10.23	0.239	0.11
	60	7 days after dosing	44.85±8.17*	42.15±5.87*	0.13	5.28	0.04	0.19
LPS (U/L)	60	1 day prior to dosing	260.06±22.08	255.37±19.16	-2.78	12.17	0.216	0.11
	60	7 days after dosing	42.48±6.99*	39.80±5.10*	0.47	4.90	0.018	0.21

*p<0.05 vs 1 day prior to dosing. AMY: serum amylase; LPS: serum lipase. Independent Samples t-test was used for between-group comparisons, and Paired Samples t-test was used for within-group comparisons.

Table 3. Comparison of C-reactive protein between the two groups of patients.

Indicator	n	Time	Mean±SD		95% CI		*p*	Effect size
			Control group	Experimental group	Lower	Upper		
CRP (mg/L)	60	1 day prior to dosing	167.25±11.62	166.50±11.92	-3.50	5.01	0.726	0.03
	60	7 days after dosing	83.24±5.32*	80.34±7.4*	0.56	5.23	0.015	0.22

*p<0.05 vs 1 day prior to dosing. CRP: C-reactive protein. Independent Samples t-test was used for comparisons between groups, and Paired Samples t-test was used for comparisons within groups.

83.24±5.32 mg/L, p<0.05; 166.50±11.92 mg/L vs. 80.34±7.4 mg/L, p<0.05), indicating that both somatostatin and octreotide can reduce inflammation in patients with acute pancreatitis. Compared with the control group (83.24±5.32 mg/L), CRP was significantly lower in the experimental group (80.34±7.4 mg/L) (95% CI: 0.56-5.23, p=0.015), suggesting that, compared with somatostatin, octreotide could normalize inflammation and tissue damage more quickly in patients with acute pancreatitis.

Comparison of IL-6, TNF-α, and PCT between the two groups

As shown in Table 4, there was no significant difference in the levels of IL-6, TNF-α, and PCT between the two groups on the first day before drug administration (p=0.222, P=0.392, p=0.546). After drug administration, the levels of these three markers decreased in both groups (all p<0.05). In addition, compared with the control group, the experimental group had lower levels of IL-6 (52.30±8.42 pg/mL vs. 55.36±8.03 pg/mL), TNF-α (40.07±5.74 ng/L vs. 42.71±7.66 ng/L), and PCT (33.80±4.70 ng/mL vs. 35.66±4.60 ng/mL), with 95% CIs of 0.08-6.03 (p=0.044), 0.19-5.09 (p=0.035), and 0.17-3.54 (p=0.031), respectively, suggesting that octreotide can normalize more quickly the degree of inflammation and infection in patients with acute pancreatitis compared to somatostatin.

Comparison of white blood cells between the two groups

As shown in Table 5, there was no significant difference in WBC between the two groups before drug administration (95% CI: -0.45 to 0.08; p=0.174). After drug administration, WBC decreased in both the control and experimental groups (13.76±1.39*109/L vs. 12.55±1.39*109/L, p<0.05; 13.94±0.69*109/L vs. 11.94 ± 1.68*109/L, p<0.05), indicating that both somatostatin and octreotide reduced leukocyte counts. Compared with the control group (12.55±1.39*109/L), the experimental group's WBC (11.94±1.68*109/L) decreased significantly (95% CI: 0.06-1.17; p=0.031), suggesting that, compared with somatostatin, octreotide could normalize infection and inflammatory responses in patients with acute pancreatitis more quickly.

Comparison of albumin between the two groups

As shown in Table 6, there was no significant difference in ALB levels between the two patient groups before drug administration (95% CI: -0.57 to 0.18; p=0.31). After drug administration, ALB levels increased in both groups (25.23±1.12 g/L vs. 36.99±1.94 g/L, p<0.05; 25.43±0.95 g/L vs. 38.47±5.12 g/L, p<0.05). Compared with the control group, ALB levels increased in the experimental group (36.99±1.94 g/L vs. 38.47±5.12 g/L; 95% CI: -2.89 to 0.07;

Table 4. Comparison of interleukin-6, tumor necrosis factor- α, and procalcitonin between the two patient groups.

Indicator	n	Time	Mean±SD		95% CI		*p*	Effect size
			Control group	Experimental group	Lower	Upper		
IL-6 (pg/mL)	60	1 day prior to dosing	98.63±9.59	100.65±8.40	-5.28	1.24	0.222	-0.11
	60	7 days after dosing	55.36±8.03*	52.30±8.42*	0.08	6.03	0.044	0.18
TNF-α (ng/L)	60	1 day prior to dosing	81.61±8.94	80.23±8.71	-1.81	4.57	0.392	0.09
	60	7 days after dosing	42.71±7.66*	40.07±5.74*	0.19	5.09	0.035	0.30
PCT (ng/mL)	60	1 day prior to dosing	73.12±5.63	73.78±6.18	-2.79	1.48	0.546	-0.21
	60	7 days after dosing	35.66±4.60*	33.80±4.70*	0.17	3.54	0.031	0.35

*p<0.05 vs 1 day prior to dosing. IL-6: interleukin-6; TNF-α: tumor necrosis factor-α; PCT: procalcitonin. Independent samples t-test was used for between-group comparisons, and Paired Samples t-test was used for within-group comparisons.

Table 5. Comparison of white blood cells between the two groups of patients.

Indicator	n	Time	Mean±SD		95% CI		*p*	Effect size
			Control group	Experimental group	Lower	Upper		
WBC (10^9/L)	60	1 day prior to dosing	13.76±0.77	13.94±0.69	-0.45	0.08	0.174	-0.12
	60	7 days after dosing	12.55±1.39*	11.94±1.68*	0.06	1.17	0.031	0.19

*p<0.05 vs 1 day prior to dosing; WBC: white blood cells; Independent Samples t-test was used for between-group comparisons, and Paired Samples t-test for within-group comparisons.

Table 6. Comparison of serum albumin between the two groups of patients.

Indicator	n	Time	Mean±SD		95% CI		*p*	Effect size
			Control group	Experimental group	Lower	Upper		
ALB (g/L)	60	1 day prior to dosing	25.23±1.12	25.43±0.95	-0.57	0.18	0.31	-0.10
	60	7 days after dosing	36.99±1.94*	38.47±5.12*	-2.89	-0.07	0.039	-0.19

*p<0.05 vs 1 day prior to dosing. ALB: serum albumin. Independent Samples t-test was used for between-group comparisons, and Paired Samples t-test for within-group comparisons.

p=0.031), suggesting that, compared with somatostatin, octreotide could more quickly normalize nutrition and osmotic pressure in patients with acute pancreatitis.

Comparison of the hospital stay duration of patients in two groups

As shown in Table 7, the hospital stay duration for the control group was (11.03±1.30) days, and for the experimental group it was (10.38±1.46) days. The hospital stay duration for patients in the experimental group was evidently shorter than that of the control group (95% CI: 0.15-1.15; p=0.011), suggesting that, compared with somatostatin, octreotide could help patients with acute pancreatitis return to normal more quickly, shorten hospitalization time, and improve the quality of medical care.

Incidence of adverse reactions during treatment in the two groups

As shown in Table 8, during hospitalization, the control group had two patients with abdominal pain, three with skin rashes, five with nausea and vomiting, and three with dizziness and headache, for an overall adverse reaction incidence of 21.7%. In the experimental group, one patient had nausea and vomiting, and two had dizziness and headache, for an adverse reaction incidence of 5%. These results suggest that, compared with somatostatin, octreotide for the treatment of patients with acute pancreatitis had a significantly lower incidence of adverse reactions (95% CI: 1.413-19.544; p=0.008).

DISCUSSION

Acute pancreatitis is mainly divided into two types: mild and severe. The mild type is mainly manifested by pancreatic edema, is mostly self-limiting, and usually resolves within a few days, with complete recovery to the pre-treatment state [20]. In severe cases, complications such as pancreatic hemorrhage, peritonitis, pancreatic necrosis, and shock are common, posing a greater threat to patients' health. The prognosis of severe acute pancreatitis is usually poor, with a high mortality rate that can reach 10%-40%[21]. In recent years, with the continuous improvement of China's medical treatment technol-

Table 7. Comparison of hospital stay duration between the two groups (days).

Indicator	n	Mean±SD		95% CI		*p*	Effect size
		Control group	Experimental group	Lower	Upper		
Hospital stay duration	60	11.03±1.30	10.38±1.46	0.15	1.15	0.011	0.23

An independent-samples t-test was used to compare groups.

Table 8. Comparison of incidence of adverse reactions between the two groups.

Indicator	n (%)		95% CI		*p*	Effect size
	Control group	Experimental group	Lower	Upper		
Abdominal pain	2	0				
Skin rash	3	0				
Nausea and vomiting	5	1	1.413	19.544	0.007	0.245
Dizziness and headache	3	2				
Adverse reactions	13(21.7%)	3(5%)				

Chi-square test was used to compare the groups.

ogy, a variety of new drugs have appeared in clinical practice, and their application has, to a certain extent, reduced morbidity and mortality in patients with severe acute pancreatitis, but some patients still die. The occurrence of acute pancreatitis is mainly due to the continuous release of pancreatic enzymes in the body, influenced by a series of intertwined factors, resulting in the activation of phospholipase A2, etc. Under the influence of the inflammatory response, the pancreas undergoes microcirculation abnormalities, accelerating pancreatic digestion, destroying the normal blood supply, and ultimately leading to pancreatic necrosis. Niu et al.[22] proposed that phospholipase D2 (PLD2) plays a crucial regulatory role. In the medical management of patients with severe acute pancreatitis, comprehensive therapeutic approaches are typically used to reduce pancreatic secretion, inhibit pancreatic enzyme synthesis, improve clinical signs, and promote recovery.

AMY and LPS are two important laboratory tests for acute pancreatitis [23]; the former is mainly due to the activation of pancreatic amylase by trypsinogen in the pancreas, which subsequently causes the elevation of AMY, and the latter is due to the activation of pancreatic lipase by lipaseogen in the pancreas; therefore, AMY and LPS are the characteristic indicators for the diagnosis of acute pancreatitis. Sun et al.[24], in a multicenter retrospective study, suggested that both somatostatin and octreotide could normalize serum AMY and LPS in patients with acute pancreatitis, and this article's research showed that octreotide could normalize pancreatic function more quickly than somatostatin. CRP, an acute-phase reactant synthesized by IL-6-stimulated hepatocytes, is one of the proteins mediating the inflammatory response in acute pancreatitis. The inflammatory response in acute pancreatitis and its concentration can reflect the presence or absence of inflammation and the intensity of the response in the organism [25]. TNF-α, mainly produced by monocytes and macrophages, can regulate immune function and enhance anti-infection capacity, and the multiple-organ damage caused by inflammation is closely associated with TNF-α [26].

IL-6 plays an important role in the proliferation and activation of lymphocytes, and can promote the synthesis of CRP and the development of blood cells, but its concentration is too high, which can stimulate the granulocytes to release a large number of oxygen-free radicals and proteases, thus destroying the vascular endothelium and the endothelial cells. However, its high concentration can stimulate granulocytes to release large quantities of oxygen-free radicals and proteases, thereby destroying the vascular endothelium and aggravating organ damage. During inflammatory reactions, macrophages and monocytes in the liver, lymphocytes and endocrine cells in the lungs and intestinal tissues can synthesize and secrete PCT in response to bacterial endotoxin, TNF-α, and IL-6; these substances work together, leading to an apparent increase in the level of PCT in the blood circulation [27]. The present study suggests that, in patients with acute pancreatitis, CRP, IL-6, TNF-α, and PCT levels in the blood were reduced more significantly in those treated with octreotide than in those treated with somatostatin, indicating that octreotide can normalize inflammatory responses and immune functions. Mao et al. [28], in a multicenter retrospective study, validated somatostatin and octreotide as widely used medications for acute pancreatitis and reported octreotide's superior therapeutic effect, which is more attuned to the results of this study. When germs invade the human body, leukocytes can pass through the capillary wall by deformation, concentrate at the site of germ invasion, surround and engulf the germs, and produce an inflammatory reaction, resulting in a higher leukocyte count than normal. ALB unequivocally expands blood volume and

preserves plasma colloid osmotic pressure, helps with blood transport and detoxification of body organs [29], and, in human metabolism, it can be used as a source of nitrogen to provide nutrients to our body tissues. Bhansali et al. [30] retrospectively studied 131 patients with infected pancreatic necrosis, and the use of octreotide increased the level of ALB, and reduced surgical complications, from the perspective of this study, it acts out the similitude to the results of the present study, in this study, compared to somatostatin, the patients with acute pancreatitis treated with octreotide had a significant reduction in the number of leukocytes, a significant increase in ALB, and a shorter hospitalization time, which suggests that octreotide can bring the inflammatory response and the osmotic pressure of the body in patients with acute pancreatitis back to a normal state more quickly.

In clinical practice, the most commonly used drugs for treating patients with acute pancreatitis are octreotide and somatostatin, which have similar pharmacological effects; octreotide is a synthetic octapeptide. When administered, octreotide mimics the action of endogenous somatostatin, inhibiting the release of inflammatory mediators and suppressing the activation of mononuclear phagocytes, thereby improving patients' hemodynamic status. In clinical practice, because the application of octreotide can inhibit a variety of enzymes in pancreatic tissue, it can not only control the digestion of pancreatic protease on its own, but also control and maintain the intestinal micro-ecological balance of the patient to avoid the generation of endotoxins, so as to improve the patient's intestinal environment, alleviate the patient's symptoms of abdominal pain and bloating, enhance the patient's intestinal and gastrointestinal peristalsis, inhibit the activity of platelets[31], reduce bile reflux, ensuring patient comfort and promoting patient recovery. In the case of injectable somatostatin, this drug is synthetic and belongs to the tetradecapeptide class; it is distributed in the human body's peripheral and central nervous systems, with higher concentrations in the gastrointestinal tract and the hypothalamus. Somatostatin can inhibit gastrin secretion[32], and also inhibit gastric acid and pepsin secretion, improve the internal secretion function and external secretion function of the pancreas, maintain balance and coordination, thus reducing the inflammatory response of the patient, and promoting the recovery of the patient, but from the current clinical situation, there are certain adverse reactions in the application of this drug, which adversely affects the safety of the patient's use of the drug [33], leading to the limitation of the promotion of this drug in the clinic. Octreotide has a stronger effect and a longer maintenance time, and it can inhibit pancreatic enzymes and gastric acid, thus reducing the amount of pancreatic secretion, improving the blood and urine amylase levels of patients, promoting the improvement of gastrointestinal digestive function, and protecting the pancreatic parenchymal cell membrane of patients, so as to improve the effect of clinical application and promote the recovery of patients.

Although studies have shown that, in the treatment of acute pancreatitis, octreotide with a specific treatment regimen yields better therapeutic outcomes than somatostatin in controlling inflammation and shortening hospital stay, these studies still have the following limitations that may affect the generalizability of the results and their long-term application value: (1) this study provides preliminary single-center evidence comparing the efficacy of octreotide and somatostatin in the treatment of acute pancreatitis. However, limited by the inherent defects of the single-center and retrospective design, it still has deficiencies in external validity, bias control, and causal inference. (2) Lack of clear evidence of survival benefit; this study did not analyze the impact of octreotide on short-term mortality

or complication rate in patients with acute pancreatitis [34]. (3) For severe acute pancreatitis, although octreotide may inhibit pancreatic juice secretion, there is currently no clear evidence that it is effective in blocking systemic inflammatory response or progressive multiple organ failure[35]. (4) The medication cycle of octreotide in this study was only seven days, and its long-term medication risks remain unclear. (5) The localization of research data is insufficient, and the classification of disease severity is not clear. Future studies should adopt a multi-center prospective cohort design, expand the sample size, include more abundant confounding factors, conduct analyses targeting severe subgroups, clarify the details of drug use, and combine dynamic inflammation index monitoring with long-term follow-up data to further verify the efficacy difference between octreotide and somatostatin, so as to provide more reliable evidence to support clinical medication.

In conclusion, octreotide in the therapy of the acute pancreatitis patients has a better effect, which is conducive to the enhancement of the body's immune function, the improvement of the patient's AMY and LPS, the body's inflammatory response, osmolality returns to normal faster, shortens the patient's hospital stay, improves the quality of medical care, and provides a scientific basis for the optimization of clinical therapeutic medication regimens.

Acknowledgment

None.

Funding

None.

ORCID ID of the authors

- Qunchao Zhu (QZ): 0009-0004-6987-6091
- Tian Jiang (TJ): 0009-0002-5083-5500
- Yan Li (YL): 0009-0002-4819-7941
- Sicong Jiang (SJ): 0000-0001-8974-6770
- Aifang Li (AL): 0009-0008-7880-6078
- Chendong Ma (CM): 0009-0003-3787-5468

Author's contributions

QZ, CM: Developed and planned the study, conducted experiments, and interpreted the results. Edited and refined the manuscript, with a focus on critical intellectual contributions. TJ, YL: Participated in collecting, assessing, and interpreting the data. SJ, AL: Made significant contributions to date interpretation and manuscript preparation.

Conflicts of interest

The authors declare no financial conflicts of interest.

Consent to publish

The manuscript has not been published previously and is not under consideration by any other journal. All authors have approved the content of the paper.

Consent to participate

We obtained a signed informed consent form from every participant.

Ethic approval

This study was approved by the Ethics Committee of The First People's Hospital of Jiashan.

Data availability statement

The data that support the findings of this study are available from the corresponding author, upon reasonable request.

REFERENCES

1. **Mederos MA, Reber HA, Girgis MD.** Acute Pancreatitis: A Review. JAMA. 2021; 325 (4): 382-90. *https://doi.org/10.1001/jama.2020.20317.*
2. **Beyer G, Habtezion A, Werner J, Lerch MM, Mayerle J.** Chronic pancreatitis. Lancet. 2020; 396 (10249): 499-512. *https://doi.org/10.1016/S0140-6736(20)31318-0.*
3. **Yang AL, McNabb-Baltar J.** Hypertriglyceridemia and acute pancreatitis. Pancreatology. 2020; 20(5): 795-800. *https://doi.org/10.1016/j.pan.2020.06.005.*
4. **Saini J, Marino D, Badalov N, Vugelman M, Tenner S.** Drug-Induced Acute Pancreatitis: An Evidence-Based Classification (Revised). Clin Transl Gastroenterol. 2023; 14(8): e00621. *https://doi.org/10.14309/ctg.0000000000000621.*
5. **Sohail Z, Shaikh H, Iqbal N, Parkash O.** Acute pancreatitis: A narrative review. J Pak Med Assoc. 2024; 74(5): 953-8. *https://doi.org/10.47391/JPMA.9280.*
6. **Gardner TB.** Acute Pancreatitis. Ann Intern Med. 2021; 174(2): ITC17-ITC32. *https://doi.org/10.7326/AITC202102160.*
7. **Horváth IL, Bunduc S, Fehérvári P, Váncsa S, Nagy R, Garmaa G, et al.** The combination of ulinastatin and somatostatin reduces complication rates in acute pancreatitis: a systematic review and meta-analysis of randomized controlled trials. Sci Rep. 2022; 12(1): 17979. *https://doi.org/10.1038/s41598-022-22341-7.*
8. **He C, Liu J, Xu L, Sun F.** The Effect of Percutaneous Catheter Drainage Combined with Somatostatin on Inflammation and Plasma Thromboxane 2, Prostacyclin I2 Levels in Patients with Severe Pancreatitis. Georgian Med News. 2024: 352/353 (7/8): 278-283.
9. **Ampofo E, Nalbach L, Menger MD, Laschke MW.** Regulatory Mechanisms of Somatostatin Expression. Int J Mol Sci. 2020; 21(11):4170. *https://doi.org/10.3390/ijms21114170.*
10. **Khedr A, Mahmoud EE, Attallah N, Mir M, Boike S, Rauf I, et al.** Role of octreotide in small bowel bleeding. World J Clin Cases. 2022; 10(26): 9192-9206. *https://doi.org/10.12998/wjcc.v10.i26.9192.*
11. **Huang ZY, Gong H, Tang CW, Wang MJ, Wang R.** Remission of organ failure in patients with predicted severe acute pancreatitis treated by somatostation, octreotide and cyclooxygenase-2 inhibitors. Pancreatology. 2024; 24(1): 24-31. *https://doi.org/10.1016/j.pan.2023.12.006.*
12. **Chinese Pancreatic Surgery Association CSoSCMA.** Guidelines for diagnosis and treatment of acute pancreatitis in China (2021). Zhonghua Wai Ke Za Zhi. 2021; 59: 578-587. *https://doi.org/10.3760/cma.j.cn112139-20210416-00172.*
13. **Cao JP, Piao XH, Zhu LX, Feng PF.** Xuebijing and somatostatin against acute pancreatitis: A systematic review and network pharmacology. Medicine (Baltimore). 2024; 103(50): e40964. *https://doi.org/10.1097/MD.0000000000040964.*
14. **Sliwinska-Mosson M, Marek G, Grzebieniak Z, Milnerowicz H.** Relationship between somatostatin and interleukin-6: A cross-sectional study in patients with acute pancreatitis. Pancreatology. 2018; 18(8): 885-891. *https://doi.org/10.1016/j.pan.2018.09.013.*
15. **Bao W, Kong R, Wang N, Han W, Lu J.** PPAR-Alpha Agonist Fenofibrate Combined with Octreotide Acetate in the Treatment of Acute Hyperlipidemia Pancreatitis. PPAR Res. 2021; 2021: 6629455. *https://doi.org/10.1155/2021/6629455.*
16. **Zheng XL, Li WL, Lin YP, Huang TL.** Computerized tomography-guided therapeutic percutaneous puncture catheter drainage-combined with somatostatin for severe acute pancreatitis: An analysis of efficacy and safety. World J Gastrointest Surg. 2024; 16(1): 59-66. *https://doi.org/10.4240/wjgs.v16.i1.59.*
17. **Rivera-Suazo Y, Vázquez-Frias R.** Factors associated with hospital length of stay in children with acute pancreatitis. Rev Gastroenterol Mex. (Engl Ed). 2023; 88(1): 4-11. *https://doi.org/10.1016/j.rgmxen. 2021.05.016.*

18. **Zhu LX, Chen Y, Chen XF, Sheng N, Feng PF.** Systematic Review and Meta-analysis of the Clinical Efficacy of Octreotide in Combination with Ulinastatin in the Treatment of Acute Pancreatitis. Drugs R D. 2025; 25(3): 195-207. *https://doi.org/10.1007/s40268-025-00518-5.*
19. **Chen ZP, Huang HP, He XY, Wu BZ, Liu Y.** Early continuous blood purification affects TNF-alpha, IL-1beta, and IL-6 in patients with severe acute pancreatitis via inhibiting TLR4 signaling pathway. Kaohsiung J Med Sci. 2022; 38(5): 479-485. *https://doi.org/10.1002/kjm2.12497.*
20. **Zerem E, Kurtcehajic A, Kunosić S, Zerem Malkočević D, Zerem O.** Current trends in acute pancreatitis: Diagnostic and therapeutic challenges. World J Gastroenterol. 2023; 29(18): 2747-2763. *https://doi.org/10.3748/wjg.v29.i18.2747.*
21. **Hong W, Pan J, Goyal H, Zippi M.** Acute pancreatitis infection: Epidemiology, prevention, clinical characteristics, treatment, and prediction. Front Cell Infect Microbiol. 2023; 13: 1175195. *https://doi.org/10.3389/fcimb.2023.1175195.*
22. **Niu JW, Zhang GC, Ning W, Liu HB, Yang H, Li CF.** Clinical effects of phospholipase D2 in attenuating acute pancreatitis. World J Gastroenterol. 2025; 31(2): 97239. *https://doi.org/10.3748/wjg.v31.i2.97239.*
23. **Wang L, Qi X, Tian F, Li H, Zhao H, Lv J, et al.** Diagnostic value of hematological parameters in acute pancreatitis. Ann Palliat Med. 2020; 9(5): 2716-2722. *https://doi.org/10.21037/apm-20-160. 2716-2722. doi: 10.21037/apm-20-160.* Epub 2020 Jul 23. PMID: 32787347.
24. **Sun C, Li Z, Shi Z, Li G.** Current diagnosis and treatment of acute pancreatitis in China: a real-world, multicenter study. BMC Gastroenterol. 2021; 21(1): 210. *https://doi.org/10.1186/s12876-021-01799-1.*
25. **Potempa M, Hart PC, Rajab IM, Potempa LA.** Redefining CRP in tissue injury and repair: more than an acute pro-inflammatory mediator. Front Immunol. 2025; 16: 1564607. *https://doi.org/10.3389/fimmu.2025.1564607.*
26. **Ashrafizadeh M.** Cell Death Mechanisms in Human Cancers: Molecular Pathways, Therapy Resistance and Therapeutic Perspective. J Can Biomol Therap. 2024; 1(1): 17-40. *https://doi.org/10.62382/jcbt.v1i1.13.*
27. **Velissaris D, Zareifopoulos N, Lagadinou M, Platanaki C, Tsiotsios K, Stavridis EL, et al.** Procalcitonin and sepsis in the Emergency Department: an update. Eur Rev Med Pharmacol Sci. 2021; 25(1): 466-479. *https://doi.org/10.26355/eurrev_202101_24416.*
28. **Mao X, Yang Z.** Current usage status of somatostatin and its analogs and trypsin inhibitors: a real-world study of 34,654 Chinese adult patients with acute pancreatitis. Ann Palliat Med. 2021; 10(2): 1325-1335. *https://doi.org/10.21037/apm-19-363.*
29. **Ullah A, Shin G, Lim SI.** Human serum albumin binders: A piggyback ride for long-acting therapeutics. Drug Discov Today. 2023; 28(10): 103738. *https://doi.org/10.1016/j.drudis.2023.103738.*
30. **Bhansali SK, Shah SC, Desai SB, Sunawala JD.** Infected necrosis complicating acute pancreatitis: experience with 131 cases. Indian J Gastroenterol. 2003; 22(1): 7-10. PMID: 12617444.
31. **Li ZF, Xu MY, Zhang DH, Gao TT, Gao Z, Li H.** Effects of ulinastatin combined with octreotide on blood coagulation function, inflammatory factors and amylase in patients with severe acute pancreatitis. J Biol Regul Homeost Agents. 2020; 34(6): 2147-2151. *https://doi.org/10.23812/20-362-L.*
32. **Chen F, Xu Y, Wang Z.** Ulinastatin combined with somatostatin enhances disease control and modulates serum inflammatory factors in patients with severe pancreatitis. Am J Transl Res. 2023; 15(9): 5797-5807. PMID: 37854214.
33. **Dou H, Kan Y, Xu Z, Wang Z, Zheng C.** Effect of probiotics combined with Ulinastatin and Somatostatin in the treatment of severe acute pancreatitis. Pak J Med Sci. 2024; 40(8): 1729-1734. *https://doi.org/10.12669/pjms.40.8.9744.*

34. Rykina-Tameeva N, Samra JS, Sahni S, Mittal A. Non-Surgical Interventions for the Prevention of Clinically Relevant Postoperative Pancreatic Fistula-A Narrative Review. Cancers (Basel). 2023; 15(24):5865. *https://doi.org/10.3390/cancers15245865.*

35. Nickel F, Anthony Wise P. Acute pancreatitis and multiple organ failure-Who beats the odds? United European Gastroenterol J. 2021; 9(2): 137-138. *https://doi.org/10.1002/ueg2.12056.*

Invest Clin 67(2): 205 - 217, 2026 https://doi.org/10.54817/IC.v67n2a04

Predictive value of carotid atherosclerotic plaques assesment, in combination with glycosylated hemoglobin A1c and C-reactive protein levels, for disease progression in young patients with acute ischemic stroke.

Shuting Jiang[1,2†], Hongquan Liu[1,2†], Chen Zhong[3,4], Jie Yang[1,2], Yue Qin[1,2], Yechen Lu[1,2] and Mingming Fang[1,2]*

[1]Affiliated Hospital of Integrated Traditional Chinese and Western Medicine, Nanjing University of Chinese Medicine, Nanjing, Jiangsu Province, China.
[2]Department of Neurology, Jiangsu Province Academy of Traditional Chinese Medicine, Nanjing, Jiangsu Province, China.
[3]Hepatobiliary Center, The First Affiliated Hospital of Nanjing Medical University, Key Laboratory of Liver Transplantation, Nanjing, Jiangsu Province, China.
[4]Chinese Academy of Medical Sciences, NHC Key Laboratory of Hepatobiliary Cancers, Nanjing Jiangsu Province, China.
[†]The two authors contributed equally to this study.

Keywords: Ischemic Stroke; Plaque, Atherosclerotic; Carotid Arteries; C-Reactive Protein; Hemoglobin HA1c.

Abstract. This study evaluated the predictive significance of combining carotid atherosclerotic plaques assesment with glycosylated hemoglobin A1c (HbA1c) and C-reactive protein (CRP) levels for disease progression in young acute ischemic stroke (AIS) patients. A total of 130 subjects were evenly recruited, comprising young patients with AIS admitted between January 2015 and March 2025 (case group) and healthy individuals undergoing physical examinations during the same period (control group). Comparisons were conducted on the incidence rate of carotid atherosclerotic plaques and serum HbA1c and CRP levels. The case group was categorized into mild-moderate and severe groups according to the National Institute of Health Stroke Scale (NIHSS) score. Significant differences were observed between the severe and mild-moderate groups in NIHSS scores, carotid atherosclerotic plaque incidence, and serum levels of HbA1c and CRP ($p<0.05$). Increased serum HbA1c levels, elevated CRP levels, and presence of carotid atherosclerotic plaques functioned as risk factors for AIS progression in young patients (odds ratio>1, $p<0.05$).

Corresponding author: Mingming Fang. Affiliated Hospital of Integrated Traditional Chinese and Western Medicine, Nanjing University of Chinese Medicine, Nanjing 210028, Jiangsu Province, China. Email: fangmmnuem@elnu-edu.cn

Serum HbA1c and CRP levels, along with the presence of carotid atherosclerotic plaques, showed a positive correlation with NIHSS scores ($r>0$, $p<0.05$). The areas under the ROC curves of serum HbA1c and CRP levels, carotid atherosclerotic plaques and their combination for assessing AIS progression in young patients were 0.810, 0.823, 0.781, and 0.905, respectively. Elevated HbA1c, CRP, and the presence of carotid plaques are associated with AIS severity in young patients. Combined detection improves predictive accuracy, suggesting clinical utility for risk stratification.

Valor predictivo de la detección de placas ateroscleróticas carotídeas, en combinación con los niveles de hemoglobina glicosilada A1c y proteína C reactiva, para la progresión de la enfermedad en pacientes jóvenes con accidente cerebrovascular isquémico agudo.

Invest Clin 2026; 67 (2): 205 – 217

Palabras clave: Accidente Cerebrovascular Isquémico; Placa Aterosclerótica; Arterias Carótidas; Proteína C-Reactiva; Hemoglobina HA1c.

Resumen. Este estudio evaluó la significancia predictiva de combinar placas ateroscleróticas carotídeas con niveles de hemoglobina glicosilada A1c (HbA1c) y proteína C reactiva (PCR) para la progresión de la enfermedad en pacientes jóvenes con accidente cerebrovascular isquémico agudo (AIS). Se reclutó de manera uniforme un total de 130 sujetos, que comprendían pacientes jóvenes con AIS ingresados entre enero de 2015 y marzo de 2025 (grupo de casos) e individuos sanos sometidos a exámenes físicos durante el mismo período (grupo de control). Se realizaron comparaciones en la tasa de incidencia de placas ateroscleróticas carotídeas y los niveles séricos de HbA1c y PCR. El grupo de casos se categorizó en grupos leve-moderado y grave según la puntuación de la Escala de Accidente Cerebrovascular del Instituto Nacional de Salud (NIHSS). Se observaron diferencias significativas entre los grupos grave y leve-moderado en las puntuaciones NIHSS, la incidencia de placa aterosclerótica carotídea y los niveles séricos de HbA1c y PCR ($p<0,05$). El aumento de los niveles séricos de HbA1c, los niveles elevados de PCR y la presencia de placas ateroscleróticas carotídeas funcionaron como factores de riesgo para la progresión del AIS en pacientes jóvenes (odds ratio > 1, $p<0,05$). Los niveles séricos de HbA1c y PCR, junto con la presencia de placas ateroscleróticas carotídeas, mostraron una correlación positiva con las puntuaciones NIHSS ($r >0$, $p<0,05$). Las áreas bajo las curvas ROC de los niveles séricos de HbA1c y PCR, las placas ateroscleróticas carotídeas y su combinación para evaluar la progresión del AIS en pacientes jóvenes fueron 0,810, 0,823, 0,781 y 0,905, respectivamente. Los niveles elevados de HbA1c, PCR y presencia de placas carotídeas se asocian con la gravedad del AIS en pacientes jóvenes. La detección combinada mejora la precisión predictiva, lo que sugiere utilidad clínica para la estratificación del riesgo.

Received: 07-10-2025 *Accepted: 02-03-2026*

INTRODUCTION

Acute ischemic stroke (AIS) is defined as a cerebrovascular disease attributed to blood supply disorders to brain tissues, which displays high mortality and disability rates. Besides, AIS exhibits a significantly increasing incidence rate in young people in recent years along with improved living standards and changed dietary patterns of people, which has become a major disease jeopardizing the health of young adults. Through extensive and in-depth research on the pathogenesis of AIS in young patients, it is discovered that atherosclerosis acts as the underlying cause. Hence, clarifying the predictors of atherosclerosis and implementing early interventions after accurately predicting the development and progression risk of AIS are of great clinical significance for reducing the incidence, mortality and disability rates of AIS in young adults. Atherosclerotic plaques are a product of atherosclerosis, and the presence of carotid atherosclerotic plaques gives rise to narrowed inner diameter of the carotid artery, leading to artery stenosis, which, when reaching a certain degree, can cause blood shortage to the brain. Once unstable plaques rupture, the dislodged plaques can result in thrombosis in distal intracranial vessels and eventually AIS [1,2]. Abnormal glucose metabolism is able to not only induce damage to vascular endothelial cells, but also facilitate smooth muscle hyperplasia and inflammatory responses, thereby triggering atherosclerosis, which serves as a crucial cause of the development and progression of cerebrovascular diseases [3]. Glycosylated hemoglobin A1c (HbA1c), formed by the binding of hemoglobin to blood glucose in red blood cells, is a frequently measured biomarker in patients with abnormal glucose metabolism. Therefore, the glucose metabolism status in the body can be effectively mastered by measuring serum HbA1c level. C-reactive protein (CRP)-mediated inflammatory responses participate in the whole process of atherosclerosis development and progression, serving as a risk factor inducing cerebrovascular diseases [4]. Research has shown that atherosclerotic plaques and levels of serum HbA1c and CRP are correlated with the onset and advancement of AIS, potentially serving as reliable indicators of the condition.

Given this, in the present study, analyses were carried out on the distribution of carotid atherosclerotic plaques and expressions of HbA1c and CRP in young patients with AIS, as well as their correlations with and predictive value for the progression of AIS.

MATERIALS AND METHODS

Subjects

A total of 65 young AIS patients admitted to our hospital between January 2015 and March 2025 were consecutively enrolled as the case group, including 59 males and 6 females, aged 23-45 years (mean age, 39.11±5.61 years). The body mass index (BMI) of the case group ranged from 21 to 26 kg/m^2, with a mean value of 23.46 ± 0.45 kg/m^2. During the same period, 65 age- and sex-matched healthy individuals undergoing routine physical examinations at our hospital were recruited as the control group, comprising 57 males and 8 females, aged 23-46 years (mean age, 38.86±5.46 years), with a BMI ranging from 21 to 26 kg/m^2 (mean, 23.42±0.48 kg/m^2).

Inclusion and exclusion criteria

Inclusion criteria for the case group were: 1) patients diagnosed with AIS via cranial Computed Tomography (CT) images [5], 2) ischemia duration of less than 72 hours, 3) informed consent obtained from family members, and 4) first episode of the disease.

The exclusion criteria were listed below: 1) patients with such diseases as brain tumors and brain traumas, 2) those with severe insufficiency of the heart, liver, kidneys or other organs, 3) those with a history of cardiogenic AIS or AIS induced by rheumatic

heart disease, atrial fibrillation, or other factors, 4) those with a history of administration of such drugs as propranolol, morphine and hydrochlorothiazide, or 5) those with a history of surgery or traumas or a history of nosocomial infection with obvious signs and clinical evidence in the past 1 week.

Blood sample collection

A 5 mL fasting venous blood sample was collected from the median cubital vein of participants in the health group during their physical examination and from the case group on the morning before treatment, then allowed to stand at room temperature for 30 minutes. After that, centrifugation was conducted (centrifugal radius: 10 cm, centrifugation speed: 2500 r/min, and centrifugation time: 10 min). The upper serum was transferred to a centrifuge tube and stored at -80°C for future analysis.

Measurement of serum HbA1c and CRP levels

The serum was removed from refrigeration, thawed at room temperature, and analyzed for HbA1c using a latex agglutination test (RB, USA) with a reference range of 3.8-5.8%, and for CRP levels using a double-antibody sandwich ELISA [Pointe Biotechnology (Nanjing) Co., Ltd.] with a reference range of 0-5 mg/L.

Detection of carotid atherosclerotic plaques

Color Doppler ultrasonic diagnostic apparatus (produced by Aloka, Japan) was employed to detect the distribution of carotid atherosclerotic plaques in both groups. During examination, the subjects were instructed should be instructed to lie in a relaxed position, with the shoulders elevated with the help of soft pads and the head turning to the opposite side to fully extend the neck. Next, a linear array probe was selected, with the frequency set at 3-11 MHz, and evenly applied with the couplant on the surface. Ultrasonic scans were performed on the common carotid artery, its bifurcation, and the carotid bulb (typically 4.0-6.0 cm above the bifurcation). The carotid intima-media thickness (IMT) was measured three times, and the results were averaged. Presence of carotid atherosclerotic plaques was considered in case of IMT ≥1.5 mm or localized thickening exceeding 50% of the surrounding intimal thickness.

Evaluation of AIS progression

The severity of AIS in the case group was evaluated using the NIHSS score (National Institutes of Health Stroke Scale) [6]. Patients with a score of ≤15 were categorized as mild-moderate, while those scoring >15 were classified as severe.

Collection of general data

The collected data included gender, age, BMI, allergic constitution (yes/no), smoking history (≥5 years, >10 cigarettes/day), drinking history (≥5 years, >1 liang/day), hypertension (yes/no), NIHSS score, and laboratory indicators such as white blood cell count (WBC), triglycerides (TG), total cholesterol (TC), high-density lipoprotein (HDL), and low-density lipoprotein (LDL).

Statistical analysis

Statistical analysis was completed with SPSS 23.0 software. Measurement data underwent normality testing. Normally distributed data were expressed as mean ± standard deviation (X±SD) and analyzed using independent-samples t-tests for intergroup comparisons and paired-samples t-tests for intragroup comparisons. A logistic regression analysis was conducted to determine risk factors influencing AIS progression in young patients. Kendall's Tau-b and Pearson correlation analyses were used to examine the relationships between NIHSS scores and carotid atherosclerotic plaques, as well as serum HbA1c and CRP levels. ROC curves were utilized to evaluate the predictive values of carotid atherosclerotic plaques, serum HbA1c levels, serum CRP levels, and their combination for AIS progression, and the optimal cut-

off values were determined using the Youden index. AUCs >0.90 indicate high predictive value, 0.71-0.90 suggest fair value, 0.50-0.70 denote low value, and <0.50 reflect no predictive value. A p-value less than 0.05 was considered statistically significant.

RESULTS

Baseline and key characteristics

Baseline demographic, clinical, and laboratory characteristics of the case and control groups are presented in Table 1. No significant differences were observed between the two groups in age, sex, BMI, allergic constitution, smoking or drinking history, hypertension status, WBC count, or lipid profiles (TG, TC, HDL-C, and LDL-C) (all $p>0.05$). In contrast, serum HbA1c and CRP levels were significantly higher in the case group, and carotid atherosclerotic plaques were more frequently detected in the case group, whereas no plaques were observed in the control group (all $p<0.001$).

Relevant data in case and health groups

The case group exhibited significantly higher serum HbA1c levels (6.05±1.84% vs. 4.26±0.50%) and serum CRP levels (3.08±2.98 mg/L vs. 0.55±0.30 mg/L) compared with the healthy group (both $p < 0.001$). In addition, carotid atherosclerotic plaques were detected in 19 patients (29.23%) in the case group, whereas no plaques were observed in the control group ($p<0.001$) (Table 2).

Disease progression in case group

Among the 65 patients in the case group, 50 patients (76.92%) were classified as having mild–moderate AIS, and 15 patients (23.08%) were classified as having severe AIS based on NIHSS scores.

Relevant data of patients in mild-moderate and severe groups

No significant differences were found between the mild-moderate and severe groups in terms of sex distribution, age, BMI, allergic constitution, smoking history, drinking history, hypertension, WBC or serum lipid profiles, including TG, TC, HDL-C, and LDL-C (all $p>0.05$). In contrast, the severe group exhibited significantly higher NIHSS scores, as well as a higher prevalence of carotid atherosclerotic plaques and significantly elevated serum HbA1c and CRP levels, compared with the mild-moderate group ($p<0.001$) (Table 3).

Results of logistic regression analysis on AIS progression in young patients

Logistic regression analysis was carried out with AIS progression in young patients as the dependent variable (1=severe, 0=mild-moderate) and variables showing statistically significant differences in univariate analyses (except NIHSS score) as the independent variables. Serum HbA1c level (OR=17.583, 95% CI: 2.545-121.500, p=0.004), serum CRP level (OR=14.391, 95% CI: 2.852-72.625, p=0.001), and the presence of carotid atherosclerotic plaques (OR=12.667, 95% CI: 2.361-67.958, p=0.003) were independently associated with an increased risk of AIS progression in young patients (Table 4 and Fig. 1).

Results of correlation analyses

Correlation analyses demonstrated that NIHSS scores were positively correlated with serum HbA1c levels ($r=0.401$, $p=0.001$), serum CRP levels ($r=0.430$, $p<0.001$), and the presence of carotid atherosclerotic plaques ($r=0.522$, $p=0.004$) in young patients with AIS (Table 5).

Value of serum HbA1c levels, serum CRP levels, carotid atherosclerotic plaques and their combination for assessing AIS progression in young patients

ROC curves analyses were performed to evaluate the ability of serum HbA1c levels, serum CRP levels, presence of carotid atherosclerotic plaques, and their combination to discriminate severe AIS from mild–mod-

erate AIS (Fig. 2). As shown in Table 6, the AUCs were 0.810 for serum HbA1c levels, 0.823 for serum CRP levels, and 0.781 for carotid atherosclerotic plaques. The combined model demonstrated the highest discriminative performance, with an AUC of 0.905 ($p<0.001$).

DISCUSSION

In the pathogenetic process of AIS, a range of extremely complex pathophysiological variations are triggered owing to ischemia and hypoxia at lesion sites, involving multiple factors.

Table 1. Baseline characteristics and key study parameters of the case and control groups.

Variable	Case group (n=65)	Control group (n=65)	Statistical test	p value
Age (years)	39.11±5.61	38.86±5.46	t=0.258	0.797
Gender, n (%)			χ^2=0.080	0.777
Male	59 (90.77)	57 (87.69)		
Female	6 (9.23)	8 (12.31)		
Body mass index (kg/m^2)	23.46±0.45	23.42±0.48	t=0.490	0.625
Allergic constitution, n (%)			χ^2=0.301	0.583
Yes	9 (13.85)	6 (9.23)		
No	56 (86.15)	59 (90.77)		
Smoking history, n (%)			χ^2=0.040	0.841
Yes	18 (27.69)	16 (24.62)		
No	47 (72.31)	49 (75.38)		
Drinking history, n (%)			χ^2=0.037	0.847
Yes	20 (30.77)	18 (27.69)		
No	45 (69.23)	47 (72.31)		
Hypertension, n (%)			χ^2=0.035	0.851
Yes	22 (33.85)	20 (30.77)		
No	43 (66.15)	45 (69.23)		
WBC ($\times10^9$/L)	6.78±1.52	6.62±1.47	t=0.610	0.543
Serum TG (mmol/L)	1.54±0.46	1.48±0.42	t=0.777	0.439
Serum TC (mmol/L)	4.62±0.71	4.58±0.69	t=0.326	0.745
Serum HDL-C (mmol/L)	1.12±0.24	1.15±0.22	t=-0.743	0.459
Serum LDL-C (mmol/L)	2.76±0.58	2.69±0.55	t=0.706	0.481
Serum HbA1c (%)	6.05±1.84	4.26±0.50	t=7.569	<0.001
Serum CRP (mg/L)	3.08±2.98	0.55±0.30	t=6.810	<0.001
Carotid atherosclerotic plaque, n (%)			Fisher's exact test	<0.001
Present	19 (29.23)	0 (0.00)		
Absent	46 (70.77)	65 (100.00)		

Data are presented as mean ± standard deviation for continuous variables and number (percentage) for categorical variables. WBC: white blood cell count; TG: triglycerides; TC: total cholesterol; HDL-C: high-density lipoprotein cholesterol; LDL-C: low-density lipoprotein cholesterol; HbA1c: glycated hemoglobin A1c; CRP: C-reactive protein. Comparisons between the case and control groups were performed using the independent-samples t test for continuous variables and the chi-square test or Fisher's exact test for categorical variables, as appropriate.

Table 2. Relevant data in case and health groups.

Group	n	Serum HbA1c level (%)	Serum CRP level (mg/L)	Carotid atherosclerotic plaque, n (%)	
				Yes	No
Control	65	4.26±0.50	0.55±0.30	0 (0.00)	65 (100.00)
Case	65	6.05±1.84	3.08±2.98	19 (29.23)	46 (70.77)
t		7.569	6.810	22.252	
p		<0.001	<0.001	<0.001	

Data are presented as mean ± standard deviation or number (percentage). HbA1c: glycated hemoglobin A1c; CRP: C-reactive protein. Comparisons between the case and control groups were performed using the independent-samples t test for continuous variables and the chi-square test for categorical variables.

Table 3. Relevant indicators of patients in mild-moderate and severe groups

Indicator		Mild-moderate group (n=50)	Severe group (n=15)	Statistical value	p
Gender, n (%)	Male	28 (56.00)	6 (40.00)	1.184	0.277
	Female	22 (44.00)	9 (60.00)		
Allergic constitution, n (%)	Yes	3 (6.00)	0 (0.00)	0.073	0.787
	No	47 (94.00)	15 (100.00)		
Smoking history, n (%)	Yes	6 (12.00)	3 (20.00)	0.130	0.718
	No	44 (88.00)	12 (80.00)		
Drinking history, n (%)	Yes	8 (16.00)	2 (13.33)	0.025	0.875
	No	42 (84.00)	13 (86.67)		
Carotid atherosclerotic plaque, n (%)	Yes	6 (12.00)	13 (86.67)	27.592	<0.001
	No	44 (88.00)	2 (13.33)		
Hypertension, n (%)	Yes	22 (44.00)	4 (26.67)	1.444	0.229
	No	28 (56.00)	11 (73.33)		
Age (year)		39.11±5.61	40.13±5.23	0.627	0.533
BMI (kg/m^2)		23.46±0.44	23.43±0.43	0.233	0.817
WBC ($\times 10^9$/L)		3.95±0.28	3.89±0.27	0.734	0.466
Serum TG (nmol/L)		2.03±0.25	2.05±0.26	0.269	0.789
Serum TC (nmol/L)		6.85±0.16	6.88±0.18	0.619	0.538
Serum HDL-C (nmol/L)		0.84±0.17	0.82±0.16	0.405	0.687
Serum LDL-C (nmol/L)		4.87±0.13	4.85±0.15	0.504	0.616
Serum HbA1c (%)		5.50±0.55	7.88±0.62	14.276	<0.001
Serum CRP (mg/L)		2.84±0.25	3.88±0.36	12.697	<0.001
NIHSS score (points)		22.15±4.24	38.24±5.12	12.282	<0.001

Data are presented as mean ± standard deviation for continuous variables and number (percentage) for categorical variables. BMI: body mass index; WBC: white blood cell count; TG: triglycerides; TC: total cholesterol; HDL-C: high-density lipoprotein cholesterol; LDL-C: low-density lipoprotein cholesterol; HbA1c: glycated hemoglobin A1c; CRP: C-reactive protein; NIHSS: National Institutes of Health Stroke Scale; AIS: acute ischemic stroke. Comparisons between mild-moderate and severe AIS groups were conducted using the independent-samples t test for continuous variables and the chi-square test or Fisher's exact test for categorical variables, as appropriate.

Table 4. Results of logistic regression analysis on acute ischemic stroke progression in young patients.

Variable	B	Standard error	Wals	p	Odds ratio	95% confidence interval
Serum HbA1c level	2.776	0.975	7.340	0.004	17.583	2.545-121.500
Serum CRP level	2.556	0.715	9.444	0.001	14.391	2.852-72.625
Presence of carotid atherosclerotic plaques	2.428	0.656	7.764	0.003	12.667	2.361-67.958

B represents the regression coefficient. Odds ratios (ORs) and 95% confidence intervals (CIs) were calculated using multivariable logistic regression. Serum HbA1c and serum CRP levels were entered into the model as continuous variables (per 1% increase in HbA1c and per 1 mg/L increase in CRP). Presence of carotid atherosclerotic plaques was entered as a binary variable (present vs. absent). HbA1c: glycated hemoglobin; CRP: C- reactive protein.

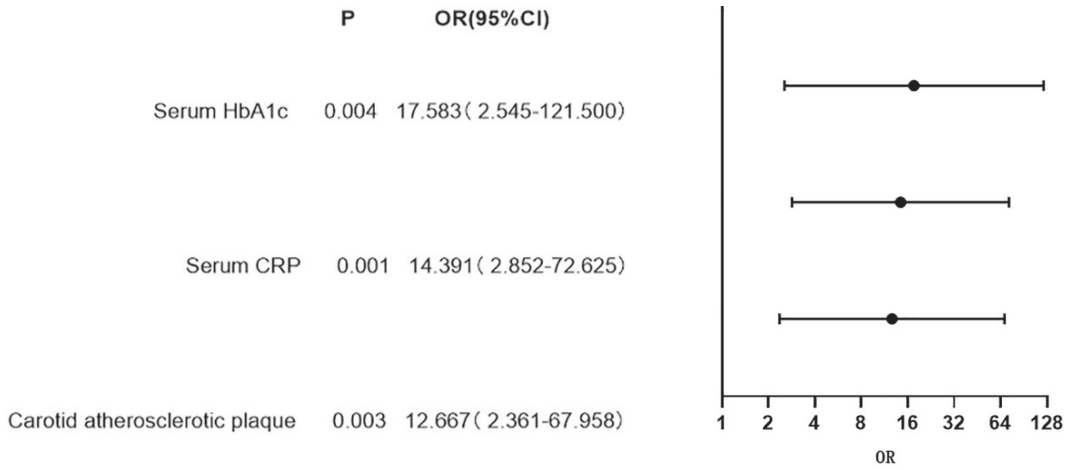

Fig. 1. Forest plot of clinical characteristics based on multivariate logistic regression analysis. Odds ratios (ORs) and 95% confidence intervals (CIs) are presented for each variable. Serum HbA1c was analyzed as a continuous variable per 1% increase, and serum CRP was analyzed per 1 mg/L increase. Presence of carotid atherosclerotic plaque was treated as a binary variable (present vs. absent). The horizontal lines represent 95% CIs, and the solid circles indicate the corresponding ORs. The x-axis is displayed on a logarithmic scale.

Table 5. Correlations of serum HbA1c and CRP levels and carotid atherosclerotic plaques with acute ischemic stroke progression in young patients.

Coefficient	Serum HbA1c level	Serum CRP level	Carotid atherosclerotic plaque
r	0.401	0.430	0.522
p	0.001	<0.001	0.004

Correlation coefficients (r) were calculated using Pearson or Kendall's Tau-b correlation analysis, as appropriate. Serum HBA1c (%) and serum CRP (mg/L) were analyzed as continuous variables. Presence of carotid atherosclerotic plaques was treated as a binary variable. p values <0.05 were considered statistically significant. HbA1c: glycated hemoglobin; CRP: C- reactive protein.

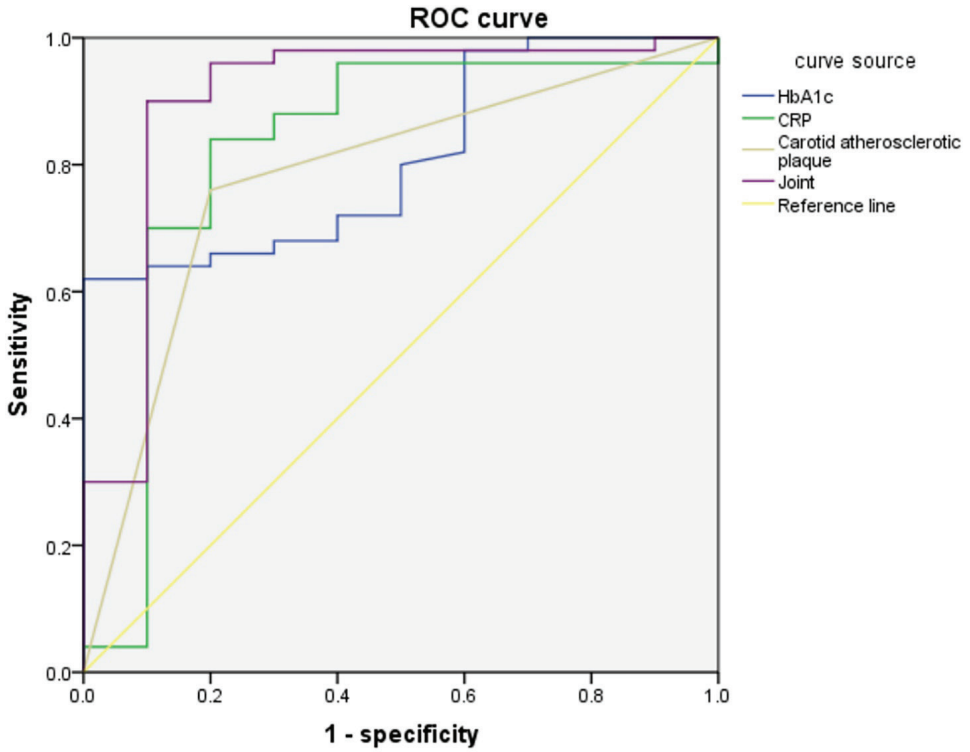

Fig. 2. ROC curves showing the predictive performance of serum HbA1c, serum CRP, carotid atherosclerotic plaque, and their combination for AIS progression in young patients. Serum HbA1c (%) and serum CRP (mg/L) were analyzed as continuous variables, and optimal cut-off values were determined using the Youden index. Presence of carotid atherosclerotic plaque was treated as a binary variable. The combined model demonstrated the highest discriminative performance, with an AUC of 0.905 ($p<0.001$).

Table 6. Value of serum HbA1c levels, serum CRP levels, carotid atherosclerotic plaques and their combination for assessing acute ischemic stroke progression in young patients.

Item	Optimal cut-off value	Area under the curve	Standard error	p	95% confidence interval	Sensitivity	Specificity	Youden index
Serum HbA1c level	7.565 %	0.810	0.063	0.002	0.688-0.934	0.640	0.900	0.540
Serum CRP level	3.015 mg/L	0.823	0.091	0.001	0.644-0.998	0.840	0.800	0.640
Carotid atherosclerotic plaque	-	0.781	0.082	0.005	0.620-0.940	0.760	0.800	0.560
Combination	-	0.905	0.067	<0.001	0.772-0.999	0.900	0.900	0.800

Receiver operating characteristic (ROC) curve analysis was performed to assess the predictive value of each parameter for AIS progression. Serum HbA1c (%) and serum CRP (mg/L) were analyzed as continuous variables, and the optimal cut-off values were determined using the Youden index. Presence of carotid atherosclerotic plaques was treated as a binary variable. The combined model was derived from multivariable logistic regression and represents the predicted probability of AIS progression. AIS: acute ischemic stroke; HbA1c: glycated hemoglobin; CRP: C- reactive protein.

A recent study reported that atherosclerotic changes in the brain and neck serve as the initiating factors for the development and progression of AIS [7]. Therefore, risk stratification of patients by identifying predictors directly associated with atherogenesis or susceptibility to atherosclerosis is conducive to more accurate implementation of interventions, and is of great clinical significance for hindering the progression of atherosclerosis to AIS.

In the present study, carotid atherosclerotic plaques were more frequently detected in the case group than in the control group, and their prevalence was significantly higher in patients with severe AIS than in those with mild–moderate AIS. Moreover, carotid atherosclerotic plaques were positively correlated with NIHSS scores and were independently associated with AIS progression in logistic regression analysis. These findings indicate that the presence of carotid atherosclerotic plaques is closely associated with disease severity and progression in young patients with AIS. Rather than establishing causality, these associations suggest that carotid atherosclerotic plaques may reflect a higher vascular risk burden in this population. It is speculated to be attributable to the following fact: Healthy arteries are elastic, but local lipid accumulation, fibrous tissue proliferation, and calcinosis of the arterial wall occur over time, starting from the intima of arteries, which gives rise to gradual hardening of arterial vessels and thus results in atherosclerosis [8,9]. As atherosclerosis progresses, atherosclerotic plaques will form in blood vessels and then gradually enlarge over time. When the plaques erode and migrate to the small blood vessels in the brain, narrowing and blockage of the arterial lumen will be induced, affecting blood flow and normal nutrient delivery and thereby arousing various symptoms and diseases associated with AIS [10,11].

Serum HbA1c and CRP levels were significantly higher in the case group than in the control group and were elevated in patients with severe AIS compared with those with mild–moderate AIS. Both biomarkers showed positive correlations with NIHSS scores and were independently associated with AIS progression in multivariable logistic regression analysis.

These results suggest that higher serum HbA1c and CRP levels are associated with greater neurological impairment and increased risk of disease progression in young AIS patients. This is ascribed to the under-mentioned facts. Elevated HbA1c levels cause a leftward shift in the oxygen dissociation curve, reducing the dissociation rate of oxyhemoglobin and increasing the affinity of red blood cells for oxygen. This results in a significant decrease in 2,3-diphosphoglycerate levels within red blood cells. If uncorrected over time, these changes can disrupt blood and oxygen supply to the brain, potentially inducing AIS [12,13]. Secondly, hypoxia-ischemia brain damage exacerbates progressively as HbA1c levels continuously increase, together with constant AIS progression in young patients. Thirdly, an elevation in HbA1c levels enhances endothelial activity, activates smooth muscle endothelin-A receptors, and stimulates the renin-angiotensin system, leading to vasoconstriction. Additionally, it enhances protein glycosylation and oxidation, with the resulting glycosylation end products stimulating LDL-C cytophagy and oxidation by lymphocytes and monocytes on the arterial wall. This process leads to foam cell formation, advancing atherosclerosis and contributing to the development and progression of AIS [14-16]. CRP is a highly sensitive inflammatory marker, typically present at very low levels in the blood, but it significantly increases during acute inflammation, trauma, or necrosis. If CRP levels increase, nuclear factor-kB is continuously activated, resulting in abnormalities in hemorheology and making the blood in the arterial blood vessels hyperviscous and hypercoagulable and flow slowly. Consequently, thrombosis is readily triggered, leading to the onset

and advancement of AIS [17-19]. Fifthly, CRP may stimulate nerve cells and glial cells to release various inflammatory factors like tumor necrosis factor-α and interleukin by activating autoreceptors and the complement system. These inflammatory factors further induce peripheral immune cells to enter the brain, exacerbating inflammatory responses, which not only aggravate brain tissue damage, but also affect the recovery of neurological function, and thus boosting the progression of AIS [20,21].

ROC curve analyses further demonstrated that serum HbA1c levels, serum CRP levels, and carotid atherosclerotic plaques each exhibited moderate discriminative ability for AIS progression, whereas their combined assessment achieved the highest predictive performance. This finding suggests that integrating metabolic, inflammatory, and vascular indicators may improve risk stratification for AIS progression in young patients. Physicians can also better understand AIS progression in young patients based on the above indicators, and thus develop more effective treatment plans. The present study clarified the correlations of carotid atherosclerotic plaques and varying serum HbA1c and CRP levels with AIS in young adults, which, however, had some shortcomings. For instance, the sample size was small, and subjects were all from the same hospital, which may result in some degree of selection bias. Besides, only univariate logistic regression analysis was conducted in data statistics, and no investigation was carried out on independent risk factors for the development and progression of AIS in young adults, which may have a certain impact on research results. Future research should increase sample sizes for multicenter prospective studies and utilize univariate and multivariate logistic regression analyses to examine the impact of independent risk factors on AIS development and progression.

In conclusion, elevated serum HbA1c and CRP levels and the presence of carotid atherosclerotic plaques were associated with increased disease severity and progression in young patients with AIS. The combined evaluation of these indicators demonstrated improved predictive performance and may provide additional value for clinical risk assessment.

Acknowledgements

None.

Funding

This study was financially supported by The Second-Level Key Project of the Sixth Phase of Jiangsu Province "333" Talent Project (No. BRA2-2201), Jiangsu Province Traditional Chinese Medicine Science and Technology Development Plan General Project (No. MS2023035), and Jiangsu Province Traditional Chinese Medicine Science and Technology Development Plan Key Project (No. ZD202415).

ORCID ID of the authors

- Shuting Jiang (SJ): 0009-0004-7236-8127
- Hongquan Liu (HL): 0009-0003-5246-3939
- Chen Zhong (CZ): 0009-0009-6729-6823
- Jie Yang (JY): 0009-0004-8218-9376
- Yue Qin (YQ): 0009-0006-7083-8679
- Yechen Lu (YL): 0009-0005-6100-435X
- Mingming Fang MF): 0009-0007-8211-0789

Conflict of interest

The authors report no conflicts of interest.

Author's contributions

SJ and MF designed the study, HL and CZ conceived and supervised the study, JY, YQ and YL performed and analyzed the experiments, SJ and MF drafted the paper. All authors read and approved the final manuscript.

REFERENCES

1. **Bos D, Arshi B, van den Bouwhuijsen QJA, Ikram MK, Selwaness M, Vernooij MW, et al.** Atherosclerotic Carotid Plaque Composition and Incident Stroke and Coronary Events. J Am Coll Cardiol. 2021;77(11):1426-1435. *http://doi.org/10.1016/j.jacc.2021.01.038.*
2. **Gerosa C, Cerrone G, Suri JS, Aimola V, Cau F, Coni P, et al.** The human carotid atherosclerotic plaque: an observational review of histological scoring systems. Eur Rev Med Pharmacol Sci. 2023;27(8):3784-3792. *http://doi.org/10.26355/eurrev_202304_32179.*
3. **Shi J, Weng J, Ding Y, Xia Y, Zhou Y, Wang X, et al.** Performance of Continuous Glucose Monitoring System Among Patients with Acute Ischaemic Stroke Treated With Mechanical Thrombectomy. Diabetes Metab Res Rev. 2024;40(8):e70001. *http://doi.org/10.1002/dmrr.70001.*
4. **Cui C, Liu L, Qi Y, Han N, Xu H, Wang Z, et al.** Joint association of TyG index and high sensitivity C-reactive protein with cardiovascular disease: a national cohort study. Cardiovasc Diabetol. 2024;23(1):156. *http://doi.org/10.1186/s12933-024-02244-9.*
5. **Mead GE, Sposato LA, Sampaio Silva G, Yperzeele L, Wu S, Kutlubaev M, et al.** A systematic review and synthesis of global stroke guidelines on behalf of the World Stroke Organization. Int J Stroke. 2023;18(5):499-531. *http://doi.org/10.1177/17474930231156753.*
6. **Candelario-Jalil E, Dijkhuizen RM, Magnus T.** Neuroinflammation, Stroke, Blood-Brain Barrier Dysfunction, and Imaging Modalities. Stroke. 2022; 53(5):1473-1486. *http://doi.org/10. 1161/STROKEAHA.122.036946.*
7. **DeLong JH, Ohashi SN, O'Connor KC, Sansing LH.** Inflammatory Responses After Ischemic Stroke. Semin Immunopathol. 2022;44(5):625-648. *http://doi.org/10.1007/s00281-022-00943-7.*
8. **Saba L, Nardi V, Cau R, Gupta A, Kamel H, Suri JS, et al.** Carotid Artery Plaque Calcifications: Lessons From Histopathology to Diagnostic Imaging. Stroke. 2022;53(1):290-297. *http://doi.org/10.1161/STROKEAHA.121.035692.*
9. **Singh RJ, Menon BK.** A Carotid Web with Atherosclerotic Plaque. Ann Neurol. 2023;94(1):203-204. *http://doi.org/10.1002/ana.26683.*
10. **van der Toorn JE, Bos D, Ikram MK, Verwoert GC, van der Lugt A, Ikram MA, et al.** Carotid Plaque Composition and Prediction of Incident Atherosclerotic Cardiovascular Disease. Circ Cardiovasc Imaging. 2022;15(3):e013602. *http://doi.org/10.1161/CIRCIMAGING.121.013602.*
11. **Boswell-Patterson CA, Hétu MF, Kearney A, Pang SC, Tse MY, Herr JE, et al.** Vascularized Carotid Atherosclerotic Plaque Models for the Validation of Novel Methods of Quantifying Intraplaque Neovascularization. J Am Soc Echocardiogr. 2021;34(11):1184-1194. *http://doi.org/10.1016/j.echo.2021.06.003.*
12. **Wang Y, Wang Y, Peng G, Liang W, Chen J, Chen K, et al.** Analysis of magnetic resonance spectroscopy characteristics in patients with type 2 diabetes complicated with stroke. Front Med. 2022;9(4):1008941. *http://doi.org/10.3389/fmed.2022.1008941.*
13. **Yang Y, Huang X, Wang Y, Leng L, Xu J, Feng L, et al.** The impact of triglyceride-glucose index on ischemic stroke: a systematic review and meta-analysis. Cardiovasc Diabetol. 2023;22(1):2. *http://doi.org/10.1186/s12933-022-01732-0.*
14. **Bruno A.** Pre-diabetes, Diabetes, Hyperglycemia, and Stroke: Bittersweet Therapeutic Opportunities. Curr Neurol Neurosci Rep. 2022;22(11):781-787. *http://doi.org/10.1007/s11910-022-01236-0.*

15. **Maida CD, Daidone M, Pacinella G, Norrito RL, Pinto A, Tuttolomondo A.** Diabetes and Ischemic Stroke: An Old and New Relationship an Overview of the Close Interaction between These Diseases. Int J Mol Sci. 2022;23(4):2397. *http://doi.org/10.3390/ijms23042397.*
16. **Liu P, Hao J, Zhang Y, Wang L, Liu C, Wang J, et al.** Acute Ischemic Stroke Comorbid with Type 2 Diabetes: Long-Term Prognosis Determinants in a 36-Month Prospective Study for Personalized Medicine. OMICS 2022;26(8):451-460. *http://doi.org/10.1089/omi.2022.0071.*
17. **Small AM, Pournamdari A, Melloni GEM, Scirica BM, Bhatt DL, Raz I,** Lipoprotein(a), C-Reactive Protein, and Cardiovascular Risk in Primary and Secondary Prevention Populations. JAMA Cardiol. 2024;9(4):385-391. *http://doi.org/10.1001/jamacardio.2023.5605.*
18. **Jiang J, Tan C, Zhou W, Peng W, Zhou X, Du J, et al.** Plasma C-Reactive Protein Level and Outcome of Acute Ischemic Stroke Patients Treated by Intravenous Thrombolysis: A Systematic Review and Meta-Analysis. Eur Neurol. 2021;84(3):145-150. *http://doi.org/10.1159/000514099.*
19. **Pastorello Y, Carare RO, Banescu C, Potempa L, Di Napoli M, Slevin M.** Monomeric C-reactive protein: A novel biomarker predicting neurodegenerative disease and vascular dysfunction. Brain Pathol. 2023;33(6):e13164. *http://doi.org/10.1111/bpa.13164.*
20. **Jang JH, Hong S, Ryu JA.** Prognostic Value of C-Reactive Protein and Albumin in Neurocritically Ill Patients with Acute Stroke. J Clin Med. 2022;11(17):5067. *http://doi.org/10.3390/jcm11175067.*
21. **Wang S, Song X, Wang Y, Gao Y, Wu J.** Elevated high-sensitivity C-reactive protein levels predict poor outcomes among patients with acute cardioembolic stroke. Ann Palliat Med. 2021;10(3):2907-2916. *http://doi.org/10.21037/apm-20-1927.*

Invest Clin 67(2): 218 - 229, 2026 https://doi.org/10.54817/IC.v67n2a05

Ensayo no aleatorizado de una intervención con terapia de la risa y su efecto en la calidad de vida de personas mayores residentes en centros gerontológicos.

Jairo L. Cardona[1], María M. Villamil[1], Ángela Quintero[1], María E. Henao[1], Laura Restrepo[2] y Daniela A. Calderón[2]

[1] Grupo de Investigación en Neurociencias y Envejecimiento (GISAM). Corporación Universitaria Remington, Medellín, Colombia.
[2] Corporación Universitaria Remington, Medellín, Colombia.

Palabras clave: Persona mayor; Terapias Complementarias; Casas para Ancianos; Salud Mental; Estudios Controlados Antes y Después.

Resumen. El incremento de personas mayores que muestran un deterioro en su calidad de vida y salud mental hace necesario profundizar en el conocimiento de los efectos de terapias complementarias en este grupo de población, por lo que se pretendió describir las variaciones en los puntajes de calidad de vida posterior a la aplicación de la terapia de la risa en personas adultas residentes en centros gerontológicos. Se realizó un estudio exploratorio con diseño cuasi-experimental, con la participación de 25 personas voluntarias mayores de 60 años, se empleó la encuesta SF-12 para medir calidad de vida relacionada con la salud, que valora las dimensiones de salud física y salud mental; aplicada antes de ocho sesiones de terapia de la risa y posterior a su terminación. Se encontraron cambios estadísticamente significativos en el puntaje total de calidad de vida una vez terminadas las secciones de terapia (p=0,001), especialmente en la dimensión de salud mental (p=0,001), sin ser significativos en la dimensión de salud física (p=0,281). Según las variables sociodemográficas quienes más se benefician de la terapia son las mujeres, los mayores de 80 años, los solteros y quienes reciben algún ingreso monetario. En cuanto a las variables de escolaridad y tipo de institución (privada o pública), todos los grupos mejoraron sus puntajes de calidad de vida. Se concluye que la terapia de la risa aplicada en adultos mayores internados incrementa los puntajes de calidad de vida en la dimensión de salud mental y el total de la escala de manera significativa.

Autor de Correspondencia: Jairo León Cardona. Corporación Universitaria Remington, Edificio Coltabaco Torre 1 Calle 51 No 51-27 Medellín, Colombia. Tel. (574) 3210000 ext 5606. Correo electrónico: jairoleon01@gmail.com

Non-randomized trial of an intervention using laughter therapy and its effect on the quality of life of older people residing in gerontological centers.

Invest Clin 2026; 67 (2): 218 – 229

Key words: Aged; Complementary Therapies; Homes for the Aged; Mental Health; Controlled Before-After Studies.

Abstract. The rise in older adults experiencing deterioration in quality of life and mental health underscores the need to deepen our understanding of the effects of complementary therapies on this population. Therefore, this study aimed to describe changes in quality-of-life scores following laughter therapy among adults residing in gerontological centers. An exploratory quasi-experimental study was conducted with 25 volunteers aged 60 and older. The SF-12 survey, which assesses physical and mental health dimensions, was administered before and after eight laughter therapy sessions. Statistically significant improvements were observed in the total quality-of-life score after completing the therapy sessions ($p = 0.001$), particularly in the mental health dimension ($p = 0.001$), whereas changes in the physical health dimension were not significant ($p = 0.281$). By sociodemographic variables, those who benefited most were women, those over 80 years of age, single individuals, and those with a monetary income. Regarding education and the type of institution (private or public), all groups improved their quality-of-life scores. In conclusion, laughter therapy applied to older adult residents in nursing homes significantly increases quality-of-life scores in the mental health dimension and on the total scale.

Recibido: 24-09-2025 Aceptado: 16-03-2026

INTRODUCCIÓN

En los adultos mayores se presentan situaciones complejas dadas las distintas condiciones que puede sufrir, entre ellas la pérdida de amigos y familiares, el padecimiento de enfermedades crónicas, la dificultad de obtener un empleo; y en algunos casos ser internados en hogares gerontológicos. Estas situaciones pueden desmejorar la calidad de vida de las personas mayores, aumentando el riesgo de enfermar o llevar a un rápido detrimento del estado de salud.

La terapia de la risa ha sido utilizada en distintos contextos, con resultados positivos importantes, especialmente en el área de la pediatría, pero también en pacientes con enfermedades más riesgosas como sida, cáncer y terminales [1].

Los efectos positivos se muestran en las esferas psicosociales y la salud física, debido a la disminución de los niveles de ansiedad y estrés, mejorando el bienestar psicológico, la satisfacción con la vida y el estado de ánimo después de la intervención [2]. La literatura reporta intervenciones en padecimientos como la depresión, la esquizofrenia, entre otras patologías mentales [3,4].

En el organismo opera con un efecto opuesto a la tensión; teniendo resultados favorables en el sistema cardiovascular [5-7], inmunológico, endocrino, entre otros [8]. Al-

gunos autores consideran la risa como predictora de la discapacidad funcional y la mortalidad [9].

Otra esfera que se afecta positivamente es la social; al incrementarse las relaciones amistosas, facilitando la comunicación entre los integrantes del grupo, resolviendo favorablemente situaciones incómodas y derrumbando barreras durante el desarrollo de la intervención [10]. Además, estas intervenciones se consideran simples y de bajo costo, ya que no se necesita realizar en ningún espacio en concreto y pueden ser administradas por personal que no requiere formación especializada [11].

Distintos estudios que se centran en la vejez, expresan la importancia de la salud física y sobre todo mental, procurando disminuir costos médicos en esta población[12]; dado que la edad está asociada con padecimientos de tipo crónico; además de sentimientos de aislamiento y ausencia de apoyo social, que afectan la calidad de vida [13].

La calidad de vida como término comprende amplios rangos y dimensiones, por lo que debe ser abordada con una visión multidimensional que incluye factores ambientales, económicos, sociales y culturales, además de la autopercepción de la salud que está afectada por las limitaciones, estado funcional, oportunidades sociales, y que se relacionan con las enfermedades, lesiones, tratamientos y atención sanitaria recibida, entre otros [14,15].

Ahora bien, el nuevo espacio en los centros gerontológicos implica en las personas mayores internadas alejamiento de su familia, de su ambiente cotidiano, incremento de los niveles de estrés, unido a la situación de salud específica que padece, pueden afectar la percepción de su calidad de vida. El aumento de personas mayores a nivel regional y global, que evidencian un deterioro en su calidad de vida y salud mental, lo convierten en un problema desafiante en salud pública que requiere intervenciones urgentes que se centren de manera integral en atender los distintos factores que deterioran la calidad de vida de este grupo poblacional [16,17].

De ahí la importancia de profundizar en el conocimiento de los efectos de la terapia de la risa aplicada en personas mayores comprobando los efectos positivos en la dimensiones física y mental que miden calidad de vida en las personas adultas internadas. Por tanto, el objetivo de este trabajo fue identificar los cambios en los puntajes de calidad de vida después de la aplicación de terapia de la risa en personas mayores residentes en hogares gerontológicos.

PACIENTES Y MÉTODOS

Estudio exploratorio con diseño cuasiexperimental; la unidad de análisis fue cada adulto mayor que participó en las 8 sesiones de terapia de la risa inducida (una semanal) y que diligenciaron ambas encuestas, una de ellas antes de las terapias y la segunda después de finalizadas, estas fueron administradas por los investigadores entre los meses de septiembre y noviembre de 2015. Este articulo forma parte de un estudio más amplio, donde se midieron otros componentes, como el nivel de estrés, la respuesta inmunológica, estado fisiológico y depresión como respuesta a una intervención con terapia de la risa [18].

Muestra a conveniencia, donde todos los adultos mayores fueron invitados a participar del estudio en dos centros gerontológicos del Valle de Aburrá, para una muestra final de 25 adultos mayores de 60 años. Uno de los centros gerontológicos es privado, sus residentes o familiares deben de pagar los costos de su permanencia, participaron 12 adultos mayores. El otro centro gerontológico es financiado por la administración municipal y acceden aquellos que no poseen recursos para su sostenimiento, han sido abandonados por sus familias o estaban en situación de calle. De este centro participaron 13 adultos mayores.

Los criterios de inclusión fueron adultos mayores de 60 años con capacidad cognitiva, este criterio fue valorado por las coordinadoras de ambos centros que emplean el cuestionario Mini Mental State Examination

(MMSE) [19] para detectar déficit cognoscitivo y la observación directa. Además, que hubieren participado en al menos cinco terapias de las ocho programadas. Los criterios de exclusión fueron adultos mayores que se encontraban en duelo (perdida afectiva cercana y resiente) trastorno del sueño y dolor o que participaran en menos de cinco secciones de terapia. Las variables utilizadas fueron edad, género, estado civil, nivel educativo, ingresos y tipo de institución. Se utilizó el instrumento SF-12 encuesta para Calidad de vida validada para Colombia [20], a partir de 12 preguntas que miden ocho conceptos de salud conformando las dimensiones de salud física (función física, rol físico, dolor corporal y salud general) y salud mental (vitalidad, función social, rol emocional y salud mental) y la sumatoria de ambas dimensiones transformada en una escala de 0 a 100 [21]. Se obtuvo la autorización de la empresa representante para utilizar la encuesta SF-12.

La terapia de la risa fue aplicada por dos payasos con vasta experiencia en ámbitos hospitalarios adscritos a la Fundación Mediclaun de Medellín, los cuales no participaron en la evaluación de los resultados del proyecto, solo se limitaron a la aplicación de la terapia dada su experticia. Estos, al ingresar a los sitios de los centros gerontológicos donde se encontraban los adultos mayores, usualmente en pequeños grupos de tres a cinco integrantes hacían intercambio de juegos entre ellos, preguntas obvias o absurdas, música, canto, entre otras actividades, induciendo a los participantes a implicarse en sus juegos. los investigadores aseguraban que la intervención en cada pequeño grupo no fuera inferior a 15 minutos. Si el participante se encontraba solo o en su habitación, también se le hacia la intervención, asegurando que se cumpliera con el tiempo establecido.

Se usó el paquete estadístico SPSS versión 24 para Windows (Licencia de la universidad). Para el análisis univariado de las variables cualitativas (género, estado civil, nivel educativo, ingresos) se emplearon frecuencias absolutas y proporciones; para las variables cuantitativas (edad, puntaje SF-12), rangos, desviación estándar y promedios. De acuerdo a la distribución normal de los datos se empleó diferencia de medias con prueba de t de Student para muestras relacionadas en la comparación de los puntajes de las variables género, estado civil, nivel educativo, ingresos y tipo de institución en la cual residía. El nivel de significancia se fija en $p<0,05$.

Al grupo de voluntarios participantes se les compartió los objetivos, posibles beneficios y riesgos en la aplicación de la terapia de la risa y se recogió su consentimiento informado. El estudio se considera con riesgo mínimo (Resolución 8430 de 1993), siguiendo los parámetros de la Declaración de Helsinki de la Asociación Médica Mundial [22] y fue aprobado por el comité de ética de la Corporación Universitaria Remington, acta de 12/08/2015. Se siguieron las recomendaciones para evaluaciones no aleatorias de intervenciones conductuales y de salud pública de la declaración TREND [23].

RESULTADOS

El 52% de los participantes eran mujeres, la edad promedio de 81,9 años y una desviación estándar (DE) de 7,6; el 64% había cursado uno o varios niveles de primaria, el estado civil más frecuente fue el soltero (60%) y el 36% percibía algún ingreso (Tabla 1).

Los resultados muestran que el puntaje de calidad de vida en la dimensión de salud física después de la aplicación de la terapia de la risa en los adultos mayores institucionalizados, aunque se incrementa, no alcanza cambios significativos ($p = 0,281$); por el contrario, en la dimensión de salud mental este pasa de un puntaje promedio al inicio de 45,6 a 56,9 indicando un cambio estadísticamente significativo ($p = 0,001$), al realizar la sumatoria de ambas dimensiones esta se incrementa en 6,9 puntos en promedio, con un resultado total de calidad de vida relacionada con la salud de 49,2 puntos ($p = 0,000$) (Fig. 1).

Tabla 1. Variables sociodemográficas de adultos mayores residentes en hogares gerontológicos.

Variable		n	%
Género	Femenino	13	52
	Masculino	12	48
Edad (en años) Promedio (81,9) Desviación estándar (DE: 7,6)	65 a 80	13	52
	> 80	12	48
Nivel educativo	Ninguno	8	32
	Primaria (Completa o Incompleta)	16	64
	Técnico Incompleto	1	4
Estado civil	Soltero	15	60
	Viudo	9	36
	Unión Libre	1	4
Recibe ingresos	Sí	9	36
	No	16	64
Tipo de centro gerontológico	Privado	12	48
	Municipal	13	52

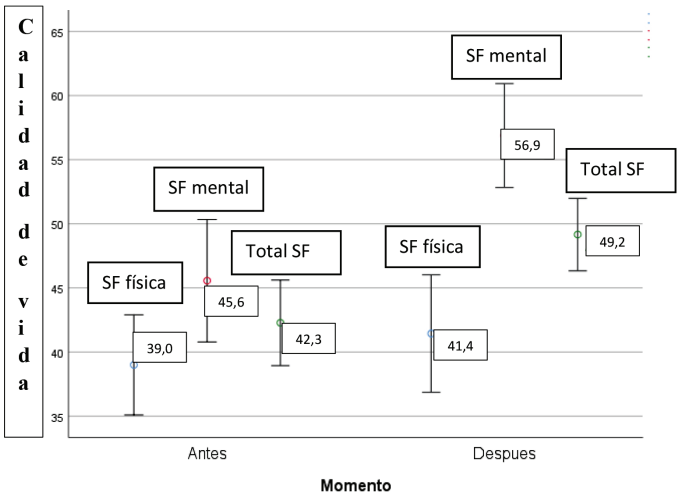

Fig. 1. Cambios en el puntaje de calidad de vida después de la terapia de la risa en adultos mayores institucionalizados. SF: Salud Física p = 0,281; SF: Salud Mental p = 0,001; Total SF: Calidad de Vida p = 0,001. p: prueba de t de Student para muestras relacionadas.

En referencia al género, se destaca que en el femenino se dan cambios significativos en las dimensiones de salud mental y en el total (p = 0,001), pero no en la dimensión de salud física. Los hallazgos obtenidos en el sexo masculino, indican una ausencia de cambios significativos en las dimensiones evaluadas, aunque aumentaron los puntajes (Tabla 2).

Respecto al grupo de edad, en menores de 80 años no se encuentran cambios significativos en las dimensiones de salud física y salud mental; sin embargo, se encontró significancia al borden line para el total de calidad de vida (p = 0,047). En mayores de 80 años, hay cambios significativos en las dimensiones de salud mental (p = 0,003) y salud total (p = 0,002) (Tabla 2).

Tabla 2. Cambios en el puntaje promedio de calidad de vida después de la terapia de la risa en adultos mayores institucionalizados según variables sociodemográficas.

Variable	Salud Física			Salud Mental			Total Calidad de vida		
	Pre	Post	p	Pre	Post	p	Pre	Post	p
Femenino	35,0±9,3	39,1±12,0	0,209	40,8±9,7	58,2±9,3	0,001	37,9±6,9	48,7±8,0	0,001
Masculino	43,3±7.9	44,0±9,9	0,841	50,8±11,6	55,4±10,5	0,306	47,0±6,6	49,7±5,6	0,163
Hasta 80 años	41,3±10,8	44,5±10,3	0,182	48,0±12,0	54,7±8,2)	0,108	44,7±8,3	49,6±6,8	0,047
Mayores de 80 años	36,5±7,4	38,1±11,4	0,699	42,9±11,0	59,3±11,1	0,003	39,7±7,4	48,7±7,2	0,002
Ningún nivel de escolaridad	37,4±8,9	35,4±13,1	0,707	40,9±12,2	58,3±9,5	0,017	39,1±8,9	46,8±7,2	0,035
Algún nivel de escolaridad	40,3±10,0	44,5±9,4	0,079	48,3±11,1	56,8±10,3	0,030	44,3±7,4	50,6±6,7	0,007
Solteros	38,9±9,0	40,1±10,5	0,693	45,6±10,4	58,9±9,9	0,005	42,2±7,4	49,5±5,5	0,004
Viudos	40,6±10,4	45,8±10,3	0,136	48,1±11,7	53,6±9,9	0,193	44,3±7,5	49,7±8,6	0,075
Reciben algún ingreso	36,3±7,5	44,6±10,6	0,035	44,7±10,5	62,0±7,2	0,003	40,5±7,3	53,3±5,7	0,005
No reciben ningún ingreso	40,5±10,3	39,7±11,3	0,765	46,1±12,4	54,0±10,1	0,056	43,3±8,6	46,8±6,5	0,060
Privado	36,3±8,3	41,9±9,8	0,102	43,7±10,	57,3±10,5	0,004	40,0±6,8	49,6±7,3	0,002
Municipal	41,5±10,1	41,0±12,6	0,859	47,3±13,0	56,5±9,5	0,067	44,4±8,8	48,8±6,7	0,035

Datos expresados en promedio ± desviación estándar. **p:** prueba de t de Student para muestras relacionadas.

En los valores de calidad de vida en adultos mayores tanto en quienes no tienen ningún nivel de escolaridad, como en aquellos que cursaron la primaria completa o incompleta, se encontraron cambios significativos en la dimensión de salud mental (p= 0,017; p= 0,030; respectivamente) y en el total de calidad de vida (p= 0,035; p= 0,007; respectivamente); en la dimensión de salud física los cambios no fueron significativos, aclarando que una persona que reportó tener estudios técnicos sin concluir, no fue integrada en este análisis (Tabla 2).

El 96% de los adultos mayores intervenidos son solteros o viudos, solo uno cuenta con pareja y fue excluido para el análisis de esta variable. En los viudos, aunque se incrementaron los puntajes en ambas dimensiones, estas no alcanzaron significancia estadística (p= 0,075), en contraposición a los resultados alcanzados por los solteros que obtuvieron cambios significativos en las dimensiones de salud mental y salud total (p = 0,005; p = 0,004, respectivamente) (Tabla 2).

En referencia a los ingresos, aquellos que manifestaron no recibir ningún tipo de ingresos, no se hallaron cambios significativos en ninguna de las dimensiones; pero quienes reciben algún tipo de ingresos, se encontraron cambios significativos en todas las dimensiones valoradas. De acuerdo al tipo de hogar donde residen, los participantes del centro gerontológico privado muestran cambios significativos tanto en salud mental, como en el puntaje total de la escala; en los participantes del centro municipal se reporta para el total de calidad de vida (Tabla 2).

DISCUSIÓN

Se ha reportado que la terapia de la risa disminuye los malestares físicos, fortalece la relación entre los adultos mayores, la distracción momentánea de sus problemas, penas y el estrés cotidiano, lo cual repercute en su calidad de vida [24]. Varios autores reportan el incremento de la calidad de vida como efecto de la terapia de la risa [13, 25-28], la discusión se centra en los aspectos de la salud que se ven impactados positivamente por la terapia y la intensidad de este impacto en el incremento de la calidad de vida. Hwang y col. [26], afirman que la terapia de la risa tiene un efecto significativo en el aumento de la calidad de vida de las personas mayores de 65 años, al igual que Kayserilioğlu y Koçaşlı[27] que expresan que la terapia de la risa aplicada a pacientes adultos es eficaz para aumentar la calidad de vida, la calidad del sueño, y también eficaz para reducir el nivel de estrés y ansiedad; además de mejorar la depresión y la soledad [28].

En este sentido Üner, Sezer y Kadıoğlu[29], encontraron que la terapia de la risa era eficaz para reducir el dolor, la depresión, el estrés y la ansiedad en las personas y aumentar la calidad del sueño, pero evidencia limitada del efecto de la terapia en la somatización, la glucosa en sangre, la presión arterial, las endorfinas y los niveles de cortisol, aunque, otros autores reportan mejoría en la fisiología corporal, como la reducción del nivel de cortisol [30], la inducción de la secreción de algunas inmunoglobulinas, endorfinas y derivados, la aceleración de la circulación, el fortalecimiento de la inmunidad y la mejora del sueño [27].

Es claro en los trabajos reportados anteriormente la mejoría en la calidad de vida y el componente mental, resultados concordantes con los obtenidos en este trabajo, que muestran un incremento significativo de la calidad de vida, específicamente en la dimensión mental, que comprende los factores de: "vitalidad, función social, rol emocional y salud mental" [21], aspecto también reportado por Bennett y col. [31]; en el mismo sentido y en población colombiana en un estudio de calidad de vida en adultos mayores no institucionalizados, donde se utilizó la escala SF-12, los mayores puntajes se obtuvieron en los componentes de salud mental [20].

En este estudio los cambios en la dimensión de salud física que comprende: "la función física, rol físico, dolor corporal y salud general" [21] y que incluye preguntas sobre limitaciones para hacer esfuerzos moderados, caminar más de una hora, subir por la escalera, dejar de hacer algunas tareas y la presencia de dolor; mejoró, pero no alcanzó diferencias significativas, lo cual pudo deberse al tamaño reducido de la muestra; pues, autores como Tamada y col. [9], encontraron un incremento del riesgo de discapacidad funcional en 1,42 veces en aquellos adultos mayores que nunca o casi nunca ríen en comparación con aquellos que lo hacen frecuentemente; resultados congruentes son reportados por Hayashi y col. [5], afirmando que la risa puede ser un factor importante para promoción de la salud general y mental de los adultos mayores, pero precisando que estos mecanismos que vinculan la risa y la salud merecen más estudio.

Mora y Ubal [32], afirman que las mujeres emplean más la risa para afrontar el estrés a nivel social que los hombres y la utilizan con mayor frecuencia para encausar emociones positivas y descargas emocionales. Esta afirmación pudiera explicar los resultados encontrados en este estudio, donde las mujeres mostraron un aumento significativo en la dimensión de salud mental y total de calidad de vida, cambios que no se encontraron en los hombres.

Se observó una mejoría de la calidad de vida en ambos grupos de edad, aunque con mayor significancia en el grupo de adultos mayores de 80 años, que podría indicar una mejor aceptación de los adultos más longevos por este tipo de terapia. López-García y col. [33] al revisar los valores referencia de la escala SF36 de calidad de vida relacionada con la salud en población española adulta,

concluyen que con el aumento de edad disminuían los valores promedios de todos los componentes de la escala, a excepción de la salud mental. Otros trabajos, por el contrario, reportan que los adultos menores de 80 años obtienen una mejor medida en el estado de salud mental que los adultos más viejos [34], y obtuvieron una mejor respuesta a la terapia de la risa en la disminución de la depresión [4].

Se observaron cambios positivos en la calidad de vida en los dos grupos de escolaridad, aunque ambos muestran los bajos niveles alcanzados, son más significativos estos cambios en los adultos mayores que cursaron la primaria o parte de esta en comparación con aquellos que no cursaron ningún grado. También, en otro estudio se reporta que aquellos que cursaron algún nivel de primaria obtuvieron mejor respuesta de la terapia de la risa y el teatro al estrés, a la depresión y mejoría en la autoestima, en comparación con aquellos que no cursaron ninguno [35].

El 60% de los adultos mayores estudiados eran solteros, los cuales reportaron cambios más significativos en el incremento de los puntajes de calidad de vida, en contraste con los puntajes de los viudos que, aunque mejoraron, estos no alcanzaron significancia estadística, lo cual puede estar influencia por el tamaño de la muestra empleado. Sin embargo; pudiera ser que la ausencia de su pareja afecte los posibles efectos benéficos de la terapia. La ausencia de compañero fue la principal variable explicativa en un modelo pronóstico de soledad [36], pero para Demakakos y col. [37], aquellos que nunca han tenido una convivencia marital (los solteros) no se relacionan con estas características. Lo anterior podría corresponder con las discrepancias halladas en este estudio entre viudos y solteros.

En cuanto a los ingresos, quienes mejores cambios en los puntajes de calidad de vida obtuvieron, fueron aquellos que expresaron recibir alguno. Lo cual puede relacionarse con los resultados de Quintero y col. [4], con adultos mayores residentes en un centro gerontológico encontrando que aquellos procedentes de estrato dos, obtuvieron un mejor efecto en la mejoría de los síntomas depresivos como respuesta a la terapia de la risa, comparados con aquellos procedentes del estrato uno. Expresa Sarabia [38] que la percepción subjetiva de la calidad del envejecimiento puede estar asociado a un alto grado de calidad de vida demostrado en estudios longitudinales, donde aquellos adultos con características específicas como "salud, estatus social, buenas relaciones interpersonales; tenían una percepción más alta de su propio bienestar comparado con las personas que carecían de estas características" [38].

Los resultados fueron positivos en el puntaje de calidad de vida; tanto, en el centro gerontológico privado, como en el municipal; lo que podría sugerir que la terapia de la risa impacta tanto para quienes han tenido condiciones adecuadas en el trascurso de vida, como en aquellos que no. Aunque los cambios más positivos se hubieren registrado en los centros privados.

Dentro las limitaciones de este estudio se tiene el pequeño tamaño de muestra elegida a conveniencia con los adultos que voluntariamente desearon participar, por lo que los resultados deben ser mirados con precaución; además, la calidad de vida se midió con un solo instrumento. Se recomienda realizar estudios experimentales con mayor tamaño de muestra que puedan corroborar los hallazgos iniciales de este trabajo.

A juzgar por la literatura revisada para la presentación de este informe, son pocos los estudios realizados en Latinoamérica que traten de medir los efectos de esta terapia en la calidad de vida y su relación con factores socio demográficos en los adultos mayores internados; además que compara estos resultados entre residentes en una institución pública con una privada.

Los resultados sugieren que la terapia de la risa en los adultos mayores institucionalizados es benéfica, ya que mejora la calidad de vida significativamente, especialmente en

la dimensión mental; además, es asequible y puede ser empleada en las instituciones para hacer la estancia de los adultos mayores más agradable, mejorando su calidad de vida [13]. Y teniendo en cuenta que el segmento de población que tiene un mayor crecimiento, tanto a nivel global como en nuestro país, es el de mayores de 60 años y son quienes sufren con mayor frecuencia el deterioro de sus funciones mentales y calidad de vida, lo convierten en un problema de salud pública [17].

Considerando, además que las acciones de intervención en salud que se centran en la curación, no son pertinentes dado que las enfermedades ya están instaladas, se sugiere que los servicios de salud deben centrarse en ralentizar, detener, o revertir el deterioro de las capacidades en los adultos mayores, por lo que debe revisarse con mayor atención el empleo de este tipo de intervenciones como la terapia de la risa [16,17].

Los próximos estudios deben ser ensayos controlados, aleatorios, estandarizados con tamaños muestrales suficientes; además de precisar el número y la frecuencia más apropiada de secciones con personal capacitado, probando los efectos de la terapia de la risa inducida tanto en adultos internados como en grupos comunitarios [11].

Agradecimiento

Nuestros más sinceros agradecimientos para todos los adultos mayores que nos acompañaron, al personal directivo de los centros participantes que abrieron sus puertas y a la Corporación Universitaria Remington por su financiación y disposición.

ORCID ID de los autores

- Jairo L. Cardona (JC): 0000-0003-3383-1401
- María M. Villamil (MV): 0000-0003-4641-9504
- Ángela Quintero (AQ): 0000-0002-2727-7312
- María E. Henao (MH): 0000-0002-9403-748-2
- Laura Restrepo (LR): 0009-0004-9675-3222
- Daniela A. Calderón (DC): 0009-0005-5733-1243

Contribución de los autores

JC: Participación en el diseño del trabajo de investigación, análisis e interpretación de los datos, construcción de tablas y figuras, aprobación de la versión final del manuscrito. MV: Participación en el diseño del trabajo de investigación, supervisión de la calidad de las encuestas, elaboración de la base de datos e interpretación de los resultados, aprobación de la versión final del manuscrito. AQ: Participación en el diseño del trabajo de investigación, contribución a la concepción del artículo, aprobación de la versión final del manuscrito. MH: Participación en el diseño del trabajo de investigación, contribución a la concepción del artículo, encargada de la logística en el desarrollo del proyecto. LR: Análisis e interpretación de los datos, aprobación de la versión final del manuscrito. DC: Análisis e interpretación de los datos, aprobación de la versión final del manuscrito.

Conflicto de interés

Los autores afirman no tener conflictos de interés.

REFERENCIAS

1. **Bennett P, Parsons T, Ben-Moshe R, Weinberg M, Neal M, Gilbert K, et al.** Laughter and Humor Therapy in Dialysis. Semin Dial. 2014; 27(5): 488–493. *https://doi.org/10.1111/sdi.12194*
2. **Demir Doğan M.** The Effect of Laughter Therapy on Anxiety. Holist Nurs Pract. 2020; 34(1):35-39. *https://doi.org/10.1097/HNP.0000000000000363.*

3. **Kafle E, Papastavrou G, Chawner D, Foye U, Declercq D, Brooks H**. Beyond laughter: a systematic review to understand how interventions utilise comedy for individuals experiencing mental health problems. Front Psychol. 2023; 14:1161703. *https://doi.org/10.3389/fpsyg.2023.1161703*
4. **Quintero Á, Henao M, Villamil M, Cardona J**. Cambios en la depresión y el sentimiento de soledad después de la terapia de la risa en adultos mayores internados. Biomédica 2015; 35(1):90-100. *http://dx.doi.org/10.7705/biomedica.v35i1.2316*
5. **Hayashi K, Kawachi I, Ohira T, Kondo K, Shirai K, Kondo N**. Laughter is the Best Medicine? A Cross-Sectional Study of Cardiovascular Disease Among Older Japanese Adults. J Epidemiol. 2016; 26(10): 546–552. *https://doi.org/10.2188/jea.JE20150196*
6. **Ikeda S, Ikeda A, Yamagishi, Hori M, Kubo S, Sata M, et al.** Longitudinal trends in blood pressure associated with the frequency of laughter: the circulatory risk in communities' study (circs), a longitudinal study of the Japanese general population. J Epidemiol. 2021; 31(2): 125–131. *https://doi.org/10.2188/jea.JE20190140*
7. **Sakurada K, Konta T, Watanabe M, Ishizawa K, Ueno Y, Yamashita H, et al.** Associations of frequency of laughter with risk of all-cause mortality and cardiovascular disease incidence in a general population: findings from the Yamagata study. J Epidemiol. 2020; 30(4): 188–193. *https://doi.org/10.2188/jea.JE20180249*
8. **Morishima T, Miyashiro I, Inoue N, Kitasaka M, Akazawa T, Higeno A, et al**. Effects of laughter therapy on quality of life in patients with cancer: An open-label, randomized controlled trial. PLoS ONE. 2019; 14(6): e0219065. *https://doi.org/10.1371/journal.pone.0219065*
9. **Tamada Y, Takeuchi K, Yamaguchi C, Saito M, Ohira T, Shirai K, et al.** Does Laughter Predict Onset of Functional Disability and Mortality Among Older Japanese Adults? The JAGES Prospective Cohort Study. J Epidemiol. 2021; 31(5): 301–307. *https://doi.org/10.2188/jea.JE20200051*
10. **Cardona J, Villamil M, Quintero A, Henao E**. Terapia de la risa en un grupo de mujeres adultas. Rev Fac Nac Salud Pública. 2013; 31(2): 202-208. https://www.redalyc.org/articulo.oa?id=12028113005
11. **Van Der Wal N, Kok R**. Laughter-inducing therapies: Systematic review and meta-analysis. Soc Sci Med. 2019; 232: 473-488. *https://doi.org/10.1016/j.socscimed.2019.02.018.*
12. **Yoshikawa Y, Ohmaki E, Kawahata H, Maekawa Y, Ogihara T, Morishita R, et al.** Beneficial effect of laughter therapy on physiological and psychological function in elders. Nurs Open. 2018; 6(1): 93–99. *https://doi.org/10.1002/nop2.190.*
13. **Rezaei S, Mahfeli M, Mousavi S, Hosseini S**. The Effect of Laughter Yoga on the Quality of Life of Elderly Nursing Home Residents. Caspian J Neurol Sci. 2019; 5(1):7-15. *https://doi.org/10.32598/CJNS.5.16.7*
14. **Villareal G, Pérez C, Usta A**. Salud y calidad de vida auto percibida de los adultos mayores en un municipio del caribe colombiano. SUN. 2022; 38(1):35-50. *https://dx.doi.org/10.14482/sun.38.1.613.042*
15. **Varela L.** Salud y calidad de vida en el adulto mayor. Rev Peru Med Exp Salud Publica. 2016; 33(2):199-201. *https://doi.org/10.17843/rpmesp.2016.332.2196*
16. **Organización Mundial de la Salud**. Informe mundial sobre el envejecimiento y la salud. E.E.U.U: OMS 2015; [citado, 2022 marzo 10] Disponible en: https://www.who.int/es/publications/i/item/9789241565042
17. **Gálvez M, Aravena C, Aranda H, Ávalos C, López-Alegría F.** Salud mental y calidad de vida en adultos mayores: revisión sistémica. Rev Chil Neuropsiquiatr. 2020; 58(4): 384-399. *http://dx.doi.org/10.4067/S0717-92272020000400384*
18. **Cardona J, Henao M, Quintero A, Villamil M, Higuita E, Ramirez L, et al**. La importancia de la RISA en la salud de los adultos mayores institucionalizados. Medellín: Corporación Universitaria Remington; 2020. *https://doi.org/10.22209/9789585321809*

19. **Rosselli D, Ardila A, Pradilla-Ardila G, Morillo L, Bautista L, Rey O, GENECO**. El examen mental abreviado (Mini-Mental State Examination) como prueba de tamizaje para el diagnóstico de demencia: estudio poblacional colombiano. Rev Neurol. 2000; 30 (5): 428-432. *https://doi.org/10.33588/rn.3005.99125*
20. **Ramírez-Vélez R, Agredo-Zuñiga R, Jerez-Valderrama A**. Confiabilidad y valores normativos preliminares del cuestionario de salud SF-12 (Short Form 12 Health Survey) en adultos colombianos. Rev Salud Pública. 2010; 12(5): 807–819. https://revistas.unal.edu.co/index.php/revsaludpublica/article/view/33328
21. **Vera-Villarroel P, Silva J, Celis-Atenas K, Pavez P**. Evaluación del cuestionario SF-12: verificación de la utilidad de la escala salud mental. Rev Med Chile. 2014; 142(10):1275-1283. *http://dx.doi.org/10.4067/S0034-98872014001000007*
22. **Asociación Médica Mundial.** Declaración de Helsinki de la AMM – Principios éticos para las investigaciones médicas en seres humanos. Helsinki, Finlandia: 75ª Asamblea General; 2024. Disponible en: https://www.wma.net/es/que-hacemos/etica-medica/declaracion-de-helsinki/.
23. **Des Jarlais DC, Lyles C, Crepaz N; TREND Group**. Improving the reporting quality of nonrandomized evaluations of behavioral and public health interventions: the TREND statement. Am J Public Health. 2004;94(3):361-366. *https://doi.org/10.2105/ajph.94.3.361*
24. **Nagai M, Ohira T, Shirai K, Kondo K**. Does variety of social interactions associate with frequency of laughter among older people? The JAGES cross-sectional study. BMJ open. 2021; 11(1): e039363 *http s://doi.org/10.1136/bmjopen-2020-039363.*
25. **Díaz de Villegas V, Medina S, Iglesias J**. Payaso terapéutico, alternativa en la Sala de Geriatría. Acta Med Cent. 2019; (13): 428-434. https://www.medigraphic.com/pdfs/medicadelcentro/mec-2019/mec193o.pdf
26. **Hwang SH, Jeong HC, Hwang JW**. Effect of laughter therapy on healthy life: a meta-analysis. J Korea Converg Soc. 2019; 10(9): 291-299. *https://doi.org/10.15207/JKCS.2019.10.9.291*
27. **Kayserilioğlu G, Koçaşlı S**. The Effect of Laughter Therapy Applied to Adult Patients on Anxiety, Stress, Sleep and Quality of Life: Systematic Review and Meta-Analysis. Acta Med Eur. 2024; 6(3):79-91. *https://doi.org/10.5281/zenodo.11543205*
28. **Zhou Z, Jia Y, Yan H, Wen J, Xu J, Wang S**. Effects of humor therapy on negative emotions, quality of life and cognitive function in older adults: A systematic review and meta-analysis. Geriatr Nurs. 2025; 61:20-26. 10.1016/j.gerinurse.2024.10.054
29. **Üner E, Sezer Balcı A, Kadıoğlu, H.** The Effect of Laughter Therapy on Physical and Mental Health: Systematic Review. Halk Sağlığı Hemşireliği Dergisi (J Public Health Nurs). 2022; 4(3): 251-269. *https://doi.org/10.54061/jphn.1102843*
30. **Cardona J, Villamil M, Henao E, Quintero Á, Gaviria O, Ortiz J, et al.** Cambios en el nivel de cortisol después de la aplicación de terapia de la risa, en adultos hospitalizados con diagnóstico de enfermedad cerebrovascular. Invest Clín. 2020; 60(3):233-242. *https://doi.org/10.22209/IC.v60n3a05*
31. **Bennett P, Hussein W, Reiterman M, Yu J, Schiller B**. The effects of laughter therapy on depression symptoms in patients undergoing center hemodialysis: A pragmatic randomized controlled trial. Hemodial Int. 2023; 24 (4): 541- 549. *https://doi.org/10.1111/hdi.12870*
32. **Mora-Ripolla R. Ubal-López R**. La risa: diferencias según el género. Rev Clin Esp. 2011; 211(7):360-366. *https://doi.org/10.1016/j.rce.2010.10.013*
33. **López-García E, Banegas JR, Pérez-Regadera AG, Gutiérrez-Fisac JL, Alonso J, Rodríguez-Artalejo F**. Valores de referencia de la versión española del Cuestionario de Salud SF-36 en población adulta de más de 60 años. Med Clin. 2003; 120(15):568–573. *https://doi.org/10.1016/s0025-7753(03)73775-0.*
34. **Cortese RH, Fernández Canales MM**. Estudio comparativo del bienestar y el ac-

ceso al bienestar en la vejez. Psicología del desarrollo[Internet]. 2021;(2):1-15. *https://doi.org/10.59471/psicologia20215*

35. **Henao M, Cardona J, Villamil M, Quintero Á.** Efectos de la terapia de la risa y teatro sobre la salud de los adultos mayores residentes en un hogar gerontológico de Medellín, 2016. En: La importancia de la RISA en la salud de los adultos mayores institucionalizados. Eds. Fondo Editorial Corporación Universitaria Remington, Medellín; 2020. p 16-32. Disponible en: https://www.uniremington.edu.co/fondo-editorial/libros-de-investigacion/la-importancia-de-la-risa-en-la-salud-de-los-adultos-mayores/
36. **Theeke L**. Predictors of loneliness in U.S. Adults over age sixty-five. Arch Psychiatr Nurs. 2009; 23(5):387-396. *https://doi.org/10.1016/j.apnu.2008.11.002*
37. **Demakakos P, Nunn S, Nazroo J.** Loneliness, relative deprivation and life satisfaction. En: Retirement, health and relationships of the older population in England: the 2004 English longitudinal study of ageing. Chapter 10. London: Institute for Fiscal Studies. Banks J, Breeze E, Lessoff C, Nazroo J, editors. 2006. p 297-337. Disponible en: https://www.researchgate.net/publication/284664030_Loneliness_relative_deprivation_and_life_satisfaction
38. **Sarabia CM**. Envejecimiento exitoso y calidad de vida. Su papel en las teorías del envejecimiento. Gerokomos 2009; 20(4): 172-174. Disponible en: https://scielo.isciii.es/scielo.php?script=sci_arttext&pid=S1134-928X2009000400005

Invest Clin 67(2): 230 - 240, 2026 https://doi.org/10.54817/IC.v67n2a06

Impact of plasma adsorption volumes (5 L vs. 6 L) on the prognosis of patients with liver failure.

Xin Zhang, Zhuoyao Zhang, Hui Chen and Huafen Zhang

State Key Laboratory for Diagnosis and Treatment of Infectious Diseases, Collaborative Innovation Center for Diagnosis and Treatment of Infectious Diseases; Department of Nursing, The First Affiliated Hospital, Zhejiang University School of Medicine, Hangzhou City, Zhejiang province, China.

Keywords: Plasma Adsorption; Liver Failure; Complications; Duration of Therapy; Blood Platelets.

Abstract. Plasma adsorption (PA) is used to improve outcomes in liver failure (LF). Data on adsorption capacity and its relationship to patient outcomes are limited. This single-center retrospective study included patients with LF who received PA at the First Affiliated Hospital of Zhejiang University School of Medicine in Hangzhou City, China, between October 2020 and October 2022, and examined the impact of adsorption volume (5 L vs. 6 L) on prognosis. The study included 230 PA treatments, of which nine were excluded due to missing data. The 5L column was used in 60 patients (118 treatments, 47 male), and the 6L column was used in 50 patients (103 treatments, 31 male). Treatment effectiveness was evaluated using length of hospital stay, liver transplantation, death, and improvement in disease-related symptoms. In both groups, PA increased white blood cells (WBC), international normalized ratio (INR), activated partial thromboplastin time (APTT), and prothrombin time (PT) but decreased hemoglobin, total bile acids, total bilirubin, and fibrinogen (all $p<0.05$). Platelet levels decreased after 6L PA ($p=0.033$) but not after 5L PA ($p=0.116$). After PA, the 6L group had lower WBC than the 5L group ($p=0.003$), but there were no significant differences in the other parameters. The 5L and 6L columns did not differ significantly in hospital stay duration, liver transplantation, mortality, or symptom improvement. However, the 5L column significantly reduced platelet destruction, shortened treatment time, and reduced the occurrence of complications, particularly thrombocytopenia-related risks. Hence, the results indicate that the 5L volume would be preferable clinically.

Corresponding author: Huafen Zhang. State Key Laboratory for Diagnosis and Treatment of Infectious Diseases, Collaborative Innovation Center for Diagnosis and Treatment of Infectious Diseases; Department of Nursing, The First Affiliated Hospital, Zhejiang University School of Medicine, No. 79 Qingchun Rd., Shangcheng District, Hangzhou City 310003, Zhejiang province, China. Tel: +86-13757120681. Email: zhanghuafen@zju.edu.cn

Impacto de los volúmenes de adsorción plasmática (5 L vs. 6 L) en el pronóstico de pacientes con insuficiencia hepática.

Invest Clin 2026; 67 (2): 230 – 240

Palabras clave: Adsorción Plasmática; Insuficiencia Hepática; Complicaciones; Duración de la Terapia; Plaquetas.

Resumen. La adsorción plasmática (AP) se utiliza para mejorar los resultados en la insuficiencia hepática (IH). Faltan datos relevantes sobre las diferentes capacidades de adsorción y su efecto en la recuperación de los pacientes. Este estudio retrospectivo unicéntrico incluyó a pacientes con IH que recibieron AP en el First Affiliated Hospital of Zhejiang University School of Medicine, Hangzhou City, China, entre octubre de 2020 y octubre de 2022, y examinó el impacto del volumen de adsorción (5 L frente a 6 L) en el pronóstico. El estudio incluyó 230 tratamientos de AP, de los cuales nueve fueron excluidos por falta de datos. Se utilizó la columna de 5 L en 60 pacientes (118 tratamientos) y la de 6 L en 50 pacientes (103 tratamientos). La efectividad se evaluó mediante la duración de la estancia hospitalaria, el trasplante hepático, la muerte y la mejoría de los síntomas relacionados con la enfermedad. En ambos grupos, la AP aumentó los leucocitos, el INR, la APTT y el PT, y disminuyó la hemoglobina, los ácidos biliares totales, la bilirrubina total y el fibrinógeno (todos $p<0,05$). Los niveles de plaquetas disminuyeron después de la AP de 6 L ($p=0,033$), pero no con la de 5 L ($p=0,116$). Tras la AP, el grupo de 6 L mostró leucocitos más bajos ($p=0,003$). Las columnas de 5 L y 6 L no mostraron diferencias significativas en los resultados clínicos principales. Sin embargo, la columna de 5 L redujo significativamente la destrucción plaquetaria y acortó el tiempo de tratamiento, lo que sugiere que el volumen de 5 L podría ser clínicamente preferible.

Received: 08-10-2025 Accepted: 05-03-2026

INTRODUCTION

Liver failure (LF) is the leading cause of death in patients with liver disease. It often progresses rapidly, with a poor prognosis and severe cases that are life-threatening[1,2]. High mortality associated with LF results from severe impairment or decompensation of hepatic synthesis, detoxification, excretion, and biotransformation functions. Among these, the accumulation of bile acids, bilirubin metabolites, and ammonia in the body is a major factor [3-5]. These metabolites are normally managed by the liver, and abnormal liver function can lead to brain dysfunction (hepatic encephalopathy), renal dysfunction (hepatorenal syndrome), and eventually death [6, 7].

Plasma adsorption (PA) has been established as a treatment for various LF conditions, providing patients with additional treatment options by temporarily and partially replacing liver function [8-12]. These treatments can remove toxins, endotoxins, and bilirubin metabolites from the blood, allowing time for liver cell recovery and func-

tion, or providing support while awaiting a donor liver. PA is preferred because it avoids plasma-dose limitations, plasma allergies, and blood transfusion-related infections [8, 11]. This method introduces the patient's blood into the external pipeline, and the plasma to be processed is separated by the plasma component separator. The separated plasma is then passed through a bilirubin adsorption column to remove pathogenic substances and returned to the patient without requiring allogeneic plasma or albumin.

Plasorba BR-350 is a commonly used bilirubin adsorption column capable of processing large volumes of plasma to remove bilirubin effectively [13, 14]. PA mainly uses an adsorption column to remove toxins from patients' plasma, including substances such as albumin-bound bilirubin, thereby improving liver cells and liver function. According to this principle, the role of the plasma bilirubin adsorption column is particularly critical [8-11]. In lipoprotein (a) apheresis, different treatment volumes affect the lipid removal rate, as well as the removal of fibrinogen and other macromolecules [15]. Data are available regarding the curative effect of the adsorption column material itself [13, 14], but there remains a lack of data on whether different adsorption capacities will produce different curative effects. Although an adsorption capacity below 7 L can be treated using the BR-350 adsorption column, current studies mostly show that the treatment adsorption time is 3-4 h (representing about 5-6 L) [13, 16-18]. In patients on hemodialysis, the volume of blood treated is associated with various outcomes, such as hemodialysis efficacy and intradialytic hypotension [19, 20]. Hence, optimizing benefits and limiting complications is an important goal during blood purification therapies.

Therefore, this study aimed to examine how adsorption volume (5 L vs. 6 L) affects clinical outcomes in patients with LF. The results could help improve treatment and nursing during PA.

MATERIALS AND METHODS

Study design and patients

This single-center retrospective study included patients with LF who received PA treatment at the First Affiliated Hospital of Zhejiang University School of Medicine from October 2020 to October 2022.

The inclusion criteria were 1) patients diagnosed with LF according to the Chinese Guidelines for Diagnosis and Treatment of Liver Failure (2018) [21], 2) aged ≥18 years, and 3) who underwent PA only. The exclusion criteria were 1) patients with incomplete clinical data, 2) patients with a malignant tumor, 3) patients with severe infection, such as pulmonary infection, or 4) patients in the ICU.

This study was approved by the Medical Ethics Committee of the First Affiliated Hospital of Zhejiang University School of Medicine. Patient informed consent was waived due to the retrospective nature of the study. All authors had full control of the data and information for this study.

Data collection and definition

According to the infection department's artificial liver center standard operating procedure and guidelines [21], an Artificial Liver Support System (ALSS) was considered for patients with LF. Vascular access was obtained with a double-lumen hemodialysis catheter placed in the femoral veins. Blood anticoagulation was managed with unfractionated heparin. The anticoagulant regimen consisted of an initial 2000 U of heparin sodium, followed by maintenance at 1000 U/h. The PA treatment device consisted of a standard hemodialysis machine with the appropriate tubing and plasma filter. The Plasorba BR-350 (B-Braun Carex) was used as the bilirubin absorption column during the study period, with a plasma processing volume of 5L or 6L. The selection of 5L versus 6L plasma processing volume was determined by the attending physician based

on clinical judgment and the department's standard operating procedures during the study period, rather than being predetermined by patient anthropometric characteristics such as height or body weight.

The patients' identities were protected. The demographic and clinical characteristics were collected from the medical records, including sex, age, height, weight, hypertension, allergies, diabetes, heart disease, kidney disease, viral hepatitis, hepatocirrhosis, hematocrit, and blood volume. The blood volume was estimated using 0.65×weight×(1-hematocrit) [22].

Blood routine and coagulation function indicators were collected, including white blood cells (WBC), hemoglobin (HGB), platelets (PLT), total bile acid (TBA), total bilirubin (TB), potassium (K+), sodium (Na+), chlorine (Cl-), calcium (Ca^{2+}), phosphorus (P), international normalized ratio (INR), fibrinogen (Fib), activated partial thromboplastin time (APTT), and prothrombin time (PT). Percentage differences were calculated as [(after treatment - before treatment) / before treatment].

Outcomes

The outcomes of this study were the length of hospital stay, liver transplant, death, and improvement in disease-related symptoms. Symptom improvement was defined as 1) clinical symptoms such as fatigue, poor appetite, abdominal distension, and bleeding were significantly improved, and hepatic encephalopathy disappeared; 2) signs such as jaundice and ascites improved significantly; and 3) liver function indices improved significantly, such as TBil <5 the upper limit of normal (ULN), PTA >40%, or INR <1.5 [21].

Statistical analysis

Continuous data were tested for normality using the Shapiro-Wilk test. Continuous variables with a normal distribution were expressed as means ± standard deviations (SD) and analyzed using Student's t-test; otherwise, they were presented as medians (interquartile ranges) and analyzed using the Mann-Whitney U-test. Categorical variables were presented as n (%) and analyzed using the chi-square test or Fisher's exact test. Data processing was performed in Python, and data analysis was conducted in SPSS 26.0 (IBM, Armonk, NY, USA). Two-sided P-values <0.05 were considered statistically significant.

RESULTS

During the study period, 230 plasma adsorption (PA) treatments were performed in 110 patients. Nine treatments were excluded for missing data, leaving 221 for analysis of laboratory parameters (118 in the 5L group and 103 in the 6L group). For patient-level analyses of baseline characteristics and clinical outcomes, 60 patients received 5L PA and 50 received 6L PA. Patients in the 5L group were significantly taller than those in the 6L group (166.14±7.18 cm vs. 163.13±7.24 cm, p=0.031), but the estimated systemic blood volume (0.65×weight×(1-hematocrit)) did not differ significantly between groups (2732.29±453.71 mL vs. 2683.34±508.21 mL, p=0.595). Other baseline characteristics, including the prevalence of viral hepatitis, hypertension, diabetes, and renal disease, were comparable between groups (Table 1).

The majority of patients were male (70.9%), and males had a higher mean systemic blood volume than females (2838±452 mL vs. 2395±387 mL). The mean age of the entire cohort was 55.4±13.8 years. Patients in the 5L group were significantly taller than those in the 6L group (p=0.031). Viral hepatitis was the most common underlying disease (30%). No significant differences were observed between groups in the prevalence of hypertension, diabetes, heart disease, or kidney disease (all p>0.05) (Table 1). Baseline laboratory parameters, including total bile acid and total bilirubin levels, were comparable between the two groups prior to treatment (all p>0.05).

Table 1. Baseline characteristics.

Variable	5L group (n=60)	6L group (n=50)	p
Sex, n (%)			
Female	13 (21.7%)	19 (38%)	0.065
Male	47 (78.3%)	31 (62%)	
Age, year, mean ± SD	54.00±12.53	57.17±15.20	0.233
Height, cm, mean ± SD	166.14±7.18	163.13±7.24	0.031
Weight, kg, mean ± SD	61.57±10.24	60.41±2.48	0.592
Hypertension, n (%)	12 (20%)	9 (18%)	0.793
Allergy, n (%)	1 (1.7%)	2 (4%)	0.459
Diabetes, n (%)	7 (11.7%)	6 (12%)	0.957
Heart disease, n (%)	1 (1.7%)	1 (2%)	0.898
Kidney disease, n (%)	4 (6.7%)	1 (2%)	0.224
Virus hepatitis, n (%)	19 (31.7%)	14 (28%)	0.679
Hepatocirrhosis, n (%)	0	1 (2%)	0.275
Hematocrit, median (interquartile range)	31.44 (5.74)	30.99 (7.49)	0.730
Blood volume, median (interquartile range)	2732.29 (453.71)	2683.34 (508.21)	0.595

Continuous variables were analyzed using Student's t-test for normally distributed data (expressed as mean ± SD) and the Mann-Whitney U-test for non-normally distributed data (expressed as median with interquartile range). Categorical variables were analyzed using the chi-square test or Fisher's exact test.

In both groups, PA treatment significantly increased white blood cell counts, INR, APTT, and PT, while decreasing hemoglobin, total bilirubin, total bile acids, and fibrinogen (all $p<0.05$) (Supplementary Table 1). Notably, platelet levels decreased significantly after 6L PA ($p=0.033$), whereas no significant reduction was observed after 5L PA ($p=0.116$).

Post-treatment comparisons between groups showed significantly lower white blood cell counts in the 6L group than in the 5L group ($p=0.003$). No significant between-group differences were observed in other post-treatment laboratory parameters, including hemoglobin, platelets, bilirubin, coagulation indices, or electrolytes (Table 2).

At the patient level, no significant differences were observed between the 5L and 6L groups in length of hospital stay, liver transplantation rates, in-hospital mortality, or improvement in disease-related symptoms (all $p>0.05$) (Table 3). Although the 5L group had a numerically longer mean hospital stay and higher transplantation and mortality rates, and the 6L group showed a slightly higher improvement rate, none of these differences reached statistical significance.

DISCUSSION

The 5L and 6L columns yield similar outcomes in terms of hospital stay duration, liver transplantation, mortality, and symptom improvement. The 5L column can reduce platelet destruction, shorten treatment time, and reduce the occurrence of complications.

In patients with LF, high bilirubin levels can be fatal in the short term [13, 14]. Low bilirubin levels can promote hepatocyte regeneration, whereas high bile acid levels can induce hepatocyte apoptosis and necrosis and delay regeneration [3, 23, 24]. Excessive bilirubin

Table 2. Laboratory indices after treatment.

Variable	5L group (n=118)	6L group (n=103)	p
WBC, x10^9/L	11.57±10.29	8.29±3.84	0.003
HGB, g/L	107.61±22.76	102.42±26.12	0.116
PLT, x10^9/L	166.43±88.66	155.70±84.15	0.359
TBA, μmol/L	170.04±115.27	152.53±104.54	0.241
TB, μmol/L	251.16±107.54	238.27±106.26	0.372
Na, mmol/L	136.81±4.6	137.79±3.25	0.068
Cl, mmol/L	101.99±4.55	102.01±3.97	0.975
Ca, mmol/L	2.13±0.12	2.15±0.13	0.493
P, mmol/L	0.98±0.24	0.92±0.26	0.125
INR	1.80±3.55	1.44±0.38	0.301
Fib, g/L	1.80±0.68	1.92±0.74	0.224
APTT, s	45.69±19.07	42.68±12.76	0.167
PT, s	17.00±4.19	16.53±4.19	0.413

White blood cells (WBC), hemoglobin (HGB), platelets (PLT), total bile acid (TBA), total bilirubin (TB), sodium (Na+), chlorine (Cl-), calcium (Ca^{2+}), phosphorus (P), international normalized ratio (INR), fibrinogen (Fib), activated partial thromboplastin time (APTT), and prothrombin time (PT). Between-group comparisons of post-treatment laboratory parameters were performed using Student's t-test for normally distributed continuous variables, with data presented as mean ± standard deviation.

Table 3. Clinical outcomes.

Variable	5L group (n=60)	6L group (n=50)	p
Length of stay (days)	23.7±19.86	19.4±8.78	0.135
Liver transplant	6 (10%)	3 (6%)	0.451
In-hospital mortality	8 (13.3%)	4 (8%)	0.376
Good prognosis	45 (75%)	42 (85%)	0.245

Length of hospital stay was analyzed using Student's t-test, and categorical outcomes (liver transplant, in-hospital mortality, and good prognosis) were analyzed using the chi-square test or Fisher's exact test. All data are presented as mean ± SD or n (%).

itself does not cause multiple organ failure, but in patients with LF it has neurotoxic and encephalopathic effects. Therefore, removing bilirubin and bile acids seems a reasonable therapeutic goal. ALSS can help remove toxic metabolites in patients with LF, which is beneficial for liver cell regeneration and functional recovery, buys time for liver transplantation, and can even allow some patients to avoid liver transplantation [8, 10, 25]. PA can selectively adsorb lipid-soluble substances such as bilirubin, aromatic amino acids, and other toxic metabolites that are tightly bound to proteins. Although many studies have examined the efficacy of ALSS [3, 8, 10,13,26,27], there are few data on different PA amounts and even fewer studies in large populations. It is unclear whether the amount of adsorption in the clinic will have the same effect across patients with LF. In the present study, bilirubin decreased in both groups after treatment, which is the goal of treatment. WBCs increased, probably due to an immune insult from the treatment. Fibrino-

gen decreased, and PT and APPT increased, suggesting reduced coagulation function, probably due to adsorption of coagulation factors by the column. HGB also decreased.

The PA treatment mode is a mature, classic method that addresses the issue of scarce plasma supply. The 5-L and 6-L adsorption capacities are routine choices in adults. This study showed that 1) the 5-L and 6-L adsorption doses could be considered effective strategies for treating patients with LF, with no differences in treatment outcomes; 2) there might be a risk of thrombocytopenia after treatment with a PA volume of 6 L, but not with 5 L; and 3) since the treatment time is shorter with 5 L, the 5-L volume could be associated with lower complication rates.

BR-350 is an anion resin plasma adsorption column with styrene-divinylbenzene as the main material. The effective use of BR-350 in LF dates back more than 30 years[8,10,25]. Previous studies have reported that the amount of PA in LF treatment ranges from 2 to 7 L, and the clearance rate of BR-350 for bilirubin decreases with increasing treatment volume and eventually tends to saturate [13]. As shown in the present study, there were no significant differences in post-treatment bilirubin and TBA between 5 and 6 L. Some researchers have suggested that a longer PA treatment time can lead to a higher incidence of complications [28]. Therefore, in the case of the same treatment effect, a 5L treatment capacity seems to be a better choice because of the shorter treatment time. Nursing care for ALSS treatment needs to be refined and individualized, and timely analysis of the cause of alarms in the treatment system and handling of emergencies are required to ensure patient safety and the smooth progress of treatment.

The most critical safety distinction between the two treatment volumes lies in their differential effects on hematological parameters. While both 5L and 6L PA effectively reduced bilirubin and bile acids, the 6L volume was associated with a significant decrease in platelet counts ($p=0.033$), whereas the 5L volume preserved platelet levels ($p=0.116$). This finding carries substantial clinical significance for patients with liver failure, who already exhibit compromised hemostasis due to impaired synthesis of coagulation factors and often baseline thrombocytopenia [29]. Further platelet reduction in this vulnerable population increases the risk of spontaneous bleeding and procedure-related hemorrhage and may necessitate platelet transfusions, thereby increasing treatment costs and risks[30,31]. Additionally, the 6L group demonstrated significantly lower post-treatment white blood cell counts compared to the 5L group ($p=0.003$). Although we did not observe a statistically significant increase in infection rates in the 6L group during the study period, leukopenia theoretically elevates infection risk, which is particularly concerning in patients with liver failure who exhibit immune dysfunction. The combination of thrombocytopenia and leukopenia suggests that the 6L volume may impose greater hematological stress or more pronounced activation of cellular adhesion to the adsorption column and extracorporeal circuit. Patients with LF are at risk of thrombocytopenia due to factors such as decreased thrombopoietin synthesis from massive necrosis of liver cells[32,33]. Blood purification treatments such as bilirubin adsorption will cause increased platelet consumption, and at the same time, there is an increased risk of HIT due to heparin anticoagulation. A researcher found that the proportion of patients with amputation or death due to HIT was as high as 20%-30% [33]. At the same time, an elevated time-to-risk of transient thrombocytopenia associated with separation membranes was associated [31]. This study found a statistically significant decrease in platelet counts with 6-L PA, suggesting that 5-L PA may be safer. A previous study of lipoprotein(a) apheresis showed that larger treatment volumes were associated with larger decreases in the levels of fibrinogen and other blood macromolecules [15], but no significant differences were

observed in the present study. The 6L group had lower WBC levels than the 5L group after treatment. Although our study did not find a significant increase in infection rates in the 6 L group, we acknowledge that leukopenia may theoretically elevate infection risk [34]. Future studies with larger cohorts and longer follow-up may further elucidate this relationship. Nevertheless, differences could be observed in larger cohorts or with longer follow-up.

We acknowledge that the 5L group had a significantly greater mean height than the 6L group. Although height can correlate with blood volume, we believe this difference is unlikely to have influenced the choice of adsorption volume or the study outcomes for several reasons. First, the estimated systemic blood volume, calculated using the formula 0.65×weight×(1-hematocrit), showed no significant difference between groups (p=0.595), suggesting that the height disparity did not translate into clinically relevant differences in total circulating volume. Second, in clinical practice, the decision to use 5L versus 6L adsorption is typically based on the severity of liver failure, baseline bilirubin levels, and physician preference rather than patient height. Nevertheless, we recognize this baseline imbalance as a limitation of our retrospective design, and we cannot entirely exclude the possibility of unmeasured confounding factors that may influence both patient selection and volume determination.

This study had limitations. It was a single-center study with a small sample size. The retrospective design limited the data to what was available in the charts. The 5-L and 6-L capacities are the most common at the authors' center, but future studies should also examine other capacities.

In conclusion, PA therapy can remove a large amount of bilirubin and also reuse the patient's plasma and albumin to reduce allergic reactions. Treatment with a 5-L plasma adsorption capacity yields outcomes similar to those of the 6-L treatment for length of stay, liver transplantation, in-hospital mortality, and prognosis. However, given smaller post-treatment platelet changes and a shorter treatment duration, the 5-L treatment volume might be more appropriate than the 6-L volume.

Acknowledgements

The authors would like to thank the State Key Laboratory for Diagnosis and Treatment of Infectious Diseases, The First Affiliated Hospital, Zhejiang University School of Medicine, for providing the research platform and support. We are also grateful to the medical and nursing staff of the Artificial Liver Treatment Center for their clinical assistance and patient care. Finally, we acknowledge all patients involved in this study.

Funding

This research received no specific grant from any funding agency in the public, commercial, or not-for-profit sectors.

ORCID ID of the authors

- Xin Zhang (XZ): 0009-0000-6607-0499
- Zhuoyao Zhang (ZYZ): 0009-0004-3294-4003
- Hui Chen (HC): 0009-0008-7594-2701
- Huafen Zhang (HFZ): 0000-0002-5371-7895

Author's contributions

XZ: Conceptualization, Methodology, Investigation, Formal Analysis, Writing – Original Draft; ZYZ: Methodology, Investigation, Formal Analysis; HC: Methodology, Investigation, Formal Analysis; HFZ: Conceptualization, Writing – Original Draft, Writing – Review & Editing, Supervision, Project Administration. All authors contributed to resources, reviewed and edited the manuscript, and approved the final version for submission.

Conflict of interest

The authors declare that they have no competing interests.

Ethics approval and consent to participate

This work has been carried out in accordance with the Declaration of Helsinki (2000) of the World Medical Association. This study was approved by the Ethic Committee of the First Affiliated Hospital, College of Medicine, Zhejiang University (IIT20230143A). The requirement for informed consent from the patients was waived due to the retrospective nature of the study. All authors had full control of the data and information regarding this study.

Consent for publication

Not applicable.

Availability of data and materials

All data generated or analyzed during this study are included in this article and supplementary information files.

REFERENCES

1. **Moreau R, Jalan R, Gines P, Pavesi M, Angeli P, Cordoba J, et al.** Acute-on-chronic liver failure is a distinct syndrome that develops in patients with acute decompensation of cirrhosis. Gastroenterology. 2013;144(7):1426-1437, 1437 e1421-1429. *https://doi.org/10.1053/j.gastro.2013.02.042.*
2. **Angeli P, Rodríguez E, Piano S, Ariza X, Morando F, Solà E, et al.** Acute kidney injury and acute-on-chronic liver failure classifications in prognosis assessment of patients with acute decompensation of cirrhosis. Gut. 2015;64(10):1616-1622. *https://doi.org/10.1136/gutjnl-2014-307526.*
3. **Lee JY, Kim SB, Chang JW, Park SK, Kwon SW, Song KW, et al.** Comparison of the molecular adsorbent recirculating system and plasmapheresis for patients with graft dysfunction after liver transplantation. Transplant Proc. 2010;42(7):2625-2630. *https://doi.org/10.1016/j.transproceed.2010.04.070.*
4. **European Association for the Study of the Liver, Electronic address eee, Clinical practice guidelines panel, Wendon J, Panel members, Cordoba J, et al.** EASL Clinical Practical Guidelines on the management of acute (fulminant) liver failure. J Hepatol. 2017;66(5):1047-1081. *https://doi.org/10.1016/j.jhep.2016.12.003.*
5. **Alarabi AA, Wikstrom B, Loof L, Danielson BG.** Treatment of pruritus in cholestatic jaundice by bilirubin- and bile acid-adsorbing resin column plasma perfusion. Scand J Gastroenterol. 1992;27(3):223-226. *https://doi.org/10.3109/00365529208999953.*
6. **Mandiga P, Kommu S, Foris LA, Bollu PC.** Hepatic Encephalopathy. In: StatPearls. Treasure Island (FL); StatPearls Publishing; 2026. Available from: https://www.ncbi.nlm.nih.gov/books/NBK430869/
7. **Francoz C, Durand F, Kahn JA, Genyk YS, Nadim MK.** Hepatorenal Syndrome. Clin J Am Soc Nephrol. 2019;14(5):774-781. *https://doi.org/10.2215/CJN.12451018.*
8. **Viggiano D, de Pascale E, Marinelli G, Pluvio C.** A comparison among three different apheretic techniques for treatment of hyperbilirubinemia. J Artif Organs. 2018;21(1):110-116. *https://doi.org/10.1007/s10047-017-0986-1.*
9. **Fuhrmann V, Horvatits T, Drolz A, Rutter K.** [Extracorporeal therapy of patients with liver disease in the intensive care unit]. Med Klin Intensivmed Notfmed. 2014;109(4):246-251. *https://doi.org/10.1007/s00063-013-0321-4.*
10. **Saliba F, Bañares R, Larsen FS, Wilmer A, Parés A, Mitzner S, et al.** Artificial liver support in patients with liver failure: a modified DELPHI consensus of international experts. Intensive Care Med. 2022;48(10):1352-1367. *https://doi.org/10.1007/s00134-022-06802-1.*
11. **Sun Y, Yu LX, Liu YH, Wang B, Lu W.** [Bilirubin adsorption therapy for two infants with liver failure]. Zhonghua Er Ke

Za Zhi. 2020;58(11):933-934. *https://doi.org/10.3760/cma.j.cn112140-20200411-00376.*

12. **Tsipotis E, Shuja A, Jaber BL.** Albumin Dialysis for Liver Failure: A Systematic Review. Adv Chronic Kidney Dis. 2015;22(5):382-390. *https://doi.org/10.1053/j.ackd.2015.05.004.*
13. **Adani GL, Lorenzin D, Currò G, Sainz-Barriga M, Comuzzi C, Bresadola V, et al.** Selective bilirubin removal by plasma treatment with Plasorba BR-350 for early cholestatic graft dysfunction. Transplant Proc. 2007;39(6):1904-1906. *https://doi.org/10.1016/j.transproceed.2007.05.010.*
14. **Geiger H, Klepper J, Lux P, Heidland A.** Biochemical assessment and clinical evaluation of a bilirubin adsorbent column (BR-350) in critically ill patients with intractable jaundice. Int J Artif Organs. 1992;15(1):35-39. PMID: 1551726.
15. **Borberg H.** Comparison of different Lp (a) elimination techniques: a retrospective evaluation. Transfus Apher Sci. 2009;41(1):61-65. *https://doi.org/10.1016/j.transci.2009.05.014.*
16. **Ihara H, Shino Y, Hashizume N, Aoki T, Suzuki Y, Igarasi Y, et al.** Decline in plasma retinol in unconjugated hyperbilirubinemia treated with bilirubin adsorption using an anion-exchange resin. J Nutr Sci Vitaminol (Tokyo). 1998;44(2):329-336. *https://doi.org/10.3177/jnsv.44.329.*
17. **Ryan CJ, Anilkumar T, Ben-Hamida AJ, Khorsandi SE, Aslam M, Pusey CD, et al.** Multisorbent plasma perfusion in fulminant hepatic failure: effects of duration and frequency of treatment in rats with grade III hepatic coma. Artif Organs. 2001;25(2):109-118.*https://doi.org/10.1046/j.1525-1594.2001.025002109.x.*
18. **Mertens PR, Schönfelder T, Handt S, Kierdorf H, Marschall H, Busch N, et al.** Long-term extracorporeal bilirubin elimination: A case report on cascade resin plasmaperfusion. Blood Purif. 1998;16(6):341-348. *https://doi.org/10.1159/000014354.*
19. **Thijssen S, Kappel F, Kotanko P.** Absolute blood volume in hemodialysis patients: why is it relevant, and how to measure it? Blood Purif. 2013;35(1-3):63-71. *https://doi.org/10.1159/000345484.*
20. **Nafisi VR, Eghbal M.** Optimized Blood Volume Monitoring during Hemodialysis Procedure based on Ultrasonic Speed Measurement. J Biomed Phys Eng. 2019;9(3):373-380. *https://doi.org/10.31661/jbpe.v9i3Jun.675.*
21. **Liver Failure and Artificial Liver Group, Chinese Society of Infectious Diseases, Chinese Medical Association, Severe Liver Disease and Artificial Liver Group, Chinese Society of Hepatology, Chinese Medical Association.** [Guideline for diagnosis and treatment of liver failure (2018)]. Zhonghua Gan Zang Bing Za Zhi. 2019;27(1):18-26. *https://doi.org/10.3760/cma.j.issn.1007-3418.2019.01.006.*
22. **Kaplan AA**. A simple and accurate method for prescribing plasma exchange. ASAIO Trans. 1990;36(3):M597-599. PMID: 2252761.
23. **Liang C, Takahashi K, Furuya K, Oda T, Ohkohchi N.** Platelets Stimulate Liver Regeneration in a Rat Model of Partial Liver Transplantation. Liver Transpl. 2021;27(5):719-734. *https://doi.org/10.1002/lt.25962.*
24. **Chamuleau RA, Aronson DC, Frederiks WM, Bosman DK, Smit JJ, Maas MA, et al.** Liver regeneration after partial hepatectomy in rats with defective bilirubin conjugation or biliary excretion. Dig Dis Sci. 1991;36(4):510-512. *https://doi.org/10.1007/BF01298884.*
25. **Larsen FS.** Artificial liver support in acute and acute-on-chronic liver failure. Curr Opin Crit Care. 2019;25(2):187-191. *https://doi.org/10.1097/MCC.0000000000000584.*
26. **Che XQ, Li ZQ, Chen Z, Guo D, Jia QY, Jiang SC, et al.** Plasma exchange combining with plasma bilirubin adsorption effectively removes toxic substances and improves liver functions of hepatic failure patients. Eur Rev Med Pharmacol Sci. 2018;22(4):1118-1125. *https://doi.org/10.26355/eurrev_201802_14400.*

27. **Senf R, Klingel R, Kurz S, Tullius S, Sauer I, Frei U, et al.** Bilirubin-adsorption in 23 critically ill patients with liver failure. Int J Artif Organs. 2004;27(8):717-722. *https://doi.org/10.1177/039139880402700810.*
28. **Schwanke AA, Danski MTR, Pontes L, Kusma SZ, Lind J.** Central venous catheter for hemodialysis: incidence of infection and risk factors. Rev Bras Enferm. 2018;71(3):1115-1121. *https://doi.org/10.1590/0034-7167-2017-0047.*
29. **Daugirdas JT, Bernardo AA.** Hemodialysis effect on platelet count and function and hemodialysis-associated thrombocytopenia. Kidney Int. 2012;82(2):147-157. *https://doi.org/10.1038/ki.2012.130.*
30. **Doi Y, Koga K, Sugioka S, Inoue Y, Arisato T, Nishioka K, et al.** Heparin-induced thrombocytopenia among incident hemodialysis patients anticoagulated with low molecular weight heparin: A single-center retrospective study. Nefrologia (Engl Ed). 2021;41(3):356-358. *https://doi.org/10.1016/j.nefroe.2020.05.007.*
31. **Hakim RM, Schafer AI.** Hemodialysis-associated platelet activation and thrombocytopenia. Am J Med. 1985;78(4):575-580. *https://doi.org/10.1016/0002-9343(85)90398-5.*
32. **Giannini EG, Peck-Radosavljevic M.** Platelet Dysfunction: Status of Thrombopoietin in Thrombocytopenia Associated with Chronic Liver Failure. Semin Thromb Hemost. 2015;41(5):455-461. *https://doi.org/10.1055/s-0035-1550432.*
33. **Fathi M.** Heparin-induced thrombocytopenia (HIT): Identification and treatment pathways. Glob Cardiol Sci Pract. 2018; 2018(2):15. *https://doi.org/10.21542/gcsp.2018.15.*
34. **Khan MTA, Patnaik R, Huang JY, Campi HD, Montorfano L, De Stefano F, et al.** Leukopenia is an independent risk factor for early postoperative complications following incision and drainage of anorectal abscess. Colorectal Dis. 2023. 25(4):717-727. *https://doi.org/10.1111/codi.16447.*

Invest Clin 67(2): 241 - 259, 2026 https://doi.org/10.54817/IC.v67n2a07

Orientin attenuates pulmonary fibrosis via TGF-β1/suppressor of mother against decapentaplegic 3 (Smad3) pathway.

Yijin Liu[1] and Yao Lu[2]

[1]Department of Pharmacy, Liaoning University of Traditional Chinese Medicine Xinglin College, Shenyang, Liaoning Province, China.
[2]Department of Thoracic Surgery, The Fourth Affiliated Hospital of China Medical University, Shenyang City, Liaoning Province, China.

Keywords: Orientin; Pulmonary fibrosis; Fibroblasts; TGF-β1/Smad3 pathway.

Abstract. Orientin, a natural flavonoid found in many medicinal plants, can improve lung injury through anti-inflammatory and antioxidant effects, but its role in pulmonary fibrosis (PF) remains unstudied. Human Fetal Lung 1 (HFL1) cells were stimulated with transforming growth factor-β1 (TGF-β1), and a single intratracheal bleomycin instillation in mice was used to establish a PF mouse model. Orientin, the TGF-β1/suppressor of mother against decapentaplegic 3 (Smad3) pathway agonist SRI-011381, and the inhibitor SB431542 were used for intervention. The proliferation and migration were evaluated using the Cell Counting Kit-8 (CCK-8), Edu staining (evaluated proliferative activity) and a scratch-healing assay. Fibers in HFL1 cells were detected by Sirius red staining. Inflammation and fibrosis in lung tissue were assessed by pathological staining and enzyme-linked immunosorbent assay (ELISA). PF and TGF-β1/Smad3 pathway protein expressions were evaluated by Western blot. Orientin significantly reduced TGF-β1, p-Smad3, alpha-smooth muscle actin (α-SMA), Collagen I, and matrix metallopeptidase (MMP)-2 levels. After Orientin treatment, the Edu positive cells, cell proliferation and migration were significantly reduced, and the number of red-stained collagen fibers was significantly reduced. After Orientin treatment, alveolar cavity collapse, inflammatory cell infiltration, and collagen fiber hyperplasia of mice were alleviated, and the contents of Hydroxyproline (HYP) and inflammatory factors in the alveolar lavage fluid were significantly reduced. SRI-011381 attenuated the effect of Orientin on the intervention, and inflammation and fibrosis levels were markedly increased. SB431542 enhanced the intervention effect of Orientin. Orientin inhibited TGF-β1/Smad3 signaling, inhibited fibroblast-to-myofibroblast transition (FMT) and extracellular matrix (ECM) production, and alleviated inflammatory and fibrotic damage.

Corresponding author: Yao Lu. Department of Thoracic Surgery, The Fourth Affiliated Hospital of China Medical University, Shenyang City, Liaoning Province, China. Email: luyao52611@hotmail.com

La orientina reduce la fibrosis pulmonar mediante la vía de señalización TGF-β1/Smad3.

Invest Clin 2026; 67 (2): 241 – 259

Palabras clave: Orientin; Fibrosis pulmonar; Fibroblastos; Vía de TGF-β1/Smad3.

Resumen. La orientina, un flavonoide natural presente en una variedad de plantas medicinales, reduce el daño pulmonar gracias a sus efectos antiinflamatorios y antioxidantes. Sin embargo, no se han reportado estudios sobre su efecto en la fibrosis pulmonar (PF). Las células Human Fetal Lung 1 (HFL1) se estimularon con el factor de crecimiento transformante β1 (TGF-β1) y se administró una dosis única de bleomicina por vía intratraqueal para establecer un modelo de PF en ratones. La intervención se realizó con orientina, el agonista SRI-011381 de la vía supresora de madre contra el decapentapléjico 3, y el inhibidor SB431542. La proliferación y migración de células HFL1 se evaluaron mediante el Kit-8 (CCK-8) para el conteo de células, la tinción de Edu (para evaluar la actividad proliferativa) y mediante el ensayo de cicatrización de heridas. Las fibras en las células HFL1 se detectaron mediante tinción con Sirius Red. La inflamación y la fibrosis del tejido pulmonar se evaluaron mediante tinción patológica y ensayo inmunoenzimático ligado a anticuerpos (ELISA). Los niveles de expresión proteica de PF y de la vía TGF-β1/Smad3 se analizaron mediante Western blot. La orientina reduce significativamente los niveles de las proteínas TGF-β1, p-Smad3, actina alfa del músculo liso (α-SMA), colágeno I y metalopeptidasa de la matriz (MMP)-2. Además, el tratamiento con orientina disminuyó significativamente las células Edu positivas, la proliferación y la migración de las células HFL1, así como la formación de fibras de colágeno teñidas de rojo. El tratamiento con orientina redujo el deterioro de la cavidad alveolar, el infiltrado de células inflamatorias y la hiperplasia de fibras colágenas en el tejido pulmonar de los ratones, y disminuyó significativamente el contenido de Hydroxyproline (HYP) y de los factores inflamatorios (TNF-α e IL-6) en el lavado alveolar. Sin embargo, SRI-011381 atenuó el efecto de la intervención con orientina, con un aumento significativo de los niveles de inflamación y fibrosis; el SB431542 lo acentuó. La orientina inhibe la vía de señalización TGF-β1/Smad3, la transición de fibroblastos a miofibroblastos (FMT) y la producción de matriz extracelular (ECM), y alivia el daño inflamatorio y fibroso.

Received: 05-11-2025 Accepted: 21-12-2025

INTRODUCTION

The main pathological features of idiopathic pulmonary fibrosis (IPF) are destruction of the lung parenchyma and accumulation of extracellular matrix (ECM) in the pulmonary interstitial and alveolar spaces, which eventually leads to destruction of alveolar structure and severe impairment of lung function, ultimately resulting in death[1]. The median survival time of IPF patients after diagnosis is short, and the prognosis is very poor [2, 3]. At present, anti-pulmonary fibrosis (PF) drugs and lung transplantation are the main treatment options for PF. Lung-derived problems limit lung transplantation.

pirfenidone and nintedanib are the main anti-fibrosis drugs. Studies have shown that pirfenidone and nintedanib slow the decline in lung function in IPF, but overall efficacy is limited, with issues such as significant side effects, high costs, and no improvement in survival rate [3]. Thus, it is vital to find safe and effective new drugs for IPF therapy.

The pathogenesis of IPF is highly complex and involves multiple mechanisms, including the inflammatory response, oxidative stress, epithelial-mesenchymal transition (EMT), and inhibition of autophagy. These mechanisms are intertwined and interact to drive IPF progression. Among them, the transforming growth factor-β1 (TGF-β1)/suppressor of mother against decapentaplegic 3 (Smad3) signaling pathway is important in regulating the PF process [4-7]. TGF-β1 is a core regulator of IPF and can promote fibrosis [8]. When TGF-β1 binds to its receptor, it can phosphorylate Smad2/3 in the cytoplasm, which in turn binds Smad2/3 to Smad4 to form a trimer, enters the nucleus, and binds to specific DNA sites, thereby regulating the expression of a series of downstream fibrosis-related genes, up-regulating alpha-smooth muscle actin (α-SMA) level, promoting the abnormal deposition of fibrosis-related proteins, and increasing and promoting fibroblast proliferation. It drives the fibroblast-to-myofibroblast transition (FMT), a classical pathway of TGF-β1-mediated fibrosis [9]. Therefore, TGF-β1/Smad signaling can regulate the transcription and protein expressions of target genes, induce PF [10]. Inhibition of the TGF-β1/Smad3 pathway reduces PF. Sinomenine alleviates inflammatory response and reverses EMT through suppressing the TGF-β1/Smad3 pathway, thereby reducing PF [5]; inhibition of AHNAK2 via suppressing the TGF-β1/Smad3 pathway regulates EMT and alleviates PF[11]; PM2.5 enhances endoplasmic reticulum stress-induced autophagy, thereby activating the TGF-β1/Smad3 pathway, promoting ECM overproduction, ultimately aggravating PF [12]. In summary, the TGF-β1/Smad3 is a classic pathway that mediates organ fibrosis and dominates the progression of fibrotic diseases [13].

As research into treating PF with herbal medicine deepens, monomers of herbal medicine have attracted considerable attention for their single-component nature, stable structures, and notable effects. Orientin is a natural flavonoid widely found in many medicinal plants, such as *Trollius chinensis Bunge*, *Odontosoria chinensis* J. Sm., and bamboo leaves. Modern pharmacological studies have shown that orientin has many biological properties, including anti-inflammatory, antioxidant, anti-aging, antibacterial, hepatoprotective, neuroprotective, and cardioprotective effects [14, 15]. Studies have shown that Orientin is a possible anti-inflammatory drug. Orientin can improve mitochondrial homeostasis, inhibit chondrocyte senescence and inflammation, and reduce osteoarthritis [16]. The lung is the primary tissue for orientin distribution, and orientin has been shown to alleviate acute lung injury in mice by exerting anti-inflammatory and antioxidant effects [17]. Therefore, we believe that orientin may be an ideal anti-PF candidate drug. However, the therapeutic effect of orientin on PF and its molecular mechanism have not been systematically elucidated.

To evaluate the therapeutic potential of orientin in PF, the effects of orientin on FMT, fibrosis, inflammatory response, and the TGF-β1/Smad3 signaling pathway were assessed, with pirfenidone as a positive control. This study aims to demonstrate that orientin can reduce PF through the TGF-β1/Smad3 signaling pathway, thereby providing an important experimental and theoretical basis for the development of safe, effective, and economical anti-PF natural drugs.

METHODS

Cell culture and modeling

Human embryonic lung fibroblasts HFL1 were purchased from Procell Life Technology Co., Ltd. (CL-0106, Wuhan, China).

HFL1 cells were cultured with HFL1 cell-specific culture medium (CM-0106, Procell, Ham's F-12K medium containing 1% penicillin-streptomycin and 10% fetal bovine serum) in a cell culture box (MCO-18 AICUUV, PHCbi, Japan) at 37℃ and 5% CO_2. The subculture medium was changed every 3 days.

HFL1 cells (1×10^5 cells/well) in the logarithmic growth phase and in good condition were inoculated into 6-well plates and routinely cultured. The next day, after adherence, orientin (S9009, Selleck, Shanghai, China) at 0, 10, 20, 40, 80, and 160 μM was added, and cells were incubated for 24 h. Then, 10 μL of Cell Counting Kit-8 (CCK-8) solution (C0037, Beyotime, Shanghai, China) was added, and cells were incubated for 2 h. The optical density (OD) at 450 nm was measured using a microplate reader (MULTISKAN, Perkin Elmer, United States), and the cell survival rate was calculated to determine the safe concentration of orientin.

HFL1 cells were divided into the control group, the model (TGF-β1) group, the positive control (TGF-β1+pirfenidone) group, the orientin low, medium, and high concentration (TGF-β1+orientin-L, TGF-β1+orientin-M, TGF-β1+orientin-H) group, the TGF-β1/Smad3 pathway agonist (TGF-β1+orientin+SRI-011381) group, and the inhibitor (TGF-β1+orientin+SB431542) group. In the TGF-β1 group, 10 ng/mL TGF-β1 (100-21, PeproTech, USA) was added to stimulate HFL1 cells for 24 h [4, 5]. After that, 10 μM pirfenidone (Y159865, Beyotime) was added to the TGF-β1+pirfenidone group to culture HFL1 cells for 24 h; HFL1 cells were cultured with 10, 20, and 40 μM orientin for 24 h in orientin low, medium, and high concentration groups, respectively. TGF-β1+orientin+SRI-011381 and TGF-β1+orientin+SB431542 groups were added with 10 μM SRI-011381 (Y112753, Beyotime) and SB431542 (SF7890, Beyotime) at the same time as orientin. Then CCK-8 was used to measure the OD at 450 nm and calculate cell viability.

Edu staining

After intervention, HFL1 cells were incubated with an equal volume of 20 μM Edu working solution (C0071S, Beyotime) for 3 h. The cells were fixed with paraformaldehyde, permeabilized with 1 mL of permeabilization solution (P0097, Beyotime) for 10 min, and incubated with 0.5 mL of Click reaction solution in the dark for 30 min. The cells were stained with DAPI reagent and mounted with anti-fluorescence quenching mounting agent (0100-01, South biotech, USA). Three fields of view were selected for each well under the fluorescence microscope (ECLIPSE TI2-A, Nikon, Japan), and Edu-positive cells were counted using Image J software.

Scratch healing experiment

HFL1 cells were inoculated into 6-well plates and cultured overnight in serum-free medium after reaching confluence. A 200 μL pipette tip was used to create vertical scratches in each well, and the culture medium was replaced. The cells were then subjected to the experimental interventions and cultured for 24 h. Images were taken under a microscope (NIKON ECLIPSE E100, Nikon) at the beginning and end of the culture, and the distance between scratches was measured using ImageJ software to calculate the scratch-healing rate.

Sirius red staining

After the HFL1 cells were cultured, 100 μL of ice-cold methanol was added to fix the cells for 5 h, and then the ice-cold methanol in the well was discarded. Hematoxylin was added to each well for staining for 20 min, and then 200 μL of Sirius red staining solution (GC307014, Servicebio, Wuhan, China) was added. The cells were incubated in the dark for 4 h. Images were observed and collected under a microscope. The collagen fibers appeared red, and the muscle fibers appeared yellow. The area of collagen fibers was analyzed using Image J software.

Immunofluorescence

HFL1 cells were fixed with 4% paraformaldehyde for 15 min, incubated with 100 μL of membrane-breaking working solution for 10 min, blocked with 3% BSA (bovine serum albumin) for 30 min, and incubated with the α-SMA antibody (67735-1-Ig, Proteintech, Wuhan, China) overnight at 4°C. Alexa 488-labeled fluorescent secondary antibody diluent (GB25303, Servicebio) was added, and the mixture was incubated for 1 h in the dark. DAPI (4′,6-diamidino-2-phenylindole) staining solution was then added, and the mixture was incubated for 10 min in the dark. Images were acquired using a fluorescence microscope, and average fluorescence intensity was analyzed with ImageJ software.

Animal grouping, modeling, and administration

A total of 48 SPF C57BL/6J mice, aged 8 weeks and weighing (20±2) g, were purchased from Sibefu Biotechnology Co., Ltd. (Beijing, China). The mice were housed in clean feeding cages (ambient temperature 20-24°C, relative humidity 50%-70%, light and dark alternating 12 h each), had free access to food and water, and strictly adhered to the '3R' principle for experimental animals. All animal experimental procedures were approved by the Fourth Affiliated Hospital of China Medical University Ethics Committee.

The mice were adaptively fed for 1 week. They were randomly assigned to the Sham group, the model (bleomycin, BLM) group, the positive control (bleomycin+pirfenidone) group, the orientin low-, medium-, and high-dose (bleomycin+orientin-L, bleomycin+orientin-M, bleomycin+orientin-H) groups, the TGF-β1/Smad3 pathway agonist (bleomycin+orientin+SRI-011381) group, and the inhibitor (bleomycin+orientin+SB431542) group using an interval random grouping method based on body weight, with 6 mice in each group. Except for the Sham group, mice in the other groups were anesthetized with an intraperitoneal injection of 2% pentobarbital sodium (30 mg/kg) and then secured to the operating table. The mouse pulmonary fibrosis model 4 was prepared by noninvasive tracheal instillation of bleomycin (BLM) (3.75 mg/kg, dissolved in normal saline), and the Sham group received the same volume of normal saline by the same route. After 24 h of modeling, mice in the bleomycin+pirfenidone group were administered 100 mg/kg pirfenidone by gavage. Mice in the low-, medium-, and high-dose groups received 10, 20, and 40 mg/kg of orientin by gavage, respectively. Mice in the SRI-011381 and SB431542 groups were injected intraperitoneally with 30 mg/kg SRI-011381 and 10 mg/kg SB431542, respectively, once daily for 28 days. Two hours after the last administration, the mice were anesthetized and sacrificed, and their lung tissues were dissected.

Western blot

After HFL1 cells were cultured, RIPA lysis buffer (P0013B, Beyotime) was added to lyse the cells, and the supernatant was collected after centrifugation (4°C, 10 000 r/min, 10 min). Mouse lung tissue was cut into small pieces and placed in a homogenizer tube. Homogenization beads and RIPA lysate were added, and the mixture was lysed on ice for 30 min. The supernatant was collected after centrifugation (4°C, 12 000 r/min, 10 min). The BCA protein concentration assay kit (P0009, Beyotime) was used to determine the total protein concentration in the supernatant. Loading buffer was added, and the protein was denatured in a metal bath at 96°C for 10 min. SDS-PAGE (Sodium Dodecyl Sulfate Polyacrylamide Gel Electrophoresis) was used to separate the protein components (voltage 70-120 V, time 1.5 h). The protein was transferred to a PVDF (polyvinylidene fluoride) membrane by wet transfer (constant current, 300 mA; 2 h), blocked with 5% skimmed milk powder for 2 h, and washed with PBST (phosphate-buffered saline) three times. The primary anti-

bodies were added and incubated overnight at 4°C. The secondary antibody (ab6734, abcam) was added and incubated for 2 h. The chemiluminescence imaging system (Chemi Doc MP, BioRad, USA) was used to expose and capture images, and the gray value of protein bands was analyzed using Image J software.

The primary antibodies: TGF-β1 (81746-2-RR, Proteintech), Smad3 (66516-1-Ig, Proteintech), p-Smad3 (ab63403, Abcam), α-SMA (67735-1-Ig, Proteintech), fibronectin (ab2413, Abcam), Collagen I (ab316222, Abcam), Vimentin (ab20346, Abcam), matrix metallopeptidase (MMP)-2 (ab181286, Abcam), MMP-9 (ab58803, Abcam), and GAPDH (ab181603, Abcam) were diluted to 1:1,000.

Pathological examination of lung tissue

The left lung tissues of mice were fixed in 4% paraformaldehyde, dehydrated, cleared, paraffin-embedded, and sectioned (4 μm thickness). Hematoxylin and eosin (HE) and Masson staining were performed routinely. Five fields of view were selected for each section. The pathological morphology of lung tissue was observed under an optical microscope, and images were collected. The collagen deposition area in Masson-stained sections was analyzed using ImageJ software.

Lung tissue inflammation scores were assessed according to the Szapiel scoring criteria: 0 score—No alveolar inflammation; 1 score—Monocyte infiltration, widened alveolar septum, limited to local and near-pleural areas, with an area less than 20% of the whole lung, and normal alveolar structure; 2 score—The affected area accounted for 20%-50% of the lung, with the area near the pleura more severe; 3 score—Alveolitis area >50%, with occasional consolidation caused by monocytes and hemorrhage in the alveolar cavity 18.

Pulmonary fibrosis was scored according to the Ashcroft scoring standard: 0 score—normal lung tissue; 1 score—slight thickening of the alveolar or bronchial walls; 3 score—moderate thickening of the alveolar or bronchial walls, with no obvious damage to the alveolar structure; 5 score—fibrous bands or small fibrous foci were formed, and the alveolar structure was markedly destroyed; 7 score—alveolar structure was severely deformed, and extensive fibrous foci were formed, showing 'honeycomb lung'; 8 score—full-field fibrosis of lung tissue; the severity of the lesions in the 2, 4, and 6 scores was between the corresponding scores 19.

Bronchoalveolar lavage fluid (BALF) analysis

After the mice were sacrificed, the chest cavity was opened and the heart removed. The lungs were washed twice with pre-cooled normal saline. The left pulmonary hilum was carefully ligated with a surgical suture, and the trachea was separated at the neck. A V-shaped incision was made at the tracheal bifurcation, and a venous indwelling needle cannula was inserted into the lower bronchus. Then, 500 μL of normal saline was slowly injected. Lung swelling was visible to the naked eye, and the lavage fluid was slowly withdrawn. After 3 repeated injections of bronchoalveolar lavage fluid, BALF was collected in a sterile tube, and the supernatant was collected after centrifugation. Tumor necrosis factor-alpha (TNF-α), interleukin (IL)-2, and IL-6 (ab208348, ab100706, ab222503, Abcam) levels in BALF were measured using enzyme-linked immunosorbent assay (ELISA) kits according to the manufacturer's instructions. At the same time, the activity of myeloperoxidase (MPO, ab275109, Abcam) in lung tissues was assessed. The total protein content in BALF was measured using a BCA protein concentration assay kit.

Determination of hydroxyproline (HYP) level

According to the HYP kit (A030-2-1, Jiancheng Institute of Bioengineering, Nanjing, China), 30-100 mg of wet-weight lung

tissue was accurately weighed and placed in a test tube. 1 mL of hydrolysate was added, and the mixture was mixed. The mixture was incubated in a 95°C water bath for 20 min, then diluted with double-distilled water to 10 mL. 4 mL of the diluted hydrolysate was mixed with an appropriate amount of activated carbon, then centrifuged for 10 min. The OD value of each group was measured using 1 mL of supernatant at 550 nm. HYP content in mice was calculated.

Immunohistochemistry

Lung sections were dewaxed, rehydrated, and antigen-repaired using citrate buffer. Endogenous peroxidase was quenched with 3% H_2O_2 for 10 min and blocked with 5% BSA for 20 min. Sections were incubated with the α-SMA antibody (67735-1-Ig, Proteintech, Wuhan, China) overnight at 4°C, then with the secondary antibody solution for 30 min. After washing, DAB (3,3′-diaminobenzidine) staining was performed, and the nuclei were counterstained with hematoxylin. α-SMA staining was brown, and the sections were evaluated under an optical microscope.

Statistical analysis

SPSS 27.0 was used for statistical analysis. All data were tested for normality and homogeneity of variance. One-way ANOVA with Tukey's post hoc test was used to compare groups. Data for each group were expressed as mean ± standard deviation. $p<0.05$ was considered statistically significant.

RESULTS

Orientin inhibited TGF-β1-activated HFL1 cell proliferation and migration

TGF-β1 was used to stimulate HFL1 cells to assess the therapeutic effect of orientin on PF, and pirfenidone served as a positive control. The structural formula of orientin is shown in Fig. 1A. First, at concentrations of ≥ 80 μM, the survival rates of HFL1 cells were markedly reduced (Fig. 1B), indicating cellular damage at this concentration. Therefore, 10, 20, and 40 μM orientin were selected for subsequent experiments. HFL1 cells were then stimulated with TGF-β1 and treated with pirfenidone and orientin. The proliferation rate of HFL1 cells increased markedly after TGF-β1 stimulation but decreased significantly after pirfenidone and orientin treatment (Fig. 1C). Edu staining showed that Edu-positive cells rose notably after TGF-β1 stimulation and decreased significantly after pirfenidone and orientin treatment (Fig. 1D), indicating that TGF-β1 promoted HFL1 cell proliferation, whereas orientin inhibited this proliferation. TGF-β1 induced the transformation of HFL1 cells into myofibroblasts, and the migration ability of myofibroblasts was enhanced compared with fibroblasts. The migration rate was significantly elevated after TGF-β1 stimulation at 24 h. However, after treatment with pirfenidone and orientin, the migration rate was significantly reduced (Fig. 1E), indicating that orientin suppressed the migratory ability of HFL1 cells. These experiments showed that pirfenidone and orientin significantly suppressed HFL1 cell growth and migration, and the inhibitory effect of high-dose orientin was comparable to that of pirfenidone.

Orientin inhibited the TGF-β1-activated TGF-β1/Smad3 pathway and inhibited cell proliferation and migration in HFL1 cells

The TGF-β1/Smad3 pathway is a well-characterized pathway implicated in PF progression. This study also found that TGF-β1 and p-Smad3 protein expression in HFL1 cells increased significantly after TGF-β1 induction but decreased significantly after pirfenidone and orientin intervention (Fig. 2A-C), indicating that TGF-β1 induced activation of this pathway, whereas orientin inhibited its activation. Since the inhibitory effect of 40 μM orientin was the most significant in previous studies, this concentration was selected for subsequent research. HFL1 cells were treated with the TGF-β1/Smad3 pathway agonist SRI-011381 and the inhibi-

tor SB431542 alongside orientin treatment. Compared with orientin treatment, TGF-β1 and p-Smad3 protein expression increased significantly after SRI-011381 treatment and decreased significantly after SB431542 treatment (Fig. 2D-F). After SRI-011381 intervention, the proliferation rate of HFL1 cells (Fig. 2G) and Edu-positive cell number (Fig. 2H) increased significantly, and the migration rate also increased significantly (Fig. 2I). SB431542 significantly reduced the proliferation rate, Edu-positive cell num-

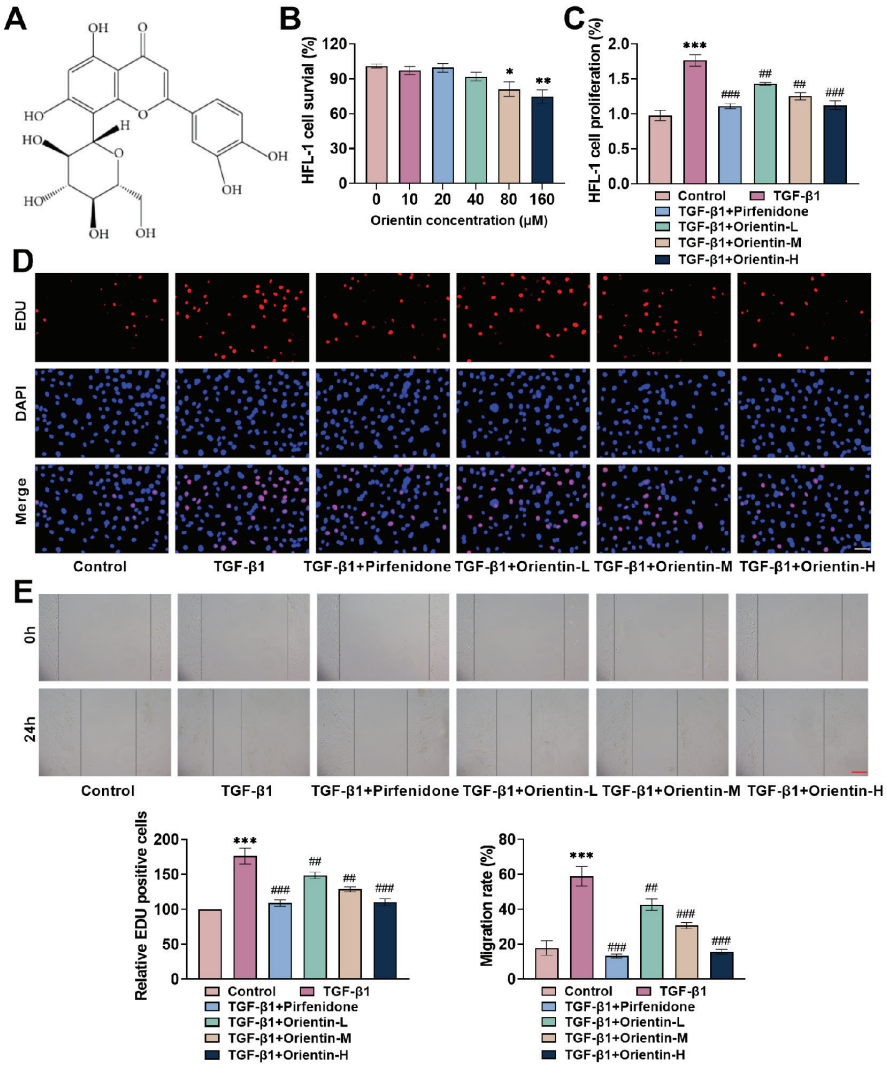

Fig. 1. Orientin inhibited TGF-β1-induced HFL1 cell growth and migration. **A:** Orientin molecular formula. **B:** HFL1 (cells derived from human fetal lung tissue) were treated with orientin for 24 h, and the survival rate was measured by CCK-8 assay (Cell Counting Kit-8). Orientin at concentrations of 40 μM or lower had no effect on cell viability (*p<0.05, **p<0.01 vs 0 group). **C:** After HFL1 cells were stimulated with TGF-β1, they were treated with pirfenidone and orientin. The proliferative ability of HFL1 cells was assessed by the CCK-8 assay. Orientin markedly inhibited cell proliferation. **D:** HFL1 cell proliferation was assessed by EdU staining (5-ethynyl-2′-12 deoxyuridine). Orientin decreased the number of EdU-positive cells (×40, 50 μm). **E:** The migration of HFL1 cells was assessed by the wound-healing assay. Orientin significantly inhibited cell migration (×10, 200 μm). 15 n=3, *p<0.05, ** p<0.01, *** p<0.001 vs 0/Control group; ## p<0.01, ### p<0.001 vs TGF-β1 group.

ber, and migration rate of HFL1 cells (Fig. 2G-I), indicating that inhibition of TGF-β1/Smad3 signaling could inhibit HFL1 cell proliferation and migration. In conclusion, orientin suppressed the TGF-β1/Smad3 pathway and inhibited HFL1 cell proliferation and migration.

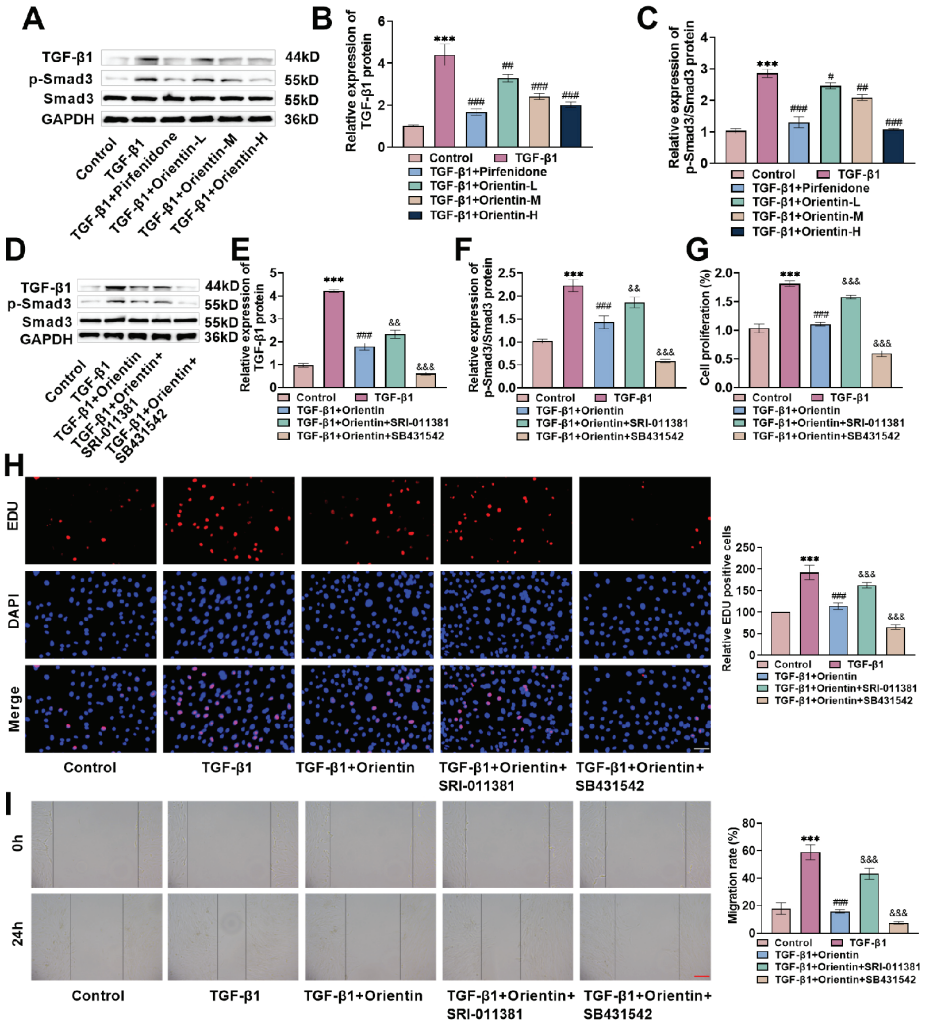

Fig. 2. Orientin inhibited TGF-β1-activated TGF-β1/Smad3 pathway and inhibited cell proliferation and migration in HFL1 cells. **A-C:** Western blot was used to detect the expression of the TGF-β1/Smad3 pathway protein in HFL1 cells (cells derived from human fetal lung tissue). Expression of TGFβ1and p-Smad3 protein increased significantly after TGF-β1 induction, and decreased significantly after orientin intervention. **D-F:** HFL1 cells were treated with the TGFβ1/Smad3 pathway agonist SRI-011381 (N′-cyclohexyl-N-(phenylmethyl)-N-(4piperidinylmethyl)-urea) and inhibitor SB431542 (TGF-β RI Kinase Inhibitor VI) alongside orientin treatment, and TGF-β1/Smad3 pathway protein levels were detected through Western blot. TGF-β1 and p-Smad3 protein expressions increased significantly after SRI-011381 treatment, and decreased significantly after SB431542 treatment. **G:** HFL1 cell proliferation was determined by CCK-8 (Cell Counting Kit-8). SB431542 markedly inhibited cell proliferation. **H:** HFL1 cell proliferation was assessed by EdU staining (5-ethynyl-2′-deoxyuridine). SB431542 significantly reduced the number of EdU-positive cells (×40, 50 μm). **I:** Migration was evaluated by the scratch-healing assay. SB431542 significantly inhibited cell migration (×10, 200 μm). n=3, *** p<0.001 vs Control group; #p<0.05, ##p<0.01, ###p<0.001 vs TGF-β1 group; &&p<0.01, &&& p<0.001 vs TGF-β1+Orientin group.

Orientin inhibited TGF-β1-induced fibroblast to myofibroblast transition (FMT) and improved extracellular matrix (ECM) through the TGF-β1/Smad3 signaling pathway

Fibroblasts are primarily responsible for producing and maintaining the ECM, and their mechanical properties can be altered. They can also transform into myofibroblasts. Myofibroblasts are cells that drive fibrotic tissue development through a sharp increase in protein deposition. The transition from fibroblasts to myofibroblasts is a well-known cellular marker of histopathological status [20]. Sirius red staining showed that collagen fiber staining increased significantly after TGF-β1 stimulation and decreased significantly after orientin treatment. However, compared with orientin treatment, red-stained collagen fibers increased significantly after SRI-011381 treatment and decreased significantly after SB431542 treatment (Fig. 3A), indicating that orientin inhibited the production and accumulation of collagen fibers induced by TGF-β1 through the TGF-β1/Smad3 pathway. α-SMA is a marker of myofibroblasts. The fluorescence intensity of α-SMA increased significantly after TGF-β1 intervention, decreased significantly after orientin treatment, increased significantly after SRI-011381 treatment, and decreased significantly after SB431542 treatment (Fig.3B). Finally, ECM-related protein expression was assessed by Western blot. α-SMA, fibronectin, Collagen I, Vimentin, MMP-2, and MMP-9 protein levels were markedly elevated after TGF-β1 stimulation but declined markedly after orientin treatment. Compared with orientin intervention, protein levels were significantly increased after SRI-011381 treatment and significantly decreased after SB431542 treatment (Fig. 3C-I), indicating that orientin improved ECM through the TGF-β1/Smad3 pathway. Overall, these experiments showed that orientin inhibited TGF-β1-induced FMT, reduced ECM deposition, and promoted ECM remodeling by suppressing the TGF-β1/Smad3 pathway.

Orientin inhibited the BLM-activated TGF-β1/Smad3 pathway in mouse lung tissue

To further verify the protective effects of orientin in vivo, this study established a BLM-induced PF mouse model to verify the in vivo mechanism and treated the mice with pirfenidone and orientin. TGF-β1 and p-Smad3 protein expression increased markedly after BLM induction but decreased significantly after pirfenidone and orientin treatment, with the high-dose orientin intervention effect comparable to that of pirfenidone (Fig. 4A-C). However, after injection of SRI-011381, TGF-β1 and p-Smad3 levels were notably raised. The protein levels were significantly reduced after injection of SB431542 (Fig. 4D-F). This indicated that orientin suppressed the BLM-induced TGF-β1/Smad3 pathway.

Orientin alleviated BLM-induced inflammatory injury in mouse lung tissue by the TGF-β1/Smad3 pathway

HE staining showed that the lung tissue structure in the bleomycin group was destroyed, with alveolar cavities collapsed, alveolar septa widened, and inflammatory infiltration within the alveolar cavities. The inflammatory score of the lung tissue increased significantly. After orientin treatment, inflammatory infiltration and the score were significantly reduced. After SRI-011381 treatment, the alveolar space in lung tissue decreased, inflammatory infiltration increased, and the score increased. Lung tissue inflammation was inhibited after SB431542 treatment (Fig. 5A). TNF-α, IL-2, and IL-6 levels in BALF, and MPO (myeloperoxidase) activity in lung tissue, increased significantly after BLM stimulation and decreased significantly after orientin treatment. Compared with orientin treatment, inflammatory factors and MPO levels were significantly increased after SRI-011381 treatment and significantly decreased after SB431542 treatment (Fig. 5B-E). The trend of total protein content in BALF was consis-

tent with that of inflammatory factors, increasing significantly after treatment with BLM and SRI-011381, and decreasing significantly after treatment with orientin and SB431542 (Fig.5F). In summary, orientin can alleviate the degree of inflammation in PF mice by suppressing the TGF-β1/Smad3 pathway.

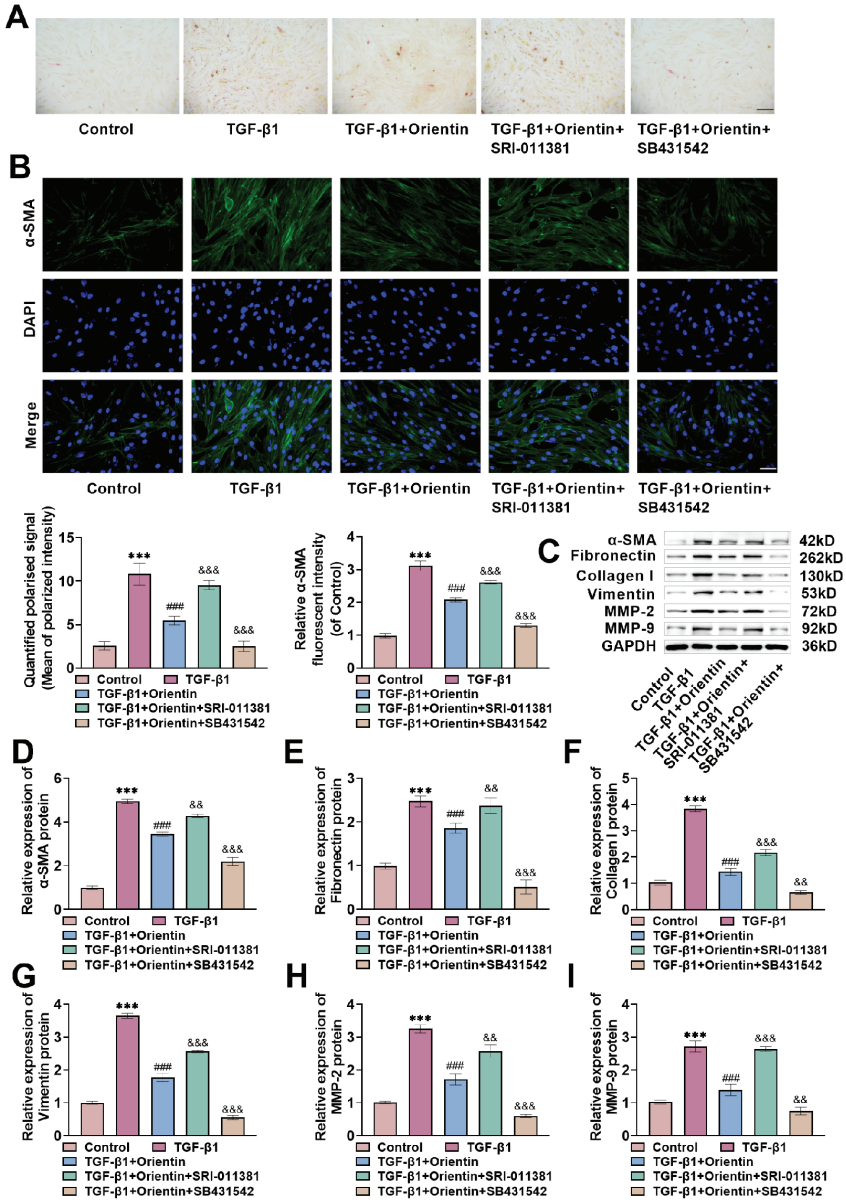

Fig. 3. Orientin inhibited TGF-β1-induced FMT and improved ECM by TGFβ1/Smad3 pathway. **A:** Sirius red staining was used to detect the type of cell collagen fibers. Red-stained collagen fibers were significantly reduced after Orientin treatment (×20, 100 μm). **B:** α-SMA levels were assessed by immunofluorescence. Orientin significantly reduced α-SMA fluorescence intensity (×40, 50 μm). **C-I:** ECM (extracellular matrix)-related protein expression was determined by Western blot. α-SMA, fibronectin, Collagen I, Vimentin, MMP-2 (matrix metalloproteinase-2), and MMP-9 (matrix metalloproteinase-9) levels were markedly decreased after Orientin therapy. n=3, *** $p<0.001$ vs Control group; ### $p<0.001$ vs TGF-β1 group; && $p<0.01$, &&& $p<0.001$ vs TGF-β1+Orientin group. TGF-β1.

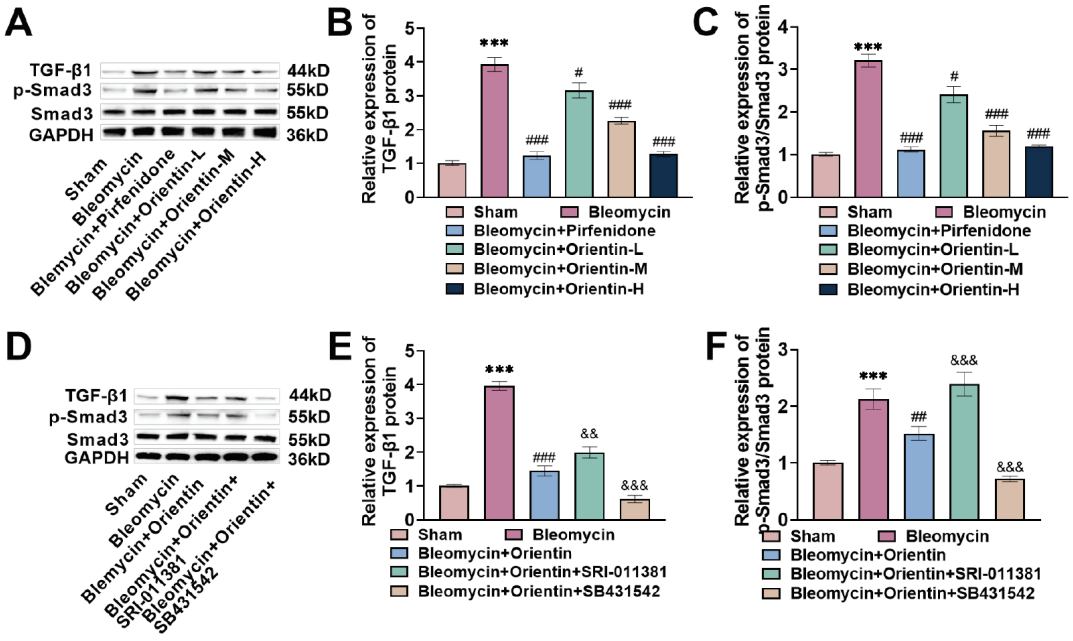

Fig. 4. Orientin inhibited BLM-induced activation of the TGF-β1/Smad3 pathway 65 in mouse lung tissue. **A-C:** Protein expression of the TGF-β1/Smad3 pathway was evaluated by Western blot. TGF-β1 and p-Smad3 protein (phosphorylated SMAD family member 3) levels were markedly increased after BLM induction, and significantly lowered after orientin intervention. **D-F:** The mice were injected with the TGF-β1/Smad3 pathway agonist SRI-011381(N′-cyclohexyl-N-(phenylmethyl)-N-(4-piperidinylmethyl)-urea) and the inhibitor SB431542 (TGF-β RI Kinase Inhibitor VI) at the same time as orientin, and TGF-β1/Smad3 pathway protein levels were determined by Western blot. p-Smad3 (phosphorylated SMAD family member 3) and TGF-β1 levels were significantly increased when SRI-011381 intervention, and significantly decreased after SB431542 treatment. n=6, ***p<0.001 vs sham group; # p<0.05, ##p<0.01, ###p<0.001 vs treatment. n=6, ***p<0.001 vs sham group; #p<0.05, ##p<0.01, ### p<0.001 vs.

Orientin alleviated BLM-induced PF injury in mice through the TGF-β1/Smad3 pathway

HYP content in lung tissue increased significantly after BLM stimulation and decreased significantly after orientin treatment. Compared with orientin treatment, HYP content increased significantly after SRI-011381 treatment and decreased significantly after SB431542 treatment (Fig. 6A). Masson staining showed that the structure of lung tissue in the bleomycin group was destroyed, collagen fibers were severely proliferated, and the collagen deposition area and pulmonary fibrosis score were significantly increased. After orientin treatment, the degree of alveolar damage and collagen fiber hyperplasia were significantly reduced, and the collagen deposition area and pulmonary fibrosis score were significantly reduced. After the SRI-011381 intervention, collagen fiber proliferation was notably elevated, and the collagen deposition area and PF score were markedly increased. After SB431542 treatment, collagen fiber proliferation was reduced, and the collagen deposition area and PF score were notably reduced (Fig.6B-D). α-SMA levels were consistent with those in cell experiments, being markedly raised after BLM and SRI-011381 treatment and significantly decreased after orientin and SB431542 treatment (Fig. 6E). Fibronectin, Collagen I, α-SMA, Vimentin, MMP-2, and MMP-9 expressions increased

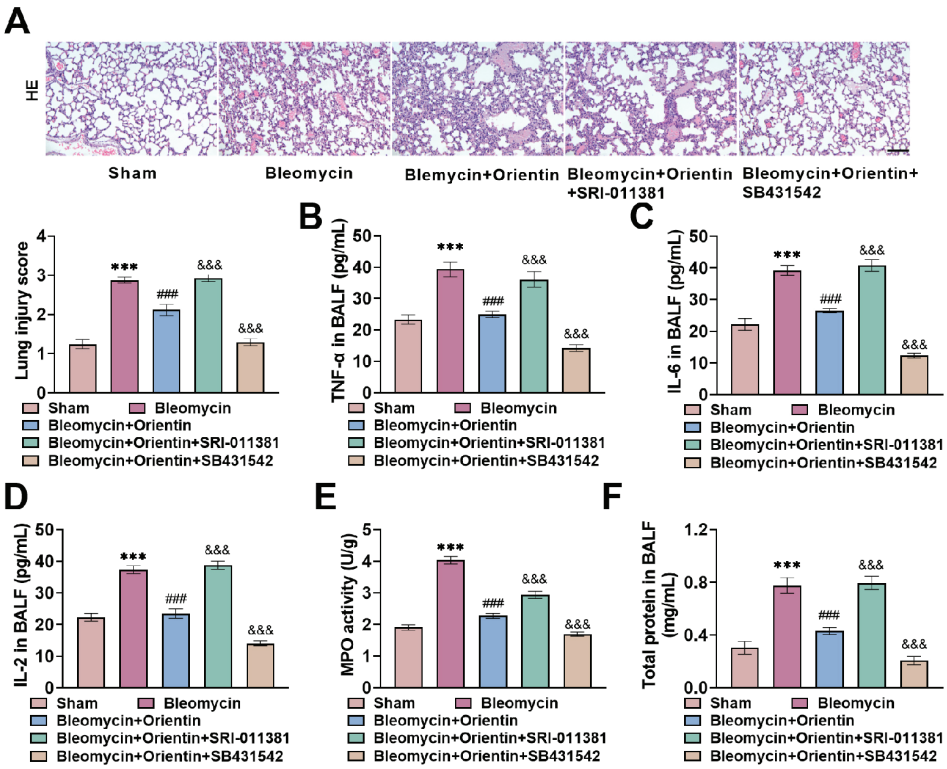

Fig. 5. Orientin alleviated BLM-induced inflammatory injury in mouse lung tissue via the TGF-β1/Smad3 pathway. **A:** Pathological damage to lung tissue in each group was observed by HE staining. After BLM stimulation, alveolar cavity collapse, inflammatory cell infiltration, and inflammatory score increased significantly. Orientin can inhibit lung inflammation (×20, 100 μm). **B-E:** TNF-α, IL-2 and IL-6 levels in BALF and MPO activity in lung tissues were determined using an ELISA kit. These were significantly reduced after Orientin treatment. **F:** The total protein content in BALF was determined by the BCA (bicinchoninic acid) method, which was significantly decreased after Orientin treatment. n=6, *** $p<0.001$ vs sham group; ###$p<0.001$ vs the bleomycin group; &&& $p<0.001$ vs the bleomycin+orientin group. SRI-011381(N′-cyclohexyl-N (phenylmethyl)-N-(4-piperidinylmethyl)-urea); SB431542 (TGF-β RI Kinase Inhibitor VI).

markedly after BLM stimulation but decreased significantly after orientin treatment. Compared with orientin intervention, protein levels were significantly increased after SRI-011381 treatment and significantly decreased after SB431542 treatment (Fig. 6F-L). These experiments showed that orientin could alleviate fibrosis damage in PF mice by suppressing the TGF-β1/Smad3 pathway.

DISCUSSION

This study was the first to systematically evaluate the therapeutic effect of orientin on PF and its underlying molecular mechanism. Orientin notably reduced pathological changes in lung tissue, inhibited FMT, improved ECM, and lessened the severity of PF. The mechanism was closely associated with reducing the inflammatory response and inhibiting the TGF-β1/Smad3 pathway.

Myofibroblasts are absent from normal lung tissue but are important producers of collagen and other matrix proteins. Promoting fibroblast apoptosis and inhibiting fibroblast-to-myofibroblast transformation can effectively inhibit PF [21]. TGF-β1, a key cytokine that promotes myofibroblast

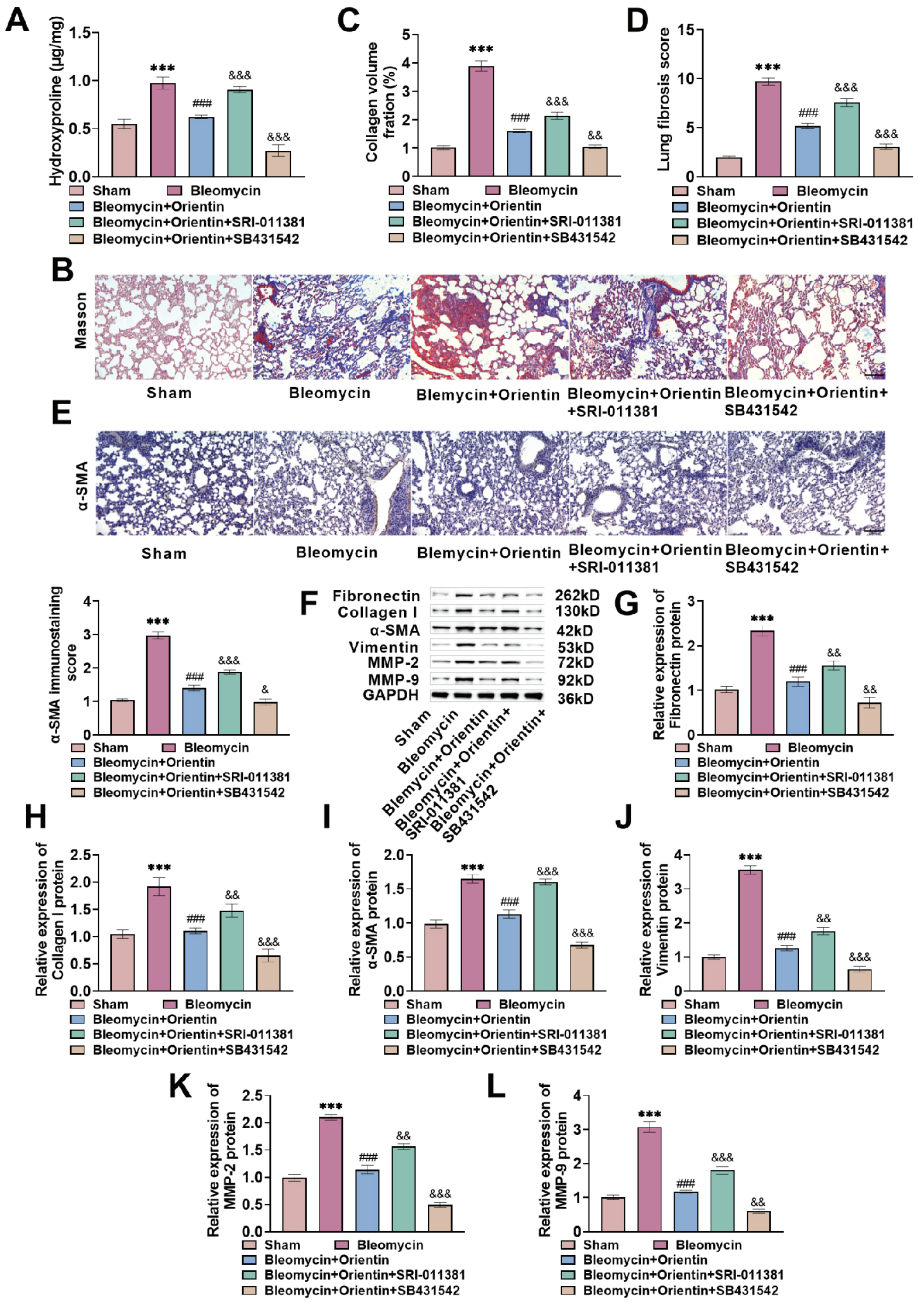

Fig. 6. Orientin alleviated BLM-induced PF injury in mice through the TGF-β1/Smad3 pathway. **A:** HYP content in lung tissue was measured by HYP assay, and was significantly reduced after orientin treatment. **B-D:** Collagen deposition and fibrosis were analyzed by Masson-Brüch staining. After BLM stimulation, collagen fibers in lung tissue proliferated significantly, and the collagen deposition area and PF score increased significantly. The collagen deposition area and pulmonary fibrosis score were markedly reduced after orientin therapy (×20, 100 μm). **E:** α-SMA) level was evaluated by immunohistochemistry. Orientin significantly reduced α-SMA level (×20, 100 μm). **F-L:** PF-related protein levels were detected by Western blot. The levels of α-SMA, fibronectin, Collagen I, Vimentin, MMP-2, and MMP-9 were markedly decreased after Orientin intervention. n=6, *** $p<0.001$ vs the sham group; ### $p<0.001$ vs the bleomycin group; & $p<0.05$, && $p<0.01$, &&& $p<0.001$ vs the bleomycin+orientin group. SRI-011381(N′-cyclohexyl-N-(phenylmethyl)-N-(4-piperidinylmethyl)-urea); SB431542 (TGF-β RI Kinase Inhibitor VI).

differentiation and collagen expression, is vital for the progression of PF. As our understanding of PF pathogenesis advances, TGF-β1 has been identified as the primary pro-fibrotic growth factor involved in fibrosis, influencing cell growth, differentiation, and programmed cell death. Excess TGF-β1 results in collagen accumulation and triggers various fibrotic conditions [22]. Therefore, this study used TGF-β1 to induce fibroblasts and construct an in vitro PF model. The results showed that orientin significantly suppressed TGF-β1-activated proliferation and migration of HEL1 cells.

In this study, the anti-fibrosis mechanism of orientin was further elucidated by systematically evaluating changes in key indicators of the TGF-β1/Smad3 pathway. At the ligand level, TGF-β1 is the central factor that initiates and maintains fibrosis, and its activity directly determines the severity of fibrosis [23]. At the level of intracellular signal transduction, the phosphorylation level of Smad3 is a direct indicator of TGF-β1 pathway activity [24]. At the effector-molecule level, α-SMA is a specific marker of fibroblast activation; its expression directly reflects the activation state of fibroblasts. At the same time, ECM remodeling is an important factor in promoting the occurrence and development of PF. Intervention in ECM remodeling can significantly improve excessive fibrosis in the lung [25, 26]. Collagen I and fibronectin are major ECM components; their high expression can lead to pulmonary interstitial collagen deposition [27, 28]. MMPs are collagenolytic enzymes that are vital to the pathophysiological process of IPF. High expression of MMPs degrades the basement membrane and lung tissue structure, collapses the alveolar cavity, aggravates lung injury, and further promotes the release of TGF-β1. TGF-β1, as an activator of MMPs, promotes their synthesis and further increases MMP expression, thus forming a vicious circle [29].

This study found that orientin significantly reduced TGF-β1 and p-Smad3 levels in HEL1 cells after TGF-β1 stimulation, indicating that orientin inhibited the TGF-β1/Smad3 pathway and that this inhibition also suppressed HEL1 cell proliferation and migration. In addition, TGF-β1 significantly increased collagen fiber formation in HEL1 cells and upregulated α-SMA, fibronectin, Collagen I, Vimentin, and MMP expression, suggesting that TGF-β1 notably promoted lung fibroblast activation, FMT, and excessive ECM deposition. Orientin could inhibit the TGF-β1/Smad3 pathway, thereby inhibiting lung fibroblast activation, improving ECM, and alleviating the PF process. ECM and collagen deposition are the key pathological changes that cause PF, indicating that Orientin improved these key pathological changes.

PF involves a series of inflammatory and fibrotic reactions that ultimately lead to ECM deposition, fibroblast foci, and fibrotic areas juxtaposed with normal lung parenchyma. In the early stage of IPF, the balance of M1/M2 macrophages is disrupted, leading to the secretion of inflammatory mediators and the recruitment of fibroblasts, which proliferate continuously. TNF-α, IL-1β, IL-6, and IL-2 are key biomarkers for assessing the inflammatory state of lung tissue. They jointly promote inflammatory injury and fibrosis in lung tissue by recruiting, activating, and expanding inflammatory cells, and by regulating the immune response and tissue repair processes in the development of PF [3]. Studies have shown that orientin can reduce LPS-induced NF-κB phosphorylation in cells, thereby lowering inflammatory factors and oxidative markers[17]. MPO activity is a marker of neutrophil infiltration in lung tissue [30]. Neutrophils release numerous toxic substances during inflammation, causing damage to the lung parenchyma and tissue structure. Neutrophils are key inflammatory cells that drive PF [31, 32]. The most commonly used and well-established drug for inducing lung fibrosis in rats is BLM [33]. In this study, lung tissues after BLM intervention were significantly damaged, with alveo-

lar collapse, atrophy, widened intervals, and inflammatory cell infiltration. In addition, a large number of inflammatory cytokines accumulated in BALF after BLM induction, and MPO activity in lung tissues was markedly elevated. However, inflammatory infiltration in the pirfenidone and orientin groups was significantly reduced, and the levels of TNF-α, IL-2, IL-6, and MPO activity were also significantly reduced. SRI-011381 significantly weakened orientin's anti-inflammatory effects, whereas SB431542 significantly enhanced them. This suggests that orientin may reduce the release of inflammatory factors and inflammatory infiltration via the TGF-β1/Smad3 axis, thereby slowing the PF process.

After modeling with BLM, the initial damage was primarily concentrated around the bronchioles; on the 7th day, the distal lung parenchyma was involved, and multiple inflammatory lesions and edema were observed in the alveolar septa. On the 14th day, regional interstitial fibrosis appeared in the lungs, manifested as extensive collagen deposition and remodeling of alveolar units. These changes are considered to reflect similar changes in PF. Based on this, the model can complete the task of studying PF mitigation drugs. HYP is a unique amino acid in collagen and is one of the main components of collagen tissue. Some data confirmed that HYP can be used as a reliable method for quantitative fibrosis[4]. In the BLM-induced PF rat model, this study, using Masson staining, observed that collagen fibers after BLM intervention were markedly proliferated, the collagen deposition area and PF score were markedly increased, and the HYP content was significantly increased. Collagen deposition in the pirfenidone and orientin groups was notably reduced, and the PF score and HYP content were significantly reduced, indicating that orientin and pirfenidone can effectively alleviate BLM-induced pulmonary fibrosis. Western blot experiments also confirmed that the expressions of fibronectin, Collagen I, α-SMA, Vimentin, MMP-2, and MMP-9 were significantly decreased after orientin treatment. However, SRI-011381 significantly weakened orientin's anti-fibrosis effect, whereas SB431542 significantly enhanced it. Therefore, orientin can inhibit lung fibroblast activation and reduce collagen deposition in the lungs of PF mice via the TGF-β1/Smad3 pathway. Combined with the results of cell experiments, Orientin can inhibit FMT through the TGF-β1/Smad3 pathway, alleviate inflammatory responses and fibrotic damage, and thereby improve PF, indicating the potential of Orientin as a therapeutic drug for PF.

In summary, orientin can inhibit inflammatory factors and FMT in a PF model, reduce ECM production, regulate key protein expression in the TGF-β1/Smad3 pathway, and demonstrate a clear anti-fibrotic effect. As a natural medicine with a wide range of sources and low cost, orientin has promising applications in PF treatment. This study provides laboratory evidence supporting the use of orientin as a therapeutic agent for PF. Follow-up studies can further explore its clinical translational value and provide new treatment options for PF patients. Although this study reveals the potential role of orientin in PF and its molecular mechanism, differences between rodents and humans introduce uncertainty in translating the results, which can be further explored and verified using PF patient samples.

List of abbreviations

TGF-β1	transforming growth factor-β1
Smad3	suppressor of mother against decapentaplegic 3
HYP	hydroxyproline
FMT	fibroblast to myofibroblast transition
PF	pulmonary fibrosis
IPF	idiopathic pulmonary fibrosis
ECM	extracellular matrix
EMT	epithelial-mesenchymal transition
α-SMA	alpha-smooth muscle actin
MMP	matrix metallopeptidase
BALF	bronchoalveolar lavage fluid
TNF-α	tumour necrosis factor-alpha
IL	interleukin
MPO	myeloperoxidase
IMP	Imperatorin
BLM	bleomycin

Acknowledgment

None.

Funding

None.

ORCID ID of the authors

- Yijin Liu (YiL): 0009-0000-9374-5973
- Yao Lu (YaL): 0009-0007-2749-1419

Author's contributions

YaL: Developed and planned the study, performed experiments, and interpreted results. Edited and refined the manuscript with a focus on critical intellectual contributions. YaL: Participated in collecting, assessing, and interpreting the date. Made significant contributions to date interpretation and manuscript preparation. Yi L: Provided substantial intellectual input during the drafting and revision of the manuscript.

Conflict of interest

The authors state that they have no conflicts of interest.

Consent to publish

The manuscript has neither been previously published nor is under consideration by any other journal. The authors have all approved the content of the paper.

Ethic approval

This study was approved by The Fourth Affiliated Hospital of China Medical University Ethic Committee (No. 21000062024112).

REFERENCES

1. **Kawano-Dourado L, Funke-Chambour M, Wells AU.** Ziritaxestat and Lung Function in Idiopathic Pulmonary Fibrosis. JAMA. 2023;330(10):973. *https://doi.org/10.1001/jama.2023.12637.*
2. **Savin IA, Zenkova MA, Sen'kova AV.** Pulmonary Fibrosis as a Result of Acute Lung Inflammation: Molecular Mechanisms, Relevant In Vivo Models, Prognostic and Therapeutic Approaches. Int J Mol Sci. 2022;23(23) :14959. *https://doi.org/10.3390/ijms232314959.*
3. **Liu GY, Budinger GRS, Dematte JE.** Advances in the management of idiopathic pulmonary fibrosis and progressive pulmonary fibrosis. BMJ. 2022;377:e066354. *https://doi.org/10.1136/bmj-2021-066354.*
4. **Zhang Y, Lu YB, Zhu WJ, Gong XX, Qian R, Lu YJ, et al.** Leech extract alleviates idiopathic pulmonary fibrosis by TGF-β1/Smad3 signaling pathway. J Ethnopharmacol. 2024;324:117737. *https://doi.org/10.1016/j.jep.2024.117737.*
5. **Yao F, Xu M, Dong L, Shen X, Shen Y, Jiang Y, et al.** Sinomenine attenuates pulmonary fibrosis by downregulating TGF-β1/Smad3, PI3K/Akt and NF-κB signaling pathways. BMC Pulm Med. 2024;24(1):229. *https://doi.org/10.1186/s12890-024-03050-5.*

6. **Yang F, Hou ZF, Zhu HY, Chen XX, Li WY, Cao RS, et al.** Catalpol Protects Against Pulmonary Fibrosis Through Inhibiting TGF-β1/Smad3 and Wnt/β-Catenin Signaling Pathways. Front Pharmacol. 2021;11:594139. *https://doi.org/10.3389/fphar.2020.594139.*
7. **Wanas H, El Shereef Z, Rashed L, Aboulhoda BE.** Ticagrelor Ameliorates Bleomycin-Induced Pulmonary Fibrosis in Rats by the Inhibition of TGF-β1/Smad3 and PI3K/AKT/mTOR Pathways. Curr Mol Pharmacol. 2022;15(1):227-238. *https://doi.org/10.2174/1874467214666210204212533.*
8. **Truchetet ME, Brembilla NC, Chizzolini C.** Current Concepts on the Pathogenesis of Systemic Sclerosis. Clin Rev Allergy Immunol. 2023;64(3):262-283. *https://doi.org/10.1007/s12016-021-08889-8.*
9. **Moss BJ, Ryter SW, Rosas IO.** Pathogenic Mechanisms Underlying Idiopathic Pulmonary Fibrosis. Annu Rev Pathol. 2021;17:515-546. *https://doi.org/10.1146/annurev-pathol-042320-030240*
10. **Wang J, Xu L, Xiang Z, Ren Y, Zheng X, Zhao Q, et al.** Microcystin-LR ameliorates pulmonary fibrosis via modulating CD206(+) M2-like macrophage polarization. Cell Death Dis. 2020;11(2):136. *https://doi.org/10.1038/s41419-020-2329-z.*
11. **Zhu D, Zhang Q, Li Q, Wang G, Guo Z.** Inhibition of AHNAK nucleoprotein 2 alleviates pulmonary fibrosis by downregulating the TGF-β1/Smad3 signaling pathway. J Gene Med. 2022;24(9):e3442. *https://doi.org/10.1002/jgm.3442.*
12. **Liu H, Lai W, Nie H, Shi Y, Zhu L, Yang L, et al.** PM(2.5) triggers autophagic degradation of Caveolin-1 via endoplasmic reticulum stress (ERS) to enhance the TGF-β1/Smad3 axis promoting pulmonary fibrosis. Environ Int. 2023;181:108290. *https://doi.org/10.1016/j.envint.2023.108290.*
13. **Ghafouri-Fard S, Askari A, Shoorei H, Seify M, Koohestanidehaghi Y, Hussen BM, et al.** Antioxidant therapy against TGF-β/SMAD pathway involved in organ fibrosis. J Cell Mol Med. 2024;28(2):e18052. *https://doi.org/10.1111/jcmm.18052.*
14. **Fahmy MI, Sadek MA, Abdou K, El-Dessouki AM, El-Shiekh RA, Khalaf SS.** Orientin: a comprehensive review of a promising bioactive flavonoid. Inflammopharmacology. 2025;33(4):1713-1728. *https://doi.org/10.1007/s10787-025-01690-5.*
15. **Long Q, Ma T, Wang Y, Chen S, Tang S, Wang T, et al.** Orientin alleviates the inflammatory response in psoriasis like dermatitis in BALB/c mice by inhibiting the MAPK signaling pathway. Int Immunopharmacol. 2024;134:112261. *https://doi.org/10.1016/j.intimp.2024.112261.*
16. **Chen H, Liu S, Xing J, Wen Y, Chen L.** Orientin alleviates chondrocyte senescence and osteoarthritis by inhibiting PI3K/AKT pathway. Bone Joint Res. 2025;14(3):245-258. Bone Joint Res. 2025 Mar 14;14(3):245-258. *https://doi.org/10.1302/2046-3758.143.BJR-2023-0383. R2.*
17. **Xiao Q, Cui Y, Zhao Y, Liu L, Wang H, Yang L.** Orientin relieves lipopolysaccharide-induced acute lung injury in mice: The involvement of its anti-inflammatory and anti-oxidant properties. Int Immunopharmacol. 2021;90:107189. *https://doi.org/10.1016/j.intimp.2020.107189.*
18. **Szapiel SV, Elson NA, Fulmer JD, Hunninghake GW, Crystal RG.** Bleomycin-induced interstitial pulmonary disease in the nude, athymic mouse. Am Rev Respir Dis. 1979;120(4):893-899. *https://doi.org/10.1164/arrd.1979.120.4.893.*
19. **Ashcroft T, Simpson JM, Timbrell V.** Simple method of estimating severity of pulmonary fibrosis on a numerical scale. J Clin Pathol. 1988;41(4):467-470. *https://doi.org/10.1136/jcp.41.4.467.*
20. **D'Urso M, Kurniawan NA.** Mechanical and Physical Regulation of Fibroblast-Myofibroblast Transition: From Cellular Mechanoresponse to Tissue Pathology. Front Bioeng Biotechnol. 2020;8:609653. *https://doi.org/10.3389/fbioe.2020.609653.*
21. **Zhang JX, Huang PJ, Wang DP, Yang WY, Lu J, Zhu Y, et al.** m(6)A modification regulates lung fibroblast-to-myofibroblast transition through modulating KCNH6 mRNA translation. Mol Ther.

2021;29(12):3436-3448. *https://doi.org/10.1016/j.ymthe.2021.06.008.*

22. **Gifford CC, Tang J, Costello A, Khakoo NS, Nguyen TQ, Goldschmeding R, et al.** Negative regulators of TGF-β1 signaling in renal fibrosis; pathological mechanisms and novel therapeutic opportunities. Clin Sci. 2021;135(2):275-303. *https://doi.org/10.1042/CS20201213.*
23. **Glass DS, Grossfeld D, Renna HA, Agarwala P, Spiegler P, Kasselman LJ, et al.** Idiopathic pulmonary fibrosis: Molecular mechanisms and potential treatment approaches. Respir Investig. 2020;58(5):320-335. *https://doi.org/10.1016/j.resinv.2020.04.002.*
24. **Ye Z, Hu Y.** TGF−β1: Gentlemanly orchestrator in idiopathic pulmonary fibrosis (Review). Int J Mol Med. 2021;48(1):132. *https://doi.org/10.3892/ijmm.2021.4965.*
25. **Ding H, Cui Y, Yang J, Li Y, Zhang H, Ju S, et al.** ROS-responsive microneedles loaded with integrin avβ6-blocking antibodies for the treatment of pulmonary fibrosis. J Control Release. 2023;360:365-375. *https://doi.org/10.1016/j.jconrel.2023.03.060.*
26. **Habert P, Puech B, Coiffard B, Secq V, Thomas P, Bec R, et al.** Angiographic and histopathological study on bronchial-to-pulmonary vascular anastomoses on explants from patients with cystic fibrosis after bronchial artery embolisation. J Cyst Fibros. 2022;21(6):1042-1047. *https://doi.org/10.1016/j.jcf.2022.04.015.*
27. **Patten J, Wang K.** Fibronectin in development and wound healing. Adv Drug Deliv Rev. 2021;170:353-368. *https://doi.org/10.1016/j.addr.2020.09.005.*
28. **Yan Y, Zhang Y, Zhang J, Ying L.** SCN-N1B regulates the proliferation, migration, and collagen deposition of human lung fibroblasts. In Vitro Cell Dev Biol Anim. 2023;59(7):479-485. *https://doi.org/10.1007/s11626-023-00787-x.*
29. **Mahalanobish S, Saha S, Dutta S, Sil PC.** Matrix metalloproteinase: An upcoming therapeutic approach for idiopathic pulmonary fibrosis. Pharmacol Res. 2020;152:104591. *https://doi.org/10.1016/j.phrs.2019.104591.*
30. **Xin Y, Zou L, Lang S.** 4-Octyl itaconate (4-OI) attenuates lipopolysaccharide-induced acute lung injury by suppressing PI3K/Akt/NF-κB signaling pathways in mice. Exp Ther Med. 2021;21(2):141. *https://doi.org/10.3892/etm.2020.9573.*
31. **Chen S, Song X, Lv C.** Macrophages and Pulmonary Fibrosis. Curr Mol Med. 2025;25(4):416-430. *https://doi.org/10.2174/0115665240286046240112112310.*
32. **Ay D, Başlılar Ş, Kulah G, Kaan Saylan B, Kalbaran Kismet G, Okutan O.** Blood Cell Counts and Inflammatory Indexes in Idiopathic Pulmonary Fibrosis. Cureus. 2025;17(1):e78319. *https://doi.org/10.7759/cureus.78319.*
33. **Allawzi A, Elajaili H, Redente EF, Nozik-Grayck E.** Oxidative Toxicology of Bleomycin: Role of the Extracellular Redox Environment. Curr Opin Toxicol. 2019;13:68-73. *https://doi.org/10.1016/j.cotox.2018.08.001.*

Invest Clin 67(2): 260 - 274, 2026 https://doi.org/10.54817/IC.v67n2a08

Circulating white blood cells and risk of tonsillar and base of tongue squamous cell carcinoma: A retrospective and mendelian randomization study.

Changyu Zhu[1], Shizhi He[2], Zhixin Li[1], Yijun Shi[1], Jingyang Zhao[1] and Wei Li[1]

[1]Cancer Center, Beijing Tongren Hospital, Capital Medical University. Beijing, China.
[2]Department of Head and Neck Surgery, Beijing Tongren Hospital, Capital Medical University.Beijing, China.

Keywords: Tonsillar Neoplasms; Leukocytes; Mendelian Randomization Analysis; Human Papillomavirus; Squamous Cell Carcinoma of Head and Neck.

Abstract. This study aimed to investigate the relationship between circulating white blood cells (cWBC) and the risk of tonsillar and base of tongue squamous cell carcinoma (TSCC/BOT SCC) using retrospective clinical data and Mendelian randomization (MR) analysis. A retrospective cohort of 239 TSCC/BOT SCC patients was analyzed for cWBC subtypes and their association with clinicopathological variables, stratified by human papillomavirus (HPV) status. Blood tests, tumor staging, and immunological markers were included. For causal inference, MR analysis was performed using genome-wide association study (GWAS) data on cWBC from the Blood Cell Consortium (UK Biobank) and TSCC/BOT SCC outcome data from the FinnGen consortium. Single-nucleotide polymorphisms (SNPs) were chosen based on genome-wide significance ($p<5 \times 10^{-8}$), low linkage disequilibrium ($r^2 < 0.001$), and F-statistic >10. The inverse-variance weighted (IVW) method was used as the primary MR approach, supplemented by MR-Egger, weighted median, and weighted mode analyses. The retrospective analysis showed significant differences in cWBC subtypes by gender, age, lifestyle factors, and HPV status. Notably, neutrophils (cNEU) and monocytes (cMON) were strongly associated with tumor stage and immune markers. MR analysis confirmed a causal link between total cWBC count and TSCC/BOT SCC risk (OR=1.516, p=0.005), with no evidence of heterogeneity or pleiotropy. No causal relationship was identified for cWBC subtypes or other head and neck squamous cell carcinoma (HNSCC) sites. This study provides the first comprehensive evidence supporting a causal role of elevated cWBC in the development of TSCC/BOT SCC. These findings indicate that cWBC may serve as a potential biomarker and therapeutic target in HPV-related or unrelated TSCC/BOT SCC.

Corresponding author: Wei Li. Cancer Center, Beijing Tongren Hospital, Capital Medical University. Beijing 100176, China. Telefax: +86-15811929005. Email: fever1988fever@sina.com

Leucocitos circulantes y riesgo de carcinoma de células escamosas de amígdalas y base de la lengua: un estudio retrospectivo y de aleatorización mendeliana.

Invest Clin 2026; 67 (2): 260 – 274

Palabras clave: Neoplasias Tonsilares; Leucocitos; Análisis de la Aleatorización Mendeliana; Virus del Papiloma Humano; Carcinoma de Células Escamosas de Cabeza y Cuello.

Resumen. Este estudio tuvo como objetivo explorar la relación entre los leucocitos circulantes (LC) y el riesgo de carcinoma de células escamosas de amígdala y de base de la lengua (CCEA/CCEB), mediante datos clínicos retrospectivos y análisis de aleatorización mendeliana (AM). Se analizó una cohorte retrospectiva de 239 pacientes con CCEA/CCEB para determinar los subtipos de LC y su asociación con variables clínico-patológicas, estratificadas según el estado del virus del papiloma humano (VPH). Se incluyeron análisis de sangre, estadificación tumoral y marcadores inmunológicos. Para la inferencia causal, se realizó un análisis de AM utilizando datos del estudio de asociación del genoma completo (GWAS) sobre LC del Consorcio de Células Sanguíneas (Biobanco del Reino Unido) y datos de resultados de CCEA/CCEB del consorcio FinnGen. Los polimorfismos de un nucleótido (SNP) se seleccionaron en función de su significancia a nivel genómico ($p<5 \times 10^{-8}$), bajo desequilibrio de ligamiento (r^2 <0,001) y un estadístico F >10. Se utilizó la ponderación por el inverso de la varianza (IVW: Inverse Variance Weighted) como método principal de AM, complementado con análisis de regresión MR-Egger, mediana ponderada y moda ponderada. El análisis retrospectivo reveló diferencias significativas en los subtipos de leucocitos totales (LCt) según el sexo, la edad, los factores del estilo de vida y el estado del VPH. Cabe destacar que los neutrófilos y monocitos se asociaron fuertemente con el estadio tumoral y los marcadores inmunitarios. El análisis de AM confirmó una asociación causal entre el recuento total de LC y el riesgo de carcinoma de células escamosas de la lengua/base de la vejiga (OR=1,516, p=0,005), sin evidencia de heterogeneidad ni pleiotropía. No se encontró ningún vínculo causal entre los subtipos de LC y otros sitios de carcinoma de células escamosas de cabeza y cuello. Este estudio proporciona la primera evidencia integrada que respalda un papel causal de los LC elevados en la patogénesis del CCEA/CCEB. Estos hallazgos sugieren que el recuento de leucocitos en sangre periférica (LC) podría servir como biomarcador y objetivo terapéutico en el carcinoma de células escamosas de la lengua/base de la lengua (CCEA/CCEB), relacionado o no con el VPH.

Received: 05-11-2025 Accepted: 19-02-2026

INTRODUCTION

The global incidence of oropharyngeal squamous cell carcinoma (OPSCC) has been gradually rising, with new cases reaching 98, 412 in 2020 [1]. Smoking, alcohol consumption, and human papillomavirus (HPV) infection are three independent risk factors for its development [2]. HPV- positive OPSCC accounts for over 70% of cases in some re-

gions, with TSCC/BOT SCC being the most common subtypes 1 [1,3-5]. The survival rate for HPV- positive OPSCC is roughly twice as high as that for HPV- negative cases [6]. Although treatments such as surgery, chemotherapy, targeted therapy, and immune checkpoint inhibitors (ICI) have improved outcomes to some extent, these tumors exhibit high heterogeneity, increasing incidence, rapid progression, and high rates of recurrence and metastasis. This highlights the urgent need for better stratification tools and immune-based biomarkers to personalize therapy and predict prognosis. The tumor immune microenvironment (TIME) involves continuous interactions between tumor cells and various immune cells, playing a key role in cancer development, progression, and response to therapy [7]. These interactions influence immune response, tumor cell proliferation, angiogenesis, and tumor recurrence and spread. Additionally, complex regulation occurs among different immune cells and their cytokines within the TIME [8]. The heterogeneity of the tumor itself can also impact the TIME [9]. Currently, immune checkpoint inhibitor (ICI) therapy is increasingly used, utilizing immunotherapy agents to boost the immune system's ability to recognize and destroy malignant cells more effectively[10]. ICI therapy is considered one of the most promising approaches for Head and Neck Squamous Cell Carcinoma (HNSCC) [11]. It has significantly improved treatment outcomes for HNSCC and has become the standard first-line therapy for advanced cases. However, despite its success, many patients still experience disease progression, recurrence, and metastasis after treatment[12, 13]. Circulating white blood cells (cWBCs), which consist of various immune cell types, reflect systemic immune status and may offer insights into the TIME [14]. Previous studies suggest that certain cWBC subsets, such as lymphocytes and monocytes, are linked to tumor immune surveillance, immunotherapy outcomes, and disease prognosis [15]. Nonetheless, the relationship between cWBCs and TSCC/BOT SCC, especially in the context of HPV infection, remains poorly understood. In this study, we explore the association between cWBC subtypes and TSCC/BOT SCC through a dual approach: retrospective clinical analysis and Mendelian randomization (MR) to assess potential causality using genome- wide association study (GWAS) data. This combined analysis aims to identify reliable immune biomarkers and clarify the immunogenic mechanisms underlying TSCC/BOT SCC pathogenesis.

MATERIALS AND METHODS

Retrospective analysis

The clinical and pathological data of all patients with TSCC/BOT SCC in our hospital from July 2020 to January 2025 were collected, including gender, age, smoking and alcohol consumption status, blood routine tests (counts of circulating white blood cells (cWBC), neutrophils (cNEU), lymphocytes (cLYM), monocytes (cMON), eosinophils (cEOS), basophils (cBAS), and derived ratios such as neutrophil-to-lymphocyte ratio (NLR) and lymphocyte-to-monocyte ratio (LMR) before biopsy or radical surgery. Tumor HPV-related status was also recorded, along with TNM staging: TI-TIV (indicating increasing size and/or local extent of the primary tumor), T stage (T1-4: tumor size and extent), and N stage (N0 to N3: spread to regional lymph nodes). The KI-67 value (a protein expressed in dividing cells and a marker for tumor cell proliferation), imaging stage or postoperative pathological stage, and Combined Positive Score (CPS) expression were included as well.

Approval from the Ethics Committee of Beijing Tongren Hospital, Capital Medical University, was obtained prior to data collection and analysis (Approval no. TREC2022-KY018.R1).

The retrospective data of patients aged ≥18 years of both genders were retrieved by passing the following criteria: pre-biopsy/radical surgery and routine blood tests con-

ducted at the host institute; pathological confirmation of TSCC/BOT SCC; available HPV and CPS data; no history of other malignancies or immunologic diseases, and no recent infection or anti-infective therapy.

The exclusion criteria included: patients under 18 years old; TSCC/BOT SCC treated at other institutions or hospitals; missing records of pre-biopsy or radical surgery; no routine blood tests performed at the host hospital; prior induction therapy before radical surgery elsewhere; recent infection or ongoing anti-infective therapy; history of other cancers or immunologic disorders; and use of hormonal drugs, anti-infective agents, or traditional medicine before blood collection.

The patients were divided into two groups based on the HPV status of TSCC/BOT SCC. Differences in cWBC were compared between the two groups, accounting for factors such as gender and age. Subsequently, subgroup analyses were performed within the HPV-positive and HPV-negative groups to assess differences in these indicators.

Mendelian Randomization

Sources of GWAS data for cWBC and HNSCC

The cWBC exposure data were obtained from the Blood Cell Consortium (BCX) meta-analysis (UKBB cohort, N=562,243) [16]. The details of the GWAS data used in this study were obtained from the FinnGen database (https://www.finngen.fi/en) [17] and are presented in Table 1.

Fig. 1 shows the MR framework used to explore the causal link between cWBCs and specific head and neck cancers. GWAS summary statistics for cWBCs served as the exposure data, while outcome data were obtained from GWAS datasets for tonsillar and base-of-tongue cancers, along with other head and neck cancer subsites, including hypopharyngeal, nasal, oral, and nasopharyngeal cancers. This method allows for the assessment of potential causal effects while reducing confounding and reverse causality.

Selection of genetic instruments

We identified SNPs strongly associated with the exposure, applying a genome-wide significance threshold of $p < 5 \times 10^{-8}$. To control for linkage disequilibrium, we applied stringent clumping parameters ($r^2 < 0.001$ within a 10,000-kb window). Palindromic SNPs with ambiguous allele frequencies were excluded to prevent strand misalignment. Additionally, we filtered out weak instruments by calculating the F-statistic (β^2/SE^2) for each SNP-exposure association, retaining only those with $F > 10$ to ensure robust instrument strength [18].

Table 1. Information of summary level genome-wide association study (GWAS) used in this study.

Phenotype	GWAS ID / Name	Sample size*	
		Patients	Controls
Malignant cancer of the tonsil and base of the tongue	Finngen_R12_C3_Malignant cancer of tonsil and base of tongue	813	378,749
Hypopharyngeal cancer	Finngen_R12_C3_Malignant neoplasm of hypopharynx	124	378,749
Nasal cavity and sinus cancer	Finngen_R12_C3_Malignant neoplasm of the nasal cavity and sinuses	345	378,749
Oral cancer	Finngen_R12_C3_Malignant neoplasm of the oral cavity	1,614	378,749
Nasopharyngeal cancer	Finngen_R12_C3_Malignant neoplasm of nasopharynx	152	378,749

*All other cancers were excluded except the selected type. Controls against each type of cancer in the patients column.

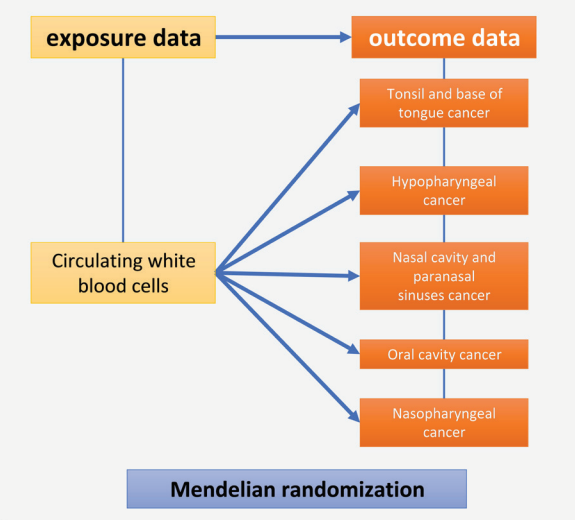

Fig. 1. Mendelian Randomization framework used to investigate the relationship between circulating white blood cell subtypes and site-specific head and neck cancers.

MR analysis

Four MR methods were used: inverse-variance weighted (IVW), MR-Egger, weighted median, and weighted mode. The IVW method served as the main approach to estimate the causal effect. By thoroughly considering the effects and precisions of multiple SNPs, the IVW method provided a solid estimate of causality. Additionally, other methods like MR-Egger, weighted median, and weighted mode were also employed in the analysis. If the statistically significant results from IVW did not agree with those from the other methods, such as MR-Egger, weighted median, and weighted mode, we compared the effect estimates (β and OR) across methods to evaluate the size and direction of the differences. Heterogeneity and horizontal pleiotropy were checked using the IVW and MR-Egger tests. A p-value above 0.05 for Cochran's Q-statistic (in MR-IVW) and Rucker's Q-statistic (in MR-Egger) suggested no heterogeneity in the MR analysis [19]. Additionally, MR-Egger could identify and assess potential pleiotropy through the MR-Egger intercept test [20]. If pleiotropy was detected, the MR results were considered invalid.

Statistical analysis

For the retrospective analysis, R software (version 4.3.1; R Foundation for Statistical Computing, Vienna, Austria) was used. Non-parametric tests were employed to compare quantitative variables: the Wilcoxon rank-sum test for two independent samples and the Kruskal-Wallis test for multiple samples. The chi-square test was used to compare proportions (rates), and analysis of variance (ANOVA) was used to compare continuous variables across groups. Statistical significance was defined as a two-sided p-value<0.05. MR analyses were performed using the TwoSampleMR software (version 0.5.11) in R (version 4.3.1). To rigorously evaluate the causal relationship, false discovery rate (FDR) correction was applied to the final results. A corrected p-value<0.05 was considered to indicate a statistically significant result.

RESULTS

Patient Baseline Characteristics

A total of 239 patients with TSCC/BOT SCC were included. Demographic and clinical characteristics are summarized in Table 2. In terms of gender distribution, there were 203 male patients, accounting for 84.94%. Regarding age, 206 patients were under 50 years old, making up 86.19%. Concerning lifestyle habits, 149 patients had a history of smoking or drinking, representing 62.34%, while 77 patients had no such habits, accounting for 32.22%. For HPV infection status, 150 patients were HPV-positive, constituting 62.76%, and 89 patients were HPV-negative, representing 37.24%. In tumor staging, T2 was the most common (40.17%), while N2 (43.10%) and N3 (33.47%) were the predominant N stages. TNM stage IV accounted for 25.10%. Regarding the immunohistochemical index Ki-67 expression level, the largest group had values >70, with 116 cases, or 48.54%. The distribution of CPS scores was as follows: 48 patients scored 1-10 (20.08%), 44 patients

Table 2. Baseline characteristics of all included oropharyngeal squamous cell carcinoma patients.

Characteristics	Patients (N=239)	Percentage
Gender		
Male	203	84.94
Female	36	15.06
Age		
≤50	33	13.81
>50	206	86.19
Smoking or Drinking		
No	77	32.22
Yes	149	62.34
NA	13	5.44
HPV status		
Positive	150	62.76
Negative	89	37.24
T Stage		
1	43	17.99
2	96	40.17
3	54	22.59
4	46	19.25
N Stage		
1	54	22.59
2	103	43.1
3	80	33.47
4	2	0.84
TNM Stage		
I	84	35.15
II	57	23.85
III	38	15.9
IV	60	25.1
Ki-67		
10-39	27	11.3
40-69	71	29.71
>70	116	48.54
NA	25	10.46
CPS		
1-10	48	20.08
11-59	44	18.41
60-99	23	9.62
<1	6	2.51
NA	118	49.37

NA: Not available (data missing); HPV: human papilloma virus; TNM system stages cancer; T stage: tumor stage; N stage: Node stage; Ki-67: proliferation index; CPS: Combined Positive Score.

scored 11-59 (18.41%), 23 patients scored 60-99 (9.62%), and 6 patients scored less than 1 (2.51%).

Correlation between cWBC and clinicopathological characteristics

In the overall cohort, circulating white blood cell subtypes (cWBC, cNEU, cEOS, cMON, and cLMR) were significantly associated with demographic and clinical variables, as shown in Fig. 2. Gender differences were particularly notable in cMON and cLMR ($p<0.001$). Smoking and drinking habits were significantly linked to cWBC, cMON, and cEOS levels ($p<0.001$). Additionally, cNEU and cNLR were associated with T-stage ($p<0.05$ and $p<0.01$, respectively), whereas cMON differed across CPS score groups ($p<0.05$). In the HPV-positive subgroup (n=150), gender had a significant impact on cMON and cLMR ($p<0.001$), with significant differences also observed in cEOS levels ($p<0.01$). Smoking and drinking were associated with higher cWBC ($p<0.01$) and cMON ($p<0.001$), while cNEU varied significantly with TNM stage ($p<0.05$). For the HPV-negative subgroup (n=89), gender-related differences were found in cMON ($p<0.05$), and smoking/drinking were linked to cMON ($p<0.05$) and cEOS ($p<0.01$). T-stage was associated with variations in cLYM and cNLR ($p<0.05$), and cMON showed differences across CPS score categories ($p<0.05$).

MR analysis

IVW analysis revealed a significant positive association between cWBC and TSCC/BOT SCC risk ($\beta=0.416$, OR=1.516, 95% CI=1.189-1.935, P/FDR=0.005). Although cMON showed a positive trend ($\beta=0.254$, OR=1.289, P/FDR=0.018), results were excluded due to significant horizontal pleiotropy ($p<0.05$). No statistically significant associations were observed between other cWBC subtypes and TSCC/BOT SCC or other HNSCC subsites. These findings are shown in Fig. 3.

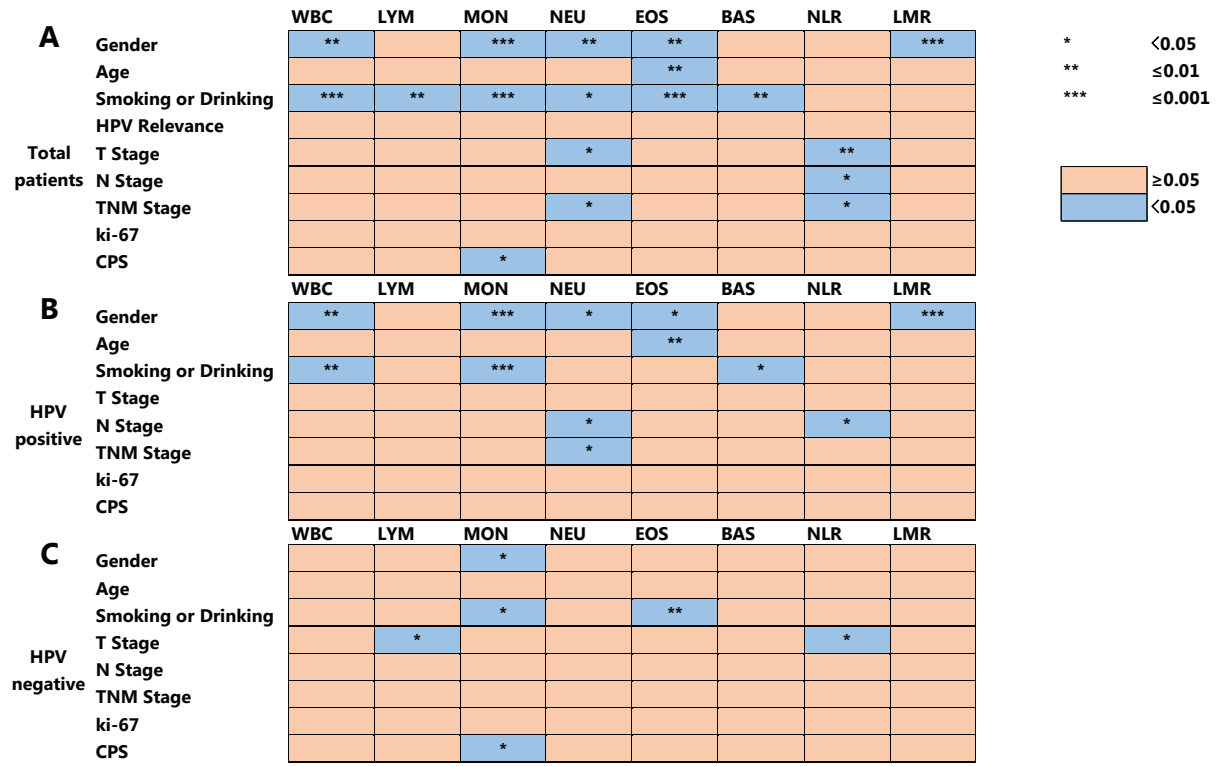

Fig. 2. Association between circulating white blood cell subtypes with demographic and clinical variables. cWBC: circulating white blood cell; cNEU: neutrophils; cLYM: lymphocytes; cMON: monocytes; cEOS: eosinophils; cBAS: basophils; NLR: neutrophils-to-lymphocyte ratio; LMR: lymphocyte-to-monocyte ratio; TNM: system stages cancer; T stage: tumor stage; N stage: Node stage; Ki-67: proliferation index; CPS: Combined Positive Score; HPV: Human Papilloma Virus.

Table 3 shows the results of heterogeneity and horizontal pleiotropy tests for the MR estimates. For the association between WBC and TSCC/BOT SCC, neither the heterogeneity nor the horizontal pleiotropy tests were statistically significant ($p>0.05$ for both). In contrast, the horizontal pleiotropy test for the association between MON and TSCC/BOT SCC was statistically significant ($p<0.05$).

DISCUSSION

Globally, the proportion of HPV-positive OPSCC has increased significantly. The cumulative risk of OPSCC is 0.21% in males and 0.05% in females, with a significantly higher proportion of male patients than female patients [1]. In this study, HPV-positive patients accounted for 62.76%, with males making up 84.94%, consistent with the global epidemiological trend in OPSCC. The biological behavior of HPV-positive OPSCC differs markedly from that of HPV-negative OPSCC. Systemic inflammatory markers have become reliable prognostic tools in HNSCC, reflecting the dynamic interaction between tumor biology and host immunity. HPV-positive OPSCC shows strong immune cell infiltration, better treatment response, and improved prognosis [21-22]. Notably, circulating leukocyte levels differ significantly between HPV-positive and HPV-negative cases, with variations in immune cell types potentially indicating differences in the tumor immune microenvironment (TIME) between these groups. These distinct immune states may influence the effectiveness of immuno-

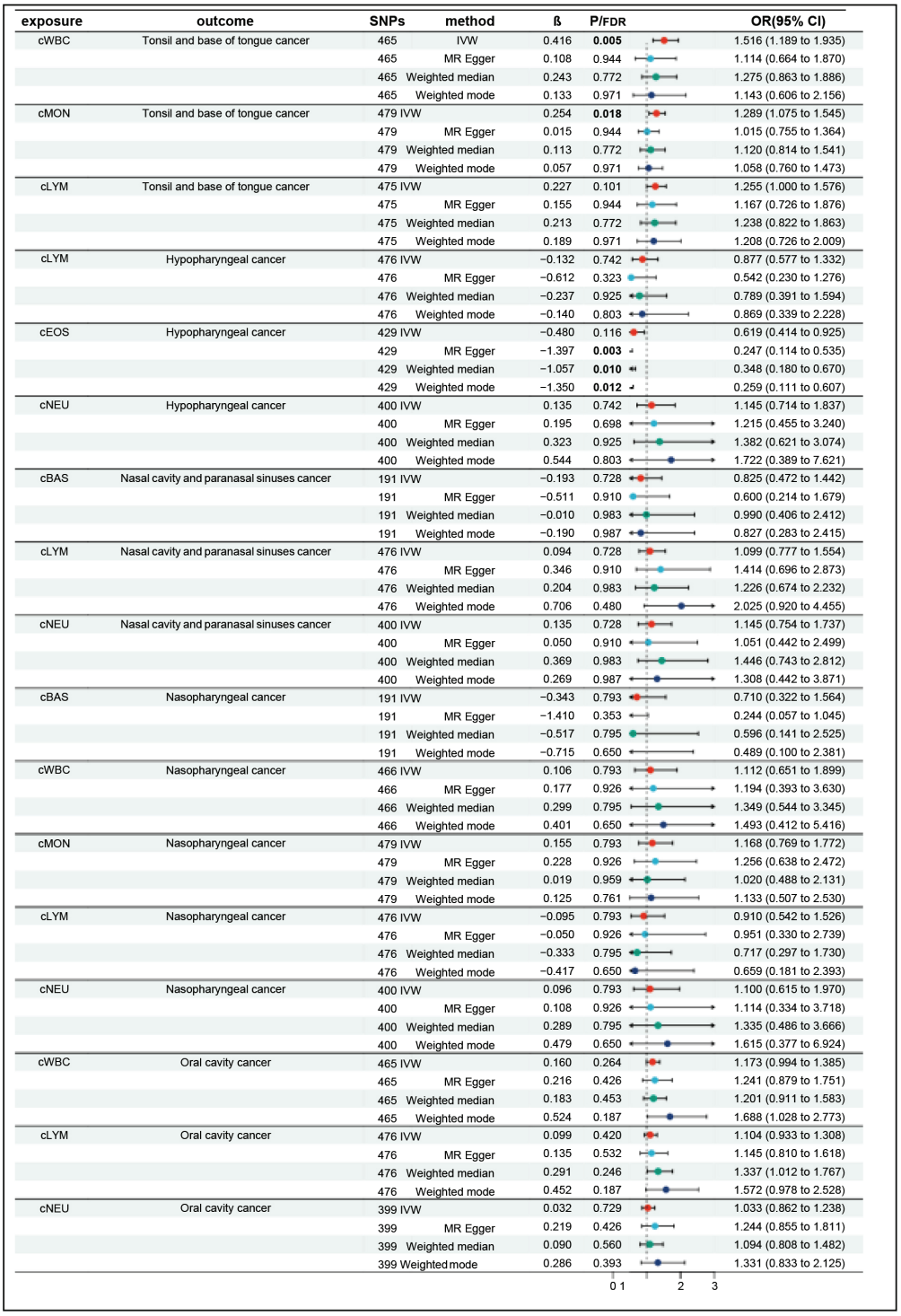

Fig. 3. Associations between circulating white blood cell (cWBC) subtypes and Tonsillar Squamous Cell Carcinoma and Base of Tongue Squamous Cell Carcinoma (TSCC/BOT SCC) or other Head and Neck Squamous Cell Carcinoma (HNSCC) subsites. cNEU: neutrophils; cLYM: lymphocytes; cMON: monocytes; cEOS: eosinophils; cBAS: basophils; LMR: lymphocyte-to-monocyte ratio; HPV: Human Papilloma Virus; IVW: Inverse variance weighted; MR-Egger: Mendelian randomization.

Table 3. Results of Mendelian Randomization heterogeneity and horizontal pleiotropy.

Exposure	Outcome	Heterogeneity			Pleiotropy		
		Method	Q	Q_pval	Egger_intercept	se	*p*val
cWBC	Tonsil and base of tongue cancer	MR-Egger	491.095	0.177	0.008	0.006	0.187
		IVW	492.95	0.17			
cMON	Tonsil and base of tongue cancer	MR-Egger	468.766	0.597	0.009	0.005	0.045*
		IVW	472.802	0.558			
cLYM	Tonsil and base of tongue cancer	MR-Egger	457.389	0.688	0.002	0.006	0.732
		IVW	457.506	0.699			
cLYM	Hypopharyngeal cancer	MR-Egger	432.64	0.914	0.013	0.011	0.208
		IVW	434.231	0.91			
cEOS	Hypopharyngeal cancer	MR-Egger	427.628	0.482	0.03	0.011	0.007*
		IVW	435.049	0.397			
cNEU	Hypopharyngeal cancer	MR-Egger	382.328	0.705	-0.002	0.011	0.893
		IVW	382.346	0.717			
cBAS	Nasal cavity and paranasal sinuses cancer	MR-Egger	215.195	0.093	0.009	0.013	0.471
		IVW	215.789	0.097			
cLYM	Nasal cavity and paranasal sinuses cancer	MR-Egger	481.968	0.39	-0.007	0.009	0.425
		IVW	482.615	0.395			
cNEU	Nasal cavity and paranasal sinuses cancer	MR-Egger	462.155	0.014*	0.002	0.01	0.826
		IVW	462.211	0.016*			
cBAS	Nasopharyngeal cancer	MR-Egger	152.792	0.975	0.032	0.019	0.088
		IVW	155.731	0.967			
cWBC	Nasopharyngeal cancer	MR-Egger	452.706	0.638	-0.002	0.013	0.886
		IVW	452.727	0.65			
cMON	Nasopharyngeal cancer	MR-Egger	409.642	0.988	-0.003	0.01	0.789
		IVW	409.713	0.989			
cLYM	Nasopharyngeal cancer	MR-Egger	462.862	0.634	-0.001	0.013	0.925
		IVW	462.871	0.646			
cNEU	Nasopharyngeal cancer	MR-Egger	395.543	0.525	0	0.014	0.982
		IVW	395.544	0.539			
cWBC	Oral cavity cancer	MR-Egger	438.241	0.79	-0.001	0.004	0.716
		IVW	438.373	0.798			
cLYM	Oral cavity cancer	MR-Egger	532.671	0.032*	-0.001	0.004	0.815
		IVW	532.733	0.034*			
cNEU	Oral cavity cancer	MR-Egger	376.332	0.765	-0.005	0.004	0.267
		IVW	377.566	0.762			

cWBC: circulating white blood cell; cNEU: neutrophils; cLYM: lymphocytes; cMON: monocytes; cEOS: eosinophils; cBAS: basophils; IVW: Inverse variance weighted; MR-Egger: Mendelian randomization Egger Regression. *p<0.05.

therapy. This study found that cWBC, cNEU, and cEOS had significant differences across various genders, ages, smoking/drinking habits, and tumor stages. In particular, among HPV-positive patients, cMON and cLMR exhibited notable differences. Previous research has demonstrated that HPV can modulate the immune microenvironment to promote tumorigenesis and progression[23]. Lower lymphocyte counts and reduced LMR are associated with poorer outcomes. A systematic review involving 5,234 HNSCC patients revealed that higher LMR (≥4) was linked to better overall survival (HR = 1.36) and disease-free survival (HR = 0.94) [24].

This threshold effect likely reflects a balance between lymphocyte-driven immune surveillance and monocyte-derived tumor-associated macrophage recruitment, which fosters immune evasion.

Circulating leukocyte subtypes such as cMON and cNEU are closely linked to immune suppression and angiogenesis in the TIME [25], and they may work together to support tumor growth. Notably, cNEU are the most common circulating leukocytes [26]. However, their levels show significant variation across different tumor stages (T/TNM stage), which could indicate different functions during disease progression in TSCC/BOT SCC. Research shows that cNEU display high plasticity within the TIME, with their roles changing based on tumor stage and microenvironmental factors. Especially in advanced tumor stages, cNEU may encourage tumor growth through mechanisms like promoting new blood vessel formation and suppressing immune responses [27]. In colorectal cancer studies, increased neutrophil levels are linked to disruptions in the intestinal microbiota and facilitate peritoneal metastasis of colorectal cancer by interacting with tumor cells [28]. Additionally, higher pretreatment neutrophil counts and NLR have been repeatedly confirmed as independent indicators of poorer overall survival (OS) and disease-free survival (DFS) in meta-analyses involving over 10,000 patients [29]. The observed correlation between cNEU and tumor stage in this study likely reflects their dynamic contribution to tumor progression.

Whether cWBC is causally associated with the occurrence of HNSCC, particularly with TSCC/BOT SCC, we conducted an MR analysis. The IVW method demonstrated a robust positive association between cWBC and TSCC/BOT SCC risk ($\beta=0.416$, OR=1.516, *P*/FDR=0.005), with consistent results across MR-Egger and weighted median methods (no evidence of heterogeneity or pleiotropy, $p>0.05$). In contrast, cMON associations were confounded by horizontal pleiotropy ($p<0.05$), limiting causal inference. This finding is consistent with previous studies, and cWBC is captured by tumour tissues to become infiltrating leukocytes that promote tumour progression [30]. The absence of significant associations between cWBC and other HNSCC subsites in our MR analysis may reflect the anatomical and biological heterogeneity of HNSCC, which could differentially influence immune cell recruitment and function. ICI therapy involves the binding of anti-programmed cell death protein 1 (PD-1)/programmed cell death ligand 1 (PD-L1) antibodies to induce autologous immune cells to kill tumors [31]. It has demonstrated significant efficacy across multiple advanced tumor types, with some patients achieving durable responses [32]. The role of cWBC in immunotherapy has also been supported by several studies. The PD-L1 status of cWBC is associated with PD-L1 expression in immune cells within the TIME [33, 34]. In melanoma patients, the efficacy of ICI therapy correlates with an adequate number of cLYM [35]. Studies have also found that the efficacy of ICI therapy is significantly associated with baseline cWBC and their subtypes (such as LYM and MON), where higher baseline cLYM is associated with better treatment responses and longer progression-free survival, while higher cNEU is associated with poorer prognosis [36, 37]. Incidental immune-related adverse events (irAEs) during im-

munotherapy are also associated with cWBC and their subtypes. Baseline cNEU, cLYM, cMON, and cEOS, baseline platelet counts, and increases in cWBC, cLYM, and cEOS during follow-up are all associated with an increased risk of irAEs [38-40]. Collectively, our data support a dual role for cWBC in TSCC/BOT SCC: they may contribute to tumor initiation and progression while concurrently modulating responses to immunotherapy. Clinically, CPS levels are typically used as a surrogate for PD-1 expression. Therefore, this study analyzed the differences between CPS expression and cWBC. Unfortunately, CPS was not detected in some patients. To exclude differences in detection results between our institution and other institutions, only patients with CPS expression detected in our hospital were included, resulting in many patients being recorded as having no CPS expression values. The results showed that different CPS expression levels were only associated with cMON in all patients and HPV-negative patients, but no differences were observed in cWBC or their subtypes in HPV-positive patients, further indicating the heterogeneity of tumor cells under different HPV infection statuses. Additionally, studies have found that retinoic acid secreted by tumor tissues can induce MON to differentiate into immunosuppressive tumor-associated macrophages (TAMs), thereby inhibiting the efficacy of immunotherapy [41]. TAMs and dendritic cells, a monocyte subset, may also indirectly promote tumor progression, which may explain the different prognoses of HPV-negative and HPV-positive tumors due to differences in immune cells [42]. This study has some limitations. First, its focus on TSCC/BOT SCC may limit the generalizability of findings to other OPSCC subsites. The retrospective design introduces potential confounding due to unmeasured clinical variables, such as treatment history. Additionally, the relatively small sample size in the HPV-negative subgroup may reduce the statistical power of subgroup analyses. Furthermore, lifestyle factors such as diet and environmental exposures, which were not assessed, could independently influence the observed associations between circulating white blood cells and tumor characteristics. Future research should further expand the sample size and incorporate more potential confounding factors to comprehensively evaluate the associations between cWBC and TSCC/BOT SCC. In-depth investigations using single-cell sequencing technology may help reveal the specific mechanisms of action of different WBC subtypes in the TIME. Finally, exploring the potential of cWBC as biomarkers and therapeutic targets for TSCC/BOT SCC will provide new insights for clinical diagnosis and treatment.

This study demonstrates a causal link between elevated cWBC and the risk of TSCC/BOT SCC through combined retrospective and Mendelian randomization analyses. Significant associations between cWBC subtypes and tumor characteristics, especially in HPV-positive cases, underscore their potential role in tumor progression and immune regulation. The findings indicate that cWBC may serve as non-invasive biomarkers for risk assessment and treatment stratification. Further research is necessary to validate these results and investigate underlying mechanisms in larger, prospective cohorts.

Funding

No sponsor or funder supported this study.

ORCID ID of the authors

- Changyu Zhu (CZ): 0009-0003-5440-0288
- Shizhi He (SH): 0009-0003-7228-943X
- Zhixin Li (ZL): 0009-0004-8248-1529
- Yijun Shi (YS): 0009-0002-0097-2654

- Jingyang Zhao (JZ): 0000-0004-5326-9537
- Wei Li (WL): 0000-0002-9991-7892

Author's contributions

Conceptualization: JZ; Methodology: CZ, JZ; Data analysis: CZ, SH, ZL, YS; Writing- original draft: CZ, SH, ZL, YS; Review & editing: CZ, JZ; Supervision: JZ. All authors read and approved the final manuscript.

Conflict of interest

The authors state that they have no conflicts of interest.

Ethical approval and informed consent

The retrospective analysis of patients at our hospital has been approved by the Ethics Committee under approval number TREC2022-KY018.R1, dated 21st April 2022. This study was performed in line with the principles of the Declaration of Helsinki.

Data availability statement

All data generated or analyzed during this study are included in this article. Further inquiries can be directed to the corresponding author.

Declaration of generative AI and AI-assisted technologies in the writing process

No generative AI or AI-assisted technology was used in the writing process.

REFERENCES

1. **Sung H, Ferlay J, Siegel RL, Laversanne M, Soerjomataram I, Jemal A, et al.** Global Cancer Statistics 2020: GLOBOCAN Estimates of Incidence and Mortality Worldwide for 36 Cancers in 185 Countries. CA Cancer J Clin. 2021;71(3):209-249. *https://doi.org/10.3322/caac.21660.*
2. **Arif RT, Mogaddam MA, Merdad LA, Farsi NJ.** Does human papillomavirus modify the risk of oropharyngeal cancer related to smoking and alcohol drinking? A systematic review and meta-analysis. Laryngoscope Investig Otolaryngol. 2022;7(5):1391-1401. *https://doi.org/10.1002/lio2.877.*
3. **Ernster JA, Sciotto CG, O'Brien MM, Finch JL, Robinson LJ, Willson T, et al.** Rising incidence of oropharyngeal cancer and the role of oncogenic human papilloma virus. Laryngoscope. 2007;117(12):2115-2128. *https://doi.org/10.1097/MLG.0b013 e31813e5fbb.*
4. **Licitra L, Zigon G, Gatta G, Sánchez MJ, Berrino F, EUROCARE Working Group.** Human papillomavirus in HNSCC: a European epidemiologic perspective. Hematol Oncol Clin North Am. 2008;22(6):1143-1153, vii-viii. h*ttps://doi.org/10.1016/j.hoc.2008.10.002.*
5. **Chaturvedi AK, Engels EA, Anderson WF, Gillison ML.** Incidence trends for human papillomavirus-related and -unrelated oral squamous cell carcinomas in the United States. J Clin Oncol. 2008;26(4):612-619. *https://doi.org/10.1200/JCO.2007.14. 1713.*
6. **Zoschke IN, Bennis SL, Wilkerson JM, Stull CL, Nyitray AG, Khariwala SS, et al.** HPV-related oropharyngeal cancer early detection in gay and bisexual men is an "orphan": A qualitative analysis among healthcare providers. Front Public Health. 2023;11:1165107. *https://doi.org/10.3389/fpubh.2023.1165107.*
7. **Shi T, Hu Z, Tian L, Yang Y. Pan-cancer landscape of CENPO and its underlying mechanism in LUAD.** Respir Res. 2023;24(1):113. *https://doi.org/10.1186/s12931-023-02408-3.*
8. **Chechlinska M, Kowalewska M, Nowak R.** Systemic inflammation as a confounding factor in cancer biomarker discovery and validation. Nat Rev Cancer. 2010;10(1):2-3. *https://doi.org/10.1038/nrc2782.*
9. **Thol K, Pawlik P, McGranahan N.** Therapy sculpts the complex interplay between cancer and the immune system during tumour evolution. Genome Med. 2022;14(1):137.

https://doi.org/10.1186/s13073-022-01138-3.

10. **Wang Y, Jiang H, Fu L, Guan L, Yang J, Ren J, et al.** Prognostic value and immunological role of PD-L1 gene in pan-cancer. BMC Cancer. 2024;24(1):20. *https://doi.org/10.1186/s12885-023-11267-6.*
11. **Xu J, Liu H, Wang T, Wen Z, Chen H, Yang Z, et al.** CCR7 Mediated Mimetic Dendritic Cell Vaccine Homing in Lymph Node for Head and Neck Squamous Cell Carcinoma Therapy. Adv Sci (Weinh). 2023;10(17):e2207017. *https://doi.org/10.1002/advs.202207017.*
12. **Cohen EEW, Soulières D, Le Tourneau C, Dinis J, Licitra L, Ahn MJ, et al.** Pembrolizumab versus methotrexate, docetaxel, or cetuximab for recurrent or metastatic head-and-neck squamous cell carcinoma (KEYNOTE-040): a randomised, open-label, phase 3 study. Lancet. 2019;393(10167):156-167. *https://doi.org/10.1016/S0140-6736(18)31999-8.*
13. **Burtness B, Harrington KJ, Greil R, Soulières D, Tahara M, de Castro G Jr, et al.** Pembrolizumab alone or with chemotherapy versus cetuximab with chemotherapy for recurrent or metastatic squamous cell carcinoma of the head and neck (KEYNOTE-048): a randomised, open-label, phase 3 study. Lancet. 2019;394(10212):1915–1928. *https://doi.org/10.1016/S0140-6736(19)32591-7.*
14. **Roxburgh CS, McMillan DC.** Role of systemic inflammatory response in predicting survival in patients with primary operable cancer. Future Oncol. 2010;6(1):149-163. *https://doi.org/10.2217/fon.09.136.*
15. **Aoki H, Ueha S, Shichino S, Ogiwara H, Hashimoto SI, Kakimi K, et al.** TCR Repertoire Analysis Reveals Mobilization of Novel CD8+ T Cell Clones into the Cancer-Immunity Cycle Following Anti-CD4 Antibody Administration. Front Immunol. 2019;9:3185. *https://doi.org/10.3389/fimmu.2018.03185.*
16. **Chen MH, Raffield LM, Mousas A, Sakaue S, Huffman JE, Moscati A, et al.** Trans-ethnic and Ancestry-Specific Blood-Cell Genetics in 746,667 Individuals from 5 Global Populations. Cell. 2020;182(5):1198-1213.e14. *https://doi.org/10.1016/j.cell.2020.06.045.*
17. **Kurki MI, Karjalainen J, Palta P, Sipilä TP, Kristiansson K, Donner KM, et al.** FinnGen provides genetic insights from a well-phenotyped isolated population. Nature. 2023;613(7944):508-518. *https://doi.org/10.1038/s41586-022-05473-8.*
18. **Bowden J, Del Greco M F, Minelli C, Zhao Q, Lawlor DA, Sheehan NA, et al.** Improving the accuracy of two-sample summary-data Mendelian randomization: moving beyond the NOME assumption. Int J Epidemiol. 2019;48(3):728-742. *https://doi.org/10.1093/ije/dyy258.*
19. **Hemani G, Zheng J, Elsworth B, Wade KH, Haberland V, Baird D, et al.** The MR-Base platform supports systematic causal inference across the human phenome. Elife. 2018;7:e34408. *https://doi.org/10.7554/eLife.34408.*
20. **Burgess S, Thompson SG.** Interpreting findings from Mendelian randomization using the MR-Egger method. Eur J Epidemiol. 2017;32(5):377-389. *https://doi.org/10.1007/s10654-017-0276-5.*
21. **Chaturvedi AK, Engels EA, Pfeiffer RM, Hernandez BY, Xiao W, Kim E, et al.** Human papillomavirus and rising oropharyngeal cancer incidence in the United States. J Clin Oncol. 2011;29(32):4294-4301. *https://doi.org/10.1200/JCO.2011.36.4596.*
22. **Pytynia KB, Dahlstrom KR, Sturgis EM. Epidemiology of HPV-associated oropharyngeal cancer.** Oral Oncol. 2014;50(5):380-386. *https://doi.org/10.1016/j.oraloncology.2013.12.019.*
23. **Gillison ML, Chaturvedi AK, Anderson WF, Fakhry C.** Epidemiology of Human Papillomavirus-Positive Head and Neck Squamous Cell Carcinoma. J Clin Oncol. 2015;33(29):3235-3242. *https://doi.org/10.1200/JCO.2015.61.6995.*
24. **Wei D, Liu J, Ma J.** The value of lymphocyte to monocyte ratio in the prognosis of head and neck squamous cell carcinoma: a meta-analysis. PeerJ. 2023;11:e16014. *https://doi.org/10.7717/peerj.16014.*

25. **Camargo S, Moskowitz O, Giladi A, Levinson M, Balaban R, Gola S, et al**. Neutrophils physically interact with tumour cells to form a signaling niche promoting breast cancer aggressiveness. Nat Cancer. 2025;6(3):540-558. *https://doi.org/10.1038/s43018-025-00924-3*
26. **Hurtado Gutiérrez MJ, Allard FL, Mosha HT, Dubois CM, McDonald PP.** Human Neutrophils Generate Extracellular Vesicles That Modulate Their Functional Responses. Cells. 2022;12(1):136. *https://doi.org/10.3390/cells12010136.*
27. **Ng M, Cerezo-Wallis D, Ng LG, Hidalgo A.** Adaptations of neutrophils in cancer. Immunity. 2025;58(1):40-58. *https://doi.org/10.1016/j.immuni.2024.12.009.*
28. **Li Q, Xiao Y, Han L, Luo W, Dai W, Fang H, et al.** Microbiome dysbiosis, neutrophil recruitment and mesenchymal transition of mesothelial cells promotes peritoneal metastasis of colorectal cancer. Nat Cancer. 2025;6(3):493-510. *https://doi.org/10.1038/s43018-025-00910-9.*
29. **Tham T, Bardash Y, Herman SW, Costantino PD.** Neutrophil-to-lymphocyte ratio as a prognostic indicator in head and neck cancer: A systematic review and meta-analysis. Head Neck. 2018;40(11):2546-2557. *https://doi.org/10.1002/hed.25324.*
30. **Tan LY, Cockshell MP, Moore E, Myo Min KK, Ortiz M, Johan MZ, et al.** Vasculogenic mimicry structures in melanoma support the recruitment of monocytes. Oncoimmunology. 2022;11(1):2043673. *https://doi.org/10.1080/2162402X.2022.2043673.*
31. **Wang J, Gai J, Zhang T, Niu N, Qi H, Thomas DL 2nd, et al.** Neoadjuvant radioimmunotherapy in pancreatic cancer enhances effector T cell infiltration and shortens their distances to tumour cells. Sci Adv. 2024;10(6):eadk1827. *https://doi.org/10.1126/sciadv.adk1827.*
32. **Kim MJ, Hong SPD, Park Y, Chae YK.** Incidence of immunotherapy-related hyperprogressive disease (HPD) across HPD definitions and cancer types in observational studies: A systematic review and meta-analysis. Cancer Med. 2024;13(3):e6970. *https://doi.org/10.1002/cam4.6970.*
33. **Liu Y, Wu X, Feng Y, Jiang Q, Zhang S, Wang Q, et al.** Insights into the Oncogenic, Prognostic, and Immunological Role of BRIP1 in Pan-Cancer: A Comprehensive Data-Mining-Based Study. J Oncol. 2023;2023:4104639. *https://doi.org/10.1155/2023/4104639.*
34. **Ilié M, Szafer-Glusman E, Hofman V, Chamorey E, Lalvée S, Selva E, et al.** Detection of PD-L1 in circulating tumour cells and white blood cells from patients with advanced non-small-cell lung cancer. Ann Oncol. 2018;29(1):193-199. *https://doi.org/10.1093/annonc/mdx636.*
35. **van Rossum PSN, Deng W, Routman DM, Liu AY, Xu C, Shiraishi Y, et al.** Prediction of Severe Lymphopenia During Chemoradiation Therapy for Esophageal Cancer: Development and Validation of a Pretreatment Nomogram. Pract Radiat Oncol. 2020;10(1):e16-e26. *https://doi.org/10.1016/j.prro.2019.07.010.*
36. **Gungabeesoon J, Gort-Freitas NA, Kiss M, Weissleder R, Klein AM, Pittet MJ, et al.** A neutrophil response linked to tumour control in immunotherapy. Cell. 2023;186(7):1448-1464.e20. *https://doi.org/10.1016/j.cell.2023.02.032.*
37. **Xu F, Xu P, Cui W, Gong W, Wei Y, Liu B, et al.** Neutrophil-to-lymphocyte and platelet-to-lymphocyte ratios may aid in identifying patients with non-small cell lung cancer and predicting Tumour-Node-Metastasis stages. Oncol Lett. 2018;16(1):483-490. *https://doi.org/10.3892/ol.2018.8644.*
38. **Diehl A, Yarchoan M, Hopkins A, Jaffee E, Grossman SA.** Relationships between lymphocyte counts and treatment-related toxicities and clinical responses in patients with solid tumours treated with PD-1 checkpoint inhibitors. Oncotarget. 2017;8(69):114268-114280. *https://doi.org/10.18632/oncotarget.23217.*
39. **Liu W, Liu Y, Ma F, Sun B, Wang Y, Luo J, et. al.** Peripheral Blood Markers Associated with Immune-Related Adverse Effects in Patients Who Had Advanced Non-Small Cell Lung Cancer Treated with PD-1 Inhibitors. Cancer Manag Res. 2021; 13:765-771. *https://doi.org/10.2147/CMAR.S29 3200.*

40. **Michailidou D, Khaki AR, Morelli MP, Diamantopoulos L, Singh N, Grivas P.** Association of blood biomarkers and autoimmunity with immune related adverse events in patients with cancer treated with immune checkpoint inhibitors. Sci Rep. 2021;11(1):9029. *https://doi.org/10.1038/s41598-021-88307-3.*
41. **Devalaraja S, To TKJ, Folkert IW, Natesan R, Alam MZ, Li M, et al.** Tumour-Derived Retinoic Acid Regulates Intratumoural Monocyte Differentiation to Promote Immune Suppression. Cell. 2020;180(6):1098-1114.e16. *https://doi.org/10.1016/j.cell. 2020.02.042.*
42. **Olingy CE, Dinh HQ, Hedrick CC.** Monocyte heterogeneity and functions in cancer. J Leukoc Biol. 2019;106(2):309-322. *https://doi.org/10.1002/JLB.4RI0818-311R.*

Invest Clin 67(2): 275 - 288, 2026 https://doi.org/10.54817/IC.v67n2a09

Neurotoxic effects of nanoplastics exposure on depression-like behavior and cognitive function in mice under chronic unpredictable mild stress.

Dewei Chang[1,#], Miao Xu[2,#], Wenning Shi[1], Yan He[3], Zhe Wu[4], Zhifeng Ning[4], Yanling Sun[4] and Jianguo Lv[5,6]

[1]School of Pharmacy, Department of Medicine, Hubei University of Science and Technology, Xianning City, Hubei Province, China.
[2]Outpatient Department, West China Emei Hospital/ Mount Emei Jingchuan Hospital, Leshan City, Sichuan Province, P. R. China.
[3]Internal Medicine Department, The Second Affiliated Hospital, Hubei University of Science and Technology, Xianning City, Hubei Province, P. R. China.
[4]School of Basic Medical Sciences, Hubei University of Science and Technology, Xianning City, Hubei Province, P. R. China.
[5]Psychiatry Department, The Second Affiliated Hospital, Hubei University of Science and Technology, Xianning City, Hubei province, P. R. China.
[6]School of Clinical Medical Sciences, Hubei University of Science and Technology, Xianning City, Hubei Province, P. R. China.
[#]These authors contributed equally to this work.

Keywords: Microplastics, Nanoparticles; Nanoplastic; BDNF/TrkB; Chronic unpredictable mild Stress; Depression-like behavior; Disease Models, Animal; Hippocampus.

Abstract. The aim was to investigate the effects of gavage exposure to nanoplastics (NPs) on cognitive decline and depression-like behavior was investigated in mice subjected to chronic unpredictable mild stress (CUMS). BALB/c mice were randomly assigned to four experimental groups: Control (Ctrl), nanoplastics (NPs), Mod (subjected to CUMS), and NPs+Mod (nanoplastics + CUMS). We evaluated the role of the brain-derived neurotrophic factor (BDNF) and its receptor, the tyrosine kinase receptor B (TrkB), signaling pathway in the hippocampus of mice. Behavioral assessments included the sucrose preference test, the open field test, the forced swim test, and the Morris water maze. Nissl staining was used to assess hippocampal neuronal morphology. BDNF and TrkB mRNA levels and protein expression in the hippocampus were measured by qPCR and Western blotting, respectively. Mice in the NPs, Mod, and NPs+Mod groups showed reduced body weight, lower sucrose preference, poorer performance in the open field test, and prolonged immobility in the forced swim test. Additionally, there was a reduction in hippocampal

Corresponding authors: Yanling Sun (Email: yanlingssmed@hotmail.com) and Jianguo Lv (Email: asljgpt@163.com), Hubei University of Science and Technology, No. 88 Xianning Avenue, Xianning 437100, China.

neurons and deficits in spatial learning and memory compared with the control group. BDNF mRNA and TrkB protein levels were decreased. Compared with the Mod group, the NPs+Mod group exhibited increased depression-like behaviors and cognitive impairments, greater hippocampal neuronal damage, and further reductions in BDNF and TrkB mRNA and protein levels. In conclusion, NP exposure has neurotoxic properties that can exacerbate CUMS-induced depression-like behavior and cognitive deficits, likely by further suppressing the hippocampal BDNF/TrkB signaling pathway.

Efectos neurotóxicos de la exposición a nanoplásticos sobre el comportamiento similar a la depresión y la función cognitiva en ratones sometidos a estrés crónico leve impredecible.

Invest Clin 2026; 67 (2): 275 – 288

Palabras clave: Nanoplásticos; Microplásticos; Nanopartículas; BDNF/TrkB; Estrés Crónico; Comportamiento similar a la depresión; Hipocampo.

Resumen. En el presente estudio se evaluó el impacto de la exposición a nanoplásticos sobre el deterioro cognitivo y el comportamiento depresivo en ratones sometidos a estrés moderado crónico e impredecible (CUMS). Ratones BALB/c fueron asignados aleatoriamente a cuatro grupos experimentales: Control (Ctrl), nanoplásticos (NPs), Mod (sometidos a CUMS) y NPs+Mod (nanoplásticos + CUMS). Se determinó el papel del factor de crecimiento derivado del cerebro (BDNF) y su vía de señalización a través del receptor de la tirosina quinasa B (TrkB) en el hipocampo. Las pruebas de comportamiento incluyeron la prueba de preferencia por la sacarosa, la actividad motora en campo abierto, el nado forzado y el laberinto de Morris. Se evaluaron la morfología neuronal y la expresión de BDNF y TrkB mediante técnicas de PCR cuantitativa y Western blot. La exposición a los nanoplásticos, así como el estrés crónico, indujeron una disminución de la actividad en las pruebas de conducta. Además, se observó una disminución de las neuronas del hipocampo y de la memoria espacial en ambos tratamientos. La combinación de estrés crónico y la exposición a los nanoplásticos tuvo un efecto sumativo sobre las pruebas conductuales y cognitivas, así como sobre la expresión de BDNF y del receptor Trak B. En conclusión, la exposición a los nanoplásticos tiene efectos neurotóxicos que pueden potenciar los efectos del estrés crónico a nivel cognitivo y conductual. Dichos efectos se mediaron mediante la supresión de la vía de señalización de BDNF y del receptor TrkB en el hipocampo.

Received: 27-11-2025 Accepted: 04-03-2026

INTRODUCTION

Nanoplastics (NPs), an emerging class of environmental contaminants, are attracting increasing attention due to their potential health hazards. Owing to their minute size, NPs can cross biological barriers, distribute widely throughout the organism, and adversely affect various physiological functions, including entry into the nervous system [1]. Accumulating evidence from experimental studies shows that exposure to

NPs can lead to heightened anxiety and depression-like phenotypes in animals [2]. While direct human epidemiological data linking NPs to specific mental health disorders remain limited, these controlled experimental models are critical because they provide a practical tool to elucidate the underlying neurotoxic mechanisms. For example, they allow precise dose control, detailed pathological examination, and the isolation of causal pathways that are not feasible in human studies. On the other hand, depression is a debilitating mental disorder characterized by low mood and significant impairments in cognition and motivation, representing a major public health concern [3,4]. Given unavoidable human exposure to plastic pollution, it is imperative to employ such experimental approaches to comprehensively investigate the impact of NPs on mental health, specifically their mechanisms for disrupting emotional regulation and cognitive function under conditions such as chronic unpredictable mild stress (CUMS) [5].

The hippocampus is a crucial brain region that regulates emotional responses and cognitive functions, and its dysfunction has been implicated in the pathogenesis of related disorders [6]. The "neuronal damage hypothesis" of depression posits that an insufficiency of neurotrophic factors plays a pivotal role in pathological changes within the hippocampus and in the pathogenesis of the disorder [7]. These neurotrophic factors are vital for neuronal survival and synaptic plasticity. Chief among them is brain-derived neurotrophic factor (BDNF), which, by binding to its receptor, the tyrosine kinase receptor B (TrkB), activates a critical signaling pathway for neuronal growth, development, and maintenance [8]. Disruption of the BDNF/TrkB signaling pathway can impair neuronal function, thereby adversely affecting emotional regulation and cognitive capabilities.

This study aims to investigate the combined neurotoxic effects of NPs and CUMS in mice, with a specific focus on depression-like behaviors and cognitive deficits. The effects were evaluated using a battery of behavioral tests, histopathological examinations, and molecular biological techniques. Furthermore, the study analyzes the involvement of the BDNF/TrkB signaling pathway in these processes, thereby providing a scientific basis for understanding the mechanisms underlying NPs-induced neurotoxicity and informing the development of potential intervention strategies.

MATERIALS AND METHODS

Experimental animals

We purchased a total of thirty-two female BALB/c mice. They were SPF-grade and 6 to 8 weeks old. The overall body weight of the mice was approximately 20-25 grams. The mice were obtained from the Hubei Provincial Research Center for Laboratory Animals (animal qualification certificate no. 42000600056335). The animal room's environmental parameters were set to maintain a temperature of 24-26°C and a humidity of 45-50%. Additionally, a 12-hour light/dark cycle was implemented. Mice had unrestricted access to food and water. This study was approved by the Ethics Committee of Hubei University of Science and Technology (Approval Certificate ID: HBUST-IACUC-2024-11-010), which is available upon request.

Reagents and kits

Polystyrene nanoparticles (PS-NPs) with a diameter of 25 nm were obtained from Zhongke Leiming Technology Co., Ltd. (Product No. PS000025). The Nissl staining solution was obtained from Shanghai Biyuntian Biotechnology Co., Ltd. (Product No. C0117). For RNA extraction, we used a kit from Shenzhen Dakewei Biotechnology Co., Ltd. (Product No. 8034111). The quantitative PCR (qPCR) kit was obtained from Beijing Quanshijin Biotechnology Co., Ltd. (Product No. Q601-02). Furthermore, antibodies against BDNF and TrKB were obtained from Abcam, USA (Product Nos. ab108319 and ab187041).

The equipment used in this research included the following: EthoVision XT Version 12.0 by Noldus (Netherlands) for recording neurobehavioral data in experimental animals; an Olympus dp73 biological microscope (Japan); a Leica RM2245 paraffin microtome (Germany); a Sartorius BAS124S electronic balance (Germany); a Sanyo MDF-U53V ultra-low-temperature freezer operating at -80 °C (Japan); an Eppendorf 5415R low-temperature centrifuge (Germany); a BioTek Epoch microplate reader (USA); a Bio-Rad CFX Connect real-time PCR system (USA); and a Bio-Rad PowerPac Basic system for Western blot electrophoresis (USA).

Animal grouping and modeling

After a week of adaptive feeding, 32 BALB/c mice were randomly assigned to four groups (n=8 per group): the control group (Ctrl), the nanoplastics group (NPs), the model group (Mod), and the combined nanoplastics and model group (NPs+Mod). The NPs and NPs+Mod groups received oral gavage with NPs (5 mg/kg/d, 10 μL/g) [9], whereas the Mod and NPs+Mod groups underwent CUMS to establish a depression model. Mice in the Ctrl group received an equivalent volume of 0.9% sodium chloride solution via gavage.

The CUMS protocol for the Mod and NPs+Mod groups consisted of a variety of unpredictable mild stressors applied over 4 weeks [10]. The stressors included tail clamping for 10 minutes, a 24-hour fast, a 24-hour water deprivation, inversion of the circadian rhythm, overnight light exposure, placement in an empty cage for 12 hours, contact with damp bedding for 12 hours, cage shaking for 15 minutes, foot shocks for 15 minutes, stroboscopic lighting for 10 minutes, refrigeration for 10 minutes, and swimming in cold water at 10°C for 10 minutes. Mice experienced 1-2 stressors each day, with the type of stressor varying daily to avoid repetition and ensure variability over a three-day period. One or two different stressors were applied daily in a random order to prevent habituation. The experimental design is shown in Fig. 1.

General condition inspection

The eating patterns, fur quality, and body weight of mice were monitored before the first exposure and after the final exposure to the experimental protocol.

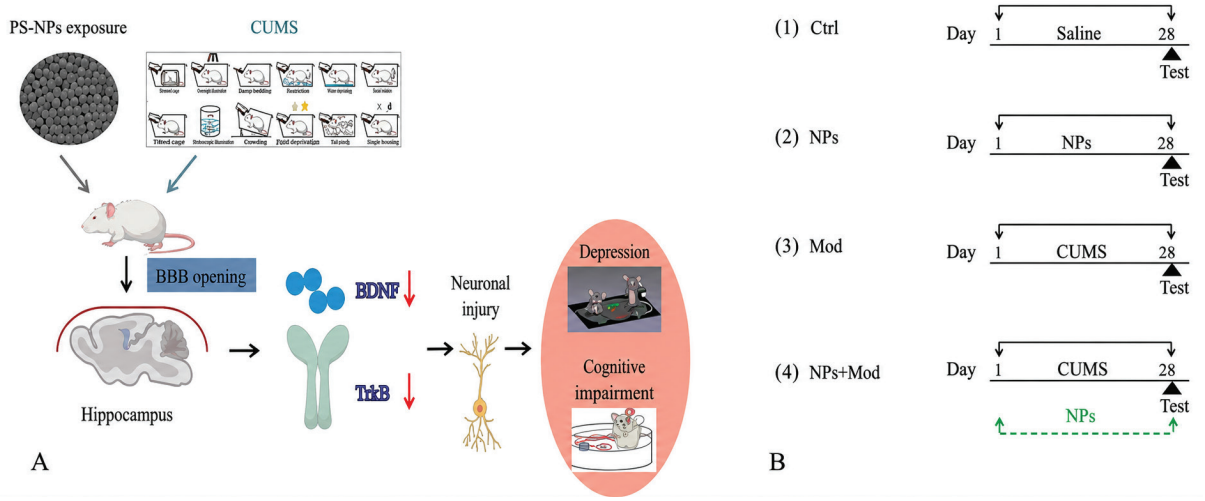

Fig. 1. Neurobiological effects of NPs on stressed mice. **A:** Scientific hypothesis of the study. **B:** Experimental groups and treatment protocol.

Behavioral testing

Sucrose preference test experiment

Before this experiment commenced, mice underwent a 3-day training phase that included sucrose water. Each cage contained two identical bottles in appearance and volume, which were rotated every 12 hours to prevent the formation of a routine memory. On the first day, each bottle was filled with a 1% sucrose solution. The next day, one bottle was replaced with an equivalent amount of distilled water. By the third day, the mice were denied access to any food or water. The evaluation took place on the fourth day, when each cage received one bottle of distilled water and another containing the 1% sucrose solution. After 24 hours, the weights of the bottles (in grams) were recorded. Sucrose solution and water consumption were determined by measuring the weight loss of each bottle. The sucrose preference rate (%) was calculated as: sucrose solution consumption / (sucrose solution consumption + water consumption) × 100%, which indicated the proportion of sucrose solution consumed by each group of mice prior to and following the final exposure.

Open field test

After the final NP administration, mice were placed at the center of an open-field reaction chamber measuring 100 cm in length, 100 cm in width, and 40 cm in height. At the same time, video recording and timing were started, and behavior was recorded for 5 minutes. The experimental data were collected and analyzed using EthoVision XT Version 13.0 software.

Forced swim test

Mice were placed in a clear acrylic cylinder, 50 cm high and 30 cm in diameter, filled with water to a depth of 30 cm at a temperature of (24±2) °C. Each mouse was carefully positioned upright in the water, ensuring that its limbs did not touch the bottom of the cylinder as it struggled and swam. The first 2 minutes were not timed, and the duration of immobility during the subsequent 4 minutes was measured. Immobility was defined as the state in which mice ceased struggling and made only minimal movements necessary to keep their heads above water. Following the swimming session, the animal was swiftly removed from the water, dried, and placed in a warm setting.

Morphological detection

After the final NPs administration, mice were anesthetized intraperitoneally with 1% sodium pentobarbital (40 mg/kg) and placed in a supine position on the surgical table. An incision was made in the chest cavity to expose the heart, and an infusion needle was carefully inserted 5-6 mm into the cardiac apex, aligned with the heart's axis. Once perfusion commenced, the right atrium was cut. The blood vessels were quickly flushed with 50 mL of warm physiological saline, followed by fixation perfusion with 450 mL of pre-cooled 4% paraformaldehyde. The whole brain was then removed and immersed in the same fixative for an additional 6 to 12 hours. Following standard paraffin embedding procedures, sections approximately 5 μm thick were prepared. These sections were stained with Nissl for 10 minutes to 1 hour, rinsed with double-distilled water, differentiated with 70% alcohol, dehydrated through a graded alcohol series, cleared with xylene, and finally mounted. Morphological alterations in hippocampal neurons were examined under an optical microscope and documented for archival records.

Cognitive function assessment

This study used the Morris water maze, a widely recognized method for assessing spatial learning and memory in rodents. The apparatus consisted of a cylindrical water tank with a diameter of 100 cm and a depth of 20 cm, maintained at a water temperature of 24±2 °C. The tank was artificially divided into four quadrants: northeast (NE), southeast (SE), northwest (NW), and southwest (SW). The escape platform was positioned at

the center of the SE quadrant, submerged 1 cm below the water's surface.

During the spatial acquisition phase, mice were placed in the water, facing the wall, at one of four designated starting points (N, E, S, W) and allowed to locate the hidden platform in the southeast quadrant. After the final trial, the swimming routes of mice from the different experimental groups, as well as the time spent in the target quadrant, were recorded. The experimental data were then collected and analyzed using EthoVision XT Version 13.0 software.

Detection of mRNA transcription levels

Total RNA was isolated from hippocampal cells of mice according to the Trizol kit instructions, and RNA concentration was measured. The extracted RNA was reverse-transcribed into complementary DNA (cDNA) using Oligo(dT) primers. Primers targeting mouse BDNF, TrkB, and β-actin were designed based on their complete GenBank sequences. The primer sequences are as follows: BDNF: forward, 5′-GTGTGACAGTATTAGCGAGTGGG-3′; reverse, 5′-ACGATTGGGTAGTTCGGCATT-3′. TrkB: forward, 5′-AGACAAACCCAAATTACCCTGA-3′; reverse, 5′-ACTTTTGTTCGTAGTATCCCCA-3′. β-actin: forward, 5′-CTCATGCCATCCTGCGTCT-3′; reverse, 5′-ACGCACGATTTCCCTCTCA-3′. These primers were synthesized by Beijing Tsingke Biotech Co., Ltd. Using the reverse-transcribed cDNA as a template, PCR amplification was performed according to the qPCR kit protocol. The reaction mixture (15 μL) consisted of 1.5 μL of cDNA, 7.5 μL of 2×SYBR Green Realtime PCR Master Mix, 0.5 μL of each primer (10 μmol·L^{-1}), and 5 μL of nuclease-free water. The PCR amplification protocol consisted of an initial denaturation at 95°C for 30 s, followed by 39 cycles of denaturation at 95°C for 5 s and annealing/extension at 60°C for 30 s.

Detection of protein expression levels

To obtain total protein from hippocampal tissue, we measured protein concentration using the BCA method. Next, protein samples were mixed with 5× SDS-PAGE loading buffer and heated for 8 minutes to denature them. Following this step, proteins were separated by electrophoresis on a 12% SDS-polyacrylamide separating gel with a 5% stacking gel. Proteins were transferred to a PVDF membrane by wet transfer for 90 minutes. The membrane was blocked with 5% skim milk for 90 minutes at room temperature with shaking. Subsequently, the membrane was incubated overnight at 4°C with primary antibodies against BDNF (1:1000) or TrkB (1:5000). After washing five times for 8 minutes each with TBST, the membrane was incubated with an HRP-conjugated secondary antibody (1:10000) for 60 minutes at room temperature. After a subsequent wash, the signal was detected using the improved chemiluminescence technique, with β-actin serving as a reference control.

Statistical analysis

Data were collected from six biological replicates, and results were reported as mean ± standard deviation (Mean ± SD). Statistical analyses were conducted in SPSS version 28.0, and GraphPad Prism 10.0 was used for data visualization. For comparisons between two groups, an independent-samples Student's t-test was used. For comparisons involving three or more groups, one-way analysis of variance (One-way ANOVA) was applied, followed by Tukey's post hoc test for multiple comparisons. A probability value (p) below 0.05 was considered statistically significant.

RESULTS

General condition of mice in each group

Before the experiment, all groups of mice had similar overall conditions. After the final exposure, mice in the Ctrl group exhibited normal food intake, shiny fur, and a significant increase in body weight (Fig. 2). In sharp contrast, mice in the NPs, Mod, and NPs+Mod groups showed reduced food intake and rough, lackluster fur. Although the

NPs and Mod groups showed a slight increase in body weight, the gain was significantly less than that in the Ctrl group. The NPs+Mod group showed little to no increase in body weight (Fig. 2).

Behavioral experiments

The effect on the sucrose preference rate in mice

A significant reduction in sucrose preference was observed in mice from the NPs, Mod, and NPs+Mod groups after the final exposure, compared with the Ctrl group ($p<0.05$). Furthermore, mice in the NPs+Mod group showed a marked decline in sucrose preference compared with the Mod group ($p<0.05$) (Fig. 3A).

The effect on the spontaneous activity of mice in the open field test

After the final exposure, mice in the NPs, Mod, and NPs+Mod groups showed reduced spontaneous activity in the open field test compared with the Ctrl group (Fig. 3B). This reduction was evidenced by a significant decrease in time spent in the central area, a concomitant increase in time spent near the walls, and reductions in total distance traveled and average speed ($p<0.05$). Moreover, compared with the Mod group, the NPs+Mod group exhibited a more pronounced decrease in spontaneous activity, characterized by an even greater preference for the periphery and further reductions in total distance traveled and average speed ($p<0.05$) (Fig. 3C).

The effect on immobility time during the forced swim test in mice

After the final exposure, the NPs-treated group, the Mod group, and the combined NPs+Mod treatment group exhibited behaviors indicative of despair. This was evidenced by a significantly longer immobility duration in these groups than in the control group. The statistical analysis confirmed that these differences were significant ($p<0.05$). Furthermore, when comparing the NPs+Mod group to the Mod group, the mice in the NPs+Mod group exhibited a longer duration of immobility, and this difference was also statistically significant ($p<0.05$) (Fig. 3D).

Morphological changes in hippocampal neurons

After the last exposure, hippocampal neurons in the control group of mice were organized in an orderly manner, with normal intercellular spaces, consistent morphology, intact structures, numerous Nissl bodies, and

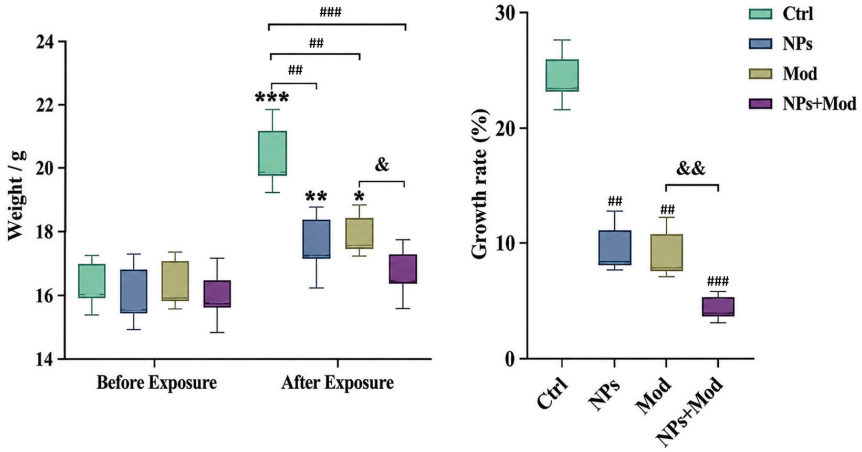

Fig. 2. Changes in body mass in each group. Note: *vs.* before poisoning, ** $p<0.01$, *** $p<0.001$; *vs.* Ctrl group, ## $p<0.01$, ### $p<0.001$; *vs.* Mod group, & $p<0.05$, && $p<0.01$.

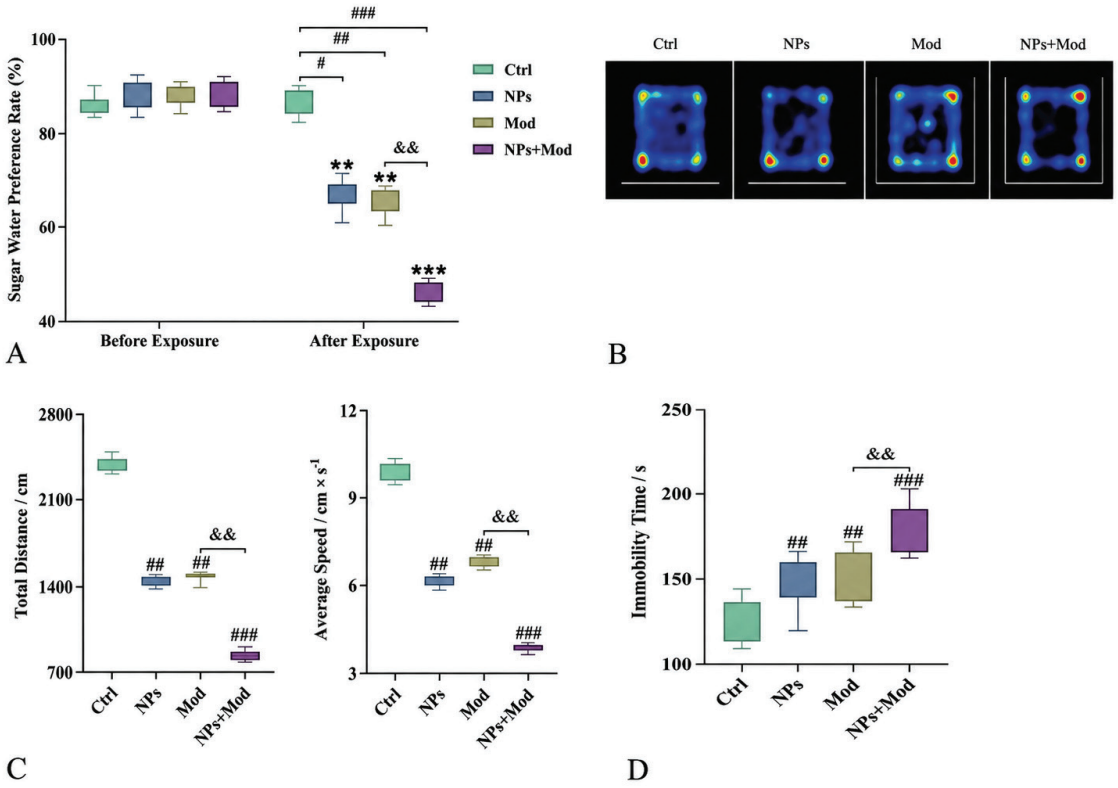

Fig. 3. Behavioral changes in each group. **A:** Sugar water preference test. **B:** Open field test (blue line: mouse path; absence of line: mouse did not enter that area). **C:** Autonomous activity. **D:** Immobility time. Note: *vs.* Ctrl group, ## $p<0.01$, ### $p<0.001$; *vs.* Mod group, && $p<0.01$.

uniform, pronounced staining. In contrast, the NPs group, Mod group, and NPs+Mod group showed disordered cell arrangements, enlarged intercellular spaces, substantial neuronal loss, and lighter staining of Nissl bodies. Importantly, the NPs+Mod group exhibited more pronounced alterations than the Mod group (Fig. 4).

The Morris water maze experiment

After the final exposure to the toxin, mice in the NPs, Mod, and NPs+Mod groups showed a significant decline in spatial memory capacity compared with the Ctrl group. This decline was evidenced by a significantly shorter time spent in the target quadrant and fewer platform location crossings during the probe trial ($p<0.05$). Furthermore, compared with the Mod group, the NPs+Mod group exhibited even more severe spatial memory impairment, with a further significant reduction in both time spent in the target quadrant and the number of platform crossings ($p<0.05$) (Figs. 5 and 6).

Changes in the expression levels of BDNF and TrkB in the hippocampal tissue

After the final exposure, reductions in BDNF and TrkB mRNA transcription and protein expression were observed in the hippocampal tissue of mice in the NPs, Mod, and NPs+Mod groups compared with the Ctrl group, demonstrating statistically significant differences ($p<0.05$). Furthermore, the NPs+Mod group showed significantly greater reductions in BDNF and TrkB mRNA and protein levels than the Mod group ($p<0.05$) (Fig. 7).

DISCUSSION

Global ecological and health implications of NPs exposure

In recent years, the widespread presence and ongoing release of NPs have become a major global environmental issue. Their high mobility enables migration across aquatic environments, terrestrial ecosystems, and atmospheric layers, ultimately disrupting ecological balance and posing significant threats to human health through bioaccumulation and trophic transfer. A notable concern is the confirmed neuroinvasive capability of NPs, as evidenced by their ability to cross the blood-brain barrier and accumulate in the central nervous system [11]. The distinct physicochemical characteristics of NPs, including a remarkably high specific surface area and surface energy, promote strong interactions with receptors on neural membranes (Fig. 2). Such interactions may impair neuronal function, leading to mood changes and cognitive challenges [12].

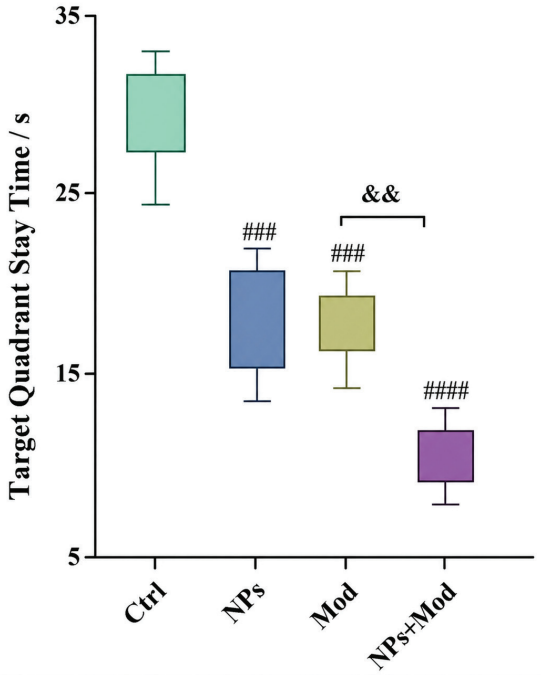

Fig. 6. Target quadrant dwell time in each group. Note: *vs.* Ctrl group, ## p<0.01, ### p< 0.001; *vs.* Mod group, && p<0.01.

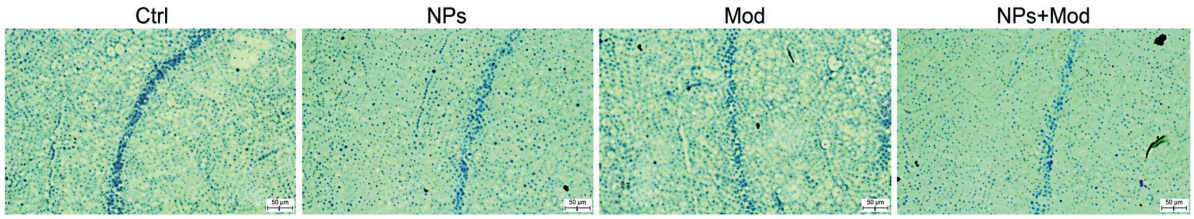

Fig. 4. Pathological changes of hippocampal neurons in each group. Nissl staining, ×100.

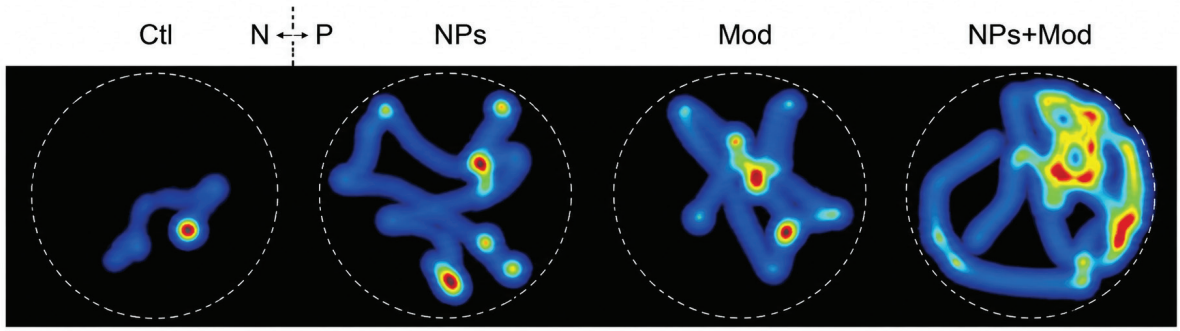

Fig. 5. Morris water maze test in each group. Blue line: mouse path; absence of line: mouse did not enter that area.

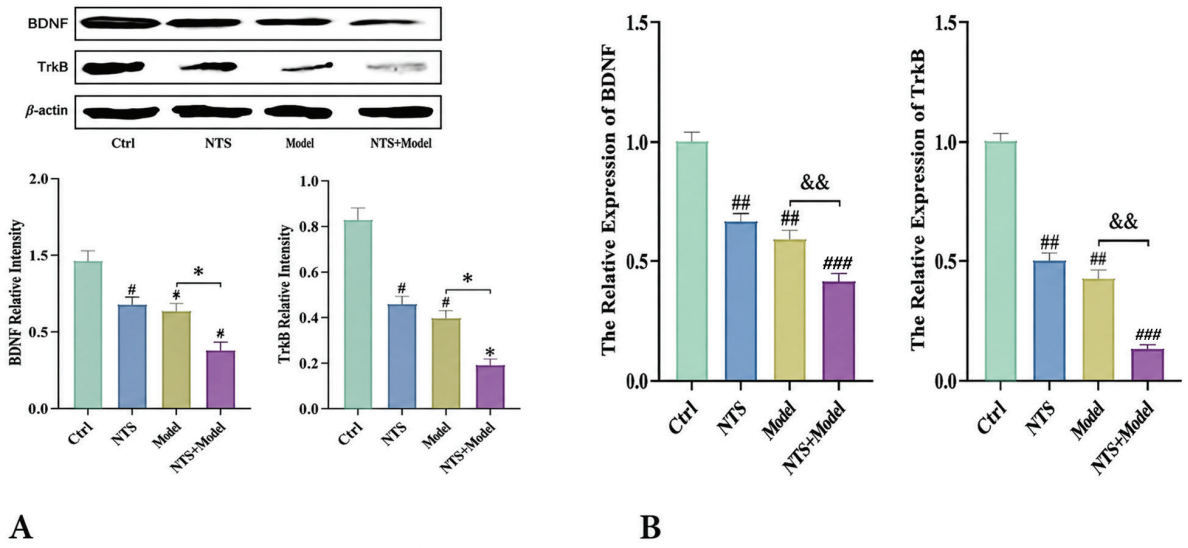

Fig. 7. Changes in the expression levels of BDNF and TrkB. **A:** Protein expression levels. **B:** mRNA transcription levels. Note: *vs.* Ctrl group, # p<0.05, ## p<0.01, ### p<0.001; *vs.* Mod group, & p<0.05, && p<0.01.

Given the neuroinvasive potential of NPs, there is growing concern about their role in mental health disorders, particularly depression [13]. The implications of depression for public health are significant; the global prevalence of depression increased by 34%, and the prevalence of major depressive disorder rose to 8%. The proportion of adolescents suffering from depression increased from 24% during 2001-2010 to 37% between 2011-2020 [14]. According to the report, in 2016, depression was among the leading global causes of disability. We therefore use the CUMS model, a widely used preclinical research framework with good construct validity and lasting behavioral outcomes. This model is highly appropriate for studying the pathogenesis of depression[8]. The objective of this study was to investigate the neurotoxicological effects of NPs and to assess their impact on depression-like behaviors and cognitive performance in CUMS mice. We also evaluated the role of the BDNF/TrkB signaling pathway in these processes.

Behavioral alterations induced by NPs exposure in mice

The current study employed an extensive behavioral battery to systematically investigate the effect of NPs exposure on depression-like behavior in mice [15]. Our results reveal that exposure to NPs causes substantial behavioral changes that correlate with states analogous to depression, as determined by three established behavioral assays. Reduced sucrose preference indicates that exposure to NPs may disrupt the reward-processing machinery, a core feature of anhedonia (Fig. 3). The changes in movement and reduced exploration of the center zone in the open field test may also reflect increased generalized psychomotor slowing or anxiety-like behaviors. Clinical reports of psychomotor agitation or retardation are consistent with these results among depressed persons he changes in movement and reduced exploration of the center zone in the open field test may reflect either generalized psychomotor slowing or anxiety-like behaviors, which is consistent with clinical

reports of psychomotor disturbances in depressed individuals (Fig. 3). The increased immobility time in the forced swim test, often interpreted as behavioral despair, further supports the emergence of a depression-like phenotype following NPs exposure (Fig. 3). Collectively, the consistent findings across these diverse behavioral paradigms robustly demonstrate that NPs exposure induces a depression-like state in mice. Our finding that NPs exposure intensifies the behavioral outcomes of CUMS is particularly significant, indicating that NPs exposure not only triggers depression-like behaviors but also amplifies the effects of CUMS. These results indicate that exposure to NPs may interfere with emotional regulation in mice and exacerbate characteristics associated with stress-induced depression.

Cognitive impairment induced by NPs exposure in mice

The hippocampus is a pivotal structure within the limbic system, widely connected to brain regions such as the prefrontal cortex and amygdala, and is critically involved in emotional processing and cognitive functions, particularly learning and memory[16]. Our histological observations show that exposure to NPs causes severe neuropathological alterations in the hippocampus, including disorganized neuronal arrangement, widened intercellular spaces, extensive neuronal loss, and markedly reduced Nissl staining. These morphological alterations were more severe in the NPs+Mod group than in the Mod group alone, strongly implying that NPs exposure exacerbates CUMS-induced hippocampal neuropathology, thereby contributing to the observed emotional dysregulation (Fig. 4).

Consistent with the hippocampus's critical role in cognition, hippocampal impairment also substantially affects spatial memory [17]. The Morris water maze test assesses spatial learning and memory in mice. Findings showed that, compared with the control group, the NPs group, Mod group, and NPs+Mod group spent less time in the target quadrant, took fewer paths within that quadrant, and exhibited reduced goal-directed movement. Additionally, compared with the Mod group, the NPs+Mod group spent even less time in the target quadrant and took fewer paths. This strongly indicates that exposure to NPs alone impairs hippocampal-related learning and memory functions and compounds cognitive deficits caused by CUMS (Figs. 5 and 6).

NPs exposure causes neuronal damage in mice

BDNF is a signaling protein essential for neuroplasticity and is primarily found in the central nervous system. It regulates neuroregeneration and neuroprotection by activating the TrkB receptor. Evidence shows that activating the BDNF/TrkB signaling pathway can reduce ischemic stroke damage while promoting the production of vascular endothelial cells [18,19]. BDNF exerts proliferative, trophic, and maturational effects on diverse neurons, promoting neuronal growth and the repair of neural structures; its expression levels can serve as a direct indicator of neural functional recovery [20,21]. Research by Liu et al. [20] indicated that enhancing the BDNF/TrkB signaling pathway may reduce neurotoxicity caused by tetrahydropalmatine, which can manifest as depression, anxiety, and cognitive deficits. Decreased expression of BDNF is associated with neuronal injury that could disrupt brain function and cause depression [22]. In this research, qPCR and Western blotting were employed to investigate mRNA transcription and protein expression levels of BDNF and TrkB in hippocampal tissues from mice across groups following the final exposure. The findings indicate that exposure to NPs significantly decreased the expression of both BDNF and TrkB. Furthermore, compared to the Mod group, the NPs+Mod group exhibited a more pronounced reduction in BDNF and TrkB levels. This downregulation of the BDNF/TrkB signaling pathway likely underlies the

observed neuronal damage in the hippocampus and, consequently, the exacerbated impairment of neuronal function, as well as the associated depression-like behavior and cognitive deficits, in CUMS mice exposed to NPs (Fig. 7).

In conclusion, this study demonstrates that NPs exposure exacerbates neurotoxicity in CUMS mice, worsening depression-like behavior and cognitive impairment. Mechanistic analysis indicates that these effects are mediated primarily through disruption of the BDNF/TrkB signaling pathway, resulting in significant hippocampal neuronal damage. These findings provide crucial insight into how NPs affect the central nervous system, offer a scientific basis for understanding NPs-induced neuropathology, and suggest potential therapeutic targets for stress-related mood and cognitive disorders.

The present study has several limitations that warrant consideration. We used a specific polystyrene NP model with a defined size, which does not capture the vast heterogeneity of environmental NPs; thus, our findings may not be fully generalizable to other particle types. Furthermore, although the study focused on the BDNF/TrkB pathway, the observed neurotoxicity is likely multifactorial, potentially involving interrelated processes such as oxidative stress, neuroinflammation, and cell death that were not fully elucidated here. Future studies should use more diverse NP models and employ multiomics approaches to systematically delineate the complex interplay of downstream mechanisms.

Funding

This work was funded by the Project of the Joint Fund for Innovative Development of the Natural Science Foundation of Hubei Province (No. 2025AFD411); the Key Project of the Special Research Fund of the School of Wuguan Medical College, Hubei Institute of Science and Technology (No. 2020WG06); the Faculty Specialized Research Fund Project of Medicine, Dental, and Optometric Medicine, Hubei Institute of Science and Technology (No. 2021WG10); and the Hubei Province Key R&D Plan (No. 2022BCE011).

ORCID ID of the authors

- Dewei Chang (DC): 0009-0006-8282-9577
- Miao Xu (MX): 0009-0008-0645-7243
- Wenning Shi (WS): 0009-0007-4977-4014
- Yan He (YH): 0009-0001-1725-3317
- Zhe Wu (ZW): 0009-0000-0465-8748
- Zhifeng Ning (ZN): 0000-0002-6700-161X
- Yanling Sun (YS): 0009-0000-1301-3730
- Jianguo Lv (JL): 0009-0005-0674-4814

Author's contributions

DC, MX, YS and JL conceiving and designing the study; DC, MX, WS, YH, ZW and ZN collecting the data; DC, MX, WS, YH, ZW and ZN analyzing and interpreting the data; DC, MX, WS, ZW, ZN and YS writing the manuscript; DC, MX, WS, YH, YS and JL providing critical revisions that are important for the intellectual content. All authors approving the final version of the manuscript.

Conflict of interests

All authors declare that they have no conflicts of interest.

Ethics approval

This study was approved by the Ethics Committee of Hubei University of Science and Technology (Approval Certificate ID:

HBUST-IACUC-2024-11-010). The approval certificate is available upon request.

Availability of data and materials

The datasets used and/or analyzed during the current study are available from the corresponding author on reasonable request.

REFERENCES

1. **Liu Q, Hu W, Zhang Y, Ning J, Pang Y, Hu H, et al.** Comprehensive analysis of lncRNA-mRNA expression profiles in depression-like responses of mice related to Polystyrene Nanoparticle exposure. Toxics. 2023;11(7):600. *https://doi.org/10.3390/toxics11070600.*
2. **Li F, Xiang H, Gu Y, Ye T, Lu X, Huang C.** Innate immune stimulation by monophosphoryl lipid A prevents chronic social defeat stress-induced anxiety-like behaviors in mice. J Neuroinflammation. 2022;19(1):12. *https://doi.org/10.1186/s12974-021-02377-8.*
3. **Simon GE, Moise N, Mohr DC.** Management of Depression in Adults: A Review. JAMA. 2024;332(2):141-152. *https://doi.org/10.1001/jama.2024.5756.*
4. **Jha MK, Mathew SJ.** Pharmacotherapies for Treatment-Resistant Depression: How Antipsychotics Fit in the Rapidly Evolving Therapeutic Landscape. Am J Psychiatry. 2023;180(3):190-199. *https://doi.org/10.1176/appi.ajp.20230025.*
5. **Sun Y, Hu N, Wang M, Lu L, Luo C, Tang B, et al.** Hippocampal subfield alterations in schizophrenia and major depressive disorder: a systematic review and network meta-analysis of anatomic MRI studies. J Psychiatry Neurosci. 2023;48(1): E34-e49. *https://doi.org/10.1503/jpn.220086.*
6. **Althammer F, Roy RK, Kirchner MK, Campos-Lira E, Whitley KE, Davis S, et al.** Angiotensin II-Mediated Neuroinflammation in the Hippocampus Contributes to Neuronal Deficits and Cognitive Impairment in Heart Failure Rats. *Hypertension*. 2023;80(6):1258-1273. *https://doi.org/10.1161/HYPERTENSIONAHA.123.21070.*
7. **Nieto-Estévez V, Defterali Ç, Vicario C.** Distinct Effects of BDNF and NT-3 on the Dendrites and Presynaptic Boutons of Developing Olfactory Bulb GABAergic Interneurons in Vitro. Cell Mol Neurobiol. 2022;42(5):1399-1417. *https://doi.org/10.1007/s10571-020-01030-x. PMC11421695.*
8. **Sharma S, Chawla S, Kumar P, Ahmad R, Kumar Verma P.** The chronic unpredictable mild stress (CUMS) Paradigm: Bridging the gap in depression research from bench to bedside. *Brain Res*. 2024;1843: 149123. *https://doi.org/10.1016/j.brainres.2024.149123.*
9. **Deng Y, Chen H, Huang Y, Zhang Y, Ren H, Fang M, et al.** Long-Term Exposure to Environmentally Relevant Doses of Large Polystyrene Microplastics Disturbs Lipid Homeostasis via Bowel Function Interference. Environ Sci Technol. 2022;56(22):15805-15817. *https://doi.org/10.1021/acs.est.1c07933.*
10. **Antoniuk S, Bijata M, Ponimaskin E, Wlodarczyk J.** Chronic unpredictable mild stress for modeling depression in rodents: Meta-analysis of model reliability. Neurosci Biobehav Rev. 2019;99: 101-116. *https://doi.org/10.1016/j.neubiorev.2018.12.002.*
11. **Xie J, Ji J, Sun Y, Ma Y, Wu D, Zhang Z.** Blood-brain barrier damage accelerates the accumulation of micro- and nanoplastics in the human central nervous system. *J Hazard Mater*. 2024;480: 136028. *https://doi.org/10.1016/j.jhazmat.2024.136028.*
12. **Khataminezhad ES, Hajihassan Z, Razi Astaraei F.** Magnetically purification/immobilization of poly histidine-tagged proteins by PEGylated magnetic graphene oxide nanocomposites. Protein Expres Purif. 2023;207: 106264. *https://doi.org/10.1016/j.pep.2023.106264.*
13. **Yang J, Li H, Hao Z, Jing X, Zhao Y, Cheng X, et al.** Mitigation Effects of Selenium Nanoparticles on Depression-Like Behavior Induced by Fluoride in Mice via the JAK2-STAT3 Pathway. ACS Appl Mater Interfaces. 2022;14(3):3685-3700. *https://doi.org/10.1021/acsami.1c18417.*

14. **Shorey S, Ng ED, Wong CHJ.** Global prevalence of depression and elevated depressive symptoms among adolescents: A systematic review and meta-analysis. Br J Clin Psychol. 2022;61(2):287-305. *https://doi.org/10.1111/bjc.12333.*
15. **Su Z, Kong R, Huang C, Wang K, Liu C, Gu X, et al.** Exposure to polystyrene nanoplastics causes anxiety and depressive-like behavior and down-regulates EAAT2 expression in mice. Arch Toxicol. 2025;99(6):2595-2609. *https://doi.org/10.1007/s00204-025-04002-6.*
16. **Wu C, Jia L, Mu Q, Fang Z, Hamoudi H, Huang M, et al.** Altered hippocampal subfield volumes in major depressive disorder with and without anhedonia. BMC Psychiatry. 2023;23(1):540. *https://doi.org/10.1186/s12888-023-05001-6.*
17. **Diersch N, Valdes-Herrera JP, Tempelmann C, Wolbers T.** Increased Hippocampal Excitability and Altered Learning Dynamics Mediate Cognitive Mapping Deficits in Human Aging. J Neurosci. 2021;41(14):3204-3221. *https://doi.org/10.1523/jneurosci.0528-20.2021.*
18. **Zhu X, Han S, Geng Y, Ren W, Quan F.** Brain-Derived Neurotrophic Factor-TrkB Pathway on Synaptic Plasticity in Ischemic Stroke Rats. Int Heart J. 2024;65(6):1095-1106. *https://doi.org/10.1536/ihj.24-312.*
19. **Yang Y, Rao C, Yin T, Wang S, Shi H, Yan X, et al.** Application and underlying mechanism of acupuncture for the nerve repair after peripheral nerve injury: remodeling of nerve system. Front Cell Neurosci. 2023;17: 1253438. *https://doi.org/10.3389/fncel.2023.1253438.*
20. **Liu L, Liu M, Zhao W, Zhao YL, Wang Y.** Tetrahydropalmatine Regulates BDNF through TrkB/CAM Interaction to Alleviate the Neurotoxicity Induced by Methamphetamine. *ACS* Chem Neurosci. 2021;12(18):3373-3386. *https://doi.org/10.1021/acschemneuro.1c00373.*
21. **Castrén E, Monteggia LM.** Brain-Derived Neurotrophic Factor Signaling in Depression and Antidepressant Action. Biol Psychiatry. 2021;90(2):128-136. *https://doi.org/10.1016/j.biopsych.2021.05.008.*
22. **Rauti R, Cellot G, D'Andrea P, Colliva A, Scaini D, Tongiorgi E, et al.** BDNF impact on synaptic dynamics: extra or intracellular long-term release differently regulates cultured hippocampal synapses. Mol Brain. 2020;13(1):43. *https://doi.org/10.1186/s13041-020-00582-9.*

Invest Clin 67(2): 289 - 00, 2026 https://doi.org/10.54817/IC.v67n2a10

Breast papillary lesions: comparative analysis of core needle biopsy and surgical excision findings in a single-center retrospective cohort with literature review.

Tuba Devrim[1], Gamze Erkılınç[1], Saniye Sevim Tuncer[2], Şaziye Ceren Pehlivan[1], Fazilet Uğur Duman[2] and Eyup Kebapci[3]

[1]Izmir Bakircay University, Çiğli Training and Research Hospital, Department of Medical Pathology, Izmir, Turkey.
[2] Ministry of Health, Çiğli Training and Research Hospital, Department of Medical Pathology, Izmir, Turkey.
[3]Izmir Bakircay University, Çiğli Training and Research Hospital, Department of General Surgery, Izmir, Turkey.

Keywords: Papillary breast lesion; Core needle biopsy; Myoepithelial cell; Estrogen receptor; Excision.

Abstract. This retrospective study aimed to identify histopathological and immunohistochemical predictors of malignancy requiring surgical excision among papillary breast lesions diagnosed by core-needle biopsy (CNB). Fifty-three women with CNB-diagnosed papillary breast lesions who subsequently underwent surgical excision at the İzmir Bakırçay University Çiğli Hospital between January 2015 and January 2025 were included. Clinical, radiological, and pathological data were analyzed. Twenty-eight patients (52.8%) were ≤50 years of age, and 21 lesions (39.6%) were larger than 3 cm. Surgical excision revealed benign lesions in 24 cases, malignant lesions in 16 cases, and intracystic solid carcinoma or atypical ductal hyperplasia in 13 cases. The malignancy/atypia group (45.2%) showed a significantly higher frequency of myoepithelial cell loss ($p<0.001$) and microcalcifications ($p=0.028$), and uniform, strong estrogen receptor positivity (100%) on CNB. Benign lesions were more commonly peripherally located ($p=0.049$). No significant associations were observed with age, Breast Imaging Reporting and Data System (BI-RADS) category, or lesion size. These findings indicate that loss of myoepithelial cells and estrogen receptor positivity are strong predictors of malignancy and support the routine incorporation of immunohistochemical evaluation into CNB-based risk stratification.

Corresponding author: Tuba Devrim, Yeni Mahalle, 8780/1 Sk 18, 35620 Cigli/Izmir, Turkiye.
Phone +905432022088. Email: tuba.devrim@bakircay.edu.tr

Lesiones papilares mamarias: análisis comparativo de los hallazgos de la biopsia con aguja gruesa y de la escisión quirúrgica en una cohorte retrospectiva de un solo centro, con revisión de la literatura.

Invest Clin 2026; 67 (2): 289 – 299

Palabras clave: Lesión papilar mamaria; Biopsia con aguja gruesa; Célula mioepitelial; Receptor de estrógeno; Escisión.

Resumen. Este estudio retrospectivo tuvo como objetivo identificar predictores histopatológicos e inmunohistoquímicos de malignidad que requieren escisión quirúrgica en lesiones papilares mamarias diagnosticadas mediante biopsia con aguja gruesa (BAG). Se incluyó a un total de 53 mujeres diagnosticadas con lesiones papilares mamarias por BAG que posteriormente fueron sometidas a escisión quirúrgica en el Hospital Çiğli de la Universidad de İzmir Bakırçay entre enero de 2015 y enero de 2025. Se analizaron datos clínicos, radiológicos y patológicos. Veintiocho pacientes (52,8%) tenían ≤50 años y 21 lesiones (39,6%) tenían un tamaño mayor a 3 cm. La escisión quirúrgica reveló lesiones benignas en 24 casos, lesiones malignas en 16 y carcinoma sólido intraquístico/hiperplasia ductal atípica en 13 casos. El grupo con malignidad/atipia (45,2%) presentó una frecuencia significativamente mayor de pérdida de células mioepiteliales ($p<0,001$) y de microcalcificaciones ($p = 0,028$), así como una positividad uniforme y fuerte para el receptor de estrógeno (100%) en la BAG. Las lesiones benignas se localizaron con mayor frecuencia en la periferia ($p = 0,049$). No se observaron asociaciones significativas con la edad, la categoría Sistema de Informes y Registro de Datos de Imagen de la Mama (BI-RADS) ni el tamaño de la lesión. Estos hallazgos indican que la pérdida de células mioepiteliales y la positividad para el receptor de estrógeno son predictores sólidos de malignidad y respaldan la incorporación sistemática de la evaluación inmunohistoquímica en la estratificación del riesgo basada en la BAG.

Received: 09-02-2026 Accepted: 21-04-2026

INTRODUCTION

Breast papillary lesions encompass a broad spectrum of entities characterized by a papillary architecture with arborizing fibrovascular cores. These lesions range from benign intraductal papillomas to atypical papillary proliferations and overt papillary carcinomas. Clinical examination and imaging modalities lack sufficient specificity to reliably distinguish among these entities, making histopathologic evaluation essential for accurate diagnosis. Classification is primarily based on the nature of the proliferating epithelial component and the presence or absence of a basal myoepithelial cell layer, which is a critical discriminator among benign, *in situ*, and invasive lesions.

Benign papillary lesions include intraductal papillomas, which may be associated with epithelial hyperplasia, metaplasia, atypical ductal hyperplasia, or ductal carcinoma in situ (DCIS). Malignant papillary neoplasms include papillary DCIS, encapsulated papillary carcinoma, solid papillary carcinoma (*in situ* and invasive), and invasive

papillary carcinoma. Despite this structured categorization, these lesions often show overlapping morphological and immunohistochemical features, posing substantial diagnostic challenges, particularly with limited tissue samples obtained by core-needle biopsy (CNB). In this setting, underdiagnosis is more common than overdiagnosis, especially when invasive components are focal or discontinuous [1].

Papillary neoplasms account for approximately 5% of all breast biopsies. However, their detection rate has risen in recent years, largely due to advances in image-guided percutaneous biopsy techniques and the widespread use of high-resolution breast ultrasonography [2]. According to the 5th edition of the WHO Classification of Breast Tumors, papillary neoplasms are classified into five major groups: intraductal papilloma, papillary DCIS, encapsulated papillary carcinoma, solid papillary carcinoma, and invasive papillary carcinoma. Although unified by their characteristic papillary architecture, these lesions exhibit considerable morphological, immunohistochemical, and biological heterogeneity, reflecting a continuum from benign to malignant disease [2-4].

Accurate distinction between noninvasive and invasive papillary carcinomas is critical for prognostic assessment and therapeutic planning. Histologic features supporting invasion include irregular clusters, tongues, and nests of tumor cells that extend into the surrounding stroma beyond a well-defined boundary. Nevertheless, limited sampling, tissue fragmentation, and artifactual distortion in CNB specimens often complicate this distinction, even when myoepithelial immunohistochemical markers [5, 6] are used.

At the molecular level, papillary carcinomas predominantly align with luminal breast cancer subtypes, consistent with their generally low-grade biology and favorable clinical behavior [1]. Papillary carcinoma of the breast is a distinct, relatively uncommon subtype that occurs predominantly in postmenopausal women and accounts for a small proportion of all breast malignancies. Histologically, it is characterized by well-formed papillary structures lined by multilayered or pseudostratified neoplastic epithelial cells, supported by delicate fibrovascular cores [7]. Importantly, neither encapsulated papillary carcinoma nor solid papillary carcinoma with associated invasive foci should be classified as invasive papillary carcinoma, as true invasive papillary carcinoma is a separate, rare entity with an excellent prognosis, low recurrence rates, and prolonged disease-free survival [8].

Preoperative CNB is widely regarded as the standard diagnostic modality for evaluating breast lesions. However, discrepancies between CNB diagnoses and subsequent surgical excision specimens remain incompletely characterized, and the overall degree of diagnostic concordance between these modalities has not been fully elucidated [9]. As reliance on CNB has increased, management strategies for benign intraductal papillomas without atypia have shifted toward more conservative, surveillance-based approaches rather than routine surgical excision [10]. Nevertheless, papillary lesions remain among the most diagnostically challenging entities in breast pathology.

Given these challenges, identifying reliable histopathological and immunohistochemical predictors of malignancy risk in papillary lesions diagnosed by CNB is of substantial clinical importance. The present study aims to contribute to this ongoing effort by evaluating key diagnostic parameters that may help stratify malignancy risk and guide decisions regarding the necessity of surgical excision.

PATIENTS AND METHODS

Study design

Between January 2015 and January 2025, 53 female patients who received a histopathological diagnosis of papillary breast lesions on CNB in the Department of Medical Pathology at İzmir Bakırçay University

Çiğli Training and Research Hospital and subsequently underwent surgical excision at the same institution were enrolled in this retrospective study. Cases were identified through a systematic search of the institutional pathology database. Ethics committee approval for this study was obtained from the İzmir Bakırçay University Non-Interventional Clinical Research Ethics Committee on 03 July 2024 (decision no. 1657).

Clinical, radiological, and pathological data were extracted from the electronic hospital information system. Collected variables included patient age at diagnosis, radiologically measured lesion size, anatomical localization within the breast parenchyma, and the Breast Imaging Reporting and Data System (BI-RADS) score assigned at the time of diagnostic imaging.

Histopathological evaluation of excision and CNB specimens included assessment of papillary architecture, the presence or absence of an intact myoepithelial cell layer, and any associated atypical or malignant epithelial proliferations. Myoepithelial cell status was determined by routine hematoxylin–eosin (H&E) staining, supplemented, when necessary, with immunohistochemical markers such as p63, CK5/6, or smooth muscle myosin heavy chain. Estrogen receptor (ER) expression was evaluated immunohistochemically in accordance with current ASCO/CAP guidelines and recorded semiquantitatively. All microscopic assessments were performed by at least two experienced breast pathologists.

Histopathologic evaluation was performed on tissue obtained via CNB. Tumors were classified by neoplastic nature, architectural features, and cytomorphologic characteristics. Biopsy sites were selected based on radiologic assessment, targeting lesions with high BI-RADS categories or clinically palpable abnormalities. CNB was the primary diagnostic procedure, with sampling directed toward the most suspicious radiologic or clinical regions.

Immunohistochemical (IHC) analysis was performed to assess estrogen receptor (ER), progesterone receptor (PR), and human epidermal growth factor receptor 2 (HER2) expression. ER and PR positivity was defined as nuclear staining in ≥1% of tumor cells. HER2 status was interpreted using standard scoring criteria (0 to 3+), with equivocal (2+) cases further evaluated by fluorescence *in situ* hybridization (FISH).

Statistical analysis

Statistical analyses were conducted using SPSS (version 22.0; IBM Corp., Armonk, NY, USA). Continuous variables were tested for normality using the Kolmogorov–Smirnov test. Descriptive statistics were reported as mean ± standard deviation (SD) or median (interquartile range, IQR) for continuous variables, and as frequencies and percentages for categorical variables.

Comparisons among diagnostic groups (benign, *in situ*/atypical, and malignant) were conducted using the Chi-square test or Fisher's exact test for categorical variables and the Student's t-test or Mann–Whitney U test for continuous variables, based on distributional characteristics. For multigroup comparisons, one-way ANOVA or the Kruskal–Wallis test was applied as appropriate.

The association between histopathological parameters (e.g., myoepithelial cell loss, ER expression), radiologic features, and final excision outcomes was examined using binary logistic regression to identify independent predictors of atypia or malignancy. A p-value <0.05 was considered statistically significant.

RESULTS

Among the 53 patients analyzed, 28 (52.8%) were ≤50 years of age, and lesions >3 cm were identified in 21 cases (39.6%). Based on excision pathology, patients were classified into benign (n = 24), malignant (n = 16), and in situ carcinoma (ISC)/

atypical ductal hyperplasia (ADH) (n = 13) groups. CNB results were classified into benign, borderline/atypical, and malignant categories, and then compared with the final excision diagnoses. This comparison allowed evaluation of diagnostic concordance and identification of underestimation or upgrade rates between biopsy and excision specimens. The grouped distribution of CNB diagnoses and their corresponding excision pathology outcomes is summarized in Table 1. A total of 53 cases were evaluated, and excision outcomes were analyzed in relation to their corresponding BI-RADS assessments to determine the association between radiological classification and final pathological diagnosis. The distribution of excision pathology results according to BI-RADS categories is presented in Table 2. Representative histopathological an d immunohistochemical features of DCIS with papillary features (Fig. 1), encapsulated papillary carcinoma (Fig. 2), and invasive encapsulated papillary carcinoma (Fig. 3) are shown.

Lesions with atypia or malignancy (combined ISC/ADH and malignant cohort; 45.2%) had a markedly higher rate of myoepithelial cell loss than benign lesions ($p<0.001$). Within this cohort, 20.7% of lesions exceeded 3 cm. The atypical group had a significantly higher frequency of microcalcifications ($p = 0.028$), and all cases (100%) showed strong ER immunoreactivity on CNB specimens, indicating uniform hormone receptor positivity.

Table 1. Distribution of core needle biopsy diagnoses and corresponding excision outcomes.

Tru-Cut Biopsi Diagnostic Group	Tru-Cut Biopsi Specific BX Diagnosis	Corresponding Excision Outcome(s)	n
Benign Papillary Lesions	IDP	IDP, ADH+IDP, FCD, Fibroadenoma, DCIS, Invasive EPC, NSTIC (rare upgrades)	23
	USD–associated papilloma	IDP	1
	Micropapilloma	FCD, FCD+fibroadenoma	2
Atypical Papillary Lesions	ADH	UDH/FCD, IDP	4
	Papillary neoplasia (atypia not excluded)	DCIS, DCIS+IDP, Sclerosing papilloma, NSTIC, EPC	8
In situ Malignant Lesions	DCIS	DCIS, DCIS+IDP, SPC, NSTIC	5
	DCIS + EPC	EPC	1
	DCIS + IDP	DCIS+IDP	1
Encapsulated / Papillary Carcinoma Spectrum	EPC ± invasive component	EPC, invasive EPC, invasive papillary carcinoma	5
	SPC	SPC	1
Invasive Carcinomas	NSTIC with EPC	Invasive EPC	1
	Invasive mucinous carcinoma with papillary component	Mucinous carcinoma	1
	Invasive papillary carcinoma	Invasive papillary carcinoma	1
Other Papillary/ Proliferative Lesions	Ductal hyperplasia with papillary structures	DCIS	1

IDP: Intraductal papilloma; ADH: Atypical ductal hyperplasia; FCD: Fibrocystic disease; NSTIC: Invasive carcinoma, no special type; EPC: Encapsulated papillary carcinoma; DCIS: Ductal carcinoma *in situ*; UDH: Usual ductal hyperplasia; SPC: Solid papillary carcinoma.

Table 2. BI-RADS-based distribution of excision results (n = 53).

BI-RADS	Benign	Malign	Total
2	5	1	6
3	6	8	14
4	14	16	30
5	2	1	3

Breast Imaging Reporting and Data System (BI-RADS).

Benign lesions were significantly more likely to be peripherally localized than atypical lesions (p = 0.049). No statistically significant intergroup differences were observed in age distribution, BI-RADS category, lesion size, or other parameters (all p>0.05).

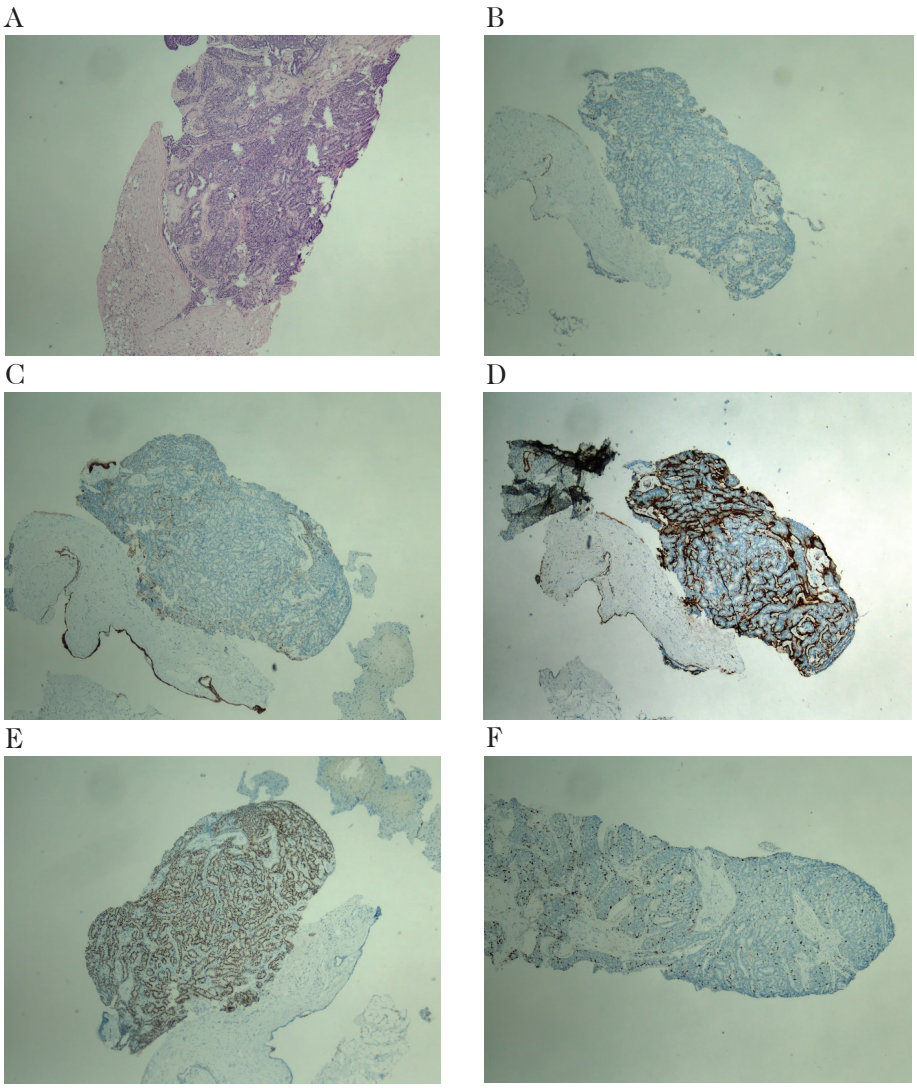

Fig. 1. Histopathological and immunohistochemical findings in a case of ductal carcinoma *in situ* with papillary features. **A:** A case diagnosed as grade 2 ductal carcinoma *in situ* on excisional biopsy; the Tru-Cut biopsy section primarily demonstrates papillary neoplasia *in situ*, stained with hematoxylin and eosin (×40); **B, C, D:** Immunohistochemical staining with p63 (B), CK5/6 (C), and smooth muscle myosin (D) demonstrating the presence of the myoepithelial layer (×40); **E:** Immunohistochemical staining for estrogen receptor (ER) showing 30% nuclear positivity (×40); **F:** Ki-67 immunohistochemical staining demonstrating a proliferative index of 10% (×40).

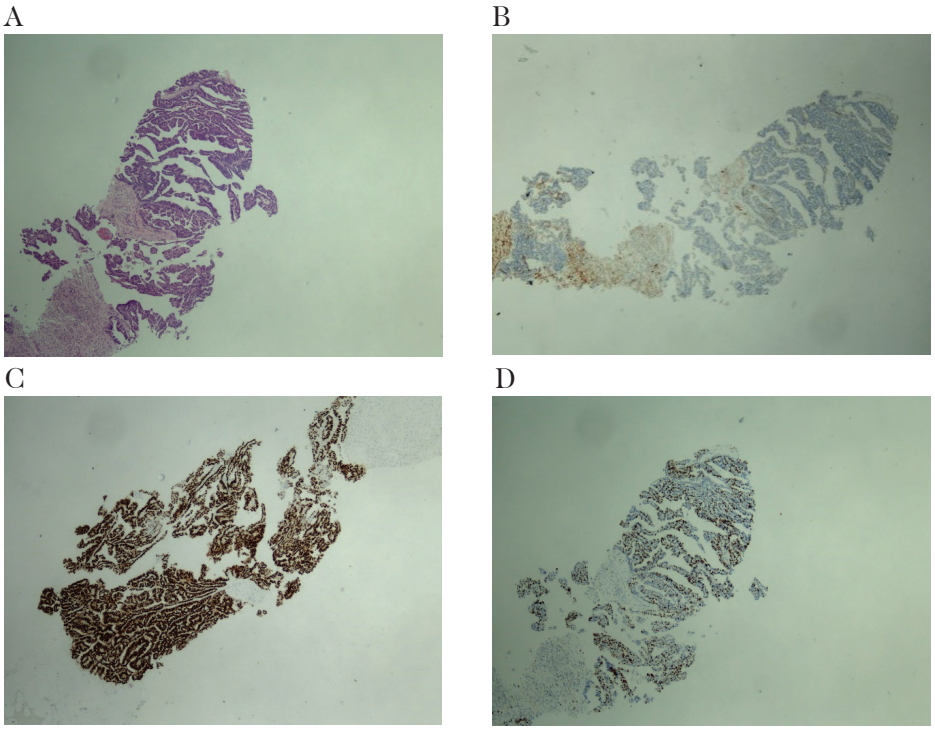

Fig. 2. Histopathological and immunohistochemical features of a case of encapsulated papillary carcinoma. **A:** Hematoxylin and eosin–stained section of a case in which encapsulated papillary carcinoma was initially suspected on Tru-Cut biopsy and subsequently confirmed on excisional material (×40); **B:** Immunohistochemical staining with p63 demonstrating absence of the myoepithelial layer (×40); **C:** Immunohistochemical staining for estrogen receptor (ER) showing diffuse, strong nuclear positivity (100%) (×40); **D:** Immunohistochemical staining for Ki-67 demonstrating a proliferative index of 30% (×40).

DISCUSSION

Papillary breast lesions constitute a diagnostically heterogeneous group, ranging from benign intraductal papillomas to atypical papillary proliferations and papillary carcinomas. Because of their complex architectural patterns and frequent histologic overlap, accurate classification based solely on CNB specimens remains challenging. Although CNB is widely accepted as a minimally invasive and effective initial diagnostic tool, its inherent sampling limitations may lead to underestimating atypia or malignancy in papillary lesions, particularly in those with focal or heterogeneous atypical components [11].

Although papillary breast lesions share a characteristic papillary architecture, they display a broad spectrum of morphological, immunohistochemical, and biological features [3,12]. Ongoing advances in diagnostic pathology, immunohistochemistry, and molecular techniques have substantially improved our understanding of these lesions; however, significant diagnostic and prognostic challenges remain. Over the past decades, numerous aspects of papillary tumor classification, biological behavior, and clinical management have been extensively investigated and, in some cases, remain controversial, with each new contribution offering incremental clarification [4,13].

More recently, molecular approaches have enabled genomic and transcriptomic characterization of papillary breast tumors, providing additional insights into their pathogenesis and potential clinical

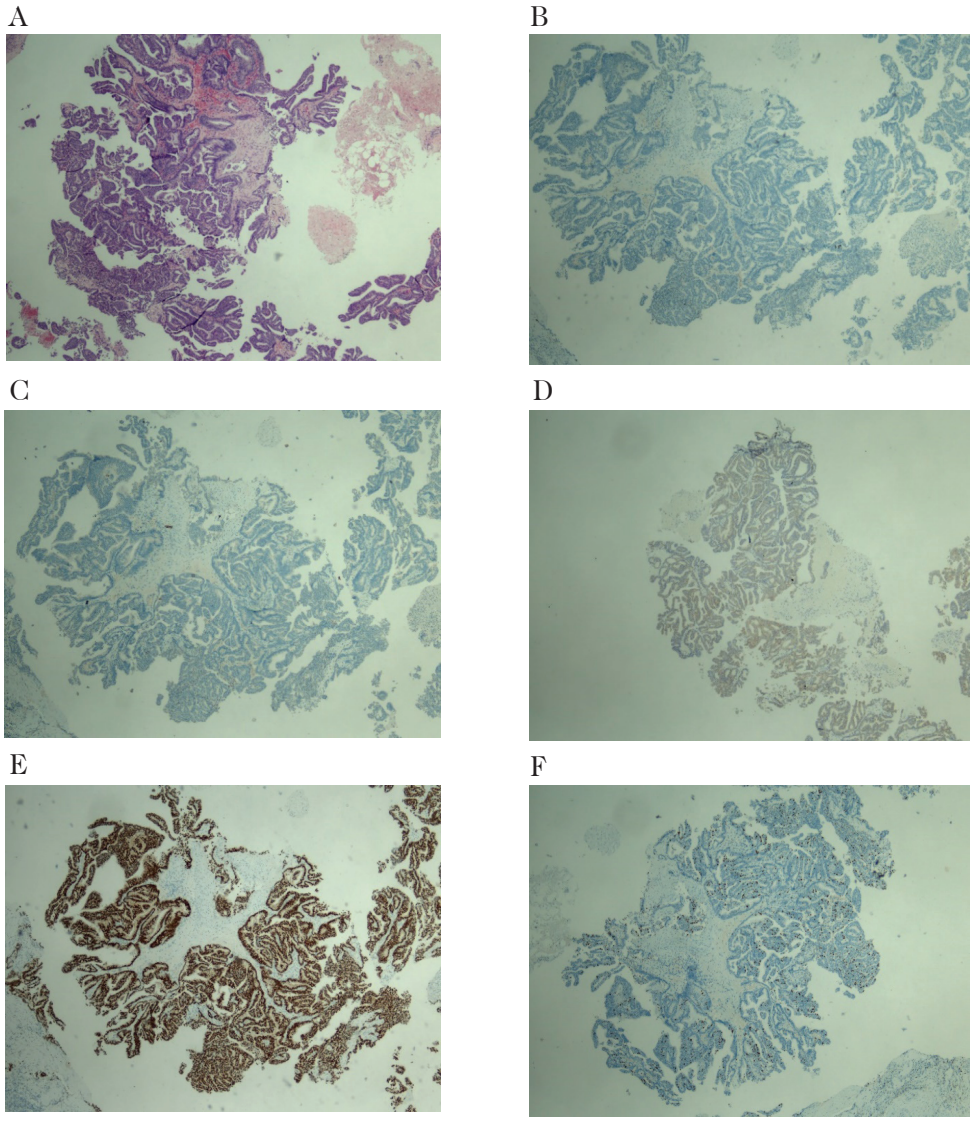

Fig. 3. Histopathological and immunohistochemical features of a case of invasive encapsulated papillary carcinoma. **A:** Hematoxylin and eosin stained Tru-Cut biopsy section (×40) from a case diagnosed with invasive encapsulated papillary carcinoma by both Tru-Cut biopsy and subsequent excisional biopsy; **B, C:** Immunohistochemical staining with p63 (B), CK5/6 (C) and SMM (**D**) showing absence of myoepithelial layer (×40); **E:** Immunohistochemical staining for estrogen receptor (ER) showing widespread strong nuclear positivity (100%) (×40); **F:** Immunohistochemical staining of Ki-67 showing a proliferative index of 15% (×40).

behavior[1,3,13,14]. Despite these advances, the biological significance and optimal management of certain papillary lesions—particularly those diagnosed from limited CNB material—remain incompletely understood, underscoring the ongoing need for comprehensive histopathological evaluation and clinicopathological correlation.

Numerous studies have examined the diagnostic performance and clinical management of papillary neoplasms identified on CNB; however, reported rates of underdiagnosis and diagnostic upgrade on excision vary widely across the literature. Epithelial atypia has consistently been associated with a substantially increased risk of upgrade to

DCIS or invasive carcinoma, supporting current recommendations for complete surgical excision in such cases. In contrast, the optimal management of papillary lesions without atypia diagnosed on CNB remains controversial, with no clear consensus on routine surgical excision versus imaging-based surveillance [2].

Consistent with the findings of Puccini et al. [2], our study showed that when diagnostic upgrades were limited to DCIS or invasive carcinoma, abnormal physical examination findings were significant predictors of malignancy. This observation underscores the limitations of CNB in fully characterizing papillary lesions and reinforces the concept that even papillary lesions without atypia diagnosed on CNB may carry a clinically meaningful risk of upgrade at excision.

Consistent with previous reports by Tian et al. [9], CNB in our cohort showed high concordance in distinguishing benign from malignant breast lesions, with only a small number of discordant cases. Notably, misclassification predominantly involved lesions with atypical ductal hyperplasia (ADH) or ADH combined with an intraductal papilloma. These lesions frequently lacked overtly suspicious sonographic features, and their maximum tumor diameter was generally less than 3 cm, factors that may partially explain the diagnostic challenges encountered.

Accurate discrimination between in situ and invasive carcinoma remains critical, as substantial differences exist in the therapeutic strategies applied to these entities [15]. Pathological grading plays a central role in guiding clinical management, influencing decisions about surgical extent, axillary evaluation, and the need for adjuvant therapy. Consequently, precise histopathological assessment is essential to optimizing patient outcomes.

Intralesional heterogeneity is a defining biological feature of papillary breast lesions and has important diagnostic implications[16]. Atypical papillary lesions, in particular, often show focal architectural atypia and localized disruptions of the myoepithelial cell layer. Immunohistochemical analysis may therefore reveal focal loss of CK5/6 expression confined to atypical regions. Similarly, proliferation indices show marked regional variability across benign, atypical, and malignant papillary lesions, with differences between low- and high-proliferative areas reported to reach up to 44%.

Collectively, these observations indicate that asymmetric growth and intralesional heterogeneity are intrinsic features of many papillary lesions. This heterogeneity highlights the inherent limitations of CNB, as limited sampling may miss the most diagnostically significant areas, potentially leading to underdiagnosis. These findings support continued recommendations for surgical excision when atypia is identified or when lesion heterogeneity raises concerns about sampling adequacy [17].

Managing patients diagnosed with benign intraductal papilloma on CNB remains particularly challenging. Although most of these lesions are truly benign, reported rates of upgrade to atypia or malignancy on excision are high enough to warrant concern. As a result, many clinicians favor routine surgical excision to establish a definitive diagnosis. However, this approach inevitably leads to overtreatment, given that the incremental breast cancer risk associated with a solitary benign papilloma is comparable to that of usual ductal hyperplasia. These considerations underscore the need for improved risk stratification strategies to more accurately identify patients who would benefit from surgical intervention [17].

Finally, the relatively low underestimation rates for DCIS and ADH reported with CNB have important implications for surgical planning. When subsequent excision is performed, surgeons may reasonably assume a low likelihood of occult invasive carcinoma, supporting breast-conserving surgical approaches. In such cases, axillary lymph node sampling may be safely omitted, given the low probability of invasive disease [18].

This review has several limitations. In several of the included studies, incomplete or inconsistent reporting limited a rigorous assessment of methodological quality and hindered accurate evaluation of the potential impact of bias on study findings. Furthermore, substantial heterogeneity in study designs, diagnostic thresholds, and histopathological criteria limited meaningful cross-study comparisons and likely contributed to variability in reported outcomes.

To strengthen the evidence base, future high-quality prospective diagnostic accuracy studies using standardized reporting frameworks are needed. Such studies would enable more robust validation of current findings and help mitigate the impact of residual methodological limitations.

In conclusion, given the well-documented potential for underestimation—not only of carcinoma but also of atypical proliferative lesions—surgical excision remains a justified and prudent management strategy for papillary breast lesions identified on CNB. When a papillary lesion is detected on CNB, surgical excision carries a substantial likelihood of revealing atypia or an associated malignancy, either within the index lesion or in adjacent breast tissue.

Funding

The authors declared that this study received no financial support.

ORCID ID of the authors

- Tuba Devrim (TD): 0000-0002-5321-2002
- Gamze Erkılınç (GE): 0000-0003-4704-7415
- Saniye Sevim Tuncer (SST): 0000-0003-0872-7493
- Şaziye Ceren Pehlivan (SCP): 0009-0002-1514-3648
- Fazilet Uğur Duman (FUD): 0000-0002-5721-9746
- Eyup Kebapci (EK): 0000-0001-8900-2325

Author's contributions

TD drafted the manuscript and conducted the statistical analyses. GE, SST, SCP, FUD, and EK contributed to the study's conception and design. All authors critically reviewed and approved the final manuscript.

Part of this study was given as an oral presentation at the 34th National Pathology Congress, held in November 12-16, 2025 in İzmir/Turkey.

Conflict of interest

All authors participating in the study declare that there is no conflict of interest.

REFERENCES

1. **Jamidi SK., Tse GM**. Papillary lesions of the breast. Diagnostic Histopathology. 2025; 31(12,):707-714. *doi:10.1016/j.mpdhp.2025.10.004.*
2. **Puccini R, Sanvido V, Waitzberg A, Facina G, Nazario A**. Underestimation in core-needle biopsies of papillary breast lesions: a retrospective cohort from a university center. In: Proceedings of the San Antonio Breast Cancer Symposium. Clin Cancer Res. 2025; 31(12): 1-10-09.
3. **Tay TKY, Tan PH.** Papillary neoplasms of the breast—reviewing the spectrum. Mod Pathol. 2021; 34: 1044–1061. *doi:10.1038/s41379-020-00732-3*
4. **WHO Classification of Tumours Editorial Board. Breast tumours.** IARC, Lyon, France, in: WHO classification of tumours. 2019; 2. Papillary Neoplasms.
5. **Naowaset P.** Prognosis and clinical outcome of papilloma neoplasm of the breast: An observational study. Cancer Treat Res Commun. 2025; 43:100900. *doi:10.1016/j.ctarc.2025.100900*

6. **Wang Y, Song, EC.** Papillary neoplasm of the breast – A review and update. Hum Pathol Rep. 2021; 26. 300581. *doi: 10.1016/j.hpr.2021.300581.*
7. **Dnyanmote A, Himashree MP.** Unusual Case of Papillary Carcinoma of the Breast. Cureus. 2024;16(7):e63568. *doi:10.7759/cureus.63568*
8. **Sukpanich R, Lertsithichai P, Chirappapha P.** Prognosis and clinical outcome of papillary carcinoma of the breast at A Tertiary Care Hospital. Thai J. Surgery. 2019; 40:101-106.
9. **Tian H, Li G, Zheng J, Ding Z, Luo Y, Mai S, et al**. Comparing core needle biopsy and surgical excision in breast cancer diagnosis: implications for clinical practice from a retrospective cohort study. Quant Imaging Med Surg. 2024;14(12):8281-8293. *doi:10.21037/qims-24-198.*
10. **Thai JN, Vickery J, Boyraz B, Crowley C, Saksena MA, Vladislav V.** Papillary Neoplasms of the Breast: WHO Classification, Multimodality Imaging, and Radiologic-Pathologic Correlation. RadioGraphics. 2025; 45(8) *doi:10.1148/rg.240091*
11. **Sydnor MK, Wilson JD, Hijaz TA, Massey HD.** Shaw de Paredes ES. Underestimation of the presence of breast carcinoma in papillary lesions initially diagnosed at core-needle biopsy. Radiology. 2007; 242(1):58-62. *doi:10.1148/radiol.2421031988.*
12. **Collins LC, Schnitt SJ.** Papillary lesions of the breast: selected diagnostic and management issues. Histopathology. 2008; 52(1):20-29. *doi:10.1111/j.1365-2559.2007.02898.x*
13. **Rakha EA, Ellis IO.** Diagnostic challenges in papillary lesions of the breast. Pathology. 2018; 50(1):100-110. *doi:10.1016/j.pathol.2017.10.005.*
14. **Piscuoglio S, Ng CK, Martelotto LG, Eberle CA, Cowell CF, Natrajanet R, et al.** Integrative genomic and transcriptomic characterization of papillary carcinomas of the breast. Mol Oncol. 2014; 8(8):1588-1602. *doi:10.1016/j.molonc.2014.06.011*
15. **Andre F, Ismaila N, Henry NL, Somerfield MR, Bast RC, Barlow W, et al.** Use of Biomarkers to Guide Decisions on Adjuvant Systemic Therapy for Women With Early-Stage Invasive Breast Cancer: ASCO Clinical Practice Guideline Update-Integration of Results From TAILORx. J Clin Oncol. 2019; 37:1956-64. *doi:10.1200/JCO.19.00945*
16. **Nuñez, DL, González FC, Ibargüengoitia MC, Fuentes Corona RE, Hernández Villegas AC, Zubiate, ML, et al.** Papillary Lesions of the Breast: A Review. Breast Cancer Management. 2020; *9*(4). *doi:10.2217/bmt-2020-0028*
17. **Pathmanathan N, Albertini AF, Provan P, Milliken JS, Salisbury EL, Bilouset AM, et al.** Diagnostic evaluation of papillary lesions of the breast on core biopsy. Mod Pathol. 2010; 23:1021–1028. *doi:10.1038/modpathol.2010.81*
18. **Bruening W, Fontanarosa J, Tipton K, Treadwell JL, Schoelles K.** Systematic review: Comparative effectiveness of core-needle and open surgical biopsy to diagnose breast lesions. Ann Intern Med. 2009; 152. 238-46. *doi:10.1059/0003-4819-152-1-201001050-00190.*

Invest Clin 67(2): 300 - 318, 2026 https://doi.org/10.54817/IC.v67n2a11

Revisión panorámica de Enterobacterales productores de carbapenemasas en Venezuela: Características microbiológicas, epidemiológicas y moleculares.

Elba Guerrero, Howard Takiff, Lizeth Caraballo y Luis Querales

Laboratorio de Genética Molecular, Centro de Microbiología y Biología Celular, Instituto Venezolano de Investigaciones científicas (IVIC). Caracas, Venezuela.

Palabras clave: *Enterobacteriaceae* Resistentes a los Carbapenémicos; Venezuela; *Klebsiella pneumoniae*; KPC.

Resumen. Las infecciones causadas por Enterobacterales resistentes a los carbapenémicos, antibióticos considerados de última línea, representan una amenaza creciente para la salud pública. El principal mecanismo de resistencia es la producción de carbapenemasas, cuya tipificación es importante para orientar las decisiones terapéuticas. Asimismo, la epidemiología molecular aporta información esencial para el monitoreo y el control de estos microorganismos. En este contexto, se realizó una revisión de los reportes sobre Enterobacterales productores de carbapenemasas en Venezuela, con el objetivo de sintetizar la información disponible, incluyendo las especies bacterianas y enzimas detectadas, la susceptibilidad antibiótica, los elementos móviles asociados y la tipificación molecular de las cepas, así como destacar las tendencias epidemiológicas en el país. El análisis de los estudios reveló que *Klebsiella pneumoniae* (*K. pneumoniae)* productora de carbapenemasas (KPC) ha sido la enterobacteria reportada con mayor frecuencia; sin embargo, la metalo-β-lactamasa de Nueva Delhi (NDM) muestra una tendencia creciente, en concordancia con la situación en América Latina. La caracterización molecular de los aislados ha sido limitada, lo que resalta la necesidad de fortalecerla en futuras investigaciones. En general, se evidencia una brecha de conocimiento que requiere estudios sistemáticos para comprender mejor la dinámica y el impacto de estos agentes patógenos en Venezuela.

Autor de correspondencia: Elba Guerrero. Laboratorio de Genética Molecular, Centro de Microbiología y Biología Celular, Instituto Venezolano de Investigaciones Científicas (IVIC), Caracas, Venezuela. Correo electrónico: eguerrero@ivic.gob.ve

Comprehensive overview of carbapenemase-producing Enterobacterales in Venezuela: microbiologic, epidemiologic, and molecular features.

Invest Clin 2026; 67 (2): 300 – 318

Key words: Carbapenem-Resistant *Enterobacteriaceae*; Venezuela; *Klebsiella pneumoniae;* KPC.

Abstract. Infections caused by carbapenem-resistant Enterobacterales, which are considered last-line antibiotics, represent a growing threat to public health. The primary resistance mechanism is carbapenemase production, and characterizing these enzymes is essential for guiding therapeutic decisions. Likewise, molecular epidemiology provides critical information for monitoring and controlling these microorganisms. In this context, we reviewed reports of carbapenemase-producing Enterobacterales in Venezuela, synthesizing available data on bacterial species, antibiotic susceptibility, resistance-conferring enzymes, associated mobile genetic elements, molecular typing, and epidemiological trends. Analysis of these studies revealed that KPC-producing Klebsiella pneumoniae has been the most frequently reported carbapenemase-producing enterobacterium, although NDM (New Delhi metallo-beta-lactamase) is on the rise, consistent with the situation in the rest of Latin America. Overall, we identified a knowledge gap, especially in the molecular characterization of carbapenem-resistant isolates, that requires systematic studies to better understand the dynamics and impact of these pathogenic agents in Venezuela.

Recibido: 05-12-2025 Aceptado: 02-03-2026

INTRODUCCIÓN

El aumento de las infecciones causadas por bacterias resistentes a antibióticos es reconocido por la Organización Mundial de la Salud (OMS) como una grave amenaza para la salud humana. En el año 2019 a nivel global se estimaron 4,95 millones de muertes asociadas a este fenómeno, de las cuales 1,27 millones fueron directamente atribuibles a esta causa [1].

El orden Enterobacterales agrupa diversas especies patógenas oportunistas que con frecuencia presentan perfiles de multirresistencia o MDR (Multidrug-Resistant, por sus siglas en inglés), definida como la resistencia simultánea a tres o más clases de antibióticos, condición que representa un desafío para el tratamiento de las infecciones asociadas [2].

La emergencia de Enterobacterales resistentes a carbapenémicos, antibióticos considerados de última línea en el manejo de infecciones graves, constituye un problema prioritario de salud pública dada su asociación con el aumento de fracasos terapéuticos, y por lo tanto de la morbilidad y mortalidad especialmente en entornos hospitalarios. Un metaanálisis publicado en 2014 estimó que hasta un 44% de las muertes en casos de infecciones por *Enterobacteriaceae* resistentes a carbapenémicos fueron directamente atribuibles a la resistencia [2], evidenciando su impacto clínico.

La resistencia a carbapenémicos puede deberse a la presencia simultánea de mecanismos como la producción de β-lactamasas de espectro extendido (BLEE) y la pérdida de porinas, pero comúnmente está asociada

a la producción de carbapenemasas. Estas enzimas, que hidrolizan a los carbapenémicos y otros β-lactámicos, se agrupan en tres de las clases moleculares de Ambler, un sistema de clasificación de las β-lactamasas, a saber: la clase A, que corresponde a serinocarbapenemasas, así denominadas porque contienen este aminoácido en su sitio activo; la clase B, conformada por metalo-β-lactamasas (MBL) que requieren de un ión metálico para su actividad y son inhibidas por agentes quelantes; y la clase D, representada por oxacilinasas que muestran niveles bajos de hidrólisis de carbapenémicos[3]. Las principales carbapenemasas por su dispersión y repercusión son las producidas por *Klebsiella pneumoniae* o KPC que pertenece a la clase A, metalo-betalactamasa New Delhi (NDM, por sus siglas en inglés) que es una MBL o clase B, y metalo-betalactamasa codificada por integrón tipo Verona (VIM, por su acrónimo en inglés), otra carbapenemasa relevante tipo MBL. KPC confiere resistencia a todos los β-lactámicos disponibles, mientras que NDM confiere resistencia a la gran mayoría de esta clase de antibióticos, pero es incapaz de hidrolizar aztreonam. A nivel mundial se han reportado más de 150, 29 y 40 variantes de KPC, NDM y VIM, respectivamente [4,5].

Se ha registrado diseminación global de las Enterobacterales productores de carbapenemasas (EPC) impulsada por el aumento en el uso de carbapenémicos para el tratamiento de infecciones causadas por bacterias Gram negativas MDR y el uso indiscriminado de estos fármacos, lo cual se acentuó con la pandemia de COVID-19 [6]. Adicionalmente, la crisis sanitaria debida a la pandemia de COVID-19 provocó una disminución en el financiamiento de actividades de vigilancia, prevención y control de la resistencia a los antimicrobianos en países de ingresos bajos y medios [7].

En Venezuela el alcance de esta problemática no se ha caracterizado de manera exhaustiva, por lo cual, el presente trabajo proporciona un análisis de los reportes publicados sobre Enterobacterales productores de carbapenemasas en el país con el objetivo de sintetizar el conocimiento actual e identificar las principales limitaciones a considerar en futuras investigaciones.

MÉTODOS

Para la búsqueda de estudios que reportan Enterobacterales productores de carbapenemasas en Venezuela se utilizaron los términos: "carbapenemase", "enterobacteria" o "Enterobacterales" y "Venezuela" o "Latin America" en las bases de datos PubMed y Google Académico. Se examinaron las 82 publicaciones que resultaron de la búsqueda en PubMed y las 150 primeras de Google Académico, así como las referencias en los artículos revisados.

Se incluyeron los estudios originales en inglés y español, en los que describen la detección de carbapenemasas en Enterobacterales aisladas en Venezuela, especificando el tipo o familia de enzima, y fecha o período de aislamiento. No se consideraron artículos de revisión ni resúmenes de presentaciones en congresos.

Adicionalmente se consultó la página web del "Programa Venezolano de Vigilancia de la Resistencia a los Antimicrobianos" (PROVENRA) (https://provenra.com.ve/). Específicamente, fueron examinados los datos de susceptibilidad a meropenem de *Klebsiella pneumoniae (K. pneumoniae)*, *Enterobacter cloacae (E. cloacae)* y *Escherichia coli (E. coli)* entre los años 2005 y 2020 (año más reciente con información disponible). La última búsqueda bibliográfica y la última consulta a la página de PROVENRA se realizaron en julio y agosto de 2025, respectivamente. Las proporciones resultantes del análisis del conjunto de estudios se presentan como porcentajes y frecuencias. Para la representación gráfica de datos se utilizó el programa Excel.

RESULTADOS

Aspectos generales

Se analizaron 33 estudios publicados entre 2008 y 2025 [7–39], de manera que se abarca un periodo de 18 años, incluyendo 5 años sin ninguna publicación (2009-2010, 2013 y 2023-2024), 5 con solo una (2008, 2011, 2012, 2018 y 2025), 2 años con dos (2015 y 2022), 3 años con tres (2014, 2019 y 2020), dos con cuatro estudios (2017 y 2021) y uno con siete publicaciones (2016).

El enfoque de los artículos evaluados es heterogéneo; unos estudian Enterobacterales en general [8–12], mientras que otros reportan un grupo de aislados de *K. pneumoniae* [13–21] *Enterobacter* spp. [22–24] o *E. coli* [25,26]. Algunos estudios también incluyen especies Gram negativas pertenecientes a otros ordenes taxonómicos como *Acinetobacter baumannii* y *Pseudomonas aeruginosa* [20,21,27] o bacterias Gram positivas y levaduras [28]. Se encontraron varios reportes de caso o de un solo aislado [29–33] y estudios internacionales que incluyen cepas productoras de carbapenemasas aisladas en Venezuela [7,24,26,27,34–39]. Algunos de los estudios internacionales no desglosan las especies bacterianas por país (3 estudios que suman 36 aislados) [36–38], y otros no especifican por país esta información ni el total de aislados positivos para carbapenemasas [34,39].

La mayoría de los estudios se centran en bacterias productoras de carbapenemasas, pero algunos se enfocan en el análisis de β-lactamasas en general [8,12,13], mientras que otros caracterizan tanto carbapenemasas como BLEE [25,28]. Casi la totalidad de aislados provenían de pacientes, solo un estudio incluyó además aislados de ambiente hospitalario y personal de salud [10]. Las fuentes de aislamiento fueron diversas, siendo frecuentes hemocultivo, urocultivo y secreciones. Los estudios analizados reportan un total de 940 aislados de Enterobacterales productores de carbapenemasas, con tres estudios concentrando más de la mitad de los mismos (662 aislados) [10,11,21].

En la Tabla 1 se indican los métodos utilizados en los estudios sobre EPC en Venezuela. Entre los trabajos que especifican los métodos para la identificación de las especies, el uso de pruebas bioquímicas convencionales fue el más frecuente, seguido de MALDI-TOF (ionización por desorción láser asistida por matriz). Para evaluar la susceptibilidad a antibióticos, se reportó difusión en disco o más comúnmente determinación de la concentración mínima inhibitoria (CMI), esta última en su mayoría por microdilución[24,25,27,33,34,37], en algunos casos usando los sistemas automatizados "microScan" [15,17,31,37] o "VITEK" [28,36]; pero también por dilución en agar [30] o dilución en caldo [16,32]. Los métodos fenotípicos utilizados para detección de carbapenemasas incluyen: sinergia de doble disco [7–9,11–16,18,19,21,25,28–32]; Test de Hodge Modificado (THM) [9–11,15–18,21,28,32]; discos combinados[10,15,22]; Blue Carba [7–9,13,20,21]; método de inactivación de carbapenémicos (CIM por sus siglas en inglés); [7,30] y Carba-NP [7,20].

Como método confirmatorio para la detección de carbapenemasas se describe el uso de Reacción en Cadena de la Polimerasa (PCR) seguida o no de secuenciación Sanger para la identificación de la variante. Tres estudios utilizaron únicamente métodos fenotípicos en la detección de carbapenemasas. Pocos estudios han incluido tipificación molecular y análisis de elementos móviles (Tabla 1). Asimismo, solo 3 estudios realizaron secuenciación de genoma completo, específicamente dos estudios de aislados colectados dentro de los programas de vigilancia global SMART ("Study for Monitoring Antimicrobial Resistance Trends") e INFORM ("International Network for Optimal Resistance Monitoring") [24,26]. Adicionalmente, un estudio analizó el genoma completo de una cepa de *E. coli* por presentar el gen de resistencia a colistina *mcr-1*, que portaba además el gen bla_{NDM-1} [33].

Especies bacterianas y tipos de carbapenemasas

El primer aislamiento reportado de una EPC en Venezuela fue obtenido en 2005 y

Tabla 1. Métodos utilizados en los estudios sobre Enterobacterales productores de carbapenemasas en Venezuela.

Objetivo	Tipo de Método	Número de estudios	Referencias
Identificación de especies	Solo pruebas bioquímicas convencionales*	9	8,9,11–13,19,21,22,30
	PCR	1	20 (1)
	MicroScan o VITEK	4	17,28,31,36
	MALDI-TOF	8	26,27,32–35,37,38 (1)
	PCR+secuenciación Sanger	1	23
Susceptibilidad a antibióticos	Difusión en disco	12	8–14,18,19,21,22,29
	Determinación de CMI	17	15–17,20,24–28,30–35,37,38
Detección e identificación de Carbapenemasas	Solo pruebas Fenotípicas*	3	8,13,25
	PCR	14	7,9–12,14,15,19,21,23,30,31,36,39
	PCR+Secuenciación Sanger	15	16–18,20,22,24,26–29,32,34,35,37,38
Tipificación molecular	Solo ERIC-PCR o REP-PCR*	3	13,14,22
	PFGE	2	15,19
	MLST	6	16–18,20,24,33 (2)
Determinación de filogrupos (*E. coli*)	PCR múltiple de Clermont	2	25,28
Análisis de plásmidos y otros MGE	Conjugación y/o transformación	3	17,18,32
	Detección de transposón	4	16–18,24 (2)

*En estudios que adicionalmente emplearon otro método, solo el confirmatorio es indicado. (1)Adicionalmente utilizaron un sistema comercial de identificación bioquímica. (2)Por secuenciación de genoma completo. MALDI-TOF: Desorción/Ionización Láser Asistida por Matriz. CMI: Concentración mínima inhibitoria; PFGE: Electroforesis en Gel de Campo Pulsado; ERIC-PCR: PCR basada en Secuencias Repetitivas Intergénicas; REP-PCR: PCR basada en Secuencias Repetitivas Extragénicas Palindrómicas; MLST: Tipificación Multilocus de Secuencia; MGE: Elementos Genéticos Móviles.

corresponde a *K. pneumoniae* portadora de bla_{VIM} [30]. En la Fig. 1 se presenta una línea de tiempo de los primeros aislamientos de cada tipo de carbapenemasa en tres especies de EPC en Venezuela. En los años 2008 y 2009, por primera vez, se aisló una EPC con KPC o NDM [19,20], respectivamente, ambas correspondientes a *K. pneumoniae.* Las primeras Enterobacterales productores de GES (una serino carbapenemasa) y de una carbapenemasa tipo OXA-48 (oxacilinasa) se aislaron en Venezuela entre 2017 y 2019, en ambos casos presentando también NDM, pero no se notificaron las especies bacterianas [34].

En Venezuela *K. pneumoniae* ha sido, por amplio margen, la especie de Enterobacterales productora de carbapenemasas reportada con más frecuencia, representando el 79,3% de los casos documentados (718 de 903 aislados). A esta le siguen miembros del complejo *E. cloacae* (7,4%, 67/903), *E. coli* (5,6% (51/903) y *K. oxytoca* (4,1%, 37/903). Otras especies observadas son: *Enterobacter aerogenes* (actualmente *Klebsiella aero-*

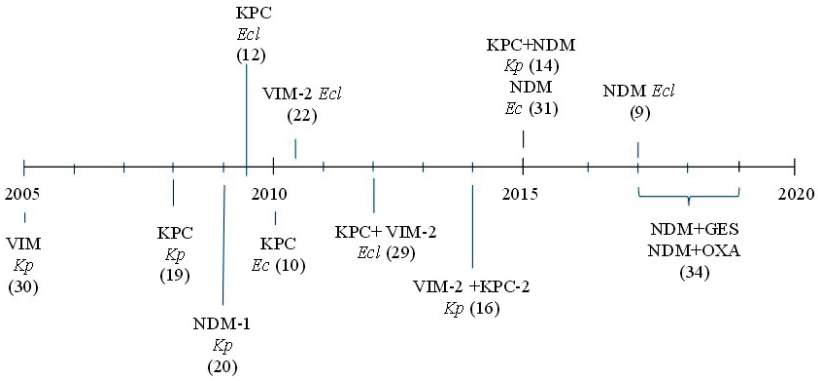

Fig. 1. Línea de tiempo del primer aislamiento reportado para cada tipo o combinación de carbapenemasas en las principales especies de Enterobacterales en Venezuela. *Kp*: *K. pneumoniae*; *Ecl*: *E. cloacae*; *Ec*: *E. coli*; KPC: *K. pneumoniae* Carbapenemasa; NDM: Nueva Delhi Metalo-β-lactamasa; VIM: Verona Metalo-β-lactamasa codificada por integrón. Entre paréntesis se indica la referencia.

genes), *Pantoea agglomerans, Citrobacter freundii, Morganella morganii, Serratia marcescens y Citrobacter koseri*, con solo 1 a 13 aislados por especie, sumando un total de 30 aislados (3,3%, 30/903) (Fig. 2A). En su mayoría, estas últimas fueron identificadas solo por pruebas bioquímicas convencionales o no se especifica la metodología empleada en su identificación [10,11]. Además, un aislado de *Enterobacter sp.* productor de carbapenemasa no fue clasificado a nivel de especie.

A continuación, se presentan las proporciones de las carbapenemasas detectadas de forma aislada, sin coproducción, excepto cuando se indique lo contrario. Las carbapenemasas KPC, NDM y VIM se encontraron en *K. pneumoniae*, complejo *E. cloacae* y *E. coli*; siendo KPC la más frecuente, con proporciones de 88% (632/718), 91% (61/67) y 70,6% (36/51), respectivamente en las tres especies. Entre el total de EPC, por detección molecular se reportó 92,3% (830/899) aislados productores de KPC, 2,7% de NDM (24/899), 2,1% (19/899) VIM y 2,9% (26/899) productores de dos carbapenemasas (Fig. 2B), específicamente KPC+NDM o KPC+VIM. De los distintos tipos de carbapenemasas detectadas, se han encontrado las variantes KPC-2, NDM-1 y VIM-2 [16–18,20,22,24,26–29,32,33,35]. Adicionalmente, por métodos únicamente fenotípicos, se detectaron 19 aislados productores de serinocarbapenemasas reportadas como KPC pero sin la confirmación molecular; así como 23 aislados con MBL no especificada, uno de los cuales portaba además el gen bla_{KPC} [8,13,15,25].

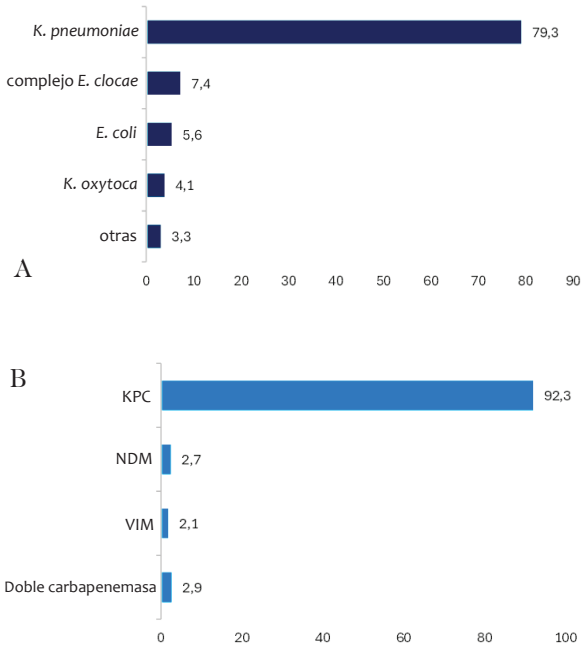

Fig. 2. Porcentaje de especies de Enterobacterales productoras de carbapenemasas (A) y de los tipos de carbapenemasas (B) reportadas en Venezuela. KPC: *K. pneumoniae* Carbapenemasa; NDM: Nueva Delhi Metalo-β-lactamasa; VIM: Verona Metalo-β-lactamasa codificada por integrón.

El estudio de Pillonetto y col. [39] que analiza aislamientos con perfil de susceptibilidad indicativo de producción de carbapenemasas, obtenidos entre 2015 y 2020 en América Latina y el Caribe, reporta 53,16% de KPC, 41,14% de NDM y 5,7% de VIM, en Enterobacterales de Venezuela, correspondientes a 158 genes de carbapenemasas detectados en 157 aislados [39]. Sin embargo, no desglosa por país la proporción atribuible a aislados productores de dos carbapenemasas ni el total de aislados positivos para cualquiera de las carbapenemasas probadas, por lo que estos datos no fueron incluidos en el análisis general.

Por otra parte, un estudio del programa de vigilancia global "Antimicrobial Testing Leadership and Surveillance" (ATLAS), analizó aislados de EPC entre 2017 y 2019 de varios países de América Latina. Este trabajo reportó la presencia en Venezuela de Enterobacterales con NDM+GES y NDM junto con una carbapenemasa tipo OXA-48 [34], sin especificar el número de aislados para cada caso. Adicionalmente, observaron una proporción de aislados productores de NDM de Venezuela en Enterobacterales no susceptibles a meropenem de 48,5% (16/33). Esta cifra es considerablemente mayor que lo reportado en un estudio previo que abarca el periodo 2015-2017, donde encontraron solo 2 aislados de *Enterobacteriaceae* con NDM-1 entre 18 productores de carbapenemasas (11%) [34,37,40]. Asimismo, dos estudios con un pequeño número de aislamientos recientes de Venezuela detectaron una proporción mayor de NDM o MBL respecto a KPC o serinocarbapenemasas, concretamente 14:2 en aislados de 2018 y 8:4 de 2018-2019, ambos en el estado Aragua [8,9].

La distribución por estados se puede apreciar en la Fig. 3. Las EPC han sido detectadas en muestras de pacientes de 10 entidades del país que incluyen la región central, occidental y oriental, específicamente: Caracas, Zulia, Aragua, Carabobo, Sucre, Anzoátegui, Miranda, La Guaira, Mérida y Bolívar. La presencia de Enterobacterales productores de dos carbapenemasas ha sido detectada en dos estados: en Sucre se halló *K. pneumoniae* productora de KPC+NDM (5 aislados), así como *E. cloacae* y *Enterobacter hormaechei* con KPC+VIM (un aislado de cada especie); y en Anzoátegui encontraron 19 aislados de *K. pneumoniae* productores de KPC+VIM [7,14,16,23,29].

Proporción de Enterobacterales no susceptibles a meropenem

La proporción (y el número) de aislados de *K. pneumoniae*, *E. cloacae* y *E. coli* no

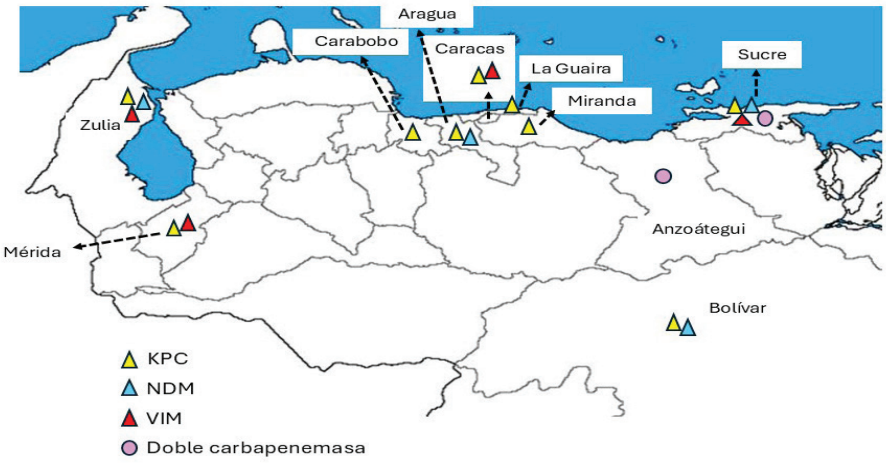

Fig. 3. Distribución geográfica de los distintos tipos de carbapenemasas detectadas en Enterobacterales en Venezuela. KPC: *K. pneumoniae* Carbapenemasa; NDM: Nueva Delhi Metalo-β-lactamasa; VIM: Verona Metalo-β-lactamasa codificada por integrón.

susceptibles a meropenem (aquellos resistentes y con susceptibilidad intermedia) en Venezuela entre 2005 y 2020 fue obtenida de la página web de PROVENRA, que recopila datos sobre resistencia a antibióticos provenientes de laboratorios clínicos ubicados en diferentes estados del país. Entre los años 2008 y 2012 se observa una tendencia creciente en la proporción de *K. pneumoniae* no susceptible, con valores en el rango de 2,2% (149/6619) a 21,1% (873/4133). Posteriormente se presentan fluctuaciones de hasta 13,7 puntos porcentuales; en 2019 hubo un repunte y para 2020 esta proporción alcanzó el 14,5% (110/759) (Fig. 4).

La proporción de *E. coli* no susceptible a meropenem fue considerablemente inferior a la observada para *K. pneumoniae* en todo el período analizado, siendo el mayor valor 6,8% (176/2605) en el año 2013 y llegando solo a 1,7% (44/2532) en 2020. No obstante, en general el número de aislados no susceptibles de *E. coli* por año fue comparable al registrado para *K. pneumoniae*, con un promedio de 149 y 232 aislados no susceptibles, respectivamente para las dos especies. Por su parte, la proporción de *E. cloacae* se asemeja a la de *K. pneumoniae* y alcanzó el 12,2% (31/254) en el año 2020 (Fig. 4).

Proporción de Enterobacterales productores de carbapenemasas

La proporción de EPC en relación al total del conjunto de Enterobacterales evaluados, o por especie, en siete estudios [8,9,12–14,37,38] se presenta en la Tabla 2. En la mayoría de estos trabajos el tipo de muestra no formaba parte de los criterios de selección. En consecuencia, se infiere que las fuentes de aislamiento fueron diversas, o bien se indica que es así, excepto en uno donde todos los aislados provenían de hemocultivos de pacientes con sepsis [8]. La proporción de aislados productores de carbapenemasas en el conjunto de especies de Enterobacterales (o *Enterobacteriaceae*) fue generalmente baja (menor a 3%), pero en el estudio de hemocultivos alcanzó 16%. Además, la proporción de aislados productores de carbapenemasas fue mucho mayor (de 6,9% a 44%) cuando se consideró únicamente *K. pneumoniae*.

Por otra parte, entre los aislados resistentes a carabepenémicos un estudio reportó 86/91 (94,5%) cepas de *Enterobacteriaceae* productoras de KPC [11].

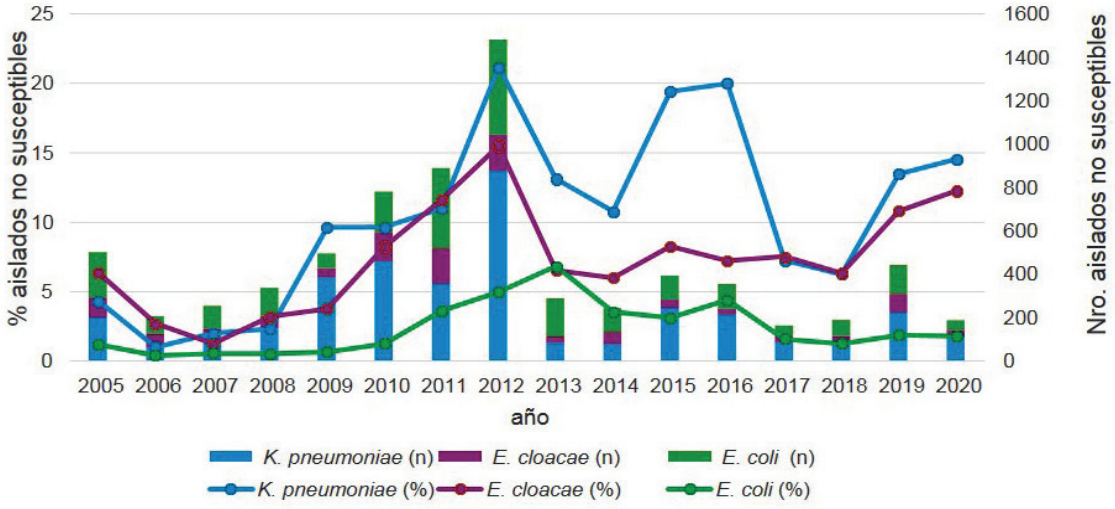

Fig. 4. Proporción (líneas) y número (barras) de aislados de *K. pneumoniae*, *E. cloacae* y *E. coli* no susceptibles (resistentes o con susceptibilidad intermedia) a meropenem en Venezuela. Gráfico realizado a partir de datos del Programa Venezolano de Vigilancia de la Resistencia a los Antimicrobianos (PROVENRA).

Tabla 2. Proporción de Enterobacterales productores de carbapenemasas en Venezuela.

Año / Periodo	Región (Institución)	Grupo/Especie	EPC/EBT (%)	Referencia
oct 2009-ene 2010	Caracas (8 hospitales)	Enterobacterales (general)	4/1235 (0,32%)	12
mar-ago 2018	Aragua-Maracay (un laboratorio clínico)	Enterobacterales (general)	16/605 (2,64%)	9
ene 2018-jun 2019	Aragua (varios centros médicos)	Enterobacterales (general)	12/73 (16%)	8
2008-2014	NE	*Enterobacteriaceae*	16/2411 (0,66%)	38
2012-2015	NE	*Enterobacteriaceae*	18/1201 (1,5%)	37
feb-mar 2015	Aragua (varios centros médicos)	*K. pneumoniae*	22/72 (30,5%)	13
ene-jun 2015	Sucre-Cumaná (un hospital)	*K. pneumoniae*	4/58 (6,9%)	14
mar-ago 2018	Aragua-Maracay (un laboratorio clínico)	*K. pneumoniae*	13/90 (14,4%)	9
ene 2018-jun 2019	Aragua (varios centros médicos)	*K. pneumoniae*	11/25 (44%)	8
mar-ago 2018	Aragua-Maracay (un laboratorio clínico)	Complejo *E. cloacae*	3/14 (21,4%)	9

EB_T: total de Enterobacterales evaluadas; NE: no especificado (estudios de vigilancia internacional).

Estas cepas fueron obtenidas de 14 centros de salud de Caracas y otras entidades del país en el período 2010-2011. En tanto que en un hospital de Maracaibo durante los años 2016-2017, 148/181 (81,8%) aislados de *K. pneumoniae* eran productores de KPC o VIM [21].

Tipificación molecular

El estudio de las relaciones genéticas entre aislados bacterianos resistentes a antibióticos es crucial para identificar patrones de diseminación y optimizar las estrategias de vigilancia y control de la resistencia antibiótica. De los estudios revisados, 13/33 presentan las relaciones genéticas entre los aislados, de los cuales 6 utilizaron tipificación multilocus de secuencia (MLST por sus siglas en inglés) [16–18,20,24,33]; cuatro de *K. pneumoniae*, uno de *E. coli* y uno de *E. cloacae*. En los dos últimos casos utilizaron MLST a partir de secuencias de genoma completo. Otros 5 trabajos usaron solo una de las siguientes técnicas de tipificación: ERIC-PCR (PCR basada en secuencias repetitivas intergénicas de enterobacterias) para *K. pneumoniae* [14] o *Enterobacter* spp. [22], REP-PCR (PCR basada en secuencias repetitivas extragénicas palindrómicas) para *K. pneumoniae* [13] o electroforesis en Gel de Campo Pulsado (PFGE por sus siglas en inglés) para *K. pneumoniae* [15,19].

El uso de técnicas basadas en la amplificación de secuencias repetidas permitió evidenciar la diseminación clonal de *K. pneumoniae* co-productora de KPC y NDM (mediante ERIC-PCR) en 3 unidades de un hospital de Cumaná durante 2015 [14]. Asimismo, mediante REP-PCR se identificó un genotipo predominante en aislados de *K. pneumoniae* productores de serinocarbapenemasa o MBL en diferentes centros de salud del estado Aragua [13].

El método MLST determina la combinación de alelos de un grupo de genes que tienen bases polimórficas, mediante la secuenciación de un fragmento de cada gen (locus), y asigna a cada perfil un tipo de secuencia

o ST ("Sequence Type") que consiste en el conjunto de alelos de todos los genes analizados. La identificación por MLST permite la comparación precisa de cepas entre laboratorios e internacionalmente. De los principales ST de *K. pneumoniae* en Venezuela, destaca ST833, con 28 aislados que provienen de Anzoátegui, Maracaibo y Caracas [16–18,20]. Le siguen ST11 con 14 aislados entre Caracas y Maracaibo [17,20]; ST273 y ST147 en 9 y 8 aislados de Maracaibo, respectivamente [18,20], y ST437 hallado en 7 aislados de Carabobo[18]. Entre los ST de *K. pneumoniae* identificados con menos frecuencia se encuentran ST15, ST17, ST1035 y ST1535, cada uno en un aislado, así como ST14 y ST45 en 3 aislados cada uno [17,18]. Adicionalmente, se identificaron cuatro nuevos ST: ST1858 en dos aislados de Carabobo, ST1859 y ST1860 cada uno en 2 aislados de Caracas y ST1857 en un aislado de la misma ciudad [17,18].

El ST833 se detectó entre los años 2009 y 2012 en un hospital de Maracaibo, indicando su persistencia en el tiempo. Mientras, dos aislados del ST147 se obtuvieron en fechas próximas en distintas salas del mismo hospital, evidenciando dispersión clonal[20]. Similarmente, mediante el análisis por PFGE de *K. pneumoniae* portadora de bla_{KPC} se detectaron clones diseminados durante 2009 y 2015 en un hospital de Cumaná, y clones persistentes en un hospital del Distrito Capital entre 2010 y 2012. La PFGE también permitió detectar una alta variabilidad genética en un grupo de cepas aisladas en varios centros de salud de diferentes estados entre 2010 y 2011 [14,19].

Por su parte, un estudio global de aislados de *Enterobacter* spp. productores de carbapenemasas, obtenidos entre 2008 y 2014, incluyó tres aislados del complejo *E. cloacae* (portadores de bla_{KPC}) de Venezuela que fueron identificados como ST516, ST523 y ST526 [24], mientras que la cepa de *E. coli* portadora de bla_{NDM-1} evaluada por MLST pertenece al ST19 [33].

Grupos filogenéticos de *E. coli*

Se han descrito ocho grupos filogenéticos en *E. coli* (A, B1, B2, C, D, E, F y G), varios de los cuales se han asociado con hábitats específicos y con infecciones de tipo intestinal o extraintestinal. Millán y col. [25] y Quijada-Martínez y col. [28] evaluaron la distribución de *E. coli* en grupos filogenéticos mediante alguno de los dos protocolos de Clermont basado en PCR múltiples. Uno de los estudios empleó el esquema clásico de 3 genes que solo puede identificar los grupos A, B1, B2 y D, mientras el otro estudio utilizó el esquema ampliado de PCR cuádruplex más dos simples que permite diferenciar además los grupos C, E and F [25,28]. En las cepas productoras de carbapenemasas se observó seis del filogrupo A, cinco del B2 y una del grupo B1 [25,28].

Elementos genéticos móviles asociados

Los plásmidos, principalmente los conjugativos, constituyen una vía fundamental para la diseminación de determinantes de resistencia a antibióticos. En tres estudios sobre Enterobacterales productores de carbapenemasas de Venezuela, utilizaron ensayos de conjugación (y en uno también de transformación) para evaluar la capacidad de transferencia y posible localización plasmídica de bla_{KPC}. Se encontró que 37/54 aislados de *K. pneumoniae* y un aislado de *K. oxytoca* portaban el gen bla_{KPC} en elementos conjugativos [17,18,32], mientras 12 de los aislados de *K. pneumoniae* lo llevaban en plásmidos presuntamente no conjugativos [17].

En 72 cepas de *K. pneumoniae* aisladas en Venezuela, de 73 cepas evaluadas mediante PCR, se ha confirmado la asociación del gen bla_{KPC-2} con el transposón Tn4401, específicamente con la isoforma "b" [16–18], una de las 8 isoformas de Tn4401 que se han descrito [41]. El transposón Tn4401b también porta bla_{KPC} en cepas del complejo *E. cloacae* aisladas en Venezuela, como fue evidenciado mediante secuenciación de genoma completo [24].

Resistencia a antibióticos no β-lactámicos

El tratamiento de infecciones causadas por Enterobacterales productores de carbapenemasas puede incluir fluoroquinolonas, aminoglucósidos, tigeciclina o colistina [42], por lo tanto, es importante conocer los niveles de resistencia a estos antibióticos entre las EPC.

La Tabla 3 presenta los resultados de 8 estudios sobre la proporción de resistencia a antibióticos no β-lactámicos en aislados de *K. pneumoniae* productores de carbapenemasas obtenidos entre 2005 y 2016. Se observa una alta proporción de resistencia frente a quinolonas, gentamicina y trimetoprim-sulfametoxazol, con valores mínimos de 50% (11/22) para gentamicina y de 63,6% (14/22) para levofloxacina. Los antibióticos con menor proporción de aislados resistentes fueron colistina (entre 0 y 3%), y tigeciclina (de 0 a 33,2%). Adicionalmente, el programa INFORM reportó, entre 2012 y 2015, datos correspondientes a 12-16 aislados de Enterobacteriacea portadores de bla_{KPC} provenientes de Venezuela, con una proporción de susceptibilidad de 37,5% para levofloxacina, 56,3% para amikacina, y 100% para colistina y tigeciclina [37].

Tabla 3. Resistencia a antibióticos no β-lactámicos en aislados de *K. pneumoniae* productores de carbapenemasas en Venezuela.

Antibiótico	Proporción de aislados resistentes (%)	Referencias
Gentamicina	224/319 (70,1) 12/22 (54,5) 11/22 (50) 8/14 (57,1) 3/3 (100) 1/1 (100)	10,15,17,20,28,30
Amikacina	212/319(66,4) 5/22 (22,7) 8/22(36,4) 12/19 (63,1) 1/1 (100)	10,15–17,30
Levofloxacina	260/319 (81,4) 14/22 (63,6) 13/14 (92,9)	10,17,20
Ciprofloxacina	267/319 (83,5) 17/22 (77,3) 18/22 (81,8) 18/19 (94,7) 4/4 (100) 3/3 (100) 1/1 (100)	10,14–17,28,30
Ácido Nalidíxico	309/319 (96,9) 19/22 (86,4) 4/4 (100) 3/3 (100)	10,14,15,28
Trimetoprim-Sulfametoxazol	277/319 (86,8) 17/22 (77,3) 13/14 (92,9) 3/4 (75)	10,14,17,20
Cloranfenicol	245/319 (76,7) 8/19 (42,1)	10,16
Tetraciclina	259/319(81) 5/22(22,7) 16/19(84,2)	10,16,17
Tigeciclina	106/319 (33,2) 0/22 (0) 3/19(15,8) 0/3(0)	10,16,17,28
Colistina	10/319 (3) 0/3 (0)	10,28

DISCUSIÓN

En Venezuela *K. pneumoniae* constituye la EPC reportada con más frecuencia, de forma similar a lo que ocurre globalmente[43]. Asimismo, la carbapenemasa más reportada ha sido KPC, no solo en *K. pneumoniae* sino también en el complejo *E. cloacae* y *E. coli*, coincidiendo con la tendencia general en América Latina [24,44]. En contraste, a nivel global, los aislados de *Enterobacter* spp. productores de carbapenemasas frecuentemente portan VIM [24], mientras que en los de *E. coli* predomina OXA o NDM [26,45].

Nueve de los estudios aquí revisados, varios de ellos relativamente recientes, usaron solo pruebas bioquímicas convencionales en la determinación de especie. En este sentido, cabe mencionar que es recomendable

confirmar la identificación fenotípica, por ejemplo, mediante métodos moleculares, para el reporte de información epidemiológica precisa. He y col. [46] indicaron que la identificación de especies en *Enterobacteriaceae* basada solo en morfología, utilización de sustratos y actividades enzimáticas no es concluyente, ya que puede resultar en perfiles fenotípicos similares a pesar de las diferencias genéticas.

En Venezuela, se ha detectado la presencia de cepas productoras de dos carbapenemasas, un hallazgo que también ha sido reportado en otros países de América Latina[6,39]. Esta co-producción de enzimas representa un mayor riesgo epidemiológico, ya que potencia la capacidad de diseminación horizontal de las carbapenemasas. Además, puede restringir aún más las opciones terapéuticas disponibles, complicando el manejo clínico de las infecciones causadas por estos patógenos.

La proporción de las distintas carbapenemasas varía por regiones a nivel mundial, siendo KPC la más común en Europa y América del norte [47]. En América Latina, estudios del periodo 2015-2017 de los programas de vigilancia global ATLAS e INFORM sobre 6 países de la región, incluyendo Venezuela, reportaron que KPC alcanzaba el 89,1% (269/302) de las carbapenemasas detectadas. Mientras, de 2017 a 2019, las bacterias Enterobacterales portadoras de bla_{KPC} representaron el 66,5% entre todas las no susceptibles a meropenem (339/510) [34,47]. Similarmente, Estabrook y col. [43] reportaron 51,6% de KPC y 25,2% de NDM para América Latina entre 2018 y 2019. Por su parte, el estudio de Wise y col. [47] también describió una tendencia creciente de NDM en el período 2018-2020 en la región, y observó que en 2022 la proporción de NDM superó la de KPC.

El aumento de la proporción de NDM puede estar relacionado al incremento en el uso de ceftazidima-avibactam, lo cual ha sido descrito en estudios de Inglaterra y EUA [48,49]. Avibactam es un inhibidor de β-lactamasas que tiene actividad sobre las carbapenemasas KPC y OXA, pero no sobre las MBL. Su uso en combinación con ceftazidima fue aprobado por la Administración de Alimentos y Medicamentos de EUA (FDA por sus siglas en inglés) en 2015 y posteriormente se observó un incremento en la resistencia a ceftazidima-avibactam en América Latina, para el periodo 2018-2020 respecto a 2015-2017, en concordancia con el aumento de NDM en la región [40].

Las variantes de carbapenemasas reportadas en Venezuela, KPC-2 y NDM-1, fueron las más comunes a nivel mundial entre 2012 y 2019. En este mismo período VIM-1 fue la variante más frecuente a nivel global [43,44]. Sin embargo, VIM-2 ha sido la única variante de esta carbapenemasa reportada en Venezuela y también se ha encontrado en otros países de América Latina [41].

La no susceptibilidad a carbapenémicos en Enterobacterales generalmente está asociada a la producción de carbapenemasas. De forma similar a lo observado en Venezuela, un estudio del período 2012 a 2017 [44] reportó la detección de algún gen de carbapenemasa en 84,5% (2253/2666) de aislados no susceptibles a meropenem obtenidos de pacientes en 39 países a nivel mundial.

Se ha descrito un incremento en la proporción de Enterobacterales no susceptibles a carbapenémicos a lo largo del tiempo en todas las regiones, incluyendo América Latina y el Caribe [7,43,50]. Específicamente en Argentina, Paraguay, Ecuador y Cuba, *K. pneumoniae* no susceptible a meropenem mostró una tendencia creciente entre 2011 y 2019, alcanzando 21%, 29%, 39% y 69%, respectivamente [7]. En contraste, la tendencia en Venezuela es similar a la de Colombia, donde el aumento es menos pronunciado que en los otros países mencionados y para 2019 llegaba solo a 15% [7].

Por otra parte, se observó que en Venezuela *E. coli* ha presentado una proporción de aislados no susceptibles a meropenem considerablemente menor que *K. pneumoniae*. Este hallazgo puede estar relacionado a que,

mientras las Enterobacterales resistentes a carbapenémicos predominan en pacientes hospitalizados, *E. coli* frecuentemente causa infecciones que solo requieren atención ambulatoria, principalmente infecciones del tracto urinario, de las cuales es el agente etiológico más común [51]. Esto coincide con el hecho de que la mayoría de los aislados de *E. coli* documentados por PROVENRA procedían de muestras de orina.

La relativamente elevada proporción de *K. pneumoniae* productora de carbapenemasas, respecto al total de aislados evaluados por estudio, es consistente con su predominio entre las EPC. Destaca el alto porcentaje reportado para esta especie en dos trabajos sobre aislados del estado Aragua. En uno de ellos [13] pudo haber influido la región y las condiciones particulares de los centros de atención médica, ya que en otros aspectos es comparable a un estudio del estado Sucre [14] que muestra una proporción aproximadamente 4 veces menor. En el otro caso se presenta una alta proporción de aislados con carbapenemasas, tanto de *K. pneumoniae* como de EPC en general, pero en hemocultivos de pacientes con sepsis [8]. En concordancia, en Brasil y en un conjunto de 7 países de América Latina [36,52] se han observado, en aislados de pacientes con infecciones del torrente sanguíneo, proporciones de EPC similares a las referidas para Venezuela.

Los transposones pueden movilizar genes de resistencia a antibióticos dentro del genoma. En Venezuela, como en muchos otros países, se ha encontrado bla_{KPC} en el transposón Tn4401 en *K. pneumoniae* y en el complejo *E. cloacae*, así como en plásmidos conjugativos de *K. penumoniae* y *K. oxytoca*. Estos hallazgos sugieren la participación de dichos elementos en la dispersión de esta carbapenemasa [35,41].

Otros elementos genéticos que pueden estar involucrados en la diseminación de determinantes de resistencia a carbapenémicos son los integrones, que contienen un gen codificante de integrasa, un sitio de recombinación y un promotor, y permiten la acumulación, expresión y reorganización de casetes genéticos de resistencia a varios antibióticos. A nivel global se conoce que en Enterobacterales, bla_{NDM} se asocia comúnmente a transposones flanqueados por IS26 o IS3000, y bla_{GES} a integrones clase 3 [53,54]. Asimismo se ha reportado que los genes codificantes de NDM, VIM y de carbapenemasas tipo OXA-48 pueden estar localizados en plásmidos conjugativos [27,53,55]. Sin embargo, la asociación de estos genes a elementos móviles no se ha evaluado en aislados de Venezuela.

El uso de métodos de tipificación molecular ha permitido observar la dispersión clonal de cepas de *K. pneumoniae* portadora de bla_{KPC} en algunos hospitales, así como una alta variabilidad genética en otros casos. Adicionalmente, tres de los ST más comunes identificados en *K. pneumoniae*, específicamente ST833, ST11 y ST437, se agrupan dentro del complejo clonal 258, el cual presenta una distribución global y predomina entre las cepas productoras de KPC, por lo que se considera un linaje de alto riesgo. De este complejo, ST11 y ST258 se han descrito como los principales ST en América Latina [16,56]. Por el contrario, de los principales clones globales descritos para miembros del complejo *E. cloacae* productores de carbapenemasas (ST114, ST93, ST90, and ST78), ninguno fue hallado entre los pocos aislados de Venezuela en los que se analizó esta característica [24].

Como en Venezuela, *E. coli* ST19 ha sido también asociada a NDM en China, pero a la variante NDM-5 [57]. Por otra parte, se ha descrito que el fondo genético de *E. coli* influye en la adquisición de genes de resistencia a antibióticos, siendo el filogrupo A uno de los más propensos a desarrollar resistencia[58]. Se identificó este filogrupo en la mayoría de cepas productoras de carbapenemasas de Venezuela. Asimismo, un trabajo que analizó más de 7000 secuencias genómicas de *E. coli* resistente a carbapenémicos portadora de genes codificantes de carbapenemasas, de la base de datos de NCBI, encontró que el

filogrupo A predominó respecto a los otros 7 grupos (B1, B2, C, D, E, F y G) con un 36,6% del total [59]. Dicho filogrupo se ha asociado a cepas comensales de origen humano, pero también puede incluir cepas patogénicas.

Generalmente, como en aislados de Venezuela, Enterobacterales resistentes a carbapenémicos también son resistentes a antibióticos no β-lactámicos, incluyendo aminoglucósidos y fluoroquinolonas [42,60], restringiendo aún más las opciones terapéuticas. Por el contrario, colistina comúnmente presenta actividad contra estas bacterias y, por lo tanto, es considerado de último recurso. Sin embargo, en un hospital de Argentina ya se ha reportado resistencia a este antibiótico en aproximadamente 40% de los aislados de *K. pneumoniae*, encontrándose cepas extensivamente o incluso pan-resistentes [60].

En el estudio de vigilancia del programa INFORM [37] en América Latina entre 2012 y 2015, la proporción de aislados de *Enterobacteraceae* productores de KPC no susceptibles a tigeciclina fue 5,2%. Mientras que en dos estudios de Venezuela que evaluaron aislamientos de *K. pneumoniae* de los períodos 2012-2013 y 2009-2013, la proporción de resistentes a este antibiótico fue 3 y 6 veces mayor [10,17]. Asimismo en un hospital de Argentina se ha informado cerca de 50% de resistencia a tigeciclina en aislados de *K. pneumoniae* productores de carbapenemasas [60]. Considerando que este antibiótico puede utilizarse para el tratamiento de infecciones causadas por EPC [42], destaca la necesidad de ampliar y actualizar la información disponible también sobre los perfiles de resistencia de estas bacterias en Venezuela.

En Venezuela la principal especie de EPC ha sido *K. pneumoniae* portadora del gen bla_{KPC}. En esta especie se ha documentado la asociación de bla_{KPC} a transposones y plásmidos conjugativos, así como la presencia de varios ST pertenecientes al complejo clonal CC258, considerado un linaje de alto riesgo. La tendencia creciente de la proporción de Enterobacterales no susceptibles a carbapenémicos, subraya la importancia de realizar más estudios sobre la presencia y caracterización de Enterobacterales productores de carbapenemasas en el país. Es fundamental realizar confirmación molecular no solo en la detección de los genes codificantes de estas enzimas, sino también para la identificación precisa de las especies. También es esencial investigar aspectos como el entorno de los genes, su potencial transferibilidad y los genotipos de las cepas mediante MLST, con el fin de contextualizar los hallazgos en el escenario internacional. Una vigilancia sostenida, que contemple estudios moleculares de amplio alcance, permitirá tener una visión más precisa de la epidemiología de las EPC en Venezuela e inferir posibles mecanismos de diseminación, contribuyendo de manera efectiva a su control.

ORCID ID de los autores

- Elba Guerrero (EG): 0000-0002-3936-9556
- Howard Takiff (HT): 0000-0002-0480-0860
- Lizeth Caraballo (LC): 0000-0003-2043-8731
- Luis Querales (LQ): 0009-0001-5542-2011

Contribución de los autores

EG: Conceptualización, investigación, análisis de datos, preparación del manuscrito y edición. HT: Conceptualización, revisión crítica del manuscrito y edición. LC: Análisis de datos, revisión crítica del manuscrito y edición. LQ: Investigación, revisión crítica del manuscrito y edición. Todos los autores leyeron y aprobaron la versión final del manuscrito.

Conflicto de interés

Los autores declaran que no existen conflictos de interés.

REFERENCIAS

1. **Antimicrobial Resistance Collaborators.** Global burden of bacterial antimicrobial resistance in 2019: a systematic analysis. Lancet. 2022; 399(10325): 629-655. *https://doi.org/10.1016/S0140-6736(21)02724-0*.
2. **Falagas ME**, **Tansarli GS**, **Karageorgopoulos DE**, **Vardakas KZ**. Deaths Attributable to Carbapenem-Resistant Enterobacteriaceae Infections. Emerg Infect Dis. 2014; 20(7): 1170-1175. *https://doi.org/10.3201/eid2007.121004*.
3. **Logan LK**, **Weinstein RA**. The Epidemiology of Carbapenem-Resistant Enterobacteriaceae: The Impact and Evolution of a Global Menace. J Infect Dis. 2017; 215(suppl_1): S28-S36. *https://doi.org/10.1093/infdis/jiw282*.
4. **Alvisi G**, **Curtoni A**, **Fonnesu R**, **Piazza A**, **Signoretto C**, **Piccinini G**, et al. Epidemiology and Genetic Traits of Carbapenemase-Producing Enterobacterales: A Global Threat to Human Health. Antibiotics. 2025; 14(2): 141. *https://doi.org/10.3390/antibiotics14020141*.
5. **Caliskan-Aydogan O**, **Alocilja EC**. A Review of Carbapenem Resistance in Enterobacterales and Its Detection Techniques. Microorganisms. 2023; 11(6): 1491. *https://doi.org/10.3390/microorganisms11061491*.
6. **Organización Panaricana de la Salud**. Alerta Epidemiológica: Emergencia e incremento de nuevas combinaciones de carbapenemasas en Enterobacterales en Latinoamérica y el Caribe. OPS 2021 [citado 20 de julio de 2025]. Disponible en: *https://iris.paho.org/handle/10665.2/55319*.
7. **Thomas G**, **Corso A**, **Pasterán F**, **Shal J**, **Sosa A**, **Pillonetto M, et al**. Increased detection of carbapenemase-producing Enterobacterales bacteria in Latin America and the Caribbean during the COVID-19 pandemic. Emerg Infect Dis. 2022; 28(11): 1-8. *https://doi.org/10.3201/eid2811.220415*.
8. **Rojas G**, **Vásquez Y**, **Rodríguez M**, **García P**, **Faraco TR**. Mecanismos de resistencia a antibióticos betalactámicos en Enterobacterales aislados en hemocultivos, Maracay, estado Aragua, Venezuela. Kasmera. 2021; 49(2): e49235057-e49235057. *https://doi.org/10.5281/zenodo.5377921*.
9. **Requena D, Vásquez Y, Gil A, Cedeño J, Chabin, M, Delgado E, et al.** Detección fenotípica y genotípica de la producción de carbapenemasas tipo NDM-1 y KPC en enterobacterias aisladas en un laboratorio clínico en Maracay, Venezuela. Rev Chil Infectol. 2021;38(2):197-203. *https://doi.org/10.4067/S0716-10182021000200197*
10. **Gómez-Gamboa L**, **Perozo-Mena A**, **Lugo J**, **Bermúdez-González J**, **Zabala I**, **Morales E**. Carbapenemasas KPC en Enterobacteriaceae aisladas en un Hospital de Maracaibo, Venezuela. Kasmera. 2014; 42(2): 89-104. Disponible en: http://ve.scielo.org/scielo.php?script=sci_arttext&pid=S0075-52222014000200002&lng=es.
11. **Luque J**, **Bohórquez P**, **Marcano D**, **Perdomo Y**, **Rodríguez C**, **Macero C**, **et al.** Diseminación de enterobacterias productoras de carbapenemasas tipo KCP en Venezuela. Bol Venez Infectol. 2012; 23(1): 13-19. Disponible en: https://www.researchgate.net/publication/312576659_Diseminacion_de_enterobacterias_productoras_de_carbapenemasas_tipo_KPC_en_Venezuela
12. **Marcano D**, **Jesús AD**, **Hernández L**, **Torres L**. Frecuencia de enzimas asociadas a sensibilidad disminuida a betalactámicos en aislados de enterobacterias, Caracas, Venezuela. Rev Panam Salud Pública. 2011; 30(6): 529-534. Disponible en: https://www.scielosp.org/pdf/rpsp/v30n6/a05v30n6.pdf
13. **Sierra L**, **Vásquez Y**, **Pérez-Ybarra L**, **Méndez-López M**. Epidemiología molecular de *Klebsiella pneumoniae* resistentes a los antibióticos betalactámicos aislados de centros asistenciales del estado Aragua-Venezuela. Kasmera. 2020; 48(2): e48232378. *https://doi.org/10.5281/ZENODO.4081865*.
14. **Martínez D**, **Caña L**, **Rodulfo H**, **García J**, **González D**, **Rodriguez L**, **et al.** Characteristics of dual carbapenemase-producing *Klebsiella pneumoniae* strains from an outbreak in Venezuela: a retrospective study.

Rev Panam Salud Pública. 2020; 44: e50. *https://doi.org/10.26633/RPSP.2020.50*.

15. **Martínez D**, **Araque Y**, **Rodulfo H**, **Caña L**, **García J**, **González D**, **et al.** Relación clonal y detección del gen *bla*$_{KPC}$ en cepas de *Klebsiella pneumoniae* resistentes a carbapenémicos, en un hospital de Venezuela. Rev Chil Infectol. 2016; 33(5): 519-523. *https://doi.org/10.4067/S0716-10182016000500006*.
16. **Falco A**, **Ramos Y**, **Franco E**, **Guzmán A**, **Takiff H**. A cluster of KPC-2 and VIM-2-producing *Klebsiella pneumoniae* ST833 isolates from the pediatric service of a Venezuelan Hospital. BMC Infect Dis. 2016; 16(1): 595. *https://doi.org/10.1186/s12879-016-1927-y*.
17. **Falco Restrepo AD**, **Velásquez Nieves MA**, **Takiff H**. Molecular characterization of KPC-producing *Klebsiella pneumoniae* isolated from patients in a Public Hospital in Caracas, Venezuela. Enferm Infecc Microbiol Clín. 2017; 35(7): 411-416. *https://doi.org/10.1016/j.eimc.2017.01.010*.
18. **Falco A**, **Barrios Y**, **Torres L**, **Sandrea L**, **Takiff H**. Epidemiología molecular de aislados clínicos de *Klebsiella pneumoniae* productores de carbapenemasas tipo KPC provenientes de dos hospitales públicos en los estados Carabobo y Zulia, Venezuela. Invest Clin. 2017; 58(1): 3-21. Disponible en: http://ve.scielo.org/scielo.php?script=sci_arttext&pid=S0535-51332017000100002&lng=es.
19. **Cuaical-Ramos NM**, **Montiel M**, **Zamora DM**. Genetic variability of carbapenemase KPC-producing *Klebsiella pneumoniae* isolated at different states in Venezuela. Enferm Infecc Microbiol Clin (Engl Ed). 2019; 37(2): 76-81. *https://doi.org/10.1016/j.eimc.2017.12.004*.
20. **Gómez-Gamboa L**, **Barrios-Camacho H**, **Durán-Bedolla J**, **Sánchez-Perez A**, **Reyna-Flores F**, **Perozo-Mena A**, **et al.** Molecular and genetic characterization of carbapenemase-producing bacteria in Venezuela. J Chemother. 2019; 31(6): 349-353. *https://doi.org/10.1080/1120009X.2019.1607452*.
21. **Gómez-Gamboa L**, **Perozo-Mena A**, **Bermudez-Gonzalez J**, **Villavicencio C**, **Villasmil J**, **Ginestre MM**, **et al.** Detection of carbapenemase-producing bacteria in a public healthcare center from Venezuela. J Infect Dev Ctries. 2020; 15(1): 163-167. *https://doi.org/10.3855/jidc.13567*.
22. **Martínez D**, **Rodulfo HE**, **Rodríguez L**, **Caña L**, **Medina B**, **Guzmán M**, **et al.** First report of metallo-β-lactamases producing Enterobacter spp. strains from Venezuela. Rev Inst Med Trop Sao Paulo. 2014; 56(1): 67-69. *https://doi.org/10.1590/S0036-46652014000100010*.
23. **Rodulfo H**, **Martínez D**, **Donato MD**. Molecular identification of multidrug resistant *Enterobacter hormaechei* in Venezuela. Invest Clin. 2016; 57(4): 402-408. Disponible en: https://ve.scielo.org/pdf/ic/v57n4/art08.pdf
24. **Peirano G**, **Matsumura Y**, **Adams MD**, **Bradford P**, **Motyl M**, **Chen L**, **et al** Genomic Epidemiology of Global Carbapenemase-Producing *Enterobacter* spp., 2008-2014. Emerg Infect Dis. 2018; 24(6): 1010-1019. *https://doi.org/10.3201/eid2406.171648*.
25. **Millán Y**, **Araque M**, **Ramírez A**. Distribución de grupos filogenéticos, factores de virulencia y susceptibilidad antimicrobiana en cepas de *Escherichia coli* uropatógena. Rev Chil Infectol. 2020; 37(2): 117-123. *https://doi.org/10.4067/s0716-10182020000200117*.
26. **Peirano G**, **Chen L**, **Nobrega D**, **Finn T**, **Kreiswirth B**, **DeVinney R**, **et al.** Genomic Epidemiology of Global Carbapenemase-Producing *Escherichia coli*, 2015–2017. Emerg Infect Dis. 2022; 28(5): 924-931. *https://doi.org/10.3201/eid2805. 212535*.
27. **Kazmierczak K**, **Rabine S**, **Hackel M**, **McLaughlin R**, **Biedenbach D**, **Bouchillon S**, **et al.** Multiyear, multinational survey of the incidence and global distribution of metallo-β-lactamase-producing Enterobacteriaceae and Pseudomonas aeruginosa. Antimicrob Agents Chemother. 2015; 60(2): 1067-1078. *https://doi.org/10.1128/aac.02379-15*.

28. **Quijada-Martínez P**, **Flores-Carrero A, Labrador I**, **Millán Y**, **Araque M**. Microbiological Profile and Molecular Characterization of Multidrug-Resistant Gram-Negative Bacilli Producing Catheter-Associated Urinary Tract Infections in the Internal Medicine Services of a Venezuelan University Hospital. Austin J Infect Dis. 2017; 4(1): 1030. Disponible en: https://austinpublishinggroup.com/infectious-diseases/fulltext/ajid-v4-id1030.php
29. **Martínez D, Marcano D, Rodulfo H, Salgado N, Cuaical N, Rodriguez L et al.** KPC and VIM producing *Enterobacter cloacae* strain from a hospital in northeastern Venezuela. Invest Clin. 2015; 56(2): 182-187. Disponible en: http://ve.scielo.org/scielo.php?script=sci_arttext&pid=S0535-51332015000200007&lng=es.
30. **Marcano D, Pasterán F, Rapoport M, Faccone D, Ugarte C, Salgado N, et al.** First isolation of a VIM-producing *Klebsiella pneumoniae* from a seven-year-old child in Venezuela. J Infect Dev Ctries. 2008; 2(3): 241-244. *https://doi.org/doi:%252010.3855/jidc.270*.
31. **De Sousa L**, **Chacare M**, **Cuaical N**, **Ashby J**. Primer aislamiento de *Escherichia coli* productora de carbapenemasa tipo New Delhi (NDM) en un hospital de Ciudad Guayana, Venezuela: A propósito de dos casos. Rev Soc Venez Microbiol. 2016; 36(2): 40-45. Disponible en: http://ve.scielo.org/scielo.php?script=sci_arttext&pid=S1315-25562016000200003&lng=es.
32. **Labrador I**, **Araque M**. First Description of KPC-2-Producing *Klebsiella oxytoca* Isolated from a Pediatric Patient with Nosocomial Pneumonia in Venezuela. Case Rep Infect Dis. 2014; 2014: 434987. *https://doi.org/10.1155/2014/434987*.
33. **Delgado-Blas JF**, **Ovejero CM**, **Abadia-Patiño L**, **González-Zorn B**. Coexistence of *mcr-1* and bla_{NDM-1} in *Escherichia coli* from Venezuela. Antimicrob Agents Chemother. 2016; 60(10): 6356-6358. *https://doi.org/10.1128/aac.01319-16*.
34. **Karlowsky JA, Kazmierczak KM, Valente MLN, Luengas EL, Baudrit M, Quintana A, et al.** *In vitro* activity of ceftazidime-avibactam against Enterobacterales and *Pseudomonas aeruginosa* isolates collected in Latin America as part of the ATLAS global surveillance program, 2017–2019. Braz J Infect Dis. 2021; 25(6): 101647. *https://doi.org/10.1016/j.bjid.2021.101647*.
35. **Kazmierczak KM**, **Biedenbach DJ**, **Hackel M**, **Rabine S**, **de Jonge B**, **Bouchillon S**, **et al.** Global Dissemination of bla_{KPC} into Bacterial Species beyond *Klebsiella pneumoniae* and In Vitro Susceptibility to Ceftazidime-Avibactam and Aztreonam-Avibactam. Antimicrob Agents Chemother. 2016; 60(8): 4490-4500. *https://doi.org/10.1128/aac.00107-16*.
36. **Villegas MV, Pallares CJ, Escandón-Vargas K, Hernández-Gómez C, Correa A, Álvarez C, et al.** Characterization and Clinical Impact of Bloodstream Infection Caused by Carbapenemase-Producing Enterobacteriaceae in Seven Latin American Countries. PLOS ONE. 2016; 11(4): e0154092. *https://doi.org/10.1371/journal.pone.0154092*.
37. **Karlowsky JA**, **Kazmierczak KM**, **Bouchillon SK**, **de Jonge BLM**, **Stone GG**, **Sahm DF**. In Vitro Activity of Ceftazidime-Avibactam against Clinical Isolates of Enterobacteriaceae and Pseudomonas aeruginosa Collected in Latin American Countries: Results from the INFORM Global Surveillance Program, 2012 to 2015. Antimicrob Agents Chemother. 2018; 62(7):e02569-17. *https://doi.org/10.1128/AAC.02569-17*.
38. **Karlowsky JA**, **Lob SH**, **Kazmierczak KM**, **Badal R**, **Young K**, **Motyl M**, **et al.** In Vitro Activity of Imipenem against Carbapenemase-Positive Enterobacteriaceae Isolates Collected by the SMART Global Surveillance Program from 2008 to 2014. J Clin Microbiol. 2017; 55(6): 1638-1649. *https://doi.org/10.1128/jcm.02316-16*.
39. **Pillonetto M, Wink PL, Melano RG, Jiménez-Pearson MA, Melgarejo Touchet NL, Saavedra Rojas SY, et al.** Carbapenemases producing gram-negative bacteria surveillance in Latin America and the caribbean: a retrospective observational study from 2015 to 2020. Lancet Reg

Health Am. 2025; 49: 101185. *https://doi.org/10.1016/j.lana.2025.101185*.

40. **Wise M**, **Karlowsky J**, **Lemos-Luengas E**, **Valdez R**, **Sahm D**. Epidemiology and in vitro activity of ceftazidime-avibactam and comparator agents against multidrug-resistant isolates of Enterobacterales and Pseudomonas aeruginosa collected in Latin America as part of the ATLAS surveillance program in 2015–2020. Braz J Infect Dis. 2023; 27(3): 102759. *https://doi.org/10.1016/j.bjid.2023.102759*.
41. **Reyes JA**, **Melano R**, **Cárdenas PA**, **Trueba G**. Mobile genetic elements associated with carbapenemase genes in South American Enterobacterales. Braz J Infect Dis. 2020; 24(3): 231-238. *https://doi.org/10.1016/j.bjid.2020.03.002*.
42. **Hughes S**, **Gilchrist M**, **Heard K**, **Hamilton R**, **Sneddon J**. Treating infections caused by carbapenemase-producing Enterobacterales (CPE): a pragmatic approach to antimicrobial stewardship on behalf of the UKCPA Pharmacy Infection Network (PIN). JAC-Antimicrob Resist. 2020; 2(3): dlaa075. *https://doi.org/10.1093/jacamr/dlaa075*.
43. **Estabrook M**, **Muyldermans A**, **Sahm D**, **Pierard D**, **Stone G**, **Utt E**. Epidemiology of Resistance Determinants Identified in Meropenem-Nonsusceptible Enterobacterales Collected as Part of a Global Surveillance Study, 2018 to 2019. Antimicrob Agents Chemother. 2023; 67(5): e0140622. *https://doi.org/10.1128/aac.01406-22*.
44. **Kazmierczak KM**, **Karlowsky JA**, **de Jonge B**, **Stone G**, **Sahm D**. Epidemiology of Carbapenem Resistance Determinants Identified in Meropenem-Nonsusceptible Enterobacterales Collected as Part of a Global Surveillance Program, 2012 to 2017. Antimicrob Agents Chemother. 2021; 65(7): e0200020. *https://doi.org/10.1128/aac. 02000-20*.
45. **Li Y**, **Sun X**, **Dong N**, **Wang Z**, **Li R**. Global distribution and genomic characteristics of carbapenemase-producing *Escherichia coli* among humans, 2005-2023. Drug Resist Updat. 2024; 72: 101031. *https://doi.org/10.1016/j.drup.2023.101031*.
46. **He Y, Guo X, Xiang S, Li J, Li X, Xiang H, et al.** Comparative analyses of phenotypic methods and 16S rRNA, khe, rpoB genes sequencing for identification of clinical isolates of *Klebsiella pneumoniae*. Antonie Van Leeuwenhoek. 2016; 109(7): 1029-1040. *https://doi.org/10.1007/s10482-016-0702-9*.
47. **Wise MG, Karlowsky JA, Mohamed N, Hermsen ED, Kamat S, Townsend A, et al.** Global trends in carbapenem- and difficult-to-treat-resistance among World Health Organization priority bacterial pathogens: ATLAS surveillance program 2018-2022. J Glob Antimicrob Resist. 2024; 37: 168-175. *https://doi.org/10.1016/j.jgar.2024.03.020*.
48. **Guy RL, Hopkins KL, Budd EL, Wilson K, Fountain H, Meunier D, et al.** The importance of monitoring a new antibiotic: ceftazidime/avibactam usage and resistance experience from England, 2016 to 2020. Euro Surveill. 2025; 30(14): 2400399. *https://doi.org/10.2807/1560-7917.ES.2025.30. 14.2400399*.
49. **Strich JR, Ricotta E, Warner S, Lai YL, Demirkale CY, Hohmann SF, et al.** Pharmacoepidemiology of Ceftazidime-Avibactam Use: A Retrospective Cohort Analysis of 210 US Hospitals. Clin Infect Dis. 2021; 72(4): 611-621. *https://doi.org/10.1093/cid/ciaa061*.
50. **Castanheira M**, **Deshpande LM**, **Mendes RE**, **Canton R**, **Sader HS**, **Jones RN**. Variations in the Occurrence of Resistance Phenotypes and Carbapenemase Genes Among Enterobacteriaceae Isolates in 20 Years of the SENTRY Antimicrobial Surveillance Program. Open Forum Infect Dis. 2019; 6(Suppl 1): S23-S33. *https://doi.org/10.1093/ofid/ofy347*.
51. **Zhou Y**, **Zhou Z**, **Zheng L**, **Gong Z**, **Li Y**, **Jin Y**, **et al.** Urinary Tract Infections Caused by Uropathogenic *Escherichia coli*: Mechanisms of Infection and Treatment Options. Int J Mol Sci. 2023; 24(13): 10537. *https://doi.org/10.3390/ ijms241310537*.

52. **de Araujo LG, Cedeño K, Bomfim AP, de Oliveira Silva M, Mendes AV, Barberino MG, et al.** Carbapenem-resistant Enterobacterales bloodstream infections related to death in two Brazilian tertiary hospitals. BMC Infect Dis. 2025; 25(1): 725. *https://doi.org/10.1186/s12879-025-11115-x*.
53. **Acman M, Wang R, van Dorp L, Shaw LP, Wang Q, Luhmann N, et al.** Role of mobile genetic elements in the global dissemination of the carbapenem resistance gene bla_{NDM}. Nat Commun. 2022; 13(1): 1131. *https://doi.org/10.1038/s41467-022-288 19-2*.
54. **Teixeira P**, **Pinto N**, **Henriques I**, **Tacão M**. KPC-3-, GES-5-, and VIM-1-Producing Enterobacterales Isolated from Urban Ponds. Int J Environ Res Public Health. 2022; 19(10): 5848. *https://doi.org/10.3390/ijerph19105848*.
55. **Solgi H, Nematzadeh S, Giske CG, Badmasti F, Westerlund F, Lin YL, et al.** Molecular Epidemiology of OXA-48 and NDM-1 Producing Enterobacterales Species at a University Hospital in Tehran, Iran, Between 2015 and 2016. Front Microbiol. 2020; 11: 936. *https://doi.org/10.3389/fmicb.2020.00936*.
56. **Karampatakis T**, **Tsergouli K**, **Behzadi P**. Carbapenem-Resistant Klebsiella pneumoniae: Virulence Factors, Molecular Epidemiology and Latest Updates in Treatment Options. Antibiotics. 2023; 12(2): 234. *https://doi.org/10.3390/antibiotics12020234*.
57. **Tian X, Zheng X, Sun Y, Fang R, Zhang S, Zhang X, et al.** Molecular Mechanisms and Epidemiology of Carbapenem-Resistant *Escherichia coli* Isolated from Chinese Patients During 2002–2017. Infect Drug Resist. 2020; 13: 501-512. *https://doi.org/10.2147/IDR.S232010*.
58. **Citterio B, Andreoni F, Simoni S, Carloni E, Magnani M, Mangiaterra G, et al.** Plasmid Replicon Typing of Antibiotic-Resistant *Escherichia coli* from Clams and Marine Sediments. Front Microbiol. 2020; 11: 1101. *https://doi.org/10.3389/fmicb.2020.01101*.
59. **Huang J, Lv C, Li M, Rahman T, Chang YF, Guo X, et al.** Carbapenem-resistant *Escherichia coli* exhibit diverse spatiotemporal epidemiological characteristics across the globe. Commun Biol. 2024; 7(1): 51. *https://doi.org/10.1038/s42003-023-05745-7*.
60. **Nastro M**. Carbapenemen-resistant Enterobacterales: An issue of global concern. Rev Argent Microbiol. 2024; 56(2): 113-114. *https://doi.org/10.1016/j.ram.2024.05.001*.

FE DE ERRATA

En el trabajo **"Withaferin-A induces apoptosis and autophagy in colorectal cancer cell lines via down-regulated expression of histone deacetylase 1"** publicado en el Vol. 67 número 1, marzo de 2026 es necesario sustituir las figuras en la pág. 82, Fig. 1 (FJ); pág. 84, Fig. 3 (C,D,H); pág. 85, Figs. 4 (C) y pág. 86, Fig. 5 (G) por las que aparecen en estas correcciones. Además, se debe hacer una modificación en la afiliación del autor Caixi Li, como se explica.

ERRATUM

In the article **"Withaferin-A induces apoptosis and autophagy in colorectal cancer cell lines via down-regulated expression of histone deacetylase 1"**, published in Vol. 67, Issue 1, March 2026, it is necessary to change the figures in pág. 82, Fig. 1 (FJ); pag. 84, Fig. 3 (C,D,H); pag. 85, Figs. 4 (C) y pag. 86, Fig. 5 (EG) for the ones shown in this new version. Besides, a correction in the affiliation of author Caixi Li, is needed.

Figure corrections:

In **Figure 1F**, the CACO2 control panel was incorrect. "Crt" was mistakenly used instead of Ctr.

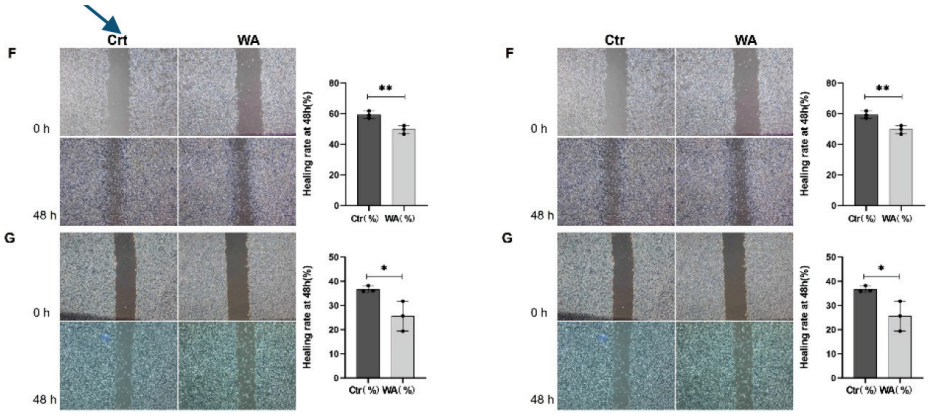

In **Figure 1J**, the CACO2 control (Ctr) and WA-treated panel were wrongly chosen.

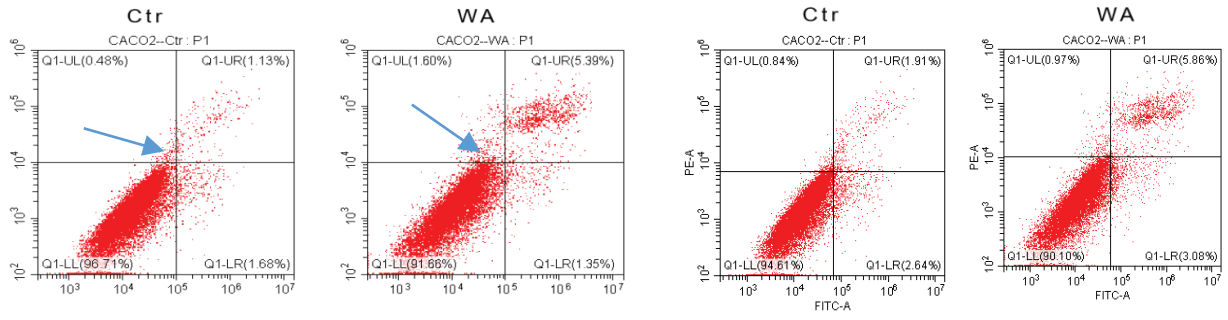

In **Figure 3C**, the molecular weight markers were inadvertently omitted. We have now added the molecular weight markers to these Western blot images. Additionally, the HT29 bands have been updated in the corrected version.

In **Figure 3D, 3H, 4C, 5E, and 5G**, the molecular weight markers were inadvertently omitted. We have now added the molecular weight markers to these Western blot images.

Figure 3D

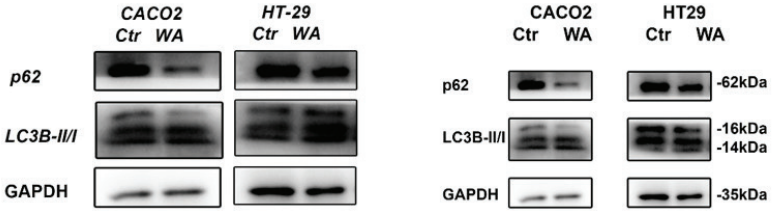

Figure 3 H

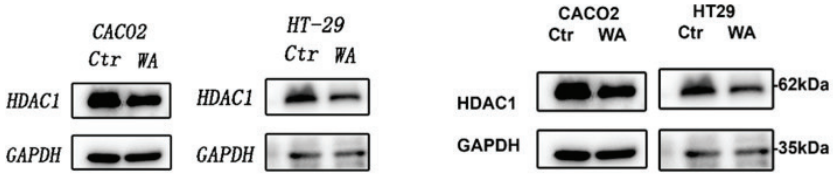

Figure 4C

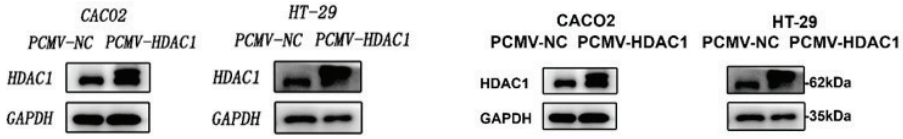

Figure 5E

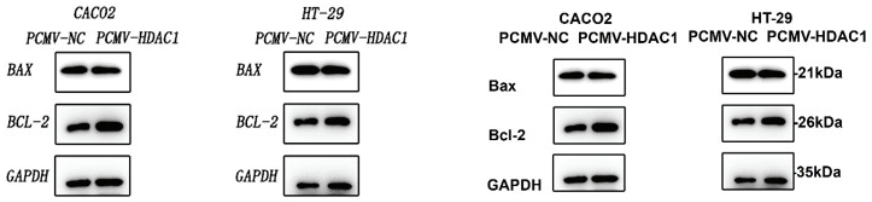

Figure 5G

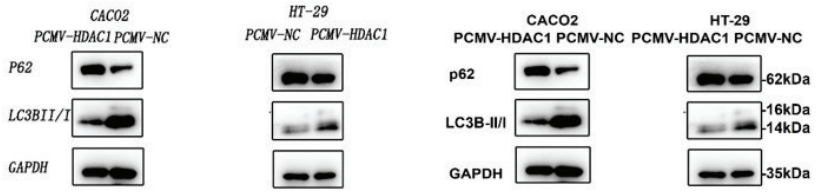

Author affiliation correction

The affiliation for author Caixia Li was listed as:

[3]Department of Stomatology, Shandong Provincial People's Hospital, Jinan, Shandong, China.

This should be corrected to:

[3]Department of Stomatology, Weifang People's Hospital, Weifang, Shandong, China. (to maintain consistency with the hospital's official designation).

Investigación Clínica
Vol. 67 Nº 2 / June 2026
Bilingual - Abstracts in Spanish and English

Contents

Investigación Clínica
Vol. 67 Nº 2 /Junio 2026
Bilingüe - Resúmenes en Español e Inglés

Contenido